

Diss. ETH No. 25863

Activation of Organic Carbonates, DMSO-based Functionalizations and Cu-catalyzed Trifluoromethylation

A thesis submitted to attain the degree of
DOCTOR OF SCIENCES of ETH ZURICH
(Dr. sc. ETH Zurich)

presented by
HARUTAKE KAJITA

Master of Engineering, Kyoto University

born on 23.07.1985

Japanese

accepted on the recommendation of
Prof. Dr. Antonio Togni, examiner
Prof. Dr. Erick M. Carreira, co-examiner

2019

Acknowledgements

A number of people from different communities have brought me to the end of my PhD life, and I wish to personally acknowledge them here.

The first and largest thanks goes to my supervisor, Prof. Antonio Togni. Your agreement with my PhD study in the group was the start of my life out of Japan. Regarding chemistry, you allowed me to pursue my interest even without fluorine and metal (I felt bad, though). Nonetheless, you guided my research to this thesis at the end. I have been amazed by your curiosity, teaching passion, decision to change the system, and generosity to accept good and bad factors inside and outside the group within your responsibility. And again, thank you very much, Antonio!

Prof. Erick M. Carreira kindly agreed to co-supervise this doctoral thesis.

Prof. Antonio Mezzetti gave instructive comments and support for my research. He is always kind to me even though I am pretty bad in his field.

Andrea Sachs is kindly acknowledged for her administrative and organizational works in Togni group. She advised me a lot about personal administrative things with the Kanton and Gemeinde, and her help is essential particularly to foreigners like me.

Because this thesis contains technical experiments and analyses, I needed supportive and skillful co-workers. Those with whom I have worked, in the past and present, are kindly acknowledged below.

Alex Lauber and Pascal Tripet helped me measuring non-standard NMR methods. Your knowledge, advice and patience led me to the right results, I believe. Alex was one of those who took care of me right after my arrival in Switzerland, and even now. My gratitude also goes for your SGU and HPLC jobs. Plus, thanks for proofreading. I will buy you beers!

Phil Liebig helped me when I started Cu–CF₃ chemistry with practical advice and a set of articles. Discussions with you were always fun and exciting.

Ewa Pietrasiak and Mona Wagner: thank you for your patience to measure my few crystals. Your advice on crystallization were very helpful because I was not trained in organometallic chemistry. Not only X-ray, but Mona also organized many group/private events, I appreciate. And thank you for the German translation for “Zusammenfassung”. With Ewa, I was happy to take care of LC-MS because of her neat attitude.

Lorena De Luca is my chromatography-mate. We have tackled “moody” GCs and HPLC together, and we managed it. You learnt the maintenance techniques so fast, which helped me a lot.

Without named group jobs, but everyone in the group was very kind and helpful. Benson Jelier and Cody Ross Pitts gave me opportunities for inspiring discussions. The speed and quality of your response to the proofreading for my thesis was amazing, too. The fun time I spent in H230 north with Rima, CP, Pascal and Cody occupied the majority of my life at ETH. Also, appreciation for the nice atmosphere of the group goes to Sebastian Küng, Dustin Bornemann, Fabian Brüning, Jorna Kalim and Dmitry Katayev.

Lorenzo Querci and Stephan Kradolfer were my co-workers in the course of the Praktikum organized by Dr. Hartmut Schönberg. We took serious amount of time and effort for student-lab because the textbook and schedule were complete mess... However, I am proud of my students and the name of best assistants!

Dr. Daniel Klose and Dr. Reinhard Kissner supported EPR and UV-VIS measurements. Even though I was not familiar with the analyses, you helped me kindly and friendly.

To all the ETH staff who help us in general, the HCI shop personnel, people at the waste station, the EA- and MS Service team: thank you for supporting us. Particularly the gas station staffs were nice and supportive during my gas cylinder responsibility although I did not speak German. Also, I appreciate the help from the administrative (department and doctoral), who took care of my position at ETH from the beginning to the end.

It was an ultra super maximum great big pleasure to share time with Remo, Lukas, Rima, Alex, Mona and Lorena for everything. Thank you for getting along with me and helping me for the five years in Zurich.

Music was another important part for my life at ETH, particularly with the core member of Sunset Hönggchestra, Jirka, Jan and Sofi. Your performances were of course great, and the energy and dynamics you brought made me unbelievably active! I hope we have more chances to play together.

Finally, I leave thank you to my family and friends in Japan. Kazuhiko Yamada, my former supervisor and my master at AGC, keeps contact with me and spares time for me. Shohei Tada was one of Japanese “H-floor friends” advised me a lot even though our fields are different. Thank you for your critical proofreading for my thesis. At the very last, I am thankful to my family in Japan. Although I made my parents worried so much, they are very supportive of me.

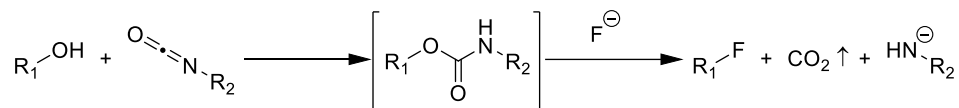
Contents

Chapter 1. General Introduction	1
1.1 Organofluorine compounds	2
1.2 Synthetic methods for organofluorine compounds	6
1.3 Organic carbamates	13
1.4 Organic carbonates	17
1.5 DMSO-based oxidations	18
1.6 Trifluoromethylation reactions	23
1.7 The aim of this thesis	28
Chapter 2. Acid-Activation of Organic Carbonates	33
2.1 Introduction	34
2.2 Preliminary investigation	35
2.3 Titanium bromide catalysis	36
2.4 Other catalysts	43
2.5 Conclusion and outlook	44
Chapter 3. Base-Activation of Organic Carbonates	47
3.1 Introduction	48
3.2 Triethylamine-catalyzed reactions	49
3.3 DABCO-catalyzed reactions	51
3.4 Hypothetic reaction mechanism	54
3.5 Conclusion and outlook	55
Chapter 4. DMSO-based Oxidative Bromination of (Hetero)Arenes	57
4.1 Introduction	58
4.2 Preliminary investigation	60
4.3 Reaction condition optimization	62
4.4 Substrate scope	64
4.5 Synthetic applications	67
4.6 Conclusion and outlook	69
Chapter 5. Exploring DMSO-based oxidative functionalizations	73
5.1 Introduction	74
5.2 DMSO-based halogenations of arenes	76
5.3 Iodine-based oxidations	80
5.4 Conclusion	84

Chapter 6. Mechanistic Study of a Copper-catalyzed Trifluoromethylation Reaction of Arenes	87
6.1 Introduction	88
6.2 Copper iodide-catalyzed reactions	89
6.3 Other copper catalysts	97
6.4 Supporting the hypothesis	104
6.5 Examination of reaction pathway	108
6.6 Conclusion and outlook	114
Chapter 7. General Conclusion and Outlook	117
7.1 Conclusion	118
7.2 Outlook	120
Chapter 8. Experimental	125
8.1 General remarks	126
8.2 Acid-activation of organic carbonate (Chapter 2)	129
8.3 Base-activation of organic carbonates (Chapter 3)	134
8.4 DMSO-based oxidative bromination of arenes (Chapter 4)	136
8.5 Exploring DMSO-based oxidative functionalizations (Chapter 5)	148
8.6 Mechanistic study of a copper-catalyzed trifluoromethylation Reaction of Arenes (Chapter 6)	152
Bibliography	174
X. APPENDIX	191
Appendix A: Abbreviations and Acronyms	192
Appendix B: Crystallographic Data	194
Appendix C: Curriculum Vitae	196

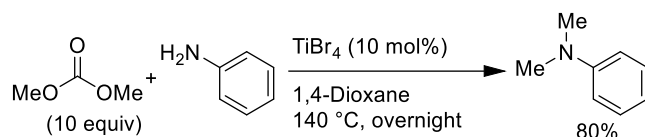
Abstract

The original goal of the thesis at hand was the development of a nucleophilic fluorination reaction of aliphatic alcohols by the use of organic carbamates as the intermediates (**Scheme 1**).



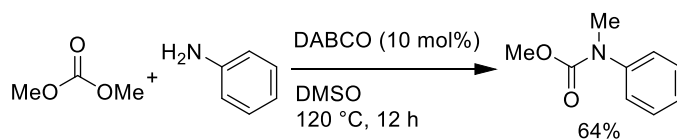
Scheme 1. Fluorination of alcohols with taking use of carbamates as intermediates.

In order to carefully examine this idea, the project was broken down into model reactions. The research started with the investigation of a model reaction of amines and organic carbonates. TiBr_4 was found to be an active catalyst for this transformation (**Scheme 2**), although this project was discontinued because the reaction did not occur at low temperatures under any conditions. However, two interesting side reactions were found during the study, which were investigated separately.



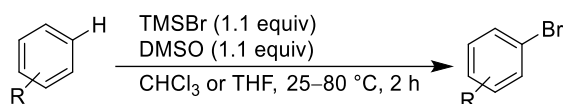
Scheme 2. The TiBr_4 -catalyzed methylation of amines by dimethyl carbonate (DMC).

One side reaction was a base-catalyzed formation of *N,N*-disubstituted carbamates from amines and organic carbonates. The transformation occurred efficiently in DMSO at 120°C , where the $\text{p}K_a$ value of the amine substrate has an influence on the reactivity (**Scheme 3**).



Scheme 3. The base-catalyzed transformation of amines and DMC to *N,N*-disubstituted carbamates.

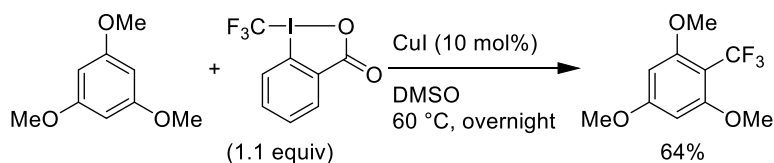
The other side reaction by TiBr_4 in DMSO led to a DMSO-based oxidative bromination of arenes. TMSBr was found to be a more efficient bromide source than TiBr_4 (**Scheme 4**). This method is suitable for large-scale syntheses because the reagents are stable and readily available, and volatile by-products can be easily removed by evaporation.



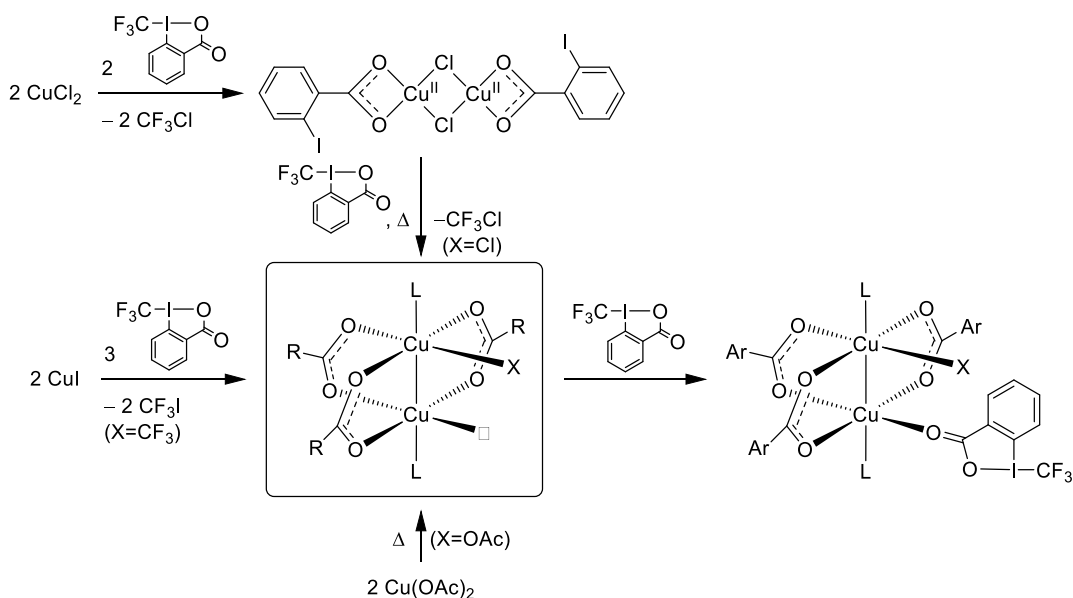
Scheme 4. The oxidative bromination of arenes in the TMSBr/DMSO system.

The use of DMSO as an oxidant was investigated further for other aromatic functionalizations, in particular fluorination and trifluoromethylation. Since positive results were not obtained, the project was turned to the mechanistic study of a model trifluoromethylation reaction.

Mechanistic studies focused on the CuI-catalyzed trifluoromethylation of a model arene (**Scheme 5**). Determination of the stoichiometric relation between CuI and the trifluoromethylating reagent, reactivity evaluations and magnetic susceptibility measurement of the reaction mixture indicate that dinuclear copper complexes $[\text{Cu}_2\text{X}(\text{OCOAr})_3]$ (X is CF_3 , halide or carboxylate) are the active catalysts for the trifluoromethylation reaction (**Scheme 6**).



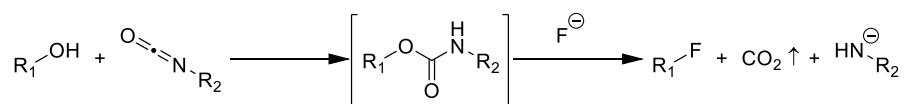
Scheme 5. CuI-catalyzed trifluoromethylation of an arene.



Scheme 6. Generations of the hypothesized active catalyst from CuI, CuCl_2 or Cu(OAc)_2 . L is solvent molecule.

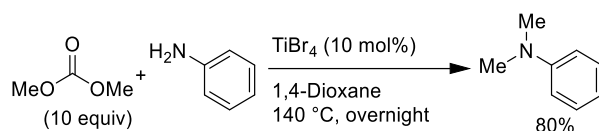
Zusammenfassung

Das ursprüngliche Ziel der vorliegenden Arbeit war die Entwicklung einer nukleophilen Fluorierungs-Reaktion von aliphatischen Alkoholen mittels organischer Carbamate als Zwischenprodukte (**Schema 1**).



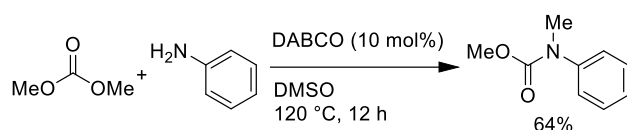
Schema 1. Fluorierungs-Reaktion eines Alkohols mit einem Carbamat als Zwischenprodukt.

Um diesen Ausgangspunkt besser zu beurteilen, wurde das Projekt zunächst vereinfacht, indem eine Modelreaktion von Aminen mit organischen Carbonaten untersucht wurde. Dabei wurde festgestellt, dass TiBr_4 als aktiver Katalysator für diese Umwandlung wirken kann (**Schema 2**). Dieses Projekt wurde allerdings eingestellt, da die gewünschte Reaktion nicht bei tiefen Temperaturen stattfindet. Nichtsdestotrotz wurden zwei interessante Nebenreaktionen beobachtet, die im Folgenden näher untersucht wurden.



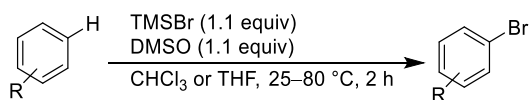
Schema 2. Methylierung von Aminen mit Dimethylcarbonat (DMC) unter der Verwendung von TiBr_4 als Katalysator.

Eine der beiden Nebenreaktionen war die basenkatalysierte Bildung von *N,N*-disubstituierten Carbamaten, ausgehend von Aminen und organischen Carbonaten. Diese Reaktion findet hauptsächlich in DMSO bei 120 °C statt, wobei auch der pK_a -Wert des Amins einen erheblichen Einfluss auf die Reaktivität hat (**Schema 3**).



Schema 3. Basenkatalysierte Umwandlung von Aminen und DMC zu *N,N*-disubstituierten Carbamaten.

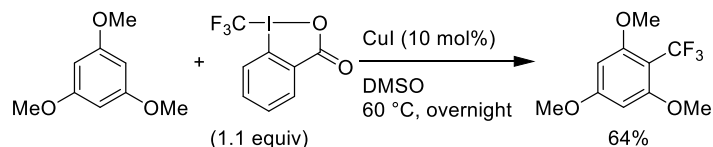
Die zweite Nebenreaktion, findet zwischen TiBr_4 und DMSO statt und führt zu einer oxidativen Bromierung von Aromaten. Im Laufe des Projektes wurde festgestellt, dass mit TMSBr bessere Ergebnisse erzielt werden können, als mit TiBr_4 (**Schema 4**). Die TMSBr Methode unterstützt Reaktionen in grossem Massstab, da die Reagenzien luftstabil und kommerziell erhältlich sind. Desweiteren können die flüchtigen Nebenprodukte, durch Verdampfen, einfach entfernt werden.



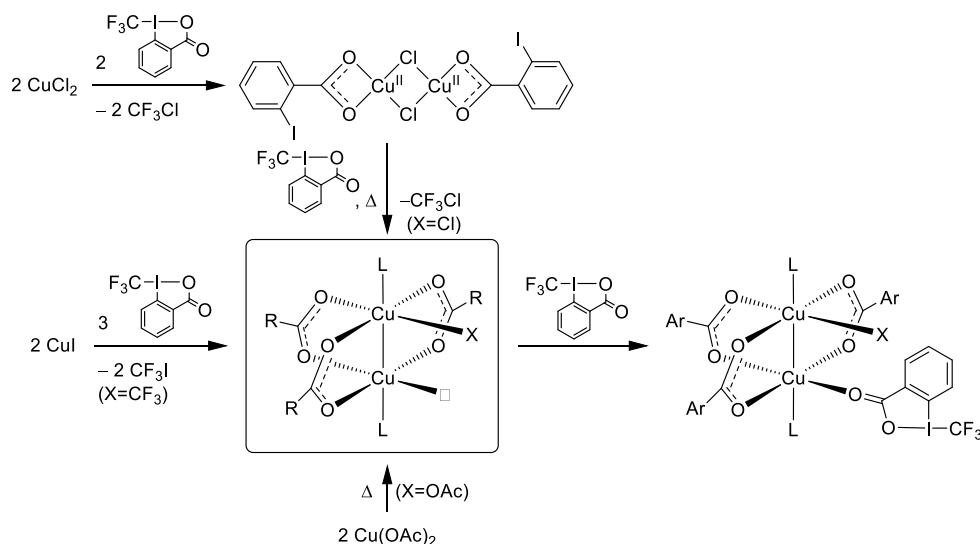
Schema 4. Oxidative Bromierung von Aromaten unter Verwendung von TMSBr und DMSO.

Um weitere Erkenntnisse über die Rolle des DMSO als Oxidationsmittel zu erhalten, wurden Reaktionen mit anderen aromatischen Funktionalisierungen durchgeführt, insbesondere im Hinblick auf Fluorierungs- und Trifluormethylierungs-Reaktionen. Da keine zufriedenstellenden Ergebnisse erhalten wurden, hat sich die Sichtweise des Projektes auf mechanistische Studien von Trifluormethylierungs-Reaktionen im Allgemeinen verlagert.

Die mechanistischen Untersuchungen konzentrierten sich auf CuI-katalysierte Trifluormethylierungs-Reaktionen von Aromaten (**Schema 5**). Diverse Experimente, wie die Ermittlung der Stöchiometrie zwischen CuI und dem Trifluormethylierungs Reagenz, die Beurteilung der Reaktivität, sowie die magnetische Suszeptibilität des Reaktionsgemisches, ergaben den Hinweis, dass zweikernige Kupferkomplexe des Typs $\text{Cu}_2\text{X}(\text{OCOAr})_3$ ($\text{X} = \text{CF}_3$, Halogen oder Carboxylat) der aktive Katalysator für die Trifluoromethylierungs-Reaktionen darstellen. (**Schema 6**).



Schema 5. CuI-katalysierte Trifluormethylierungs-Reaktion von Aromaten.



Schema 6. Mögliche Synthesewege zum hypothetisch aktiven Katalysator, ausgehend von CuI, CuCl_2 und $\text{Cu}(\text{OAc})_2$. L = Lösungsmittel.

Introductory remarks

The thesis at hand presents synthetic methods of organic and organometallic compounds. In general, the reactions were carried out in glassware under argon in order to prevent undesired oxidations of the compounds by atmospheric oxygen. The term “overnight” means approximately 12–20 hours reaction time.

Chapter 1

General Introduction

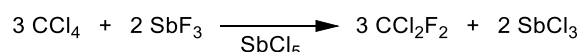
This study started with the attempt to develop a nucleophilic fluorination of aliphatic alcohols. Accordingly, the properties and the importance of organofluorine compounds and their synthetic methodologies are illustrated herein. Since this thesis contains other different topics, organic carbamates, organic carbonates, DMSO-based oxidations and trifluoromethylation reactions are subsequently described.

1.1 Organofluorine compounds

Organofluorine compounds generally exhibit high induction effects, modified lipophilicity, reduced van der Waals interactions and modified bulkiness.^[1-4] Because these characteristics can be advantageous when compared to non-fluorinated compounds, in many cases, organofluorine products are well developed and are used for a broad range of applications.^[5]

1.1.1 Halocarbons

The first use of organofluorine compounds was halocarbons, which were developed and commercialized as heat transfer fluids, better known as refrigerants.^[6] Halocarbons for refrigerants are small molecules that are highly functionalized with halogens, since they are required to be non-flammable gases or liquids. The demanded boiling point depends on the target use.^[7] However, chlorinated and brominated compounds are toxic and relatively flammable, and many of them possess too high boiling points as refrigerants. In 1928, Midgley synthesized fluorinated halocarbons (**Scheme 7**),^[8] using the method developed by Swarts in 1892.^[9] Chlorine atoms of carbon tetrachloride are substituted with fluorine atoms by antimony trifluoride in the presence of antimony pentachloride. Midgley and his co-workers selected dichlorodifluoromethane (CCl_2F_2) because it has a suitable boiling point for commercial mechanical refrigeration.^[10] Also, the molecule exhibits non-toxicity, non-flammability and high thermostability, benefitting from stable C–F bonds. Decades later, however, chlorofluorocarbons (CFCs) including CCl_2F_2 were found to damage the ozone layer.^[11] Furthermore, most of the halocarbons used as refrigerants have a negative impact on global warming.^[12] Therefore, fluorinated refrigerants with lower ozone depletion potential (ODP) and global warming potential (GWP) have been continuously developed (**Figure 1**).^[13,14] The latest studies on low GWP HFO refrigerants are described in comprehensive reviews.^[12,14]



Scheme 7. The production of dichlorodifluoromethane (CCl_2F_2) by Midgley.^[10]

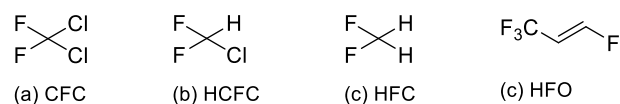


Figure 1. Selected examples of developed refrigerants. (a) CFC-12 (1930s) (b) HCFC-22 (1980s) (c) HFC-32 (1990s) (d) HFO-1234ze (2010s). The decades of their major market appearance are shown in parentheses.

1.1.2 Fluoropolymers

The development of the fluoropolymer industry began in 1938 with the discovery of poly(tetrafluoroethylene) (PTFE) (**Figure 2a**), as generally known as Teflon[®].^[15,16] Its thermo- and photo-stabilities, and non-stick and friction-reducing properties are very attractive for engineering polymer applications. It is therefore used in a broad application, for example, additive in printing inks, friction-reducing additive in thermoplastics and food contact coatings.^[17] However, conventional PTFE products have some limitations such as poor weldability, low creep resistance, low wear resistance, low tensile strength and high microvoid content.^[18] Therefore, modified fluoropolymers have been developed to overcome this problem while keeping attractive properties.^[19]

ETFE (**Figure 2b**) shows high tensile strength, high flexibility, excellent impact strength, good abrasion resistance and high cutting resistance. PFA (**Figure 2c**) is one of a few transparent fluoropolymers thanks to its low crystallinity. Also, because of its high chemical resistance it found use in the semiconductor manufacturing industry for high purity moldings. PFSA (**Figure 2d**) is suitable for many membrane applications such as sensors, drug release, gas drying or humidification, and electrochemical cells and devices including fuel cells. Since fluoropolymers in general show properties which non-fluorinated products cannot achieve, new product developments, applications and synthetic processes have continued to flourish.^[20] It is advised to read the latest reviews^[21] for details, because the variety of newly developed fluoropolymers are very broad.

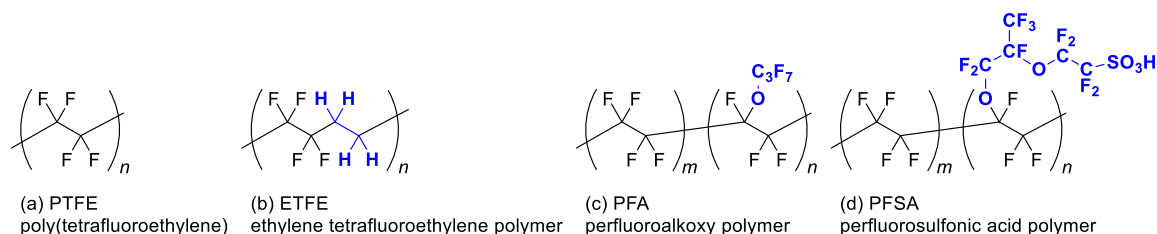


Figure 2. Chemical structures of the most used fluoropolymers. Modifications from PTFE are emphasized.

1.1.3 Fluorinated oligomers

Fluorinated oligomers found unique uses and are leading in several markets.^[19] The general characteristics of fluorosurfactants (**Figure 3a**) are low surface tension, unique optical properties and high chemical resistance. Their major use is that of hydraulic fluids for aircrafts, antireflection layers in photolithographic processes, firefighting foams and electroplating baths.^[22] Another popular use concerns lubricants such as Krytox[®] (**Figure 3b**).^[23] They are chemically and thermally stable to be used under harsh environments.^[24]

Additionally, fluorinated oligomers are used as monomers to produce partly fluorinated copolymers. Oil and water repellants for textile fabrics are widely used in society (**Figure 3c**).^[25] Such materials are acrylic polymers consisting of pendant perfluoroalkyl groups (R_f) and hydrocarbon groups (R_h). Fluorocarbon groups tend to assemble intra- and intermolecularly into small domains, and this feature improves their efficiency as repellants. Perfluoro(polyether silanes) (**Figure 3d**) are found in every smartphone, since they make touch panel displays resist-smudging and confer an anti-fingerprint function. The low surface energy given by R_f groups are responsible for these unique properties. R_h groups are generally installed to increase the flexibility of the molecules because R_f groups alone are highly crystalline and stiff for coating applications. Solvent-soluble fluorinated copolymers for paints and coatings (**Figure 3e**) maintain the excellent appearance of buildings and other structures for long periods by protecting them from sunshine, wind, rain and corrosion.^[26] Fluorinated chain is essential for the resistance to climate while side chains improve solubility to the used solvent.

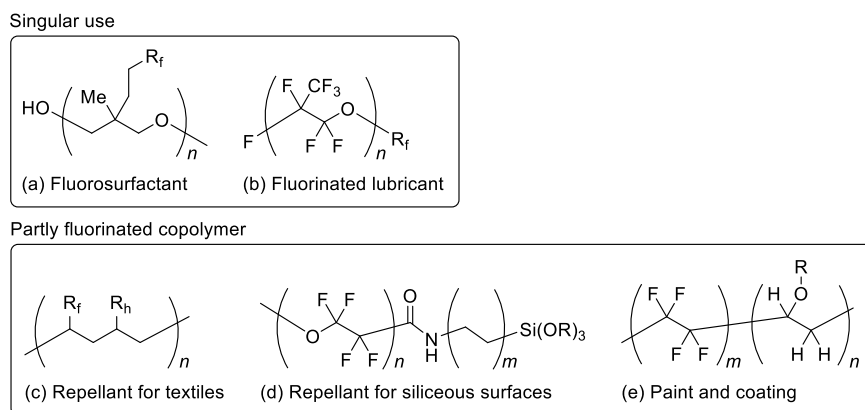


Figure 3. General structures of selected fluorinated oligomers and partly fluorinated copolymers. R_f =fluorocarbon group, R_h =hydrocarbon group.

1.1.4 Fluorinated bioactive compounds

The use of fluorinated compounds in medicinal chemistry was pioneered by Fried in 1954. The potential role of fluorine in bioactive molecules was indicated while screening the substituent for

9 α -hydrogen of cortisone and hydrocortisone.^[6,27] As a result, fluorocortisone became the first fluorinated pharmaceutical approved into the market (**Figure 4a**).^[28] Around the same time, Heidelberger showed that the fluorine atom in fluoroacetic acid was responsible for inhibition of a vital enzyme. Combining this idea with the report that uracil was absorbed into experimental rat liver tumors more rapidly than into normal liver cells,^[29] he and his coworkers synthesized and assessed 5-fluorouracil in 1957, which is one of the first anticancer drugs (**Figure 4b**).^[30,31]

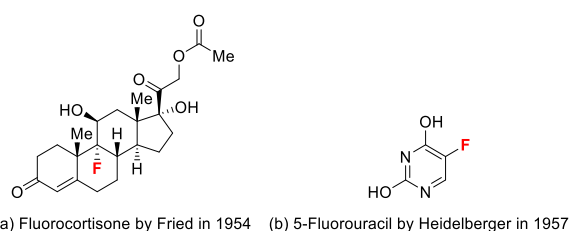


Figure 4. The structure of (a) fluorocortisone^[27] and (b) 5-fluorouracil.^[30]

Nowadays it is commonly understood that the introduction of fluorine atoms into bioactive molecules shows a substantial improvement of their potency in many cases.^[32] Many beneficial effects of fluorinated molecules in comparison to their nonfluorinated counterparts have been reported, for example, the modulation of the acidity and lipophilicity, as well as the control of conformational bias. Another useful role of fluorine substitution is the blocking of potential oxidation sites in order to prevent undesired metabolic pathways.^[33] As a result, approximately 20% of medicinal products in the current market contains at least one fluorine atom in the molecule of the active ingredient (**Figure 5**).^[34] This is also true for agrochemical science and the proportion of fluorinated active ingredients on the market is significantly higher than in medicinal chemistry (**Figure 6**).^[5,35]

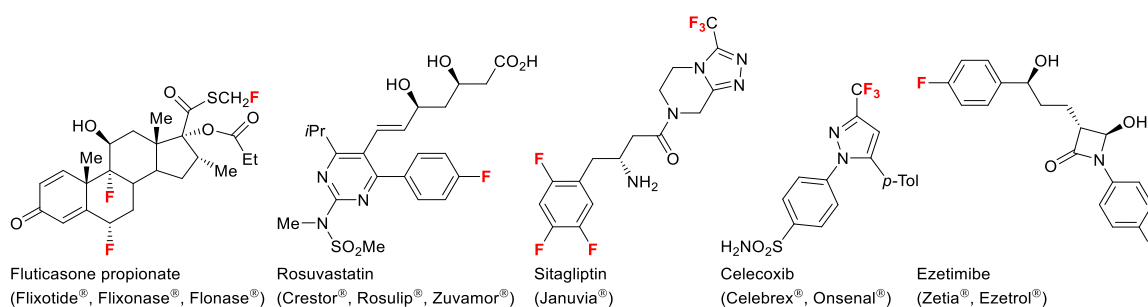


Figure 5. Fluorine-containing blockbuster pharmaceuticals.^[34]

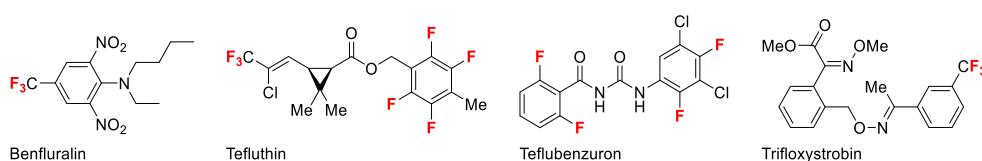
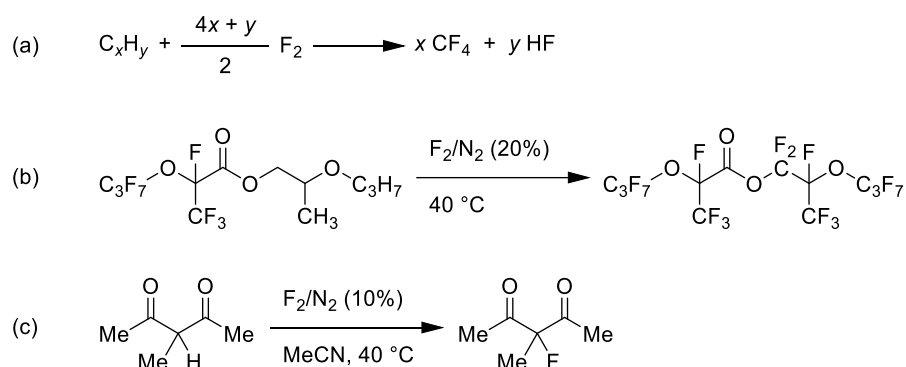


Figure 6. Popular fluorinated agrochemicals.^[5,35]

1.2 Synthetic methods for organofluorine compounds

1.2.1 Perfluorination by using fluorine gas

The first reaction of hydrocarbons and elemental fluorine was reported by Moissan himself in 1890 after the first isolation of fluorine in 1886.^[36] He and his followers faced the difficulty of controlling the reactivity of elemental fluorine. Organic compounds were burnt in elemental fluorine and the according undesired C–C bond cleavages were the major problem (**Scheme 8a**). Since 1933, Bigelow led projects of direct fluorinations of small organic molecules and suppressed C–C bond cleavage by optimizing gas-phase reactors to control perfluorination reactions.^[37] In later decades, direct fluorinations have been further studied and liquid-phase direct fluorinations have been developed to produce perfluorinated products (**Scheme 8b**).^[38] Furthermore, microfluidic techniques have made fluorine gas to be utilized for selective direct fluorinations (**Scheme 8c**).^[39]



Scheme 8. Examples of direct fluorinations. (a) Early problems of C–C cleavages.^[36] (b) A controlled perfluorination in liquid phase.^[38] (c) A selective direct fluorination by a microfluidic system.^[39]

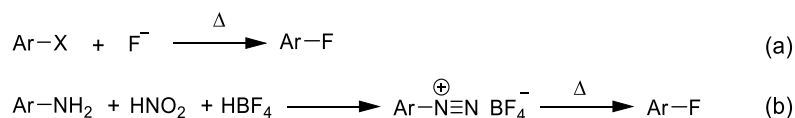
On the other hand, by using other fluorine sources, a variety of methodologies of single fluorination have been developed and are used to prepare organofluorine compounds in controlled ways. They are described in the following sections.

1.2.2 General remarks about aromatic fluoride syntheses

Synthetic strategies towards aromatic fluorides have been developed in a wide variety,^[40,41] and accordingly aryl and heteroaryl fluorides make up a notable part of commercial fluorinated products.^[42]

1.2.3 Nucleophilic aromatic fluorination

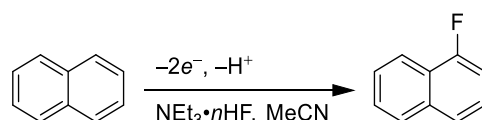
The conventional synthetic methods of aromatic fluorination are nucleophilic aromatic substitutions (S_NAr), including the Balz–Schiemann reaction (**Scheme 9**).^[43,44] They usually require electron deficient aromatic systems and high temperature. Therefore, the substrate scope of these methods is limited.



Scheme 9. (a) S_NAr of aryl halides. (b) The Balz–Schiemann reaction.

1.2.4 Electrofluorination of aromatic compounds

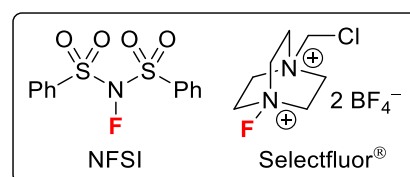
Electrochemistry was applied for the synthesis of organofluorides in 1941 by Simons and coworkers.^{1,[45]} They applied high voltage (5 – 6 V) to the cell to oxidize fluoride anion to fluorine radical, but this reaction usually occurs exhaustively and often gives undesired perfluorocarbons.^[46] In 1970, Knunyants revealed that anodic oxidation can be used to generate organic cations that then react with fluoride anion to achieve monofluorination at a potential below 2.85 V (**Scheme 10**).^[47] Following this report, controlled electrofluorinations of aromatic compounds have been studied. In particular, selectivities of monofluorinations were improved by optimizing the solvent–electrolyte system.^[48]



Scheme 10. The electrofluorination of naphthalene by Knunyants in 1970.^[49]

1.2.5 Electrophilic aromatic fluorination by organic fluorinating reagents

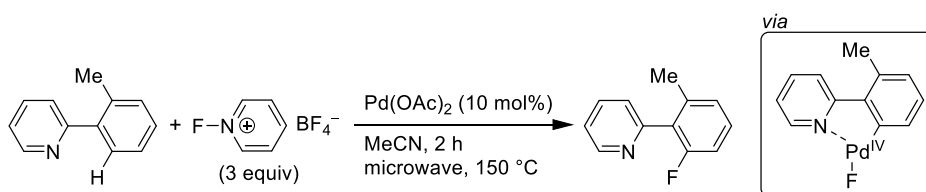
Organic electrophilic fluorinating reagents came into use after the 1980s. The illustrious examples are *N*-fluorobenzenesulfonimide (NFSI)^[50] and Selectfluor[®],^[51] which are still the mainly used fluorinating reagents. A wide range of aromatic nucleophiles such as electron-rich arenes, heteroarene, organometallic compounds, aryl silanes and aryl boranes can be fluorinated by them.^[42]



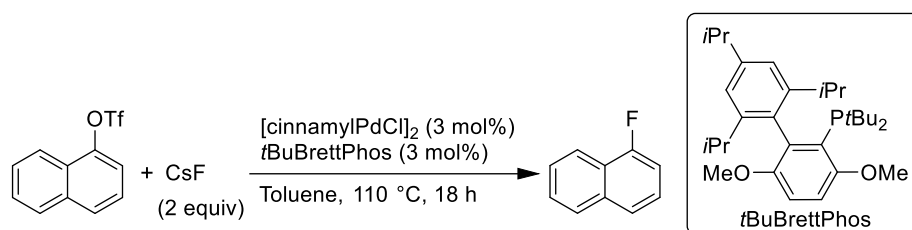
¹ The original report was withdrawn for safety reasons and was reissued in 1949.

1.2.6 Transition metal-catalyzed aromatic fluorination

The breakthrough that further broadened the scope of aromatic fluorinations has occurred when transition metal-catalyzed fluorinations were reported. This includes both nucleophilic and electrophilic fluorinations. In 2006, a Pd-catalyzed C–H activation using electrophilic fluorinating reagents was reported by the group of Sanford (**Scheme 11**).^[52] This reaction is believed to proceed *via* the generation of a Pd(IV) species from a C–Pd(II) species and an oxidative fluorinating reagent, followed by reductive elimination leading to C–F bond formation. In fact, the same group reported that the combination of an external oxidant and a metal fluoride could achieve the same reaction instead of electrophilic fluorinating reagents.^[53] Soon after that, the group of Buchwald reported that a palladium complex catalyzed a nucleophilic fluorination of aryl sulfonates (**Scheme 12**).^[54] This reaction supposedly occurs through Pd(0)/Pd(II) catalytic cycles, where they need phosphine ligands with electron rich biaryl substituents. Following these reports, researchers have studied catalysts, reagents and directing groups to achieve broader scopes and milder conditions.^[55]



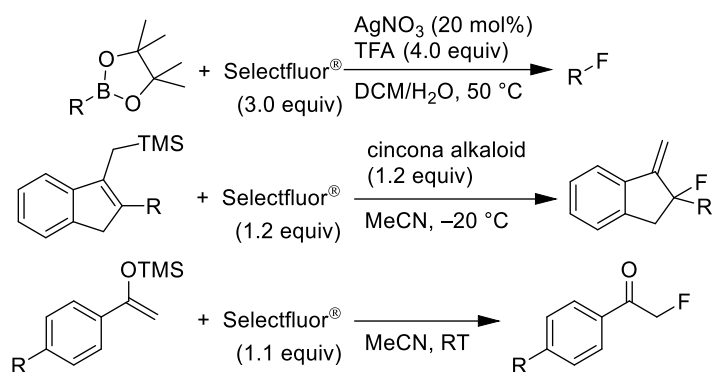
Scheme 11. The aromatic fluorination *via* C–H activation by Sanford.^[52]



Scheme 12. The Pd-catalyzed fluorination of aryl sulfonate by Buchwald.^[54]

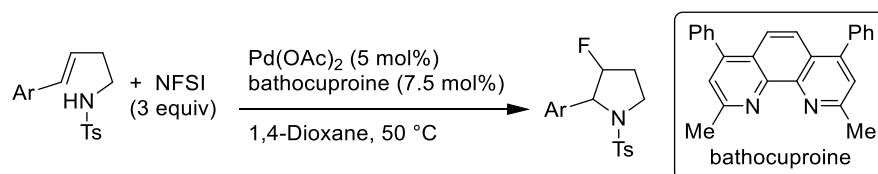
1.2.7 Electrophilic aliphatic fluorination

Electrophilic fluorinations of aliphatic compounds provide rich variations thanks to diverse aliphatic nucleophiles ranging from organoboranes to carbonyl compounds (**Scheme 13**).^[42]



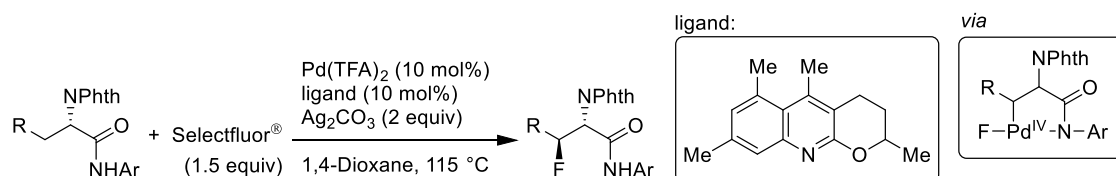
Scheme 13. Electrophilic fluorinations of aliphatic compounds.^[56–58]

Particularly, various addition reactions of olefins have been reported where often catalysts are necessary. Electrophilic fluorinating reagents are used with a nucleophile such as organoboranes, borohydrides and amines (**Scheme 14**).^[59–61]



Scheme 14. A palladium-catalyzed aminofluorination of olefins.^[61]

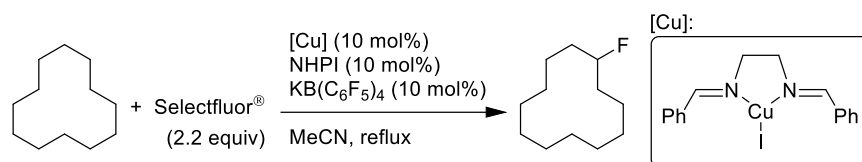
Aliphatic compounds bearing directing groups are fluorinated by Pd-catalyzed C–H activation techniques (**Scheme 15**).^[62] The mechanism is thought to involve C–H insertion and oxidative fluorination to generate Pd(IV)–F complexes (shown in the scheme). The optimal ligand suppresses β-hydride elimination and promotes reductive elimination to yield the corresponding β-fluoro amino amides. The stereoselectivity is also high (diastereoselectivity > 20:1) for most of the presented examples.



Scheme 15. An enantioselective synthesis of β-fluoro-α-amino amides.^[62] NPhth=N-phthalimido group.

1.2.8 Synthesis of aliphatic fluorination *via* radical pathways

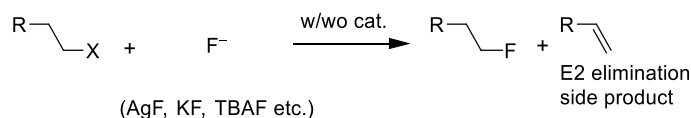
The involvement of radical species is suggested in some cases where electrophilic fluorinating reagents are used (**Scheme 16**).^[63] C(sp³)-H bonds are oxidatively cleaved to generate alkyl radicals, which react with fluorinating reagents to produce alkyl fluorides.



Scheme 16. A radical-based fluorination of alkanes.^[63] NHPI=*N*-Hydroxyphthalimide.

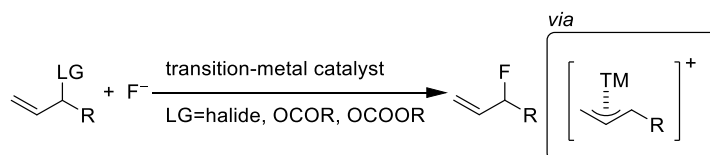
1.2.9 Nucleophilic aliphatic fluorination

The scope of nucleophilic fluorination of aliphatic compounds is more limited than that of electrophilic fluorination.^[64] The traditional S_N2 fluorination of aliphatic halides or other electrophiles suffers from side reactions such as E2 elimination to give olefins, although this approach is synthetically promising to obtain fluorinated alkanes (**Scheme 17**).^[65–68]



Scheme 17. S_N2 fluorination of aliphatic halides.

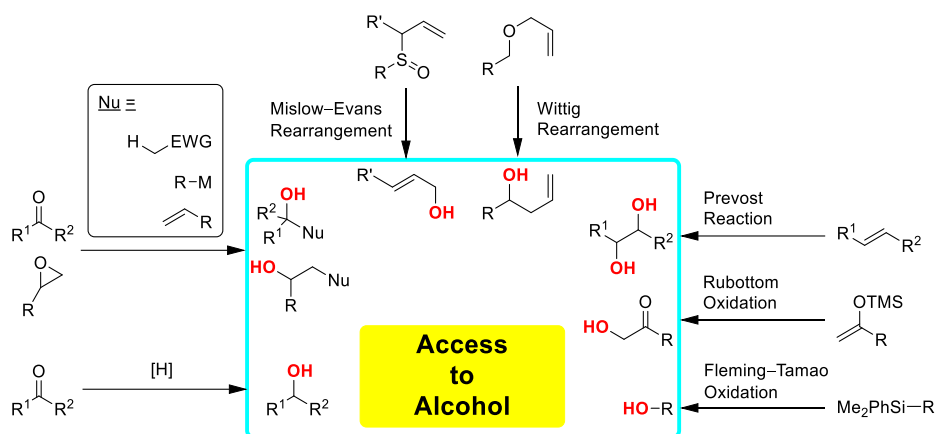
Allyl halides,^[69] allyl esters^[70] and allyl carbonates^[71] are converted to the corresponding fluorides in the presence of transition-metal catalysts (**Scheme 18**). The intermediates in this methodology are transition-metal allyl complexes and, therefore, the scope of this methodology is limited to allyl fluorides.



Scheme 18. Transition metal-catalyzed syntheses of allyl fluorides.

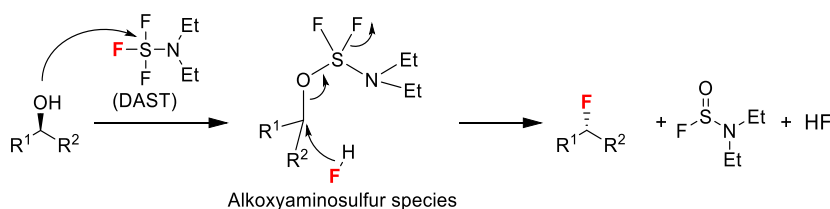
1.2.10 Deoxyfluorination

A popular methodology of nucleophilic aliphatic fluorination is deoxyfluorination because alcohols constitute very common substrates from a synthetic point of view.^[72] Alcohols can be prepared by many reactions as shown in **Scheme 19**.^[73]



Scheme 19. Synthetic methods for alcohols.

The first successful deoxyfluorinating reagent is diethylaminosulfur trifluoride (DAST) (**Scheme 20**).^[74] This reagent was introduced as a user-friendly derivative of the reactive gas SF_4 , which earlier had offered valuable methods for deoxyfluorinations but it is toxic and is difficult to handle. DAST still remains the most commonly used deoxyfluorinating reagent since its development in 1975, although it is thermally unstable and must be stored under $10\text{ }^\circ\text{C}$.



Scheme 20. The structure of DAST and its reaction.^[75]

DAST converts hydroxy groups *in situ* to alkoxyaminosulfur species, followed by nucleophilic attack by fluoride at the substitution center to yield the corresponding aliphatic fluoride with inverted configuration. Following the emergence of DAST, relevant reagents with improved stability have been developed (**Figure 7**).^[75] Yet, their chemoselectivity is not sufficient for late-stage fluorinations^[72] because of elimination reactions (see **Scheme 17**). Another problem in the case of chiral substrates is that stereoselectivity may decrease due to competing $\text{S}_{\text{N}}1$ reactions.^[75]

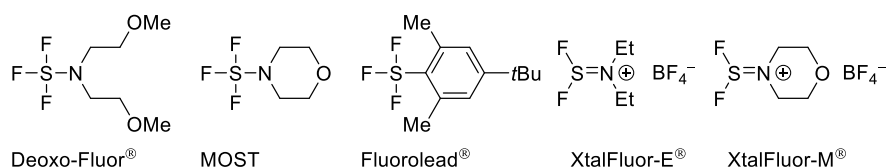
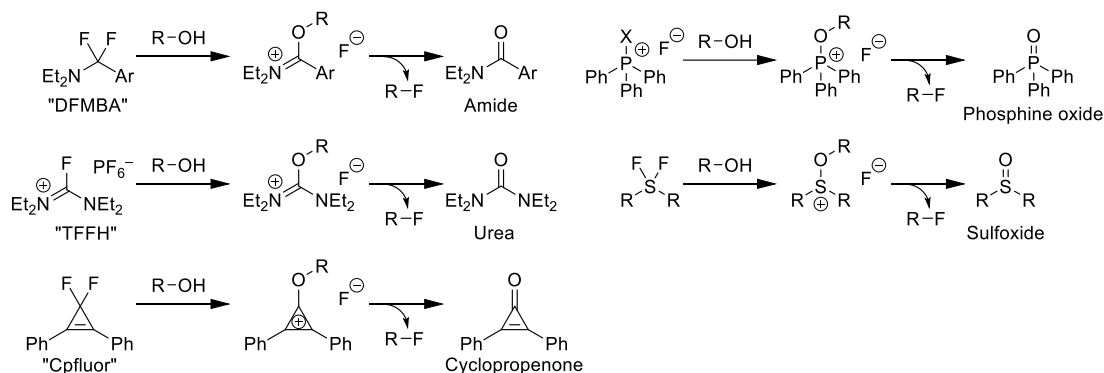


Figure 7. Popular deoxyfluorinating reagents containing S–F bonds.^[75]

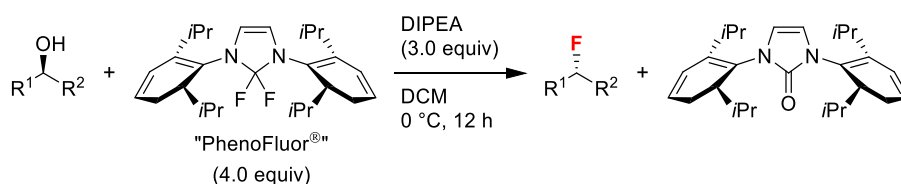
1.2.11 Variations of OH conversion

Besides DAST and similar reagents, it is a popular idea to convert a hydroxy group *in situ* into a good leaving group, because a hydroxy group is rarely eliminated as such. There are known methods to activate and remove hydroxy group as amides,^[76] ureas,^[77] cyclopropanones,^[78] phosphine oxides^[79–81] or sulfoxides^[75] (**Scheme 21**).



Scheme 21. Activation and elimination methods of hydroxy groups for deoxyfluorination.

Recent progresses are characterized by the development of PhenoFluor[®] and Pyfluor.^[72] PhenoFluor[®] was developed by the group of Ritter (**Scheme 22**).^[82,83] It is interesting that this reagent is effective for deoxyfluorination not only of aliphatic alcohols but also of phenols.^[84] However, PhenoFluor[®] is readily hydrolyzed by ambient moisture and therefore is required to be stored with special care. To overcome this problem, bench-stable reagents such as PhenoFluorMix[®]^[85] and AlkylFluor[®]^[86] have been developed (**Figure 8**).



Scheme 22. Deoxyfluorination by PhenoFluor[®].^[83] DIPEA=*N,N*-diisopropylethylamine.

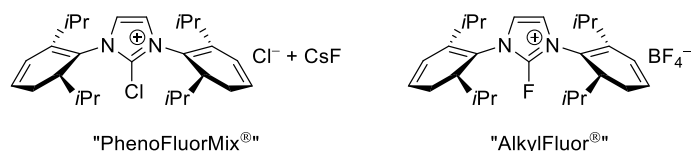
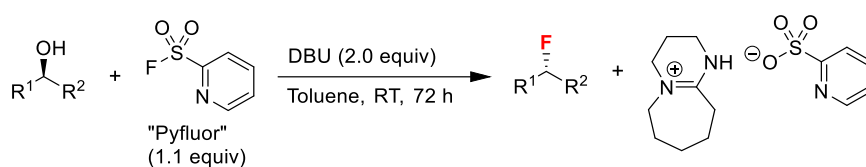


Figure 8. Variations of PhenoFluor[®]: PhenoFluorMix[®][85] and AlkylFluor[®].^[86]

Pyfluor shows high efficiency and selectivity for deoxyfluorination (**Scheme 23**), and is prepared very easily at low cost.^[87] It is stable even in non-basic aqueous solutions. Following this report, other sulfonyl fluoride reagents have been evaluated for deoxyfluorination (**Figure 9**).^[88,89]



Scheme 23. Deoxyfluorination by Pyfluor.^[87] DBU=1,8-diazabicyclo-[5.4.0]undec-7-ene.

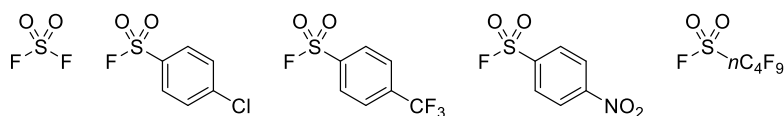


Figure 9. Sulfonyl fluoride^[88] and sulfonyl fluorides^[89] used for deoxyfluorination.

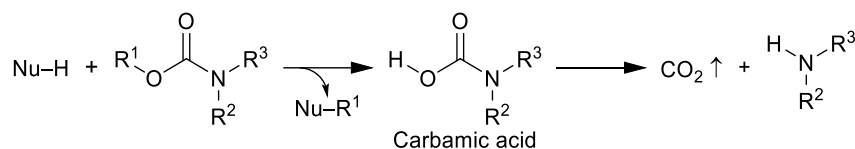
1.3 Organic carbamates

Organic carbamates were selected as activated leaving groups for deoxyfluorination. See Section 1.7 for details. Additionally, syntheses of organic carbamates will be described in Chapter 3.

1.3.1 Organic carbamates in synthetic chemistry

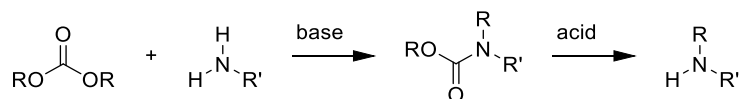
Organic carbamates are regarded in the field of organic chemistry generally as protecting groups,^[90–92] directing groups^[93–96] or ligands,^[97–100] but their use as leaving groups should not be neglected.^[101,102] When carbamates behave as leaving groups, the resulting carbamic acids are not stable and decompose into amines and CO₂ (**Scheme 24**). The elimination of CO₂ gas from the

reaction system may drive the reaction forward by entropy, on top of its high formation enthalpy.^[103,104]

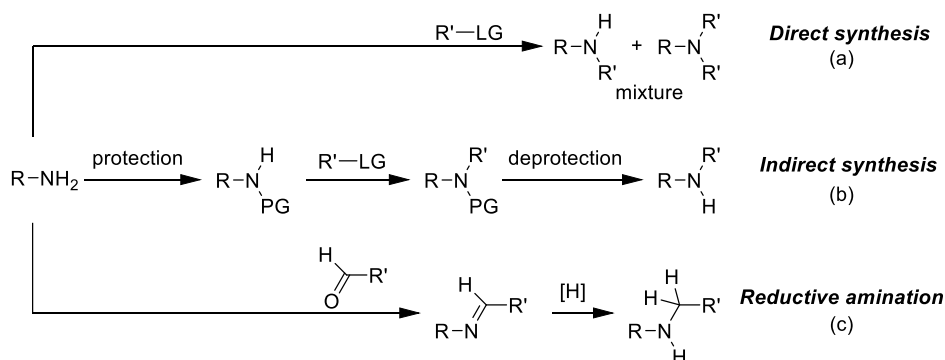


Scheme 24. The behavior of an organic carbamate as a leaving group.

It is also attractive that *N,N*-disubstituted carbamates are stable precursors for the corresponding secondary amines by acidification (**Scheme 25**).^[105–107] It has been a challenge in organic synthesis to produce secondary amines from primary amines selectively,^[108] because direct syntheses tend to give mixtures of mono- and dialkylated products (**Scheme 26a**). Indirect syntheses require at least 3 steps – protection, alkylation and deprotection. (**Scheme 26b**). Reductive amination is another popular method for preparing secondary amines, but its substrate scope is limited due to its reaction mechanism (**Scheme 26c**).^[73] Thus, it is attractive to synthesize *N,N*-disubstituted carbamates under catalytic conditions with a simple base, and to produce secondary amines by acidification.



Scheme 25. Transformations of primary amines towards secondary amines *via* carbamation.



Scheme 26. (a) Direct and (b) indirect syntheses of secondary amines from primary amines. PG = protecting group. (c) Reductive amination.

1.3.2 Organic carbamates in medicinal chemistry and material science

There is an increasing number of approved drugs and prodrugs containing carbamate groups in their structure (**Figure 10**).^[109–111] Replacing peptide bonds with carbamate groups offers opportunities for high chemical stability, increased cell membrane permeability and modulated inter- and intramolecular interactions such as conformational restriction and hydrogen bonding.^[111]

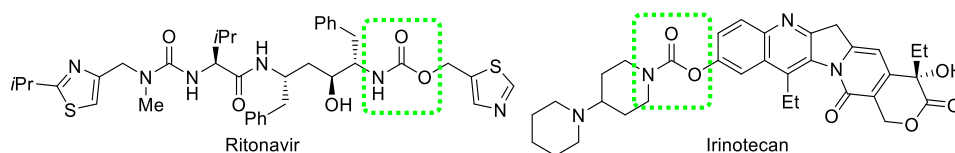


Figure 10. Examples of bioactive organic carbamates.

Carbamate polymers (polyurethanes) draw widespread attention and show variable properties in diverse applications (**Figure 11**).^[112] General advantages of polyurethanes are their high thermostability and relatively low viscosity. Also, polyurethane foams are characteristic cushioning materials because of flexible ether chains and their 3D molecular structure.^[113] In particular, it should be recognized that polyurethane thermal insulations save a significant amount of energy comparing to conventional insulators such as porous concrete and mineral wools.^[114]

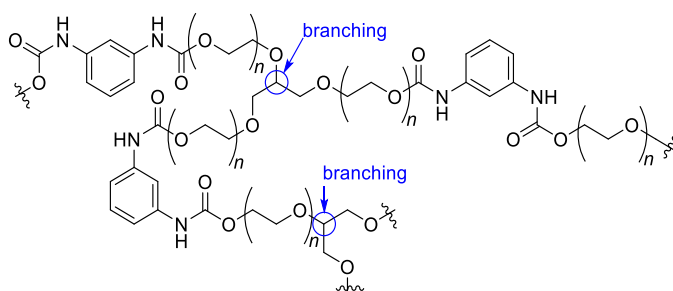


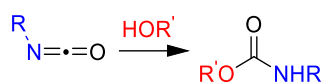
Figure 11. The represented chemical structure of polyurethanes. The branching ether centers build 3D structure and it is the source of their cushioning characteristic.

1.3.3 Synthetic methods for organic carbamates

Efficient and practical methods of carbamate syntheses have been developed,^[111] particularly in order to avoid the use of highly toxic phosgene.^[115]

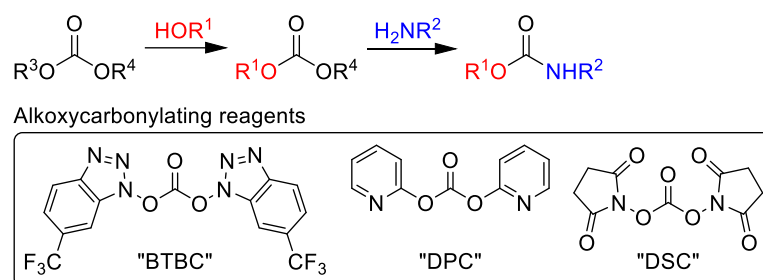
The formation of organic carbamates from isocyanates is a fundamental methodology in polyurethane industries (**Scheme 27**).^[116] The synthetic limitations and toxicity issues of isocyanates, however, are associated with the use of phosgene, which is a common route to obtain isocyanates. To solve these problems, phosgene-free synthetic methods for isocyanates have been developed.^[117–119]

Although the Bhopal accident attracted a widespread attention to the risks of isocyanates,^[120] their acute toxicity is generally low.^[121] The exposure to isocyanates and according injuries are related to the vapor pressures of the compounds.^[122] Low-molecular-weight isocyanates volatilize around room temperature, creating a vapor inhalation hazard.² Conversely, isocyanates with high molecular weight do not readily cause health impact. This excludes inhalation hazards in spraying applications, where they may be aerosolized or heated in the work environment.^[123]



Scheme 27. Synthesis of organic carbamates from alcohols and isocyanates.

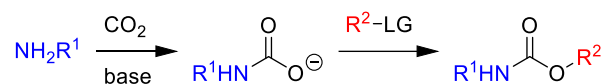
Another low-cost and benign alternative to phosgene is reactive organic carbonates (**Scheme 28**).^[124–126] They first react with an alcohol to give mixed carbonates, then react with an amine to afford the targeted organic carbamates. These methods show very broad scopes and are often used for the synthesis of complex organic carbamates in drug design.^[111]



Scheme 28. The synthesis of organic carbamates by alkoxy-carbonylating reagents. BTBC=1,1-bis[6-(trifluoromethyl)benzotriazolyl]carbonate, DPC=di(2-pyridyl) carbonate, DSC=N,N'-disuccinimidylcarbonate.

² Methyl isocyanate, the cause of the Bhopal accident, has a boiling point of 39 °C.

A new generation of organic carbamate syntheses uses CO₂, where an amine reacts with CO₂ to generate a carbamate anion, followed by a reaction with an electrophile (**Scheme 29**). A variety of methods have been investigated such as the use of solid-support reagents,^[127] supercritical CO₂^[128] and the addition of activators.^[129]



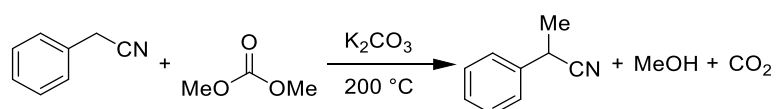
Scheme 29. A CO₂-utilizing synthesis of organic carbamates.

1.4 Organic carbonates

Organic carbonates will be employed as electrophiles in Chapter 2.

1.4.1 The use of organic carbonates

The use of organic carbonates as electrophilic alkylating reagents has been studied extensively since the 1990s because their environmental friendliness became widely recognized (**Scheme 30**).^[130]

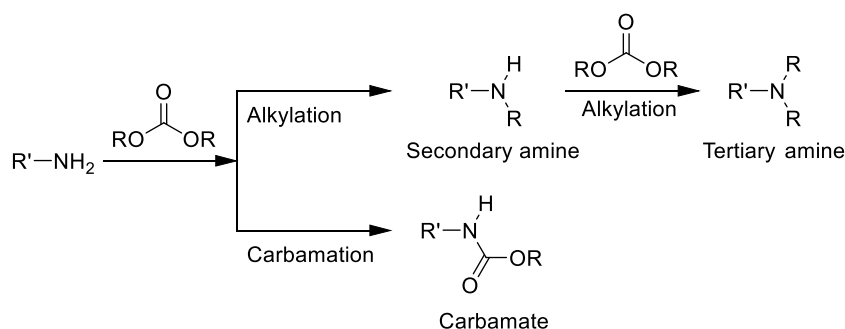


Scheme 30. A reaction of an organic carbonate as an electrophile.^[131]

Alkylation reactions are one of the most popular organic reactions,^[132] but the influence of conventional reagents such as alkyl halides and alkyl sulfonates on the environment and on human health was concerned. In this context, the use of organic carbonates has drawn the widespread attention of chemists, because of their low toxicity and easy degradability.^[133] Additionally, organic carbonates possess the reactivity features which make them attractive for general synthetic applications.^[130,133–136] Particularly regarding dimethyl carbonate (DMC), the synergy between its non-toxicity, good biodegradability, and clean industrial syntheses^[133] make it an appealing alternative to conventional methylating reagents.^[132,137,138]

1.4.2 Reactions of organic carbonates and amines

Amines are often used as nucleophiles for reactions with organic carbonates. Since primary amines and dialkyl carbonates can produce different products (**Scheme 31**), the reactions are mainly categorized into 3 groups by the target product – carbamates, secondary amines and tertiary amines.



Scheme 31. Possible products from an amine and a dialkyl carbonate.

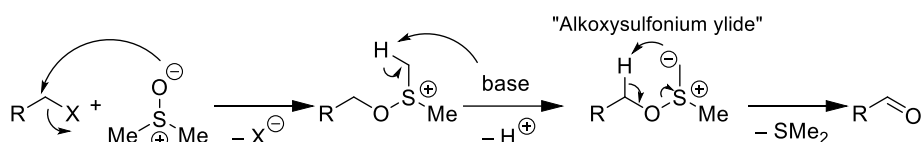
For carbamate syntheses, zinc catalysts such as $\text{Zn}(\text{OAc})_2$ and ZnCO_3 often show high conversions and selectivities,^[139,140] while a $\text{Sc}(\text{OTf})_3$ -catalyzed carbamation at ambient temperature was reported recently.^[141] The reaction control towards secondary amines is very important since a further alkylation produces tertiary amines. Nevertheless, good yields have been reported by using catalysts such as ZrOCl_2 and several zeolites.^[142–144] In the research for dialkylation, acidic catalysts such as tertiary ammonium salts and aluminium compounds as well as transition metals showed excellent performance.^[117,145,146]

1.5 DMSO-based oxidations

DMSO-based oxidations will be described in Chapter 4 and 5.

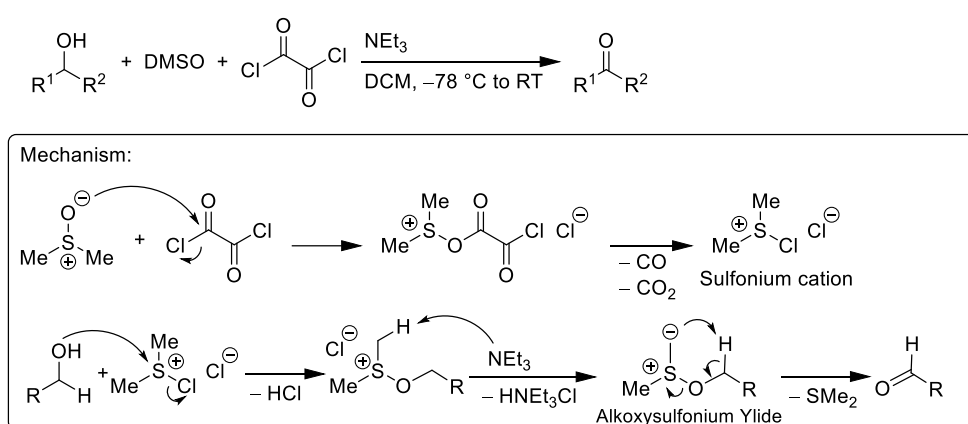
1.5.1 The Kornblum oxidation and the Swern oxidation

DMSO is used for many chemical reactions as an oxidant.^[147] The first DMSO-based oxidation is supposedly the Kornblum oxidation (**Scheme 32**).^[148,149] In this reaction, DMSO substitutes the leaving group of the substrate, followed by deprotonation at the α -position of the sulfonium cation to generate the corresponding alkoxy-sulfonium ylide. This species transfers the α -proton of the ether to the ylide and produces aldehydes or ketones.



Scheme 32. The reaction mechanism of the Kornblum oxidation.

The Swern oxidation is one of the first mild oxidations of primary alcohols to aldehydes (**Scheme 33**).^[73,150] Oxalyl chloride activates DMSO to generate a reactive sulfonium cation. The reaction of this sulfonium cation with an alcohol leads to the alkoxysulfonium ylide in basic conditions, which yields the corresponding aldehyde.



Scheme 33. The Swern oxidation and its mechanism.

The Swern oxidation was developed after examining many other activators (**Figure 12**). The first approach was by Pfitzner and Moffatt in 1963, where a carbodiimide was employed to activate DMSO.^[151] After acetic anhydride, phosphorus pentoxide (P₄O₁₀), sulfur trioxide pyridine complex and trifluoroacetic anhydride,^[152–155] oxalyl chloride was found to be very efficient for this transformation by Swern^{[156],3,[157,158]} and this protocol is the most used procedure nowadays.

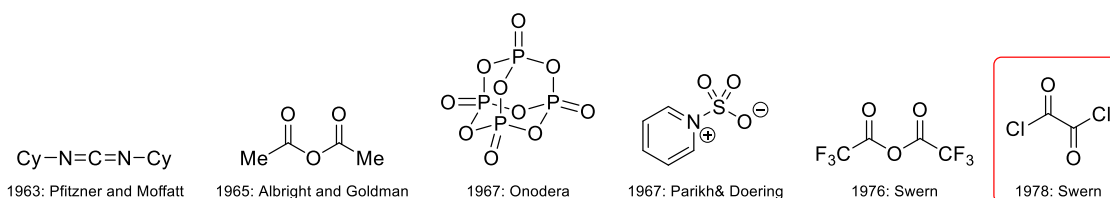


Figure 12. Activators for DMSO-based oxidation of alcohols. Cy=cyclohexyl group.

³ Swern and Albright screened activators including (sulfonyl)acid halide/anhydride, cyanuric chloride, phosphine(oxide) trihalides, thionyl chloride. Some of them were reinvestigated later.

Even after the development of the Swern oxidation, alternative activators were examined to replace oxalyl chloride, in order to carry out the oxidations at ambient temperature^[159,160] or to avoid side reactions by the Pummerer rearrangement.^[161–163] DMSO-based oxidation of alcohols using phosphorus compounds,^[161–164] carbon-based activators,^[159,165] silyl chlorides^[166,167] have been developed (**Figure 13**). Recently, Burgess reagent was employed to achieve a simple and efficient oxidation at ambient temperature.^[160]

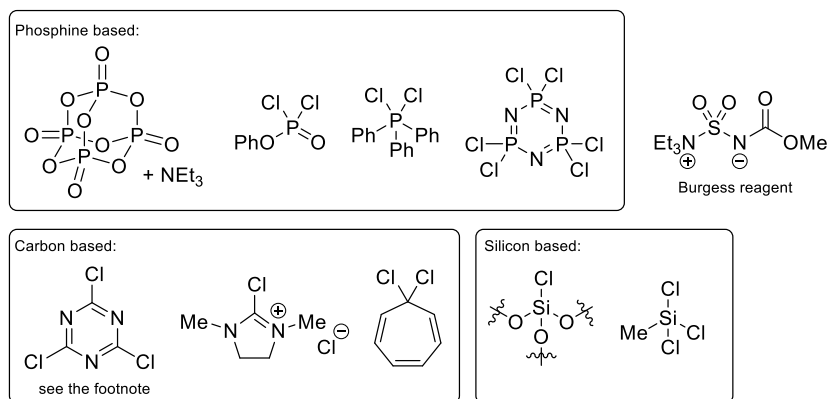
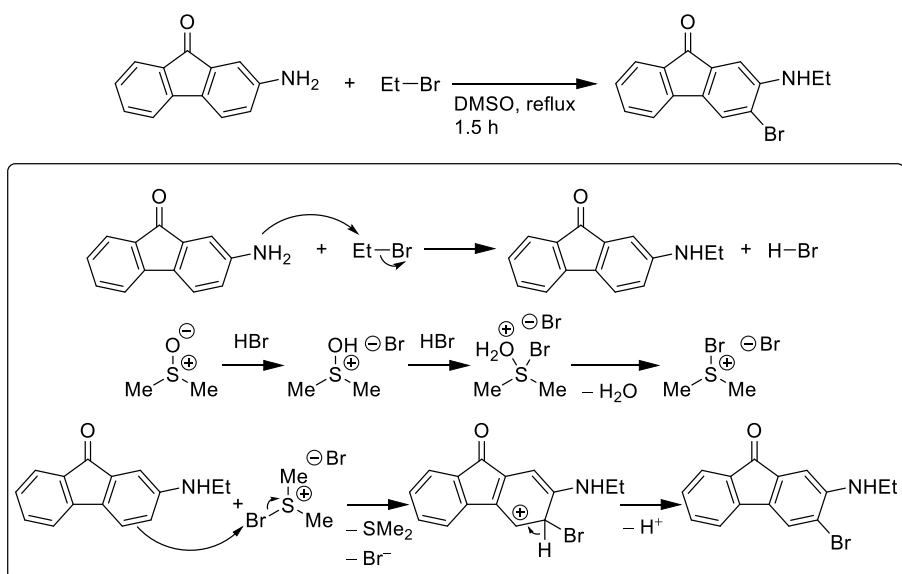


Figure 13. New activators of DMSO for alcohol oxidations.

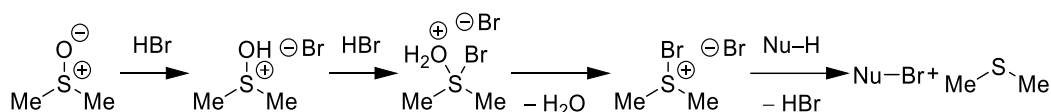
1.5.2 DMSO-based aromatic oxidation

DMSO-based aromatic oxidations were reported earlier than oxidations of alcohols, when an oxidative bromination was reported in 1956 by Fletcher (**Scheme 34**).^[168] He mixed an aromatic amine and ethyl bromide in DMSO, and unexpectedly found the brominated compound. Decades later, it was revealed that HBr generated *in situ* activates DMSO.^[169]



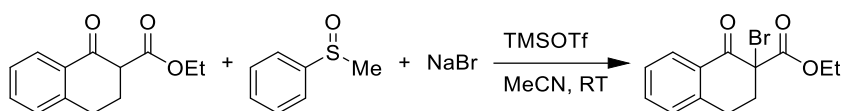
Scheme 34. DMSO-based oxidative bromination found by Fletcher.^[168]

Following the Fletcher's report, a variety of DMSO-based oxidative brominations have been developed.^[170–176] Among them, the combination of aqueous HBr and DMSO became the most popular system (**Scheme 76**),^[169,177–182] because aqueous HBr is the cheapest bromide source.



Scheme 35. General mechanism of oxidative brominations in the HBr/DMSO system.^[181]

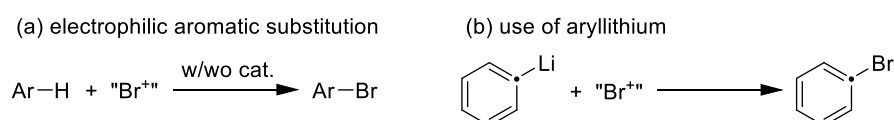
Although metal bromides are also cheap bromide sources, the combination of sulfoxide and metal bromide has been rarely reported.^[183–185] One of a few examples is described in **Scheme 36**, where a β -ketoester was brominated by using sulfoxides as oxidants.^[185] TMSOTf as a DMSO-activator and NaBr as a bromide source were used to achieve this oxidative bromination reaction.



Scheme 36. An oxidative bromination of dicarbonyl compounds with sulfoxides as oxidants.^[185]

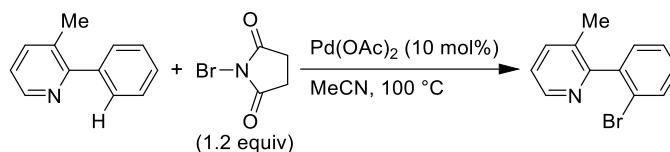
1.5.3 General methods of aromatic brominations

The most popular method for preparing aryl bromides is electrophilic aromatic substitution of electron-rich arenes (**Scheme 37**) by using electrophilic brominating reagents such as molecular bromine and *N*-bromosuccinimide (NBS).^[186] A range of Lewis-acid catalysts have been studied and even unactivated arenes can be brominated.^[187] For example, benzene is brominated by molecular bromine at ambient temperature in the presence of FeBr₃.^[188] Another methodology is the use of organometallic species, for example, phenyl lithium. They react very fast with electrophilic brominating reagents, and the lithiated position is selectively brominated.^[186]



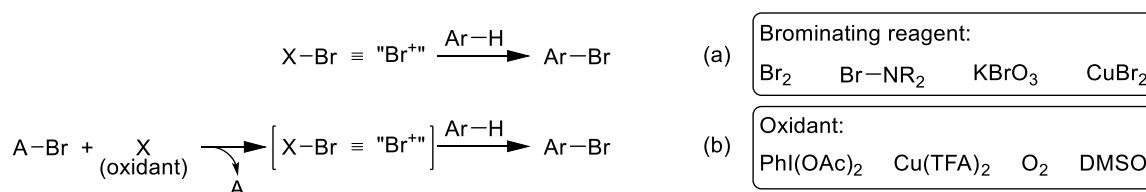
Scheme 37. Types of electrophilic bromination. (a) Electrophilic aromatic substitution where catalysts are effective for unactivated arenes. (b) The reaction of organometallic species and electrophilic brominating reagents.

Also by using electrophilic brominating reagents, transition metal-catalyzed C–H activations have been applied for bromination (**Scheme 38**).^[189] It is believed that organopalladium species are oxidized by oxidative brominating reagents to generate Pd(IV)–Br species, followed by reductive elimination to afford the corresponding aryl bromide.



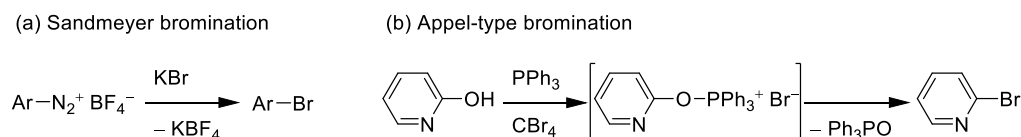
Scheme 38. An aromatic bromination *via* C–H activation.^[189]

There are two main variations to achieve these electrophilic brominating species (**Scheme 39**). One is the direct use of oxidative brominating reagents including molecular bromine. The other one is oxidative bromination, where inorganic bromides and oxidants generate electrophilic brominating intermediates *in situ*.^[190]



Scheme 39. (a) Direct bromination, (b) oxidative bromination and the used reagents and oxidants.

On the other hand, nucleophilic brominations of arenes have been utilized to a lesser extent than electrophilic brominations. For example, the Sandmeyer reaction^[191] and Appel-type reactions^[192] are known (**Scheme 40**), but they need very reactive electrophiles due to the low nucleophilicity of bromide. Although the reactions with nucleophilic bromide sources have been reported recently, the majority of them use additional oxidants, such as H₂O₂,^[193] oxone^[194] and hypervalent iodine reagents.^[195] Thus, they belong to oxidative bromination described above.



Scheme 40. Nucleophilic aromatic brominations. (a) The Sandmeyer reaction^[191] (b) An Appel-type reaction.^[192]

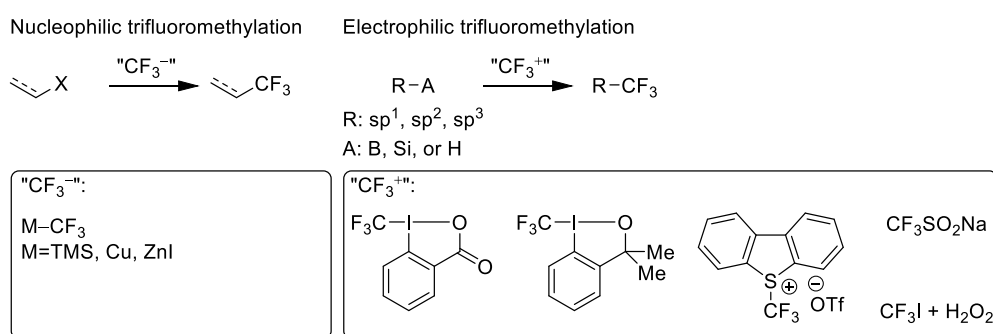
1.6 Trifluoromethylation reactions

Trifluoromethylation reactions will be described in Chapter 5 and 6.

1.6.1 The use and synthesis of CF₃-containing compounds

CF₃-containing compounds have drawn the attention in the field of organic and organometallic chemistry in the last decade, showing a surge in the developments of trifluoromethylation reactions.^[196,197] At the same time, an increasing number of CF₃-containing drugs have been developed and approved.^[198] According to the literature,^[199] the introduction of the trifluoromethyl group may have an influence on altered conformation, induction effect, modified lipophilicities and metabolic stabilities of drug molecules.

Synthetic procedures of trifluoromethylation reactions have been developed with both nucleophilic and electrophilic trifluoromethylating reagents (**Scheme 41**). Early developments of reactive trifluoromethylating reagents, for example, (trifluoromethyl)trimethylsilane (Me₃SiCF₃),^[200] (trifluoromethyl)dibenzothio-, -seleno- and -tellurophenium salts^[201–203] and hypervalent iodine reagents,^[204] facilitated the development of trifluoromethylation reactions.



Scheme 41. Nucleophilic and electrophilic trifluoromethylations and commonly used reagents.

Particularly, our group is interested in trifluoromethylation reactions and has contributed to their development.^[205] In fact, our hypervalent iodine(III) trifluoromethylating reagents are ones of the most accepted trifluoromethylating reagents (**Figure 14**),^[204,206] which have been employed in a notable part of the reported trifluoromethylation reactions.^[205]

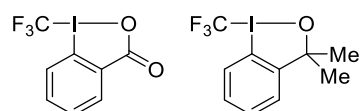
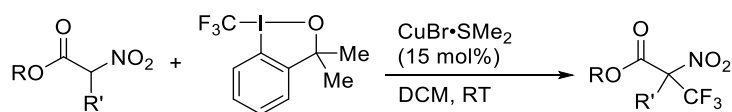


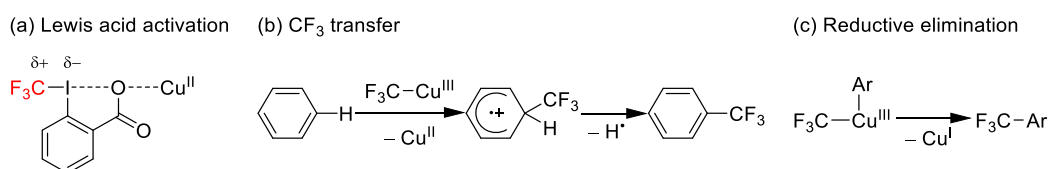
Figure 14. The structure of so-called “Togni’s reagents”.

1.6.2 Copper-catalyzed trifluoromethylations with the hypervalent iodine reagents

The first copper-catalyzed trifluoromethylation reaction with our reagent was reported in 2007 (**Scheme 42**).^[207] Now it is generally recognized that copper compounds often catalyze trifluoromethylation reactions.^[208–211] Many mechanistic studies about our reagents have been done and different suggestions have been made (**Scheme 43**). For example, Cu(II) species activating trifluoromethylating reagents as Lewis acids, Cu(III)–CF₃ species transferring the CF₃ group and reductive elimination from Ar–Cu(III)–CF₃ species has been invoked.^[212–216]



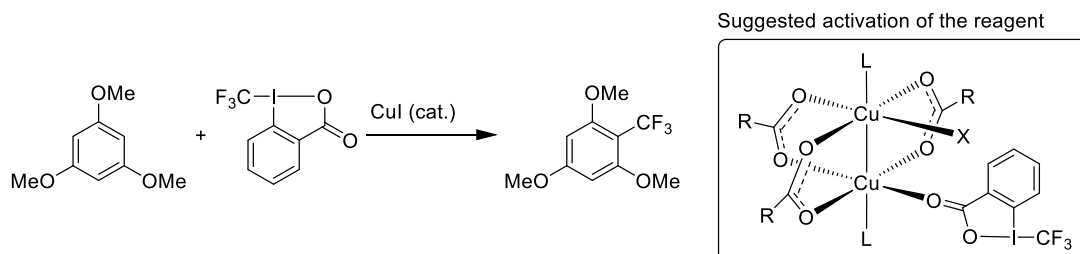
Scheme 42. The first copper-catalyzed trifluoromethylating reaction.^[207]



Scheme 43. Different types of trifluoromethylating reaction mechanisms. (a) Cu(II) Lewis acid-activation of a trifluoromethylating reagent. (b) CF₃ group transfer of Cu(III)–CF₃ species to an arene. (c) Reductive elimination from Ar–Cu(III)–CF₃ species.

1.6.3 Metal–metal bond-containing complexes

In the study of trifluoromethylation reactions, dinuclear copper(II) complexes were indicated to be an active catalyst (**Scheme 44**). Such dinuclear complexes and, more in general, polynuclear complexes are obviously not limited to copper species, but are known for many other transition metals.^[217]



Scheme 44. Copper-catalyzed trifluoromethylation of an arene (Chapter 6). Dinuclear copper complexes are proposed to activate the trifluoromethylating reagent.

Evidence of the first metal–metal bond was confirmed in the dinuclear carbonyls $\text{Mn}_2(\text{CO})_{10}$ and $\text{Re}_2(\text{CO})_{10}$ in 1957.^[218] Besides, extensive studies on rhenium(III) halides have been published in the 1960s.^[219] The studies of these Re(III) complexes by MO analysis revealed a quadruple Re–Re bond (the bond distance is 2.24 Å) in the $[\text{Re}_2\text{Cl}_8]^{2-}$ anion^[220] and a Re_3 triangle with three Re–Re double bonds (the bond distance is 2.47 Å) in the $[\text{Re}_3\text{Cl}_{12}]^{3-}$ anion.^[221–223] These Re–Re distances are much shorter than those in metallic rhenium (2.75 Å) corroborating the higher bond orders postulated by the MO analysis. These works present the first explicit recognition that direct metal–metal bonds can be very strong and can play a crucial role in the formation of polynuclear transition-metal complexes.^[217] Since then, polynuclear complexes based on most of the transition-elements have been prepared.^[224]

The structure of polynuclear complexes depends on the M–M interaction, the nature of the ligands (mono- or polydentate) and the type of coordination (σ or π). The main types of dinuclear complexes are depicted in **Figure 15**,^[225] where the precise geometry, the number of ligands and the formal bond order depend on the complex. In the simplest form, the dimetal core is bonded directly by the M–M bond as drawn in **Figure 15a**, typified by the $[\text{Me}_4\text{Cr–CrMe}_4]^{2-}$ anion. Bidentate ligands such as the acetate anion may bridge the dimetal core to facilitate the formation of polynuclear structures (**Figure 15b**). Some monodentate ligands also can connect the dimetal core (**Figure 15c**). Ligands like CO, carbenes, hydride and halides are often seen in this type of complexes. Since such M–L–M structures stabilize the complex by three-center two-electron bonding, M–M bond is not strictly necessary to form stable complexes (**Figure 15d**).

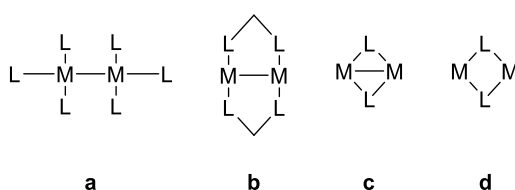


Figure 15. Dinuclear complexes of various types, categorized by their structure.

A key parameter for describing M–M interactions is the M–M distances, which is essentially related to their formal bond order. In fact, the shortest known M–M distance for a stable compound is 1.7293(12) Å with a formal bond order of five in a dichromium(II) complex with a guanidinate ligand.^[226,227] However, ligands also have an influence on the M–M distance. For example, the design of the guanidinate ligand was optimized towards obtaining this very short Cr–Cr distance.

In comparison, another dichromium(II) complex $[\text{Cr}_2(\text{OAc})_4(\text{H}_2\text{O})_2]$ has a bond distance of 2.362(1) Å.^[228] Furthermore, the bond distance also depends on the type of metal due to its own electron configuration and orbital energies. Although a selection of M–M bond distance of dimetal carboxylates is presented in **Table 1** for comparison, more examples and discussions of M–M interactions can be found in the literature.^[217,224,225]

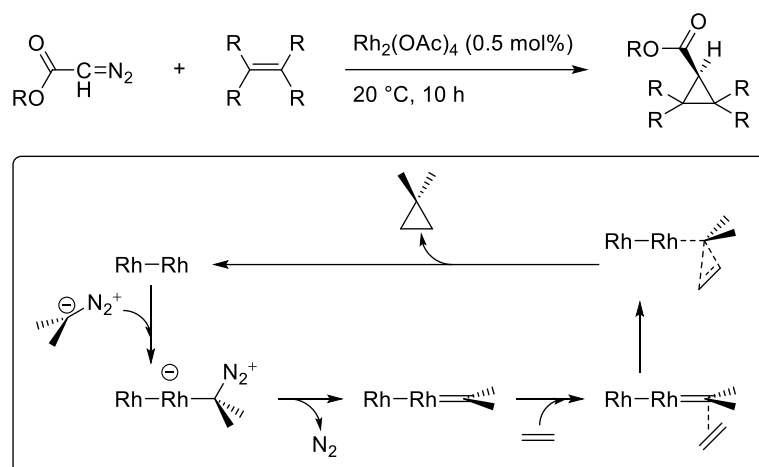
Table 1. M–M bond distance of $\text{M}_2(\text{II,II})$ tetracarboxylates (left column) and similar carboxylato complexes (right column).

$\text{M}_2(\text{II,II})$ tetracarboxylates		Similar carboxylato complexes	
Compound	(Å)	Compound	(Å)
$[\text{Cr}_2(\text{OAc})_4(\text{H}_2\text{O})_2]$ ^[228]	2.362(1)	$[\text{Nb}_2\text{Cl}_2(\text{THT})(\text{OAc})_5]^-$ ^{[c] [229]}	2.764(1)
$[\text{Mn}_2(\text{OPiv})_4\text{L}_2]$ ^{[a] [230]}	3.059	$[\text{Tc}_2(\text{OPiv})_4\text{Cl}_2]$ ^[231]	2.1758(3)
$[\text{Fe}_2(\text{OPiv})_4\text{L}_2]$ ^{[b] [232]}	2.866(9)	$[\text{Pd}(\text{OAc})_4(\text{DAF})]$ ^{[d] [233]}	3.301
$[\text{Co}_2(\text{OBz})_4(\text{quin})_2]$ ^[234]	2.83	$[\text{Ag}_2(\text{OAc})_2]$ ^[235]	2.806
$[\text{Ni}_2(\text{OAc})_4(\text{DMSO})_2]$ ^[236]	2.610	$[\text{W}_2(\text{OPiv})_6]$ ^[237]	2.2922(8)
$[\text{Cu}_2(\text{OAc})_4 \cdot (\text{H}_2\text{O})_2]$ ^[238]	2.64	$[\text{Re}_2(\text{OAc})_4\text{Cl}_2]$ ^[239]	2.2240(5)
$[\text{Mo}_2(\text{OAc})_4]$ ^[240]	2.0934(8)	$[\text{Os}_2(\text{OAc})_2(\text{CO})_6]$ ^{[e] [241]}	2.731
$[\text{Ru}_2(\text{OAc})_4(\text{H}_2\text{O})_2]$ ^[242]	2.262(3)	$[\text{Ir}_2(\text{OAc})_2\text{Cl}_2(\text{CO})_2(\text{NCMe})_2]$ ^{[f] [243]}	2.569(1)
$[\text{Rh}_2(\text{OAc})_4(\text{H}_2\text{O})_2]$ ^[228]	2.3855(5)	$[\text{Pt}_2(\text{CH}_2\text{COO})_2(\text{OAc})_2\text{Cl}_2]^{2-}$ ^{[g] [244]}	2.451(1)
$[\text{W}_2(\text{OPiv})_4(\text{PPh}_3)_2]$ ^[245]	2.218(1)		

Piv=Pivaloyl group, Bz=Benzoyl group, quin=Quinoline, THT=Tetrahydrothiophene, DAF=4,5-Diazafluoren-9-one. ^[a] L=2,6-(NH₂)₂-Py ^[b] L=2,3-Lutidine ^[c] Coordinated by two bidentate bridging acetates, monodentate bridging THT and acetate, two terminal chloride ions and two chelating acetates. ^[d] Coordinated by two bidentate bridging acetates and bidentate bridging DAF and two terminal monodentate acetates. ^[e] Coordinated by two bidentate bridging acetates, four equatorial carbonyl groups and two axial carbonyl groups. ^[f] Coordinated by two bidentate bridging acetates, two equatorial chlorides, two equatorial carbonyl groups and two terminal MeCN. ^[g] Coordinated by two bidentate bridging acetates, two bidentate bridging “CH₂COO²⁻” ligands and two terminal chlorides.

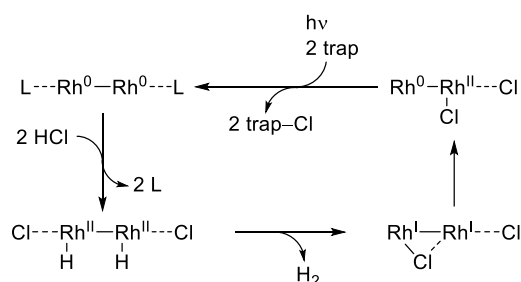
In catalysis, Rh₂ complexes display a long standing importance.^[224] Accordingly, synthetic and mechanistic investigations have revealed the involvement of intact dinuclear complexes and the effect of Rh–Rh bonds in catalysis.^[224] The first reported reaction catalyzed by M–M bond-containing compounds is the Rh₂(OAc)₄-catalyzed reactions of organic diazo compounds with alcohols^[246] or olefins^[247] yielding ethers or cyclopropanes, respectively (**Scheme 45**). Activation of diazo compounds is proposed to be initiated by coordination of the diazo compound to the Rh₂ core, followed by N₂ extrusion to generate a Rh₂ carbenoid.^[248] The three-centers-four-electron

bond of this Rh₂ carbenoid is weak, and thus, the terminal Rh–C groups are very reactive.^[249] Such a Rh₂ carbenoid intermediate has been spectroscopically characterized in form of a metastable derivative.^[250]



Scheme 45. Rh₂(OAc)₄-catalyzed cyclopropanation of alkenes with alkyl diazoacetates^[247] and its proposed mechanism.^[248]

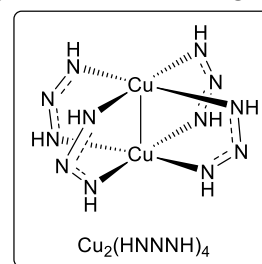
Another example using dirhodium complexes is the photocatalytic splitting of HX (X = Cl, Br) to H₂.^[251] This type of research stems from a report in 1977 where Rh(I) dimers reduce HCl to H₂ upon irradiation (λ=546 nm).^[252] Mixed valent complexes Rh(0)–Rh(II) are proposed to be an important intermediate in the reaction mechanism (**Scheme 46**).^[253,254]



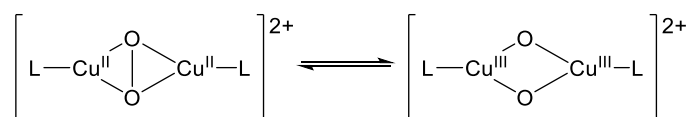
Scheme 46. The photocycle for H₂ generation by a Rh₂ photocatalyst.^[253] In the scheme, “trap” is usually an external reductant.

Dinuclear copper complexes are mostly known with the copper centers in the Cu(I) oxidation state, as well as some species with mixed valent Cu(I)–Cu(II) cores. On the other hand, fewer Cu(II) dimers have been studied.^[225] Crystal structures of Cu₂(II) complexes with bridging ligands such as carboxylates,^[238] amidinates,^[255,256] triazinates^[257,258] and pyridonates^[259–261] have been reported. The Cu–Cu interaction in Cu(II) dimers has been discussed for a long time. In the early 1960s, σ bond^[262] and δ bond^[263] were independently proposed to explain the Cu–Cu interaction, based on

theoretical calculations, the visible and electron-spin-resonance spectroscopies. Later in 1965, however, a study on the nuclear quadrupole splitting of ^{63}Cu in the single-crystal dimer strongly supported the existence of δ Cu–Cu bond.^[264,265] Furthermore, a DFT study on Cu–Cu bonding in the model paddlewheel dicopper complex $\text{Cu}_2(\text{HNNNH})_4$ invoked strong antiferromagnetic coupling mediated by the bridging ligands and disagree with Cu–Cu bonding.^[266] Still today, experimental and theoretical studies are discussed whether the Cu–Cu interaction is assigned to a δ bond or the antiferromagnetic coupling mechanism through a ligand bridge.^[267,268]



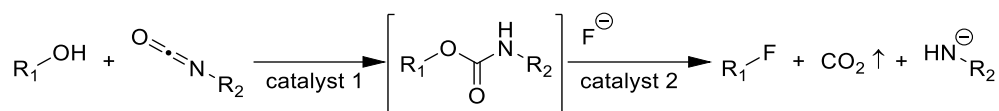
The involvement of dicopper complexes in catalysis has been proven in a few reports, including Lewis-acid activation of epoxides^[269] and aerobic oxidation reactions.^[270–272] For oxidation reactions, Cu(I) species react with O_2 to form Cu– O_2 –Cu species (**Scheme 47**). The resultant Cu(III) dinuclear complexes oxidize phenols to produce the corresponding catechols.^[273] This motif is commonly found in the active sites of several metalloproteins.^[274]



Scheme 47. Redox equilibrium of Cu_2O_2 species.

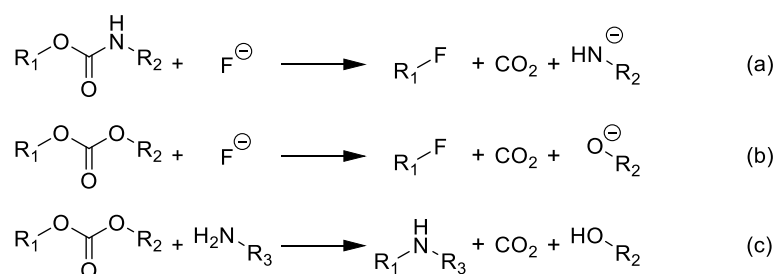
1.7 The aim of this thesis

First, the study towards the development of a new deoxyfluorination is discussed. We selected to investigate the methodology to activate hydroxy group as an organic carbamate. The idea is described in **Scheme 48**. A carbamate is formed *in situ* from an alcohol and an isocyanate. The carbamate is attacked by fluoride to give the corresponding alkyl fluoride,^[101,102] where the extrusion of CO_2 may drive the reaction forward. Accordingly, the development of the catalytic system both for the carbamate formation and for the fluorination is recognized as central aspects of this project.

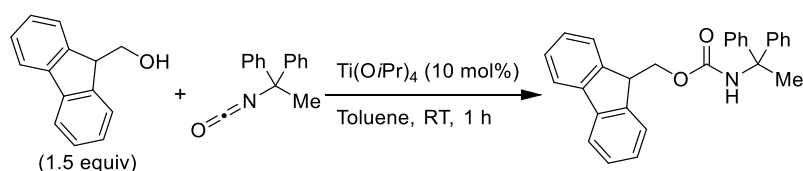


Scheme 48. The target reaction: fluorination of alcohols *via* carbamation.

The idea shown in **Scheme 48** was broken down into several steps. Before one-pot procedures are investigated, the fluorination of isolated carbamates should be examined (**Scheme 49a**). The conversions of an alcohol to a carbamate have been well investigated and several catalysts such as Sn, Ti, Sm and Mo compounds have been found effective (**Scheme 50**).^[275–277]



Scheme 49. Project breakdown. (a) Fluorination of isolated organic carbamates. (b) Fluorination of organic carbonates. (c) Amination of organic carbonates.

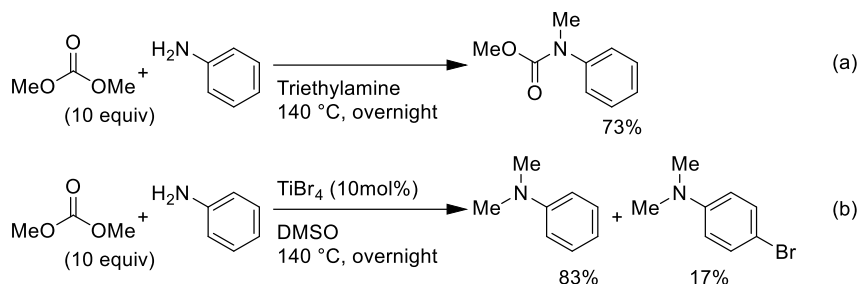


Scheme 50. A carbamate formation from alcohols and isocyanates.^[277]

In order to facilitate the investigation, organic carbamates are replaced with organic carbonates that are more reactive nucleophiles (**Scheme 49b**).^[132,137,138] The nucleophilicity of fluoride is known to be relatively low.^[65–68] Amines therefore are employed as model nucleophiles (**Scheme 49c**),^[278] so that the investigation of the activation of organic carbonates is in the focus. Accordingly, the reactions of organic carbonates and amines are the topic of Chapter 2.

During the study of the reaction between organic carbonates and amines, interesting side reactions were found when the reaction was conducted in triethylamine or DMSO (**Scheme 51**). When triethylamine was used as a solvent, an *N,N*-disubstituted carbamate was produced from an

organic carbonate and an amine. This base-catalyzed transformation will be described in Chapter 3. On the other hand, the combination of a metal bromide and DMSO produced a brominated compound (**Scheme 51b**). DMSO-based reactions were found useful and interesting, and thus, the investigation of this reaction is to be presented in Chapter 4.



Scheme 51. Side reactions found in the reaction of dimethyl carbonate and aniline, (a) in triethylamine (b) in DMSO.

The study of sulfoxide-based oxidative bromination (Chapter 4) is to be extended to other functionalizations. In particular, fluorinations and trifluoromethylations are the main targeted functionalizations. The goal of Chapter 5 is to evaluate the potential of this type of reactions.

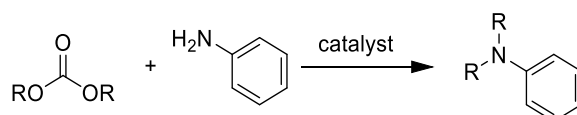
Finally, mechanistic studies of a trifluoromethylation reaction are discussed in Chapter 6. The purpose of this part is the determination of reactive intermediates in a model trifluoromethylation reaction, in order to possibly obtain ideas for the development of a new DMSO-based trifluoromethylation reaction.

Chapter 2

Acid-Activation of Organic Carbonates

2.1 Introduction

The alkylation reactions of amines with organic carbonates were investigated and are reported herein (**Scheme 52**). The purpose of this project was to investigate the activation of organic carbonates by catalysts with amines as model nucleophiles (see Section 1.7 for details).



Scheme 52. Alkylation reactions of aniline with organic carbonates which are targeted in this chapter.

2.1.1 General motivation for use of organic carbonates

Organic carbonates are regarded as environmentally friendly chemicals for various industrial applications because of their unique profile, such as low toxicity and high biodegradability.^[130,133–136] In this context, alkylation reactions using organic carbonates as alternatives to conventional alkylating reagents have attracted the attention of researchers (**Figure 16**).^[137] Section 1.4.1 describes details of the advantages of organic carbonates.

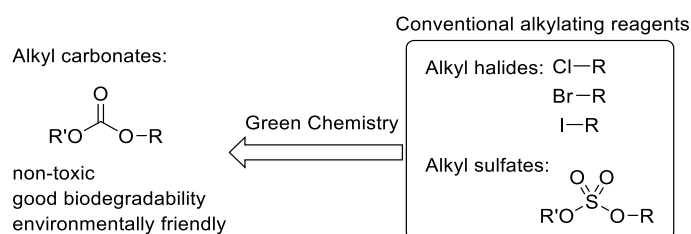
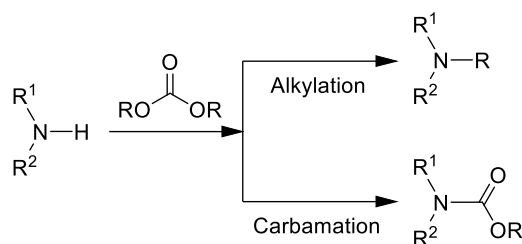


Figure 16. Substituting conventional alkylating reagents by organic carbonates.

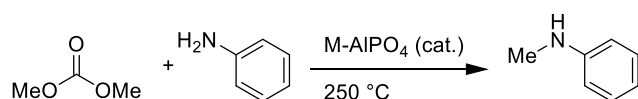
2.1.2 Known catalysts for alkylation of amines by organic carbonates

Alkylation reactions of amines with organic carbonates have been investigated in depth.^[145,279–281] However, the majority of the reported procedures require harsh conditions, for example, 345 °C and 10 MPa,^[282] which may be difficult to apply to delicate compounds. Moreover, chemoselectivity must be controlled well, because amines and organic carbonates may also produce carbamates (**Scheme 53**).^[283] These problems demand the development of milder catalytic systems for alkylation of amines by organic carbonates with high efficiency and chemoselectivity.^[134] To



Scheme 53. Alkylation or carbamation by the reaction of amines and organic carbonates.

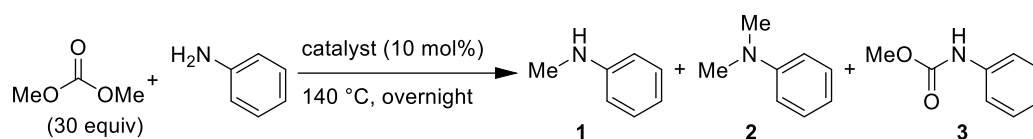
solve these problems, methylation reactions with various kinds of metal catalysts have been reported.^[142,146,284] For example, aniline is methylated with dimethyl carbonate (DMC) in the presence of Lewis acids on AlPO_4 supports (M- AlPO_4) (**Scheme 54**).^[284] While the report covers a variety of AlPO_4 -supported Lewis acids, titanium and vanadium catalysts stood out by showing an excellent selectivity towards alkylation. Therefore, we launched our study on methylation of aniline with DMC focusing on titanium and vanadium compounds as Lewis acids.



Scheme 54. Lewis acid-catalyzed methylation of aniline with DMC.^[284]

2.2 Preliminary investigations

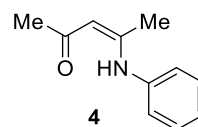
Lewis acid catalysts were screened for methylation of aniline using DMC as an electrophile and as a solvent (**Table 2**). In the presence of $\text{Ti}(\text{OEt})_4$, aniline was fully converted but carbamate **3** was produced (entry 1). Vanadium(III) acetylacetonate ($\text{V}(\text{acac})_3$) also showed a good conversion of aniline, but the methylated products were detected only in trace amounts (entry 2). In the same reaction mixture, compound **4** was detected, which should be produced by a reaction of aniline and acetylacetone. Although many other Lewis acids did not promote the reaction (entries 3–6), titanium bromide (TiBr_4) produced *N,N*-dimethylaniline (**2**) in high yield (entry 7). Since it was the only catalyst that afforded product **2** with a high conversion, the project focused on this catalyst for further investigation.

Table 2. Screening of Lewis acid catalysts for methylation of aniline by DMC.^[a]

entry	Catalyst	Products (yields) ^[b]
1	Ti(OEt) ₄	3 (99%)
2	V(acac) ₃	1 (7%) ^[c]
3	NiCl ₂	3 (5%)
4	SiO ₂	1 (5%) and 3 (10%)
5	ZrF ₄	1 (3%)
6	VOSO ₄ ·5H ₂ O	1 (10%) and 2 (1%)
7	TiBr ₄	2 (81%)
8	none	1 (5%)

^[a] Reaction conditions: aniline (1.0 mmol), DMC (2.6 mL, 30 mmol), catalyst (0.1 mmol), 140 °C, overnight.

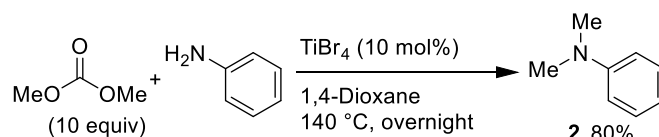
^[b] Determined by ¹H NMR with dibromomethane as the internal standard based on aniline. ^[c] Aniline seemed to react with acetylacetone to give compound **4** (15% yield).



2.3 Titanium bromide catalysis

2.3.1 TiBr₄-catalyzed methylation of aniline with DMC in 1,4-dioxane

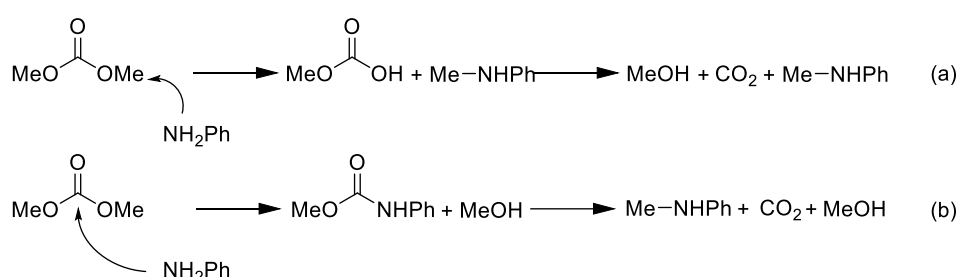
In order to use DMC as a reagent instead of a solvent, the choice of the solvent was examined. One criterion is the formation of homogenous solutions in the presence of TiBr₄, because coagulated catalysts would not be ideal due to their small surface area.^[285] Coordinating solvents should be a good choice to overcome this problem. Ethers such as 1,4-dioxane are known to coordinate to TiBr₄.^[286,287] Therefore, 1,4-dioxane was introduced as a solvent and the used amount of DMC was decreased from 30 equivalents to 10 equivalents with respect to aniline to yield product **2** in 80% yield (**Scheme 55**).



Scheme 55. The methylation reaction of aniline catalyzed by TiBr₄ in 1,4-dioxane. Reaction conditions: aniline (1.0 mmol), DMC (10 mmol), TiBr₄ (0.1 mmol), 1,4-dioxane (3 mL), 140 °C, overnight. The yield was determined by GC-FID with decane as the internal standard based on aniline.

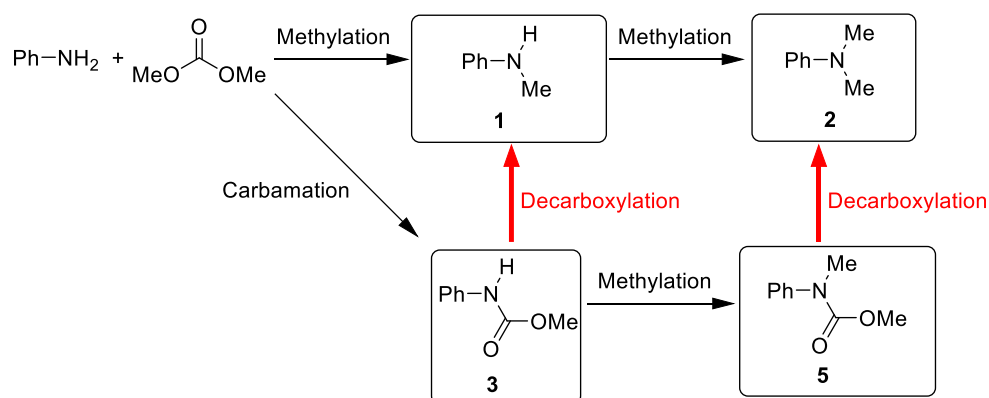
2.3.2 Examination of reaction pathways

There are two different possibilities to achieve methylation of aniline with DMC (**Scheme 56**).^[283] One is a nucleophilic attack by aniline on the methyl group to leave monomethyl carbonate, which is unstable and decomposes to CO₂ and MeOH (**Scheme 56a**). The other possibility is that the nucleophile attacks the carbonyl group to generate a carbamate as an intermediate, followed by decarboxylation giving the methylated product (**Scheme 56b**). Considering that nucleophilic fluorination is the ultimate purpose of this project (see Section 1.7), the nucleophilic substitution on the methyl group (**Scheme 56a**) should be the desired mechanism.



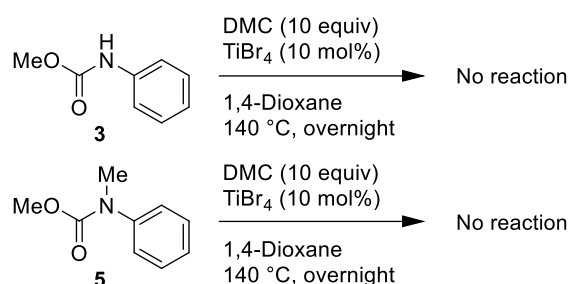
Scheme 56. Possible nucleophilic attacks of aniline onto DMC towards methylation. (a) Nucleophilic attack of aniline onto the methyl group of DMC. (b) Nucleophilic attack of aniline onto the carbonyl group of DMC.

Thus, the reaction pattern of the TiBr₄-catalyzed methylation of aniline described in **Scheme 56a** or **b** must be distinguished. Possible products and intermediates by the reaction of aniline and DMC are depicted in **Scheme 57**. Methylated product **1** can be obtained by direct methylation or carbamation-decarboxylation *via* carbamate **3**. Similarly, *N,N*-dimethylaniline (**2**) can be produced by direct methylation of monomethylaniline (**1**) or decarboxylation of carbamate **5**. If



Scheme 57. Possible products of the reaction of aniline and DMC.

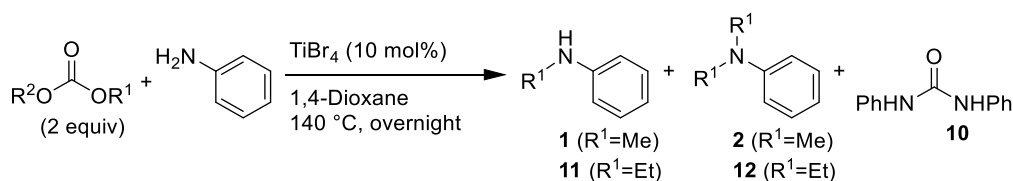
decarboxylation of carbamates occurs under reaction conditions (corresponding to **Scheme 56b**), carbamates **3** and **5** should produce anilines **1** and **2**, respectively. Thus, each carbamate was exposed to the reaction conditions in order to examine these possibilities (**Scheme 58**). Both carbamates **3** and **5** remained intact under the given conditions. This result disagrees with the carbamation-decarboxylation pathway, and therefore indicates that TiBr_4 catalyzes the direct nucleophilic attack onto the methyl group of DMC (**Scheme 56a**). Therefore, the research on this TiBr_4 -catalyzed methylation was judged to be on track towards fluorination as expected.



Scheme 58. Examination of the possible decarboxylation of carbamates. Reaction conditions: carbamate (1.0 mmol), DMC (10 mmol), TiBr_4 (0.1 mmol), 1,4-dioxane (3 mL), 140 °C, overnight. The reaction mixtures were analyzed by GC-FID.

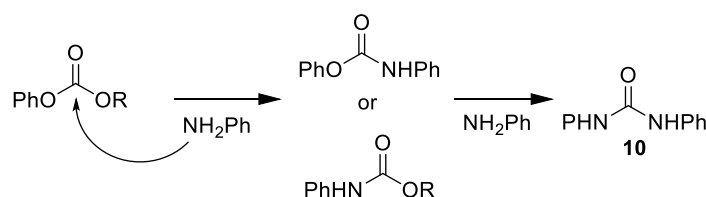
2.3.3 Use of other organic carbonates

To examine the effect of the substituents of organic carbonates, other organic carbonates were employed as electrophiles (**Table 3**). Diethyl carbonate (**6**) showed much lower reactivity than DMC (entries 1 and 2). When phenylcarbonates were used (entries 3–5), 1,3-diphenylurea (**10**) was produced. This indicates that the phenyl group promotes nucleophilic attacks onto the carbonyl center of organic carbonates instead of direct nucleophilic attacks on the alkyl group (**Scheme 59**). This characteristic of the electrophile suggests that aryl carbonates should be avoided in the design of organic carbonates for future experiments.

Table 3. Effect of substituents of organic carbonates on TiBr₄-catalyzed alkylation of aniline.^[a]

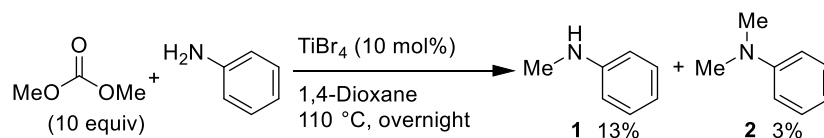
entry	Carbonate	R ¹	R ²	Yield ^[b]		
				Monoalkyl	Dialkyl	Urea 10
1	6	Et	Et	11 7%	0%	0%
2 ^[c]	6	Et	Et	11 36%	12 4%	0%
3	7	Me	Ph	1 25%	2 11%	24% ^[d]
4	8	Et	Ph	11 2%	0%	82% ^[d]
5	9	<i>n</i> C ₁₂ H ₂₅	Ph	0%	0%	92% ^[d]

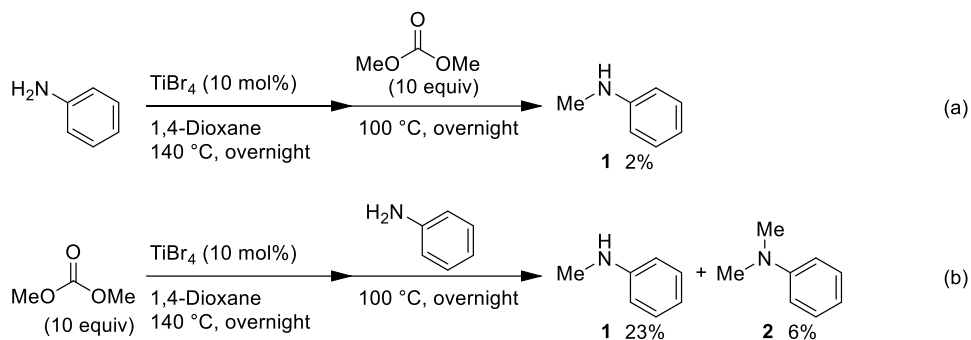
^[a] Reaction conditions: aniline (1.0 mmol), carbonate (2.0 mmol), TiBr₄ (0.1 mmol), 1,4-dioxane (3 mL), 140 °C, overnight. ^[b] Determined by GC-FID with decane as the internal standard based on aniline. ^[c] Diethyl carbonate was used as a solvent instead of 1,4-dioxane. ^[d] Calculated as the consumed aniline for **10**. For example, in entry 2, 1 mmol of aniline yielded 0.12 mmol of **10**.

**Scheme 59.** Assumed formation of urea **10** by the reactions of a phenylcarbonate and aniline.

2.3.4 Examination of the methylation reaction of aniline at lower temperature

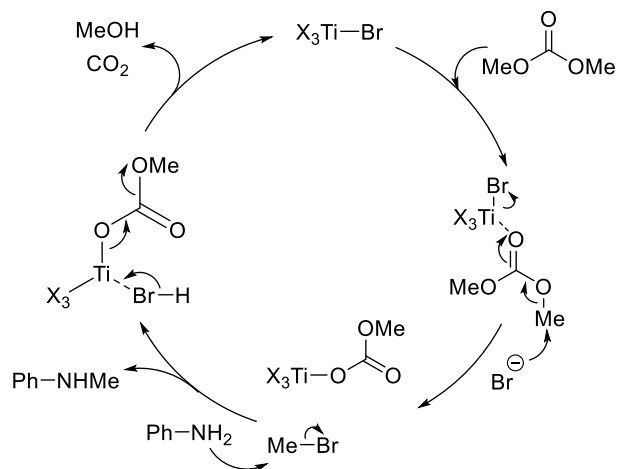
The reaction of aniline and DMC was carried out at 110 °C to evaluate the effect of the reaction temperature (**Scheme 60**). As a result, the yields of the products were very low. In order to identify the reaction step that requires a high activation energy, the reagents were added under different conditions (**Scheme 61**).

**Scheme 60.** Examination of the reaction of aniline and DMC at 110 °C. Reaction conditions: aniline (1.0 mmol), DMC (10 mmol), TiBr₄ (0.1 mmol), 1,4-dioxane (3 mL), 110 °C, overnight. The yields were determined by GC-FID with decane as the internal standard based on aniline.



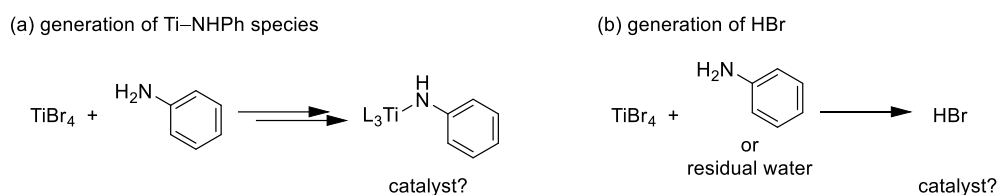
Scheme 61. Reaction of aniline and DMC at different temperature in each step. Reaction conditions (a): aniline (1.0 mmol), TiBr_4 (0.1 mmol), 1,4-dioxane (3 mL), 140 °C, overnight; then DMC (10 mmol), 100 °C, overnight. Reaction conditions (b): DMC (10 mmol), TiBr_4 (0.1 mmol), 1,4-dioxane (3 mL), 140 °C, overnight; then aniline (1.0 mmol), 100 °C, overnight. The yields were determined by GC-FID with decane as the internal standard based on aniline.

In the first experiment (**Scheme 61a**), aniline and TiBr_4 were heated at 140 °C overnight, and then DMC was added and heated at 100 °C. Only 2 % of product **1** was obtained from this reaction mixture. On the other hand, when DMC and TiBr_4 were heated at 140 °C before aniline was added and heated at 100 °C, alkylated products were detected in the amount that indicates a stoichiometric reaction with respect to the catalyst (**Scheme 61b**). These experiments seem to show that the reaction of TiBr_4 and DMC needs a temperature as high as 140 °C and possibly generates a reaction intermediate which in turn can react with aniline at 100 °C. Considering this activation of DMC by TiBr_4 , a possible reaction mechanism is described in **Scheme 62**. Ti–Br species activate DMC as Lewis acids, which bromide may attack on the methyl group. Methyl bromide is known to easily react with amines to produce methylated amines.^[288] To recover Ti–Br species, bromide should substitute the methyl carbonate group on the titanium carbonate species generating MeOH and CO_2 .



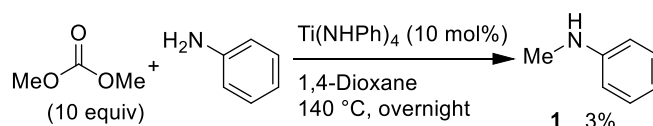
Scheme 62. A possible reaction mechanism for TiBr_4 -catalyzed methylation of aniline with DMC.

Although it is assumed that the generation of alkyl bromide is the key step of this reaction, a few experiments were carried out to exclude other possibilities (**Scheme 63**).

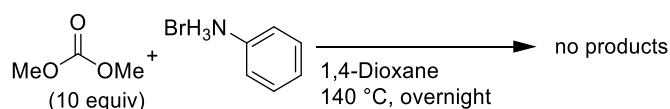


Scheme 63. Possible active catalysts generated in the reaction mixture. L = Br or NPh.

TiBr₄ and aniline may form titanium anilide species, whose catalytic activity was to be evaluated (**Scheme 63a**). Titanium tetrakis(anilide) (Ti(NHPh)₄) was employed as a catalyst, but only 3% of product **1** was obtained (**Scheme 64**). Another possibility is that TiBr₄ can generate HBr by the reaction with aniline or residual water in solvents (**Scheme 63b**). Thus, phenylammonium bromide (PhNH₃Br) was used as a substrate to test the involvement of HBr in the reaction. However, this experiment yielded no product (**Scheme 65**). Therefore, these two possibilities can be excluded for the TiBr₄-catalyzed methylation of aniline with DMC.



Scheme 64. Titanium tetrakis(anilide)-catalyzed reaction of DMC and aniline. Reaction conditions: aniline (1.0 mmol), DMC (10 mmol), Ti(NHPh)₄ (0.1 mmol), 1,4-dioxane (3 mL), 140 °C, overnight. The yields were determined by GC-FID with decane as the internal standard based on aniline.

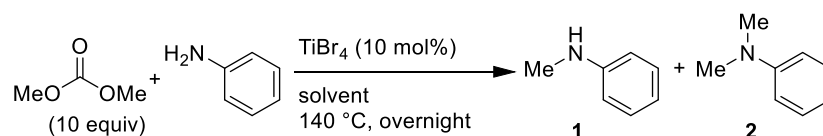


Scheme 65. Experiment to examine the involvement of HBr. Reaction conditions: PhNH₃Br (1.0 mmol), DMC (10 mmol), 1,4-dioxane (3 mL), 140 °C, overnight. The reaction mixture was analyzed by GC-FID.

2.3.5 Solvent screening

The effect of the solvent on the TiBr_4 -catalyzed methylation of aniline with DMC was examined and is summarized in **Table 4**. Apolar solvents did not dissolve the catalyst and the yields were low (entries 1 and 2). When triethylamine was used as a solvent, methyl *N*-methyl-*N*-phenylcarbamate (**5**) was unexpectedly formed in 75% yield (entry 3). It was found that TiBr_4 was not necessary for the formation of this compound (entry 4). Although this product is not desirable in this project, this transformation triggered our curiosity. (The investigation of this reaction will be described in Chapter 3.) Polar solvents formed a clear reaction mixture and the yields were high (entries 5–8). Interestingly, *p*-bromo *N,N*-dimethylaniline (**13**) was detected when the reaction was conducted in DMSO (entry 6). Because this transformation was also found interesting and useful, it was to be investigated separately. (The detail will be presented in Chapter 4.) For further studies, 1,4-dioxane was chosen for the practical reason that DMSO, NMP and sulfolane have too high boiling points to be removed *in vacuo*.

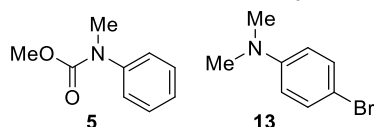
Table 4. Solvent screening for TiBr_4 -catalyzed methylation of aniline by DMC.^[a]



entry	solvent	Yield ^[b]	
		1	2
1	CCl_4	16%	2%
2	Toluene	19%	31%
3	NEt_3 ^[c]	5%	8%
4	NEt_3 ^[d]	4%	2%
5	1,4-Dioxane	13%	64%
6	DMSO ^[e]	0%	83%
7	NMP	0%	99%
8	Sulfolane	0%	99%

^[a] Reaction conditions: aniline (1.0 mmol), DMC (10 mmol), TiBr_4 (0.1 mmol), solvent (3 mL), 140 °C, overnight. ^[b] Determined by GC-FID with decane as the internal standard based on aniline.

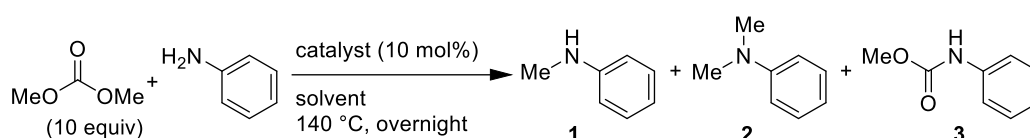
^[c] Carbamate **5** was produced in 75% yield. ^[d] Without TiBr_4 . Carbamate **5** was produced in 73% yield. ^[e] Bromide **13** was detected and identified by GC-MS and ^1H NMR.



2.4 Other catalysts

Other Lewis acids were screened for methylation of aniline with DMC (**Table 5**). Unfortunately, no improvement of conversion or selectivity was found compared to TiBr_4 . However, an interesting trend was observed. On one hand, acidic catalysts such as HfCl_4 and VCl_3 showed good selectivity towards methylation (entries 3–4). On the other hand, catalysts containing strongly basic ligands such as $\text{Ti}(\text{NMe}_2)_4$, $\text{Zn}(\text{OMe})_2$ and AlMe_3 produced carbamate **3** selectively (entries 7, 12 and 15). $\text{Zn}(\text{OTf})_2$ gave a mixture of methylated products and carbamate **3** (entry 14). As the triflate anion is very labile, the by-product methanol might coordinate to the Zn center to form $\text{Zn}(\text{OTf})(\text{OMe})$ or $\text{Zn}(\text{OMe})_2$, which in turn catalyzes the carbamation (entry 12).

Table 5. Catalyst screening of aniline and DMC in 1,4-dioxane.^[a]



entry	catalyst	solvent	Yield ^[b]		
			1	2	3
1	TiBr_4	1,4-Dioxane	7%	73%	0%
2	ZrCl_4	1,4-Dioxane	19%	24%	21%
3	HfCl_4	1,4-Dioxane	25%	13%	7%
4	VCl_3	1,4-Dioxane	24%	30%	3%
5	$\text{Zn}(\text{OTf})_2$	1,4-Dioxane	4%	0%	0%
6	ZnBr_2	1,4-Dioxane	17%	6%	4%
7	$\text{Ti}(\text{NMe}_2)_4$	Toluene	0%	0%	16%
8	TiCp_2Cl_2	Toluene	0%	0%	0%
9	$\text{TiCp}_2(\text{OTf})_2$	Toluene	17%	3%	8%
10	ZnCl_2	Toluene	0%	0%	0%
11	ZnBr_2	Toluene	3%	0%	0%
12	$\text{Zn}(\text{OMe})_2$	Toluene	0%	0%	80%
13	$\text{Zn}(\text{NTf}_2)_2$	Toluene	4%	36%	17%
14	$\text{Zn}(\text{OTf})_2$	Toluene	10%	47%	54%
15	AlMe_3	Toluene	0%	0%	30%
16	$\text{B}(\text{C}_6\text{F}_5)_3$	Toluene	3%	0%	0%
17	TMSOTf	Toluene	7%	0%	0%
18	MoCl_5	Toluene	8%	1%	0%

^[a] Reaction conditions: aniline (1.0 mmol), DMC (10 mmol), catalyst (0.1 mmol), solvent (3 mL), 140 °C, overnight. ^[b] Determined by GC-FID with decane as the internal standard based on aniline.

2.5 Conclusion and outlook

It is particularly remarkable that TiBr_4 catalyzes the formation of *N,N*-dimethylaniline (**2**) from aniline and DMC at 140 °C, which is a much lower reaction temperature than previously described in the literature.^[145,279,282] However, at even lower reaction temperatures, reactions were significantly slower. As a possible reaction mechanism, we suggest that TiBr_4 converts the alkyl group of organic carbonates into reactive species, followed by a nucleophilic attack by aniline to form alkylated anilines.

The design of the organic carbonate turned out to be critical. The bulkiness of the attacked alkyl group is significantly influential on reactivity. Additionally, in the case of aryl carbonates, nucleophilic attack on the carbonyl group is accelerated to produce carbamates and ureas.

Interesting transformations were observed when triethylamine or DMSO was used as a solvent. Triethylamine catalyzed the formation of methyl *N*-methyl-*N*-phenylcarbamate (**5**), and in DMSO brominated product **13** was produced. These transformations will be described in the next two chapters.

The acidity of the catalyst seems to play the major role in controlling the chemoselectivity. Whilst acidic catalysts produce alkylated products, catalysts with basic ligands lead to carbamate formation. It must be noted that ligand exchange *in situ* may form basic alkoxy species, leading to a mixture of alkylated amines and carbamates as it was observed when $\text{Zn}(\text{OTf})_2$ was used as a Lewis-acid catalyst. Considering these trends, it is speculated that a complex **14** depicted in **Figure 17** would be an ideal catalyst where acidic multidentate ligands control selectivity while being reluctant towards ligand exchange with the by-product alcohol.

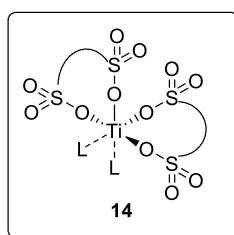


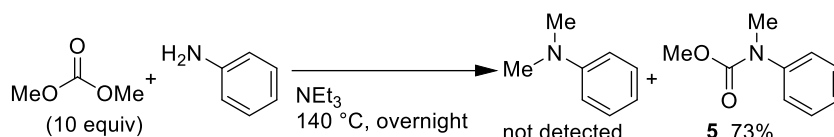
Figure 17. Suggested type of complex to improve the catalytic activity for methylation of amines with DMC.

Chapter 3

Base-Activation of Organic Carbonates

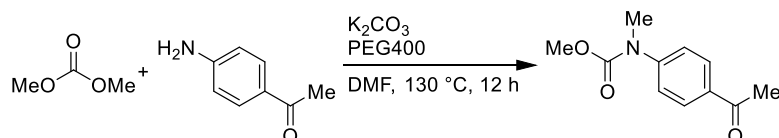
3.1 Introduction

The transformation of dimethyl carbonate (DMC) and aniline to methyl *N*-methyl-*N*-phenylcarbamate (**5**) (**Scheme 66**) was investigated and is described in this chapter. This transformation was found when TiBr₄-catalyzed methylation of aniline with DMC was carried out in triethylamine (Chapter 2).



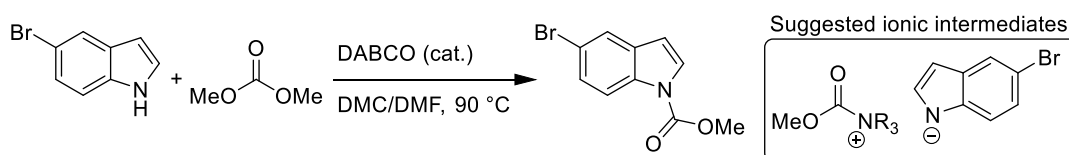
Scheme 66. The formation of *N,N*-disubstituted carbamate **5** from DMC and aniline as reported in Chapter 2.

Base-catalyzed transformations of amines and organic carbonates to *N,N*-disubstituted carbamates have been reported usually as side reactions while methylation of amines was the actual intent.^[279–281] Only a few studies focusing on such transformations have been reported.^[107,289] For example, K₂CO₃ was used as a base catalyst for the reaction of DMC and amines with polyethylene glycol (PEG) as a promoter (**Scheme 67**).^[107]



Scheme 67. Reaction of DMC and amines in the presence of K₂CO₃ and PEG.^[107] PEG400 = PEG with average molecular weight of 400 g/mol.

Organic bases have been used for the formation of carbamates from amines and organic carbonates as well, although primary amines were not presented in the report (**Scheme 68**).^[290] It is proposed that ionic liquids generated by organic bases and DMC are involved as intermediates in the reaction mechanism. Furthermore, ionic liquid-catalyzed carbamations have been reported.^[291,292] Therefore, ionic liquid catalysts or intermediates are possibly involved in this type of transformation.



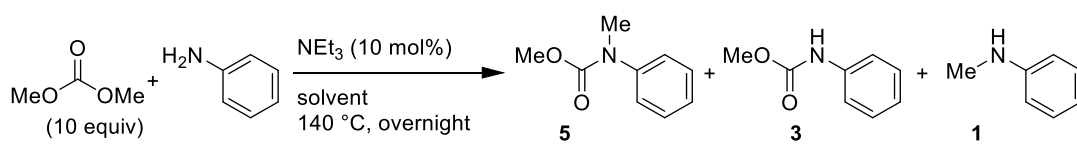
Scheme 68. Organic base-catalyzed carbamation of indoles.^[290] DABCO = 1,4-Diazabicyclo-[2.2.2]octane.

3.2 Triethylamine-catalyzed reactions

3.2.1 Reduction of the base loading to catalytic amounts

To examine the assumption that triethylamine is not only a solvent but also serves as a catalyst, 10 mol% of triethylamine was used while other solvents were introduced (**Table 6**). Although the desired product was barely obtained in 1,4-dioxane or toluene (entries 2 and 3), the yield was high when running the reaction in DMC itself (entry 1). Interestingly, DMSO also was found to be a good solvent for this transformation (entry 4).

Table 6. Solvent screening for the triethylamine-catalyzed transformation of DMC and aniline.^[a]



entry	solvent	Yield (%) ^[b]		
		5	3	1
1	DMC	73	1	4
2	1,4-Dioxane	1	2	3
3	Toluene	2	0	1
4	DMSO	91	4	4

^[a] Reaction conditions: aniline (1.0 mmol), DMC (10 mmol), NEt₃ (0.1 mmol), solvent (3 mL), 140 °C, overnight. ^[b] Determined by GC-FID with decane as the internal standard based on aniline.

3.2.2 Elucidation of the role of DMSO

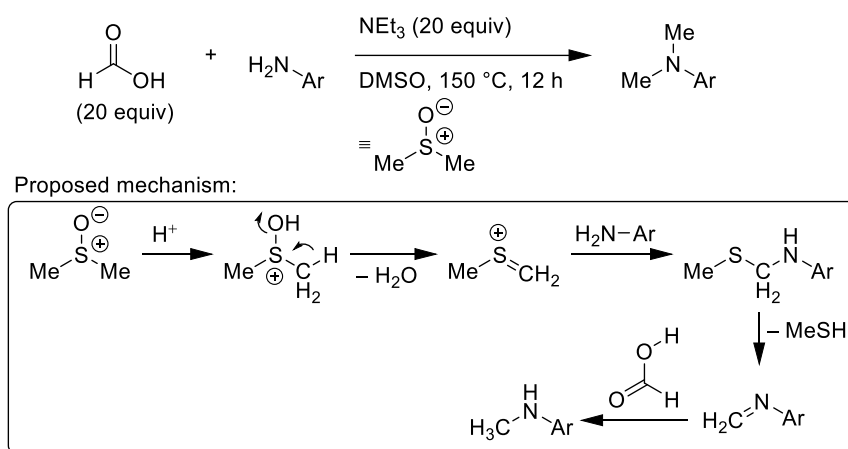
The effect of the use of DMSO on the reaction is to be discussed herein. One possibility is stabilization of ionic species. As described above (Section 3.1), ionic species may be involved in this type of reaction as intermediates or catalysts. In fact, a phase separation was observed (**Figure 18**) in the reaction mixture corresponding to **Scheme 66** where the solvent was triethylamine, although all the ingredients were dissolved before the mixture was heated. The stability of ionic



Figure 18. Phase separation was observed after the reaction in triethylamine. Reaction conditions: aniline (1.0 mmol), DMC (10 mmol), triethylamine (3 mL), 140 °C, overnight.

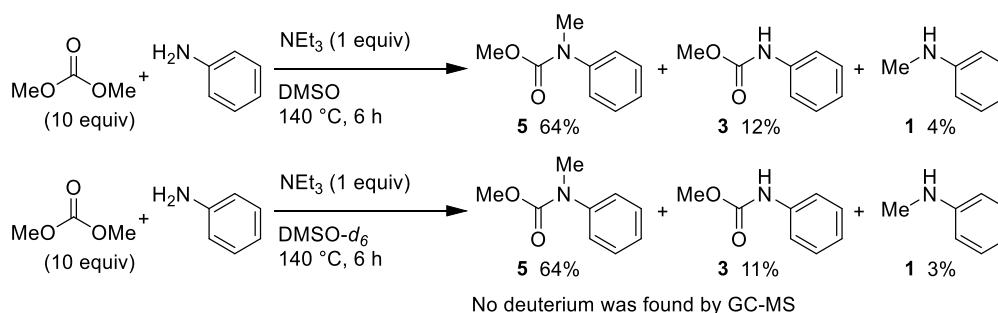
species is known to increase in polar solvents^[104] and, therefore, the high polarity of DMSO may assist the generation of ionic intermediates or catalysts.

Another possible role of DMSO was invoked by a reported methylation of amines (**Scheme 69**) where DMSO serves as an electrophile.^[293] The activated DMSO and amines could form imine intermediates,^[147] which may be reduced by formic acid. Triethylamine is necessary to improve the yield of the product. It may play a role in tuning the acidity of the reaction system, so that free amine substrates are available for the nucleophilic attack.



Scheme 69. Methylation of amines with formic acid and DMSO.^[293]

Thus, the possibility that DMSO is an electrophile in our methylation reaction was examined by using deuterated DMSO as a solvent (**Scheme 70**). ¹H NMR integration and GC-MS analyses of the reaction mixtures displayed no differences between runs in DMSO and DMSO-*d*₆. These results exclude the possibility that DMSO is a methyl source.

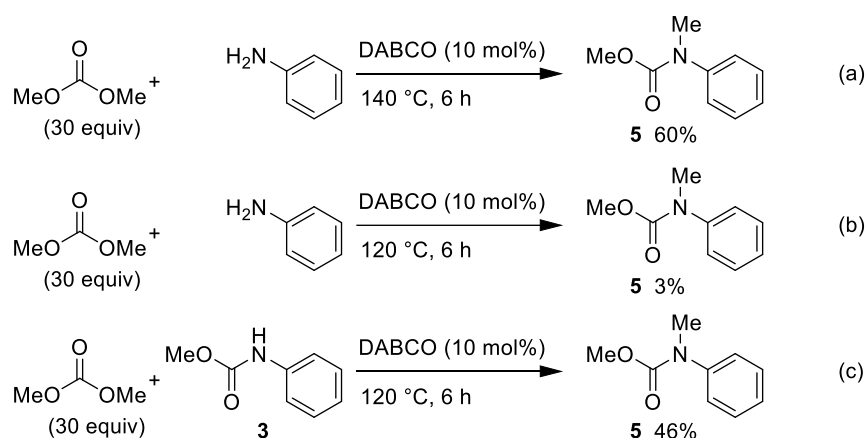


Scheme 70. The triethylamine-catalyzed reaction of DMC and aniline in deuterated DMSO. Reaction conditions: aniline (1.0 mmol), DMC (10 mmol), NEt₃ (0.1 mmol), solvent (3 mL), 140 °C, 6 h. The yields were determined by ¹H NMR of the crude mixture with CH₂Br₂ as the internal standard.

3.3 DABCO-catalyzed reactions

3.3.1 Electron-deficient amines

1,4-Diazabicyclo[2.2.2]octane (DABCO) was employed as a catalyst for the formation of carbamate **5** from aniline and DMC (**Scheme 71a**). Carbamate **5** was obtained in 60% yield at 140 °C, although the yield was low when the experiment was carried out at 120 °C (**Scheme 71b**). Interestingly, when carbamate **3** was used as a substrate at 120 °C, the yield of carbamate **5** was 46% (**Scheme 71c**). These results indicate that the deprotonation of the amine substrate is important in the reaction mechanism, as an electron-deficient N–H nucleophile seemed to react efficiently. (pK_a value in DMSO is 31 for aniline,^[294] and is estimated around 20 for carbamate **3**.^[295,296])



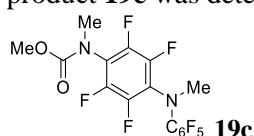
Scheme 71. DABCO-catalyzed formation of carbamate **5**. Reaction conditions: substrate (1.0 mmol), DMC (2.6 mL, 30 mmol), DABCO (0.1 mmol), 6 h. The yields were determined by GC-FID with decane as the internal standard based on aniline.

Accordingly, other electron-deficient amines were tested under similar conditions (**Table 7**). As expected, electron-deficient amines reacted with DMC to form the corresponding carbamates (entries 1–3). 4-Fluoroaniline (**18**) is apparently not electron-deficient enough (entry 4). Pentafluorophenyl amine (**19a**) produced carbamate **19b** and S_NAr -reaction product **19c** (entry 5). Diamine **20a** gave a perimidone scaffold although the yield was not very high (entry 6).

Table 7. Electron deficient amines as substrates for the formation of carbamates.^[a]

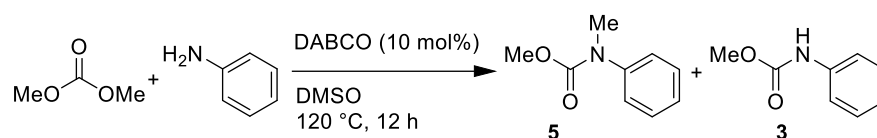
entry	Substrate	Product and yield ^[b]
1	15a	15b 51%
2	16a	16b 83%
3	17a	17b 85%
4	18	No product
5 ^[c]	19a	19b 14%
6	20a	20b 24%

^[a] Reaction conditions: substrate (1.0 mmol), DMC (2.6 mL, 30 mmol), DABCO (0.1 mmol), 120 °C, 6 h. ^[b] Determined by GC-FID with decane as the internal standard based on substrate. ^[c] S_NAr-reaction product **19c** was detected by GC-MS.



3.3.2 DABCO-catalyzed reactions in DMSO

Since DMSO showed an excellent solvent effect with triethylamine for the transformation of DMC and aniline to carbamate **5**, reactions with DABCO in DMSO were tested at 120 °C (**Table 8**). Compared to the reaction of aniline in DMC (**Scheme 71b**), better yields were observed in DMSO (entry 1). By optimizing the solvent ratio of DMSO and DMC, carbamate **5** was obtained in 64% yield at 120 °C (entry 2). Interestingly, higher proportions of DMSO produced higher yields of carbamate **3**, although the conversion of carbamate **3** to product **5** should be fast, as observed in **Scheme 71b** and **c**. The presence of DMSO may have an influence on the reaction mechanism and the reaction rate of carbamate **3** to product **5**.

Table 8. Effect of DMSO on DABCO-catalyzed carbamation.^[a]

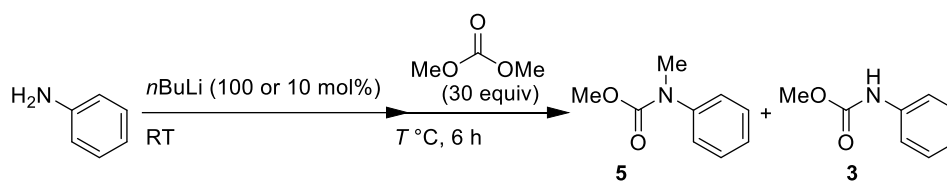
entry	solvent (mL)		Yield (%) ^[b]	
	DMSO	DMC	5	3
1	3.0	1.0 ^[c]	26	41
2	1.0	3.0	64	17
3	0.5	3.5	47	19

^[a] Reaction conditions: aniline (1.0 mmol), DMC (10 mmol), DABCO (0.1 mmol), solvent (4 mL), 120 °C, 12 h. ^[b] Determined by GC-FID with decane as the internal standard based on substrate.

^[c] 10 equivalents with respect to aniline.

3.3.3 Deprotonation of amine substrates

According to the assumption that deprotonation of the amine substrate is critical for the reaction, the base does not have to be an amine. Thus, *n*BuLi was used as a base for the reaction of aniline and DMC (**Table 9**). At 140 °C, carbamate **5** was produced in good yield with 10 mol% or 1.0 equivalent of *n*BuLi (entries 1 and 2). However, the conversion of aniline was low at 120 °C (entry 3).

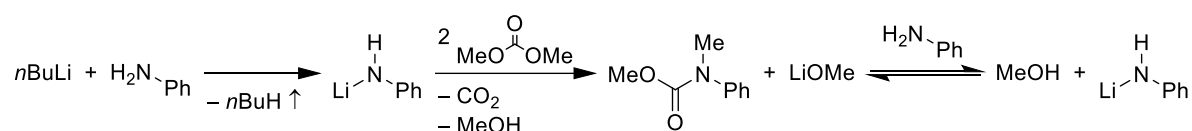
Table 9. Deprotonation of amines by *n*BuLi towards methylation with DMC.^[a]

entry	<i>n</i> BuLi	<i>T</i> (°C)	Yield ^[b]	
			5	3
1	100 mol%	140	45%	13%
2	10 mol%	140	42%	18%
3	10 mol%	120	3%	3%

^[a] Reaction conditions: aniline (1.0 mmol), DMC (2.6 mL, 30 mmol), *n*BuLi (0.1 or 1.0 mmol). *n*BuLi was added to aniline at room temperature, then diluted in DMC and heated for 6 hours.

^[b] Determined by GC-FID with decane as the internal standard based on aniline.

With a catalytic amount of *n*BuLi, LiOMe should be generated by the reaction of aniline and DMC as illustrated in **Scheme 72**. Considering that the pK_a value of MeOH in DMSO is 29,^[297] which is very close to that of aniline, the deprotonation of aniline by LiOMe should be viable. If only the deprotonation of the substrate is essential for this transformation, the yield with *n*BuLi should be similar to that of reactions with electron-deficient amines (**Table 7**). Therefore, the poor results with *n*BuLi in the absence of amine catalysts mean that the deprotonation alone does not dominate the reaction, but also the activation of DMC by an amine catalyst is important in the reaction mechanism.



Scheme 72. Deprotonation of aniline by *n*BuLi and the equilibrium of lithium species.

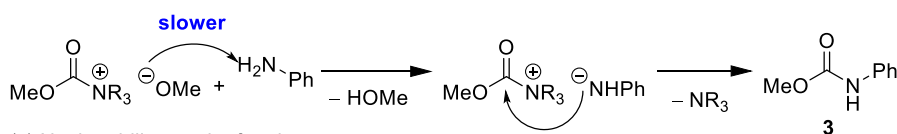
3.4 Hypothetic reaction mechanism

Phase separation in the reaction mixture indicates a positive involvement of ionic intermediates. Amine substrates of different electron density show clear reactivity differences towards carbamate formation. However, simple deprotonation by *n*BuLi to form lithium amides leads to carbamate **5** in lower yield than organic base catalysts. These observations may suggest the reaction mechanism depicted in **Scheme 73**.

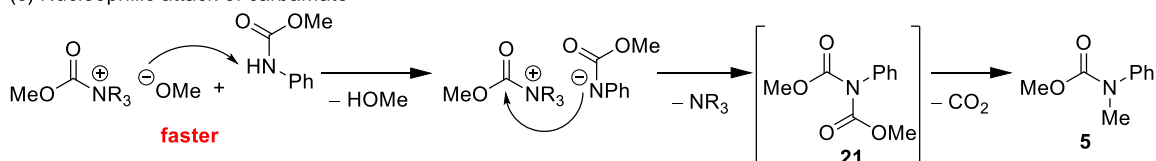
(a) Activation of DMC



(b) Nucleophilic attack of aniline

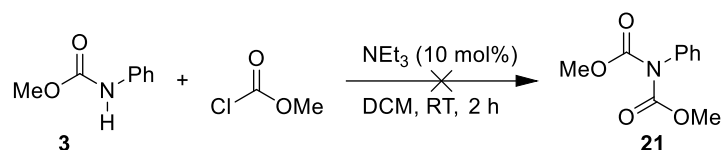


(c) Nucleophilic attack of carbamate



Scheme 73. Hypothesized reaction mechanism. (a) Activation of DMC by an amine catalyst. (b) Deprotonation of aniline followed by nucleophilic attack. (c) Deprotonation of carbamate substrates followed by nucleophilic attack and decarboxylation.

Amine catalysts first activate DMC to form ammonium cation species (**Scheme 73a**). Then, the counter anion deprotonates amine substrates (**Scheme 73b**) where electron-deficient substrates are favoured. The cationic electrophile and anionic nucleophile may stay associated as an ion pair, so the carbamation could occur fast. In the case of carbamate substrates (**Scheme 73c**), azamalonate **21** should be formed by carbamation of carbamate **3**, followed by decarboxylation to produce carbamate **5**.^[289] To test this assumption, the synthesis of azamalonate **21** was attempted but with no success (**Scheme 74**). Also, no synthesis of azamalonate **21** has been reported. These data could explain that azamalonate **21** is too unstable to be isolated.



Scheme 74. Attempted synthesis of azamalonate **21**. Reaction conditions: **3** (10 mmol), methyl chloroformate (24 mmol), NEt₃ (1 mmol), DCM (20 mL), RT, 2 h. The reaction mixture was analyzed by ¹H NMR.

3.5 Conclusion and outlook

The base-catalyzed formation of carbamate **5** from aniline and DMC was studied. The influence of solvents on the reaction was remarkable. In particular, DMSO accelerated the reaction, and high yields were achieved with catalytic amounts of base. Furthermore, electron-deficient amine substrates were favoured for this transformation. As for the reaction mechanism, both base-activation of DMC and deprotonation of an amine substrate seem to be important.

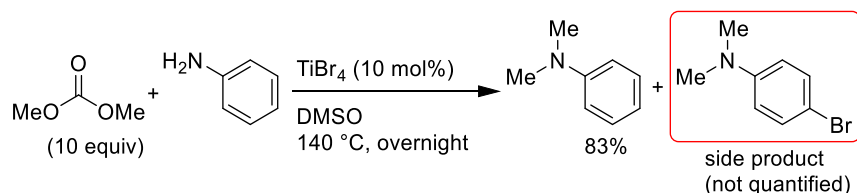
Yet, the role of DMSO is not clear. It might be just a polar solvent possibly stabilizing ionic species, but its involvement in the reaction mechanism cannot be excluded based on the observations reported in **Table 8**. Experiments to examine the solvent effect of DMSO on the stability of ionic intermediates and Lewis-base activity of DMSO would be useful to improve the understanding of the reaction.

Chapter 4

DMSO-based Oxidative Bromination of (Hetero)Arenes

4.1 Introduction

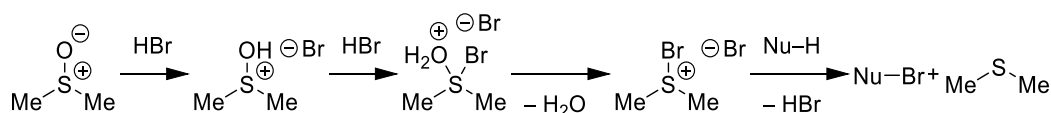
This chapter describes an oxidative bromination of arenes and heteroarenes using DMSO as an oxidant. This reaction was found when the TiBr_4 -catalyzed methylation reaction of DMC and aniline in DMSO led to bromination of dimethylaniline (Chapter 2) (**Scheme 75**). In this reaction TiBr_4 seems to activate DMSO to generate an oxidative brominating species in a similar way to other DMSO-based oxidative bromination reactions.^[181] It is attractive that aryl bromides are produced by using DMSO as an oxidant. DMSO is a nontoxic, cheap, abundant, stable and mild oxidant; all of which are preferred properties for potential industrial uses.^[147] It is also important to develop synthetic methods for aryl bromides, because they are extensively used building blocks in synthetic chemistry.^[298] Details of DMSO-based oxidations and preparations of aryl bromides are described in Section 1.5. Pursuing these expected advantages, this bromination reaction was investigated and developed.



Scheme 75. The formation of an oxidative bromination side product discovered in Chapter 2.

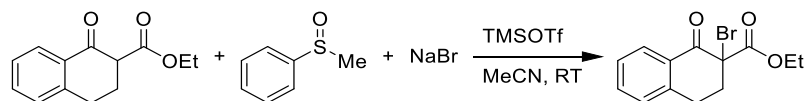
4.1.1 DMSO-based oxidative brominations

The first DMSO-based oxidative bromination of arenes was reported in 1956.^[168] Since then, brominations utilizing DMSO as an oxidant have been continuously developed.^[170–176] Among the variations, the HBr/DMSO system is the most popular because aqueous HBr is the cheapest bromide source (**Scheme 76**).^[169,177–182] Section 1.5.2 describes details of DMSO-based brominations. However, the HBr/DMSO aqueous system is not always the best choice. One of its drawbacks is that a variety of functional groups do not tolerate acidic aqueous conditions and they must be excluded from substrate scopes.^[92] The general description of aqueous reaction systems is found in Section 4.1.2.



Scheme 76. General mechanism of oxidative brominations in the HBr/DMSO system.^[181]

Unlike the HBr/DMSO system, combinations of sulfoxides and metal bromides have been rarely reported,^[183–185] although metal bromides are also cheap bromide sources. One of a few examples is described in **Scheme 77**, where a β -ketoester is brominated by using sulfoxides as an oxidant.^[185] In this reaction, an oxidative brominating species is generated by TMSOTf as a DMSO-activator and NaBr as a bromide source.



Scheme 77. A bromination reaction of carbonyl compounds with sulfoxides as oxidants.^[185]

4.1.2 Organic reactions in aqueous media

A number of studies on organic reactions using water as a solvent were reported in the 2000s.^[299] In addition to water being environmentally friendly, the reactions where reactivities and selectivities were improved by using water as a medium attracted scientific interest and encouraged researchers to develop organic reactions in water.^[300–302] Water is a green solvent because of its abundance, environmental compatibility, nontoxicity and nonflammability. However, organic reactions carried out in water rarely meet the requirements to be regarded as green reactions.^[303–305] This is mainly because chemical-contaminated aqueous wastes have a high impact on the environment,^[306,307] and the energy and cost for purifying contaminated water is significantly high.^[308] In fact, the calculation of its impact on the environment has been conducted and disagrees with the concept of green chemistry.^[309] Although new technologies such as bio-, chemical-, electrochemical-, and photochemical purification of wastewater are investigated,^[310] their efficiency is not sufficient and further improvement is necessary.^[311] Additionally, integrated synthetic systems such as sequential procedures are favourable in industry, because it is important to shorten chemical processes in order to minimize production cost.^[285] However, the majority of organic reactions are not compatible with water.^[73] Thus, possible designs of sequential procedures containing aqueous reactions are limited. Furthermore, the heterogeneity of aqueous reaction systems may cause unstable results in large-scale reactions.^[285]

4.2 Preliminary investigations

4.2.1 Bromide source optimization

TiBr₄ must have served as a bromide source instead of a catalyst for the formation of the brominated side product observed in the methylation reaction of aniline in the presence of TiBr₄ and DMSO (**Scheme 75**), because it was the only bromide source in the reaction system. This fact was confirmed by using different stoichiometric ratios of TiBr₄ to dimethylaniline (**Table 10**). The more TiBr₄ was used, the higher composition of product **13** in the crude reaction mixture was observed. TiBr₄ seems to provide 2 equivalents of bromide, and thus, 0.5 equivalent of TiBr₄ with respect to the substrate should be enough for completion of the reaction. Yields were not determined because decane, the GC-FID internal standard, and DMSO formed a heterogeneous mixture and the GC-FID analysis was unreliable (entries 1–3). By introducing CHCl₃ as a solvent, a homogeneous reaction mixture was obtained, and the yield was determined to be 82% with 0.5 equivalents of TiBr₄ (entry 4).

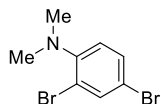
Table 10. Bromination reaction with varied equivalents of TiBr₄.^[a]

entry	x (mol%)	DMSO/CHCl ₃ (mL)	Composition (mol%) ^[b]	
			2	13
1	10	3/0	83	17
2	25	3/0	43	57
3	50	3/0	0	93 ^[c]
4	50	1/2	0	82 ^[d]

^[a] Reaction conditions: **2** (1.0 mmol), 80 °C, overnight.

^[b] Determined by ¹H NMR analysis of the crude reaction mixture.

^[c] *o*-,*p*-Dibromide derivative was detected (7 mol%).



^[d] Yield determined by GC-FID analysis of the reaction mixture with decane as the internal standard.

Other bromide sources were tested for the reaction (**Table 11**). The reaction temperature was decreased to 60 °C, because it is difficult to compare reactivities when the starting material is fully converted. The yield of bromide **13** with TiBr₄ decreased to 34% (entry 1). As a comparison, *N*-

bromosuccinimide (NBS) was used (entry 5), but other brominated products such as *o*-bromide and *o,p*-dibromide derivatives were also detected. Trimethylsilyl bromide (TMSBr) was found to be as active as TiBr₄ (entry 3). The advantages of the TMSBr/DMSO system are described in the next section.

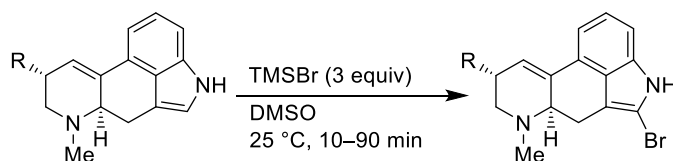
Table 11. Screening of bromide sources.^[a]

entry	bromide	x (equiv)	Yield (%) ^[b]	
			13	Others ^[c]
1	TiBr ₄	0.5	34	0
2	CuBr ₂	1.0	30	4
3	TMSBr	1.0	39	0
4	MnBr ₂	1.0	0	0
5	NBS ^[d]	1.0	36	30

^[a] Reaction conditions: **2** (1.0 mmol), DMSO (10.0 mmol), CHCl₃ (3 mL), 60 °C, overnight. ^[b] Determined by GC-FID analysis of the reaction mixture with decane as the internal standard. ^[c] *o*-Bromide and *o,p*-dibromide derivatives were detected. ^[d] Without DMSO.

4.2.2 The TMSBr/DMSO system

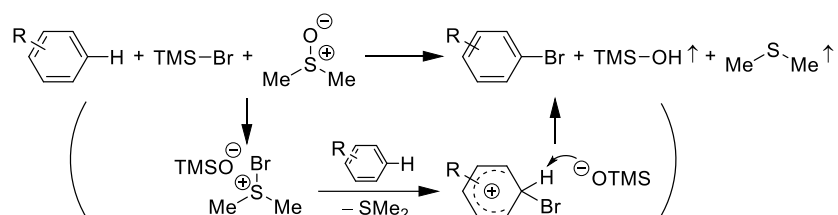
TMSBr is a readily available bromide source that is commonly used in organic reactions.^[312] The combination of TMSBr and DMSO has been known in a limited number of examples, including bromination of indole alkaloids reported by Megyeri and Keve in 1989 (**Scheme 78**).^[313] Other reports using the TMSBr/DMSO system studied bromination of aliphatic nucleophiles.^[314,315]



Scheme 78. Bromination of indole alkaloids in the TMSBr/DMSO system.^[313]

The reaction protocol with TMSBr appears to be suitable for potential large-scale applications. The by-products from this system are dimethyl sulfide and trimethylsilanol (**Scheme 79**). They are volatile enough to be removed *in vacuo* from reaction mixtures (the boiling point is 37 °C for dimethyl sulfide, 99 °C for trimethylsilanol). Thus, simply by applying vacuum to the reaction mixture, the products can be obtained in good purity. Therefore, the use of the TMSBr/DMSO

system does not need aqueous workup after the reaction. This is advantageous comparing to NBS, because this produces succinimide, which has a boiling point of 288 °C and is usually removed by aqueous workup. Furthermore, the dry conditions of this protocol avoid all the aforementioned disadvantages of aqueous systems. These properties of the TMSBr/DMSO system allow facile and cheap bromination procedures and can reduce the production time.^[285] Also, this system does not produce any solid unlike TiBr₄, and accordingly should be suitable for flow chemistry applications.^[316] Therefore, we focused on investigating the reaction in the TMSBr/DMSO system.



Scheme 79. DMSO-based oxidative bromination of arenes with TMSBr.

4.3 Reaction condition optimization

4.3.1 Solvent and reaction time

Several solvents were tested for the reaction with TMSBr as a bromide source (**Table 12**). No large differences were observed between the used solvents, but a phase separation occurred when using hexane (entry 1).

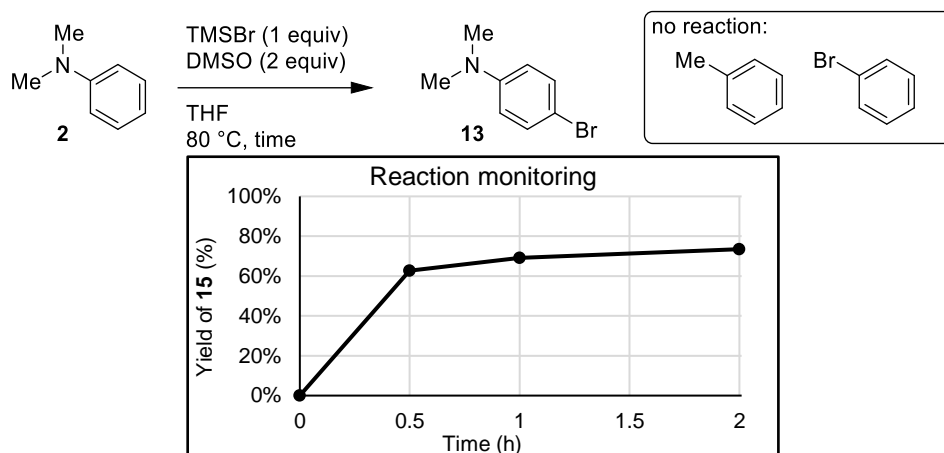
Table 12. Solvent screening of the bromination reaction.^[a]

entry	solvent	Yield of 13 (%) ^[b]
1	Hexane ^[c]	68
2	CHCl ₃	87
3	MeCN	62
4	THF	67
5	1,4-Dioxane	76

^[a] Reaction conditions: **2** (1.0 mmol), TMSBr (1.0 mmol), DMSO (10.0 mmol), solvent (3 mL), 80 °C, overnight.

^[b] Determined by GC-FID analysis of the reaction mixture with decane as the internal standard. ^[c] Liquid-liquid phase separation was observed after the reaction.

The reaction in THF was monitored in short time intervals (**Scheme 80**). Although toluene and bromobenzene were also employed as substrates, only electron-rich arene **2** yielded the brominated product. The reaction was found to go to completion in ca. 2 hours.



Scheme 80. Monitoring of the bromination reaction by GC-FID. The yields were determined by GC-FID with decane as the internal standard. Reaction conditions: arene (1.0 mmol), TMSBr (1.0 mmol), DMSO (2.0 mmol), THF (3 mL), 80 °C.

4.3.2 Effects of electron-donating groups

Bromination reactions of three different types of electron-rich arenes were compared in THF or CHCl_3 (**Table 13**). Arene **2** ($\text{R}=\text{NMe}_2$) was efficiently brominated in THF (entry 1), but the yield in CHCl_3 was lower (entry 4). In contrast, anisole ($\text{R}=\text{OMe}$) showed a good yield in CHCl_3 , but the yield was lower in THF (entries 2 and 5). In the case of phenol, conversions were high in both solvents, but *o*-bromide and *o,p*-dibromide derivatives were also detected (entries 3 and 6).

Table 13. Reactions of electron-rich arenes in THF or CHCl_3 .^[a]

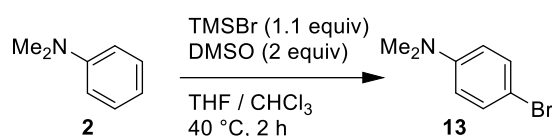
Solvent = THF			Solvent = CHCl_3		
entry	-R	Yield (%) ^[b]	entry	-R	Yield (%) ^[b]
1	-NMe ₂	100	4	-NMe ₂	52
2	-OMe	13	5	-OMe	40
3	-OH	74	6	-OH	63

^[a] Reaction conditions: arene (1.0 mmol), TMSBr (1.1 mmol), DMSO (2.0 mmol), solvent (3 mL), 80 °C, 2 h.

^[b] Determined by GC-FID analysis of the reaction mixture with decane as the internal standard.

In order to examine the solvent effect carefully with arene **2** as a substrate, the reactions in mixtures of THF and CHCl₃ as solvents were carried out (**Table 14**). While the yield of product **13** in THF at 40 °C was 65% (entry 1), the bromination of arene **2** was suppressed by the presence of CHCl₃ (entries 2–4). A possible explanation for this observation is the involvement of radicals in the reaction of arene **2**,^[317] which may be quenched by hydrogen abstraction from CHCl₃.^[318] Since the optimal solvent seems to depend on the substrate, the substrate screening was to be carried out in both solvents.

Table 14. Bromination of arene **2** in THF and/or CHCl₃.^[a]



entry	THF (mL)	CHCl ₃ (mL)	Yield of 13 (%) ^[b]
1	3	0	65
2	1	2	4
3	0.1	3	5
4	0	3	8

^[a] Reaction conditions: **2** (1.0 mmol), TMSBr (1.1 mmol), DMSO (2.0 mmol), 40 °C, 2 h.

^[b] Determined by GC-FID analysis of the reaction mixture with decane as the internal standard.

4.4 Substrate scope

The substrate scope was examined in CHCl₃ and THF at different temperatures (**Table 15**). In general, arenes bearing electron-donating groups (EDGs) were brominated at their *para* position. Aniline derivatives were brominated efficiently in this reaction (entries 1–8), although aniline itself gave little product (entries 9 and 10).⁴ Di- and trimethoxybenzene were electron-rich enough to give bromide **27** and **28**, respectively, in high yield (entries 13–16). The yield of bromide **26** was low (entries 11 and 12), and no conversion of ester **29** was observed (entries 17 and 18). Phenols **30** and **33** were the only cases where *o*-bromides derivatives were observed in the range of 9–13% yield.

⁴ A dark insoluble solid was found in the reaction mixture and only a small amount of aniline and the product **25** was detected in GC-FID analysis. Aniline is known to polymerize under oxidative conditions. For an early example, see: A. G. Green, A. E. Woodhead, *J. Chem. Soc., Trans.* **1910**, 97, 2388-2403. For more recent review, see: G. Ćirić-Marjanović, M. Milojević-Rakić, A. Janošević-Ležaić, S. Luginbühl, P. Walde, *Chem. Pap.* **2017**, 71, 199.

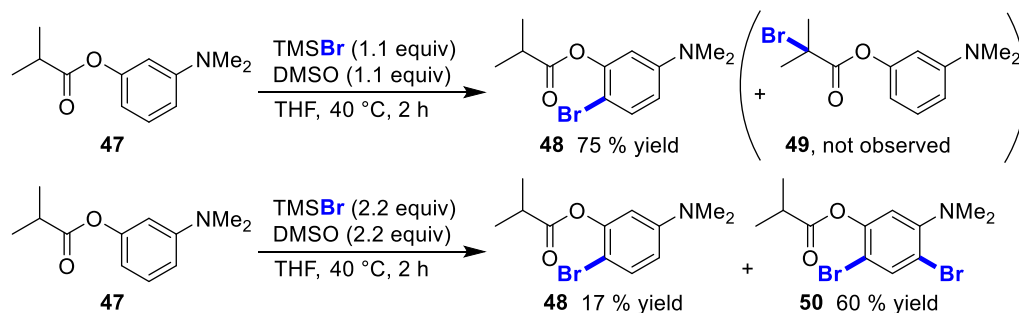
Table 15. Substrate scope of the bromination in the TMSBr/DMSO system.^[a]

entry	Product	Solvent, <i>T</i>	Yield ^[b]	entry	Product	Solvent, <i>T</i>	Yield ^[b]
1		CHCl ₃ , 80 °C	25%	27		CHCl ₃ , 80 °C	20%
2	13	THF, 60 °C	69%	28	34	THF, 40 °C	38%
3		CHCl ₃ , 80 °C	22%	29		CHCl ₃ , 40 °C	13%
4	22	THF, 80 °C	87%	30	35	THF, 25 °C	22%
5		CHCl ₃ , 60 °C	(47%) ^{[c][d]}	31		CHCl ₃ , 40 °C	43% ^[e]
6	23	THF, 60 °C	(87%) ^{[c][d]}	32	36	THF, 25 °C	75% ^[e]
7		CHCl ₃ , 40 °C	49% ^[e]	33		CHCl ₃ , 40 °C	45%
8	24	THF, 80 °C	19% ^[e]	34	37	THF, 40 °C	47%
9		CHCl ₃ , 25 °C	0%	35		CHCl ₃ , 40 °C	34% ^[c]
10	25	THF, 25 °C	17%	36	38	THF, 60 °C	64% ^[c]
11		CHCl ₃ , 40 °C	36%	37		CHCl ₃ , 25 °C	39%
12	26	THF, 40 °C	13%	38	39	THF, 25 °C	72%
13		CHCl ₃ , 25 °C	93%	39		CHCl ₃ , 25 °C	77%
14	27	THF, 25 °C	93%	40	40	THF, 25 °C	93%
15		CHCl ₃ , 25 °C	89%	41		CHCl ₃ , 25 °C	70%
16	28	THF, 40 °C	63%	42	41	THF, 60 °C	52%
17		No reaction		43		CHCl ₃ , 25 °C	86%
18	29			44	42	THF, 60 °C	73%
19		CHCl ₃ , 25 °C	68%	45		CHCl ₃ , 80 °C	87%
20	30	THF, 25 °C	69%	46	43	THF, 80 °C	82%
21		CHCl ₃ , 25 °C	95%	47		No reaction	
22	31	THF, 40 °C	81%	48	44		
23		CHCl ₃ , 25 °C	90%	49		No reaction	
24	32	THF, 25 °C	84%	50	45		
25		CHCl ₃ , 25 °C	66%	51		No reaction	
26	33	THF, 25 °C	48%	52	46		

^[a] Reaction conditions: arene (1.0 mmol), TMSBr (1.1 mmol), DMSO (1.1 mmol), solvent (3 mL), 2 h. ^[b] Isolated yield. ^[c] Molecular sieve 4 Å was used. ^[d] Determined by GC-FID due to the decomposition during purification. ^[e] Inseparable mixture of the substrate and the product. The yield was calculated from the mole ratio as determined by ¹H NMR.

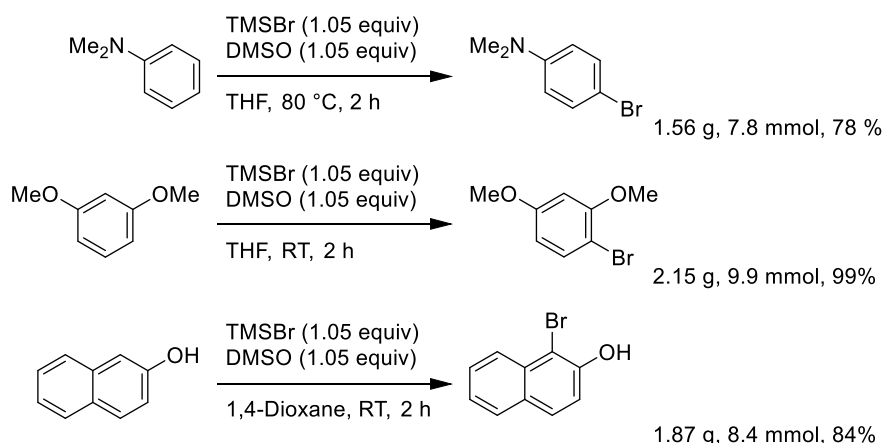
In the case of arenes functionalized with two different EDGs (entries 27–32), the dimethylamino group showed stronger influence on regioselectivity than methoxy, hydroxy and ester groups. Different regioisomers from the ones shown in **Table 15** were not detected. The regioisomers obtained from the reactions were identified by NMR techniques (^1H – ^{13}C HSQC and HMBC). The screening revealed that amide, ester, aldehyde and acetal moieties remained untouched (entries 7–8 and 31–36). It is remarkable that an acetal group was tolerated and produced bromide **38** thanks to the dry conditions of the reaction (entries 35 and 36). Heteroarenes were also employed as substrates (entries 37–52). Various structures were brominated successfully, although erosion of the yield of 3-bromo-2-indolinone (**39**) was observed due to further bromination of the product giving 3,3-dibromo-2-indolinone (11% yield in CHCl_3 and 13% in THF). 2-Methylpyrazole required high temperatures (entries 45 and 46), whereas pyridine, quinoline and 1-methylimidazole did not react at all (entries 47–52).

In order to additionally assess the chemoselectivity of this reaction, an electron-rich arene containing an ester group (**47**) was employed as a substrate (**Scheme 81**).^[319] Bromination at the α -carbon of the ester, which would produce α -bromide **49**, was not observed at all even when 2.2 equivalents of the reagents were used.



Scheme 81. Bromination of an electron-rich arene containing an ester group (**47**). Reaction conditions: arene (1.0 mmol), TMSBr (1.1 or 2.2 mmol), DMSO (1.1 or 2.2 mmol), THF (3 mL), 40 °C, 2 h. Isolated yields are shown.

Brominations of several substrates on gram-scale were carried out to confirm the suitability of this protocol for synthetic applications on a larger scale (**Scheme 82**). The yields were high in each case and products on a 2-gram scale could be obtained. No issues were encountered during the procedures.



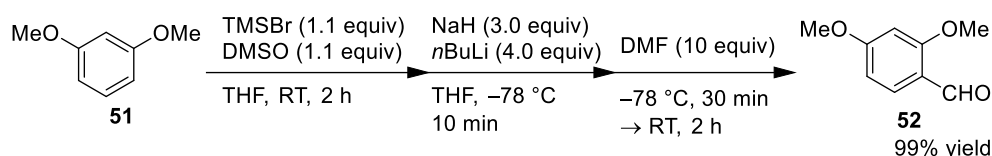
Scheme 82. Larger-scale brominations of electron-rich arenes. Reaction conditions: arene (10.0 mmol), TMSBr (10.5 mmol), DMSO (10.5 mmol), solvent (15 mL), 2 h. Isolated yields are shown.

4.5 Synthetic applications

Three synthetic applications were performed to demonstrate the advantages of this protocol allowing oxidative brominations to occur under mild conditions in non-aqueous media.

4.5.1 Lithium–halogen exchange reactions

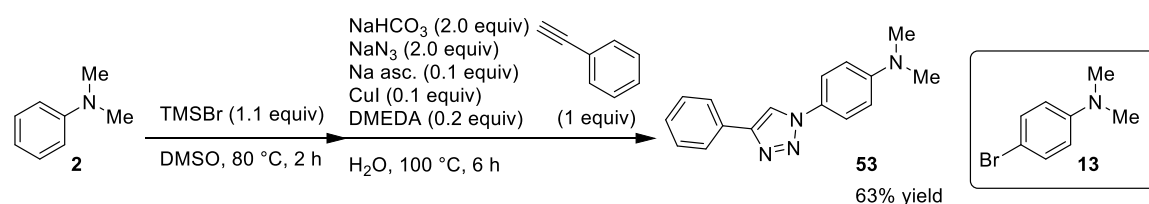
To utilize the advantage that our bromination is carried out under non-aqueous conditions, lithiation reactions were conducted (**Scheme 83**).^[320] The comparison of aqueous and non-aqueous reaction systems is described in Section 4.1.2. First, arene **51** was brominated in the TMSBr/DMSO system. The reaction mixture was treated with NaH, then *n*BuLi was added to the mixture at $-78\text{ }^{\circ}\text{C}$, followed by the addition of DMF to obtain aldehyde **52** in 99% yield. Without NaH treatment, protonated compound **51** was recovered, although arene **51** was completely consumed after the bromination. This indicates that the aryl lithium species, which is generated by the reaction of the bromide intermediate and *n*BuLi, was protonated by TMSOH before the addition of DMF. In general, lithium–halogen exchange reactions are known to be faster than protonation of alkyl lithium reagents.^[321]



Scheme 83. A sequential synthesis: bromination, lithium–bromine exchange and aldehyde formation. Reaction conditions: **51** (1.0 mmol), TMSBr (1.1 mmol), DMSO (1.1 mmol), THF (3 mL), RT, 2 h; NaH (3.0 mmol), THF (2 mL), 0 °C, 5 min; *n*BuLi (4.0 mmol), THF (3 mL), -78 °C, 5 min; DMF (10.0 mmol), -78 °C to RT, 2 h.

4.5.2 Azidation and Cu-catalyzed 1,2,3-triazole formation

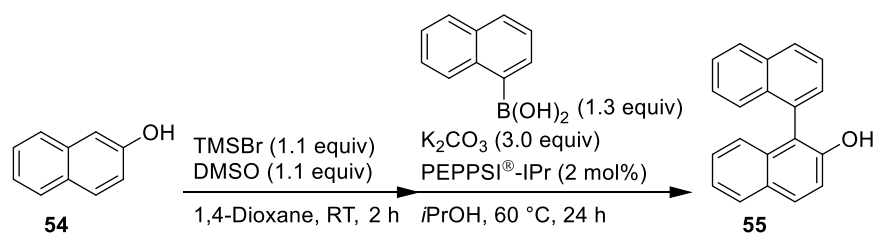
Cu-catalyzed 1,2,3-triazole formation from organic azides and alkynes is a popular reaction to link building blocks under mild conditions.^[322] Also, it is known that azidation of organic bromides and triazole formation can be carried out in a one-pot procedure.^[323] Arene **2** was therefore brominated using the developed TMSBr/DMSO protocol and subsequently subjected to azidation and triazole formation. Triazole **53** was obtained in 63% yield, and 34% of unreacted bromide **13** was recovered (**Scheme 84**).



Scheme 84. A sequential synthesis: bromination, azidation and triazole formation. DMEDA=1,2-dimethylethylenediamine, Na asc.=sodium L-ascorbate. Reaction conditions: **2** (1.0 mmol), TMSBr (1.1 mmol), DMSO (3 mL), 80 °C, 2 h; NaHCO₃ (2.0 mmol), NaN₃ (2.0 mmol), Na asc. (0.1 mmol), CuI (0.1 mmol), DMEDA (0.2 mmol), phenylacetylene (1.0 mmol), H₂O (1 mL), 100 °C, 6 h.

4.5.3 Palladium-catalyzed coupling reaction

Aryl bromides are often used for Pd-catalyzed cross-coupling reactions.^[298] To confirm that our bromination protocol is compatible with them, the bromination of 2-naphthol (**54**) was followed by Suzuki–Miyaura coupling to form a biaryl structure (**Scheme 85**).^[324] Binaphthyl compound **55** was produced in 92% yield.



Scheme 85. Suzuki–Miyaura cross-coupling to form a binaphthyl backbone. PEPPSI[®]-IPr = [1,3-bis(2,6-diisopropylphenyl)imidazol-2-ylidene](3-chloropyridyl)palladium(II) dichloride. Reaction conditions: **54** (1.0 mmol), TMSBr (1.1 mmol), DMSO (1.1 mmol), 1,4-dioxane (3 mL), RT, 2 h; 1-naphthaleneboronic acid (1.3 mmol), K₂CO₃ (3.0 mmol), PEPPSI[®]-IPr (0.02 mmol), *i*PrOH (4 mL), 60 °C, 24 h.

4.6 Conclusion and outlook

A non-aqueous, mild and facile bromination reaction of arenes and heteroarenes in the TMSBr/DMSO system has been developed. Electron-rich arenes are brominated with good tolerance of sensitive functional groups. The position *para* to the EDG was selectively brominated, while *ortho* bromide derivatives were detected only in a few cases. This method is suitable for large-scale syntheses because the reagents are stable and readily available, and the volatile by-products can be easily removed by evaporation. Furthermore, three synthetic applications were implemented to show that our bromination can be directly combined with other transformations to synthesize complex molecules in short and efficient procedures. The lithiation reaction, in particular, highlights the advantage of our non-aqueous protocol.

For further investigations, mechanistic studies focusing on the relationship between substrate and solvent could be useful for a deeper insight into this reaction. Also, this work is particularly amenable to an application for flow chemistry which could maximize the advantages of this protocol. For example, a flow of arenes and DMSO could be mixed with a TMSBr solution at low temperature before a heating column, followed by a continuous evaporation treatment to remove TMSOH and SMe_2 (**Figure 19**).

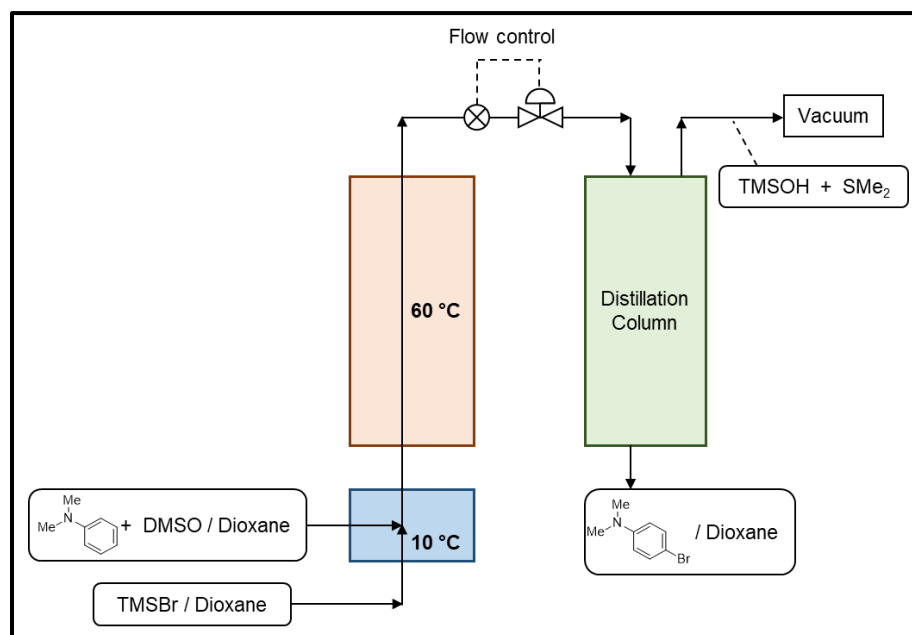


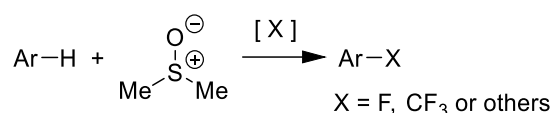
Figure 19. Diagram of a suggested flow system.

Chapter 5

Exploring DMSO-based Oxidative Functionalizations

5.1 Introduction

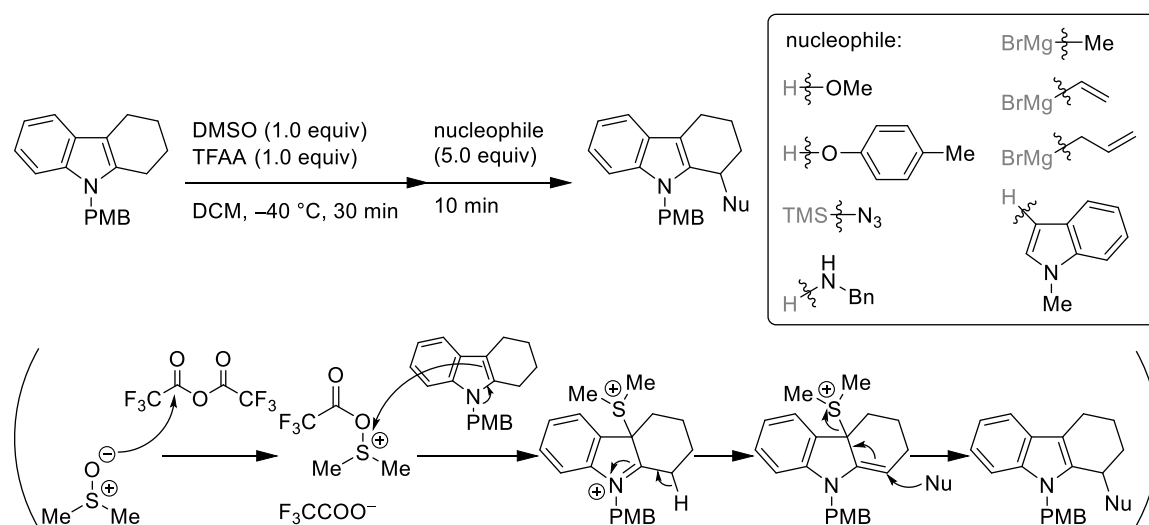
The investigations of oxidative functionalizations of arenes is described herein. Since the DMSO-based bromination of arenes (Chapter 4) was successfully developed, other functionalizations were attempted with DMSO as an oxidant (**Scheme 86**). Particularly, fluorination reactions and trifluoromethylation reactions were in the focus. General overviews about fluorination and trifluoromethylation are described in Sections 1.2 and 1.6.2, respectively.



Scheme 86. DMSO-based oxidative functionalizations of arenes described in this chapter.

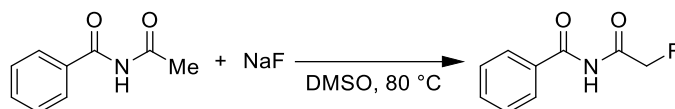
5.1.1 DMSO-based oxidative functionalizations in the literature

DMSO-based oxidative functionalizations have been developed in a wide variety.^[147] For example, arenes have been functionalized with Cl, I, O-, S-, Se- and Te moieties.^[325–329] Apart from aromatic oxidations, DMSO-based oxidative transformations of thiols to disulfides,^[330] alkynes to 1,2-diketones,^[331] hydrazones to diazo compounds^[332] and isonitriles to isocyanates^[333] as well as oxidations of alcohols^[150] and oxidative additions of olefins^[334,335] are known. More recently, oxidative functionalizations of *N*-substituted indoles by the combination of DMSO and trifluoroacetic anhydride (TFAA) have been reported (**Scheme 87**).^[185] The reactions at indole 2 α -position with various nucleophiles such as alcohols, amines and carbon-based nucleophiles including indoles were demonstrated.



Scheme 87. Activation of DMSO by TFAA for C–H functionalizations of *N*-substituted indoles.^[185] PMB=*p*-Methoxybenzyl group.

Additionally, an interesting DMSO-based fluorination with NaF and DMSO was reported (**Scheme 88**).^[336] This simple procedure is very attractive and does not require any DMSO-activator. However, we could not reproduce this procedure and no signals were detected in ¹⁹F NMR spectrum of the crude mixture.

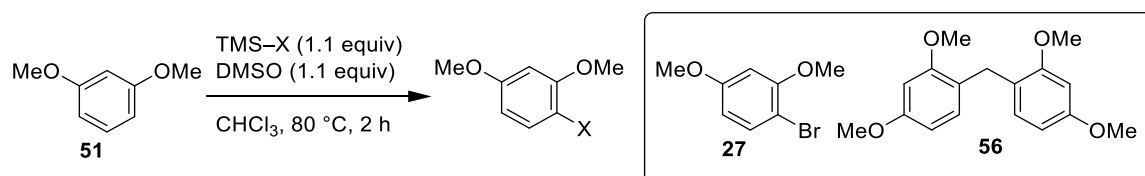


Scheme 88. DMSO-based oxidative fluorination at α -position of carbonyl compounds.^[336]

5.1.2 Preliminary experiments

Under similar reaction conditions as for the bromination reaction of Chapter 4, various trimethylsilyl compounds were tested for functionalizations of arene **51** with DMSO as an oxidant (**Table 16**). The desired product was obtained only in the case of TMSBr (entry 3), while TMSCl produced a small amount of methylene-bridged compound **56** (entry 2). The formation of such compounds where DMSO serves as an electrophile have been reported (**Scheme 89**).^[147] Since the

Table 16. Screening of trimethylsilyl compounds for DMSO-based functionalizations.^[a]

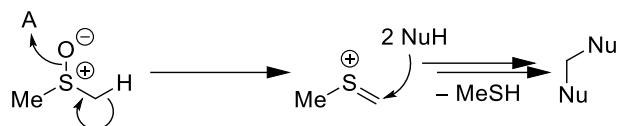


entry	-X	Result
1	-F	No Products ^[b]
2	-Cl	A trace amount of compound 56 . ^[c]
3	-Br	Brominated product 27 in 99% yield. ^[d]
4	-I	No Products ^[b]
5	-CN	No Products ^[b]
6	-CF ₃	No Products ^[b]
7	-N ₃	No Products ^[b]
8	-OTf	No Products ^[b]
9	-1-imidazole	No Products ^[b]
10	-TMS	No Products ^[b]

^[a] Reaction conditions: **51** (1.0 mmol), TMSX (1.1 mmol), DMSO (1.1 mmol), CHCl₃ (3 mL), 80 °C, 2 h. ^[b] Analyzed by ¹H NMR.

^[c] Compound **56** was detected by GC-MS. ^[d] Determined by GC-FID with decane as the internal standard.

application of these conditions was found to be limited to bromination, other reaction conditions were to be studied for DMSO-based oxidative functionalizations.

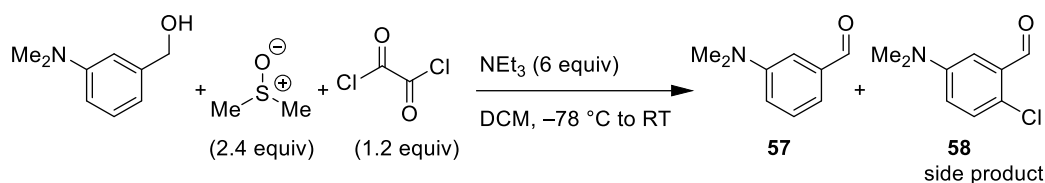


Scheme 89. The formation of methylene-bridged compounds with DMSO as an electrophile.^[147] “A” represents a DMSO-activator.

5.2 DMSO-based halogenations of arenes

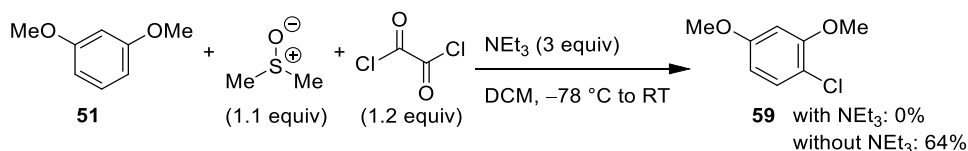
5.2.1 Oxidative chlorinations with oxalyl chloride

When preparing aldehyde **57** (used in Chapter 4), an aromatic chlorination was observed in the Swern oxidation giving chlorinated side product **58** (**Scheme 90**). Although similar side reactions in the Swern oxidation are known,^[337,338] no studies on such chlorinations have been reported.



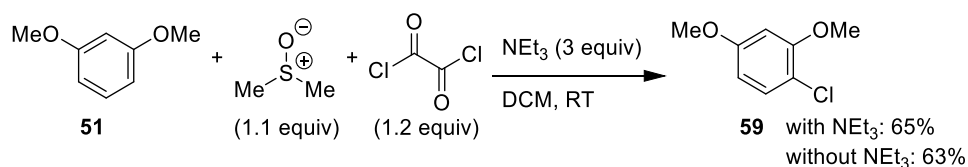
Scheme 90. The formation of a side product in the Swern oxidation. Reaction conditions: oxalyl chloride (6 mmol), DMSO (12 mmol), 3-(*N,N*-dimethylamino)benzyl alcohol (5.0 mmol), triethylamine (30 mmol), DCM (35 mL), -78°C to RT, 2 h. Side product **58** was identified by ^1H NMR and GC-MS after purification by column chromatography on silica gel.

To evaluate the oxalyl chloride/DMSO system, oxalyl chloride was employed as a DMSO-activator for the oxidative chlorination of arene **51** (**Scheme 91**). However, similar conditions did not yield chlorinated products. The role of bases in the Swern oxidation is the deprotonation for the formation of alkoxy-sulfonium ylides (See Section 1.5.1 for the mechanism of the Swern oxidation). Therefore, bases should be unnecessary in this aromatic chlorination. Thus, the same reaction but without bases was carried out and the expected chlorination was achieved giving product **59** in 64 % yield.



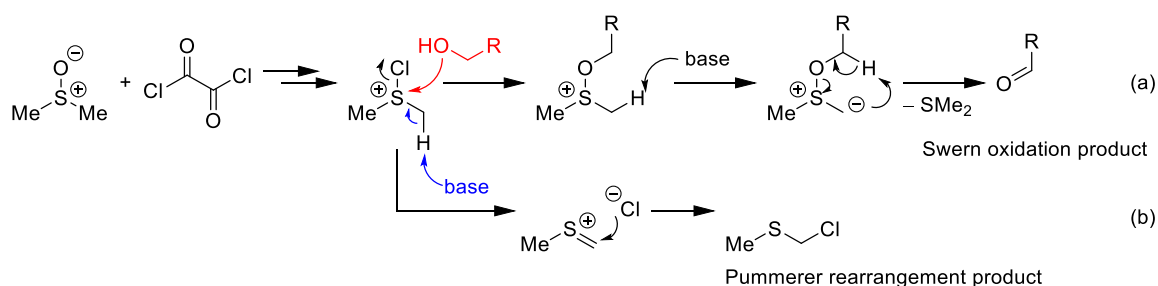
Scheme 91. Oxidative chlorination of arene **51** in oxalyl chloride/DMSO system. Reaction conditions: **51** (1.0 mmol), DMSO (1.1 mmol), oxalyl chloride (1.2 mmol), triethylamine (0 or 3.0 mmol), DCM (3 mL), $-78\text{ }^\circ\text{C}$ to RT, 2 h. The yields were determined by GC-FID with decane as the internal standard.

Surprisingly, the reaction mixture did not have to be cooled down unlike for the Swern oxidation; the aromatic chlorination of arene **51** in the oxalyl chloride/DMSO system at room temperature with or without a base produced chlorinated product **59** (**Scheme 92**). Therefore, the aromatic chlorination is inhibited by triethylamine at $-78\text{ }^\circ\text{C}$.



Scheme 92. Oxidative chlorination of arene **51** in the oxalyl chloride/DMSO system at room temperature. Reaction conditions: **51** (1.0 mmol), DMSO (1.1 mmol), oxalyl chloride (1.2 mmol), triethylamine (0 or 3.0 mmol), DCM (3 mL), RT, 2 h. The yields were determined by GC-FID with decane as the internal standard.

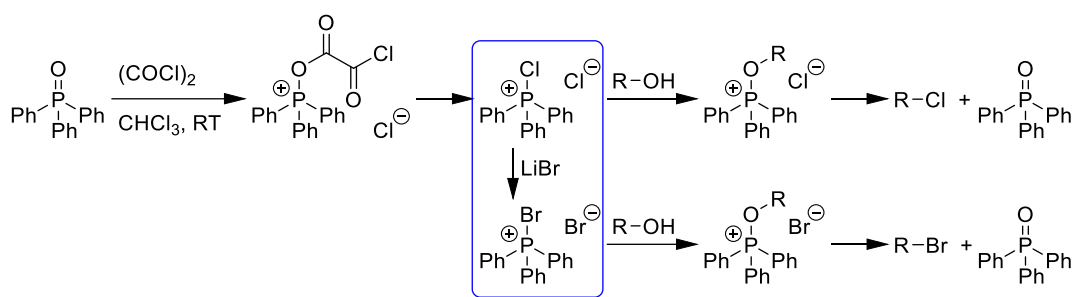
A possible explanation for the inhibition of the chlorination by triethylamine is the Pummerer rearrangement.^[73,339,340] In the Swern oxidation, the sulfonium cation reacts with alcohols at $-78\text{ }^\circ\text{C}$ before a base is added (**Scheme 93a**). The formed alkoxy-sulfonium cation is inactive for the elimination reaction^[341] and produces no Pummerer rearrangement products. In our case (**Scheme 92**), however, arene **51** seems to be reluctant for the reaction with the sulfonium cation at $-78\text{ }^\circ\text{C}$. Furthermore, the deprotonation at the α -position of the sulfonium cation towards the Pummerer



Scheme 93. Reactions of the sulfonium cation. (a) Swern oxidation. (b) Assumed acceleration of the Pummerer rearrangement by a base.

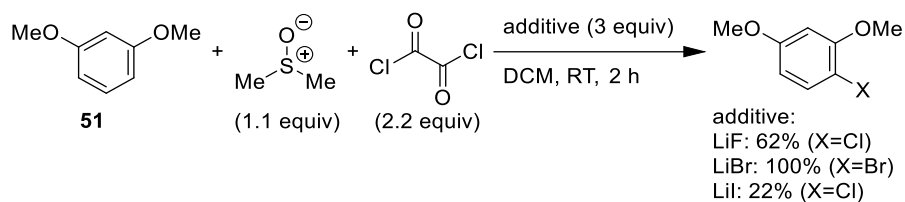
rearrangement may be accelerated by a base (**Scheme 93b**).^[342] At room temperature, however, chlorinated product **59** was obtained in the presence of a base (**Scheme 91**). This indicates that the reaction of arene **51** with the sulfonium cation is faster at room temperature than the base-promoted Pummerer rearrangement.

The group of Denton reported that the halide of the oxidative heteroatom–halogen species can be replaced by external halides.^[343,344] Their original intention was deoxychlorination of alcohols with the P(V)–Cl species that is formed by the reaction of oxalyl chloride and triphenylphosphine oxide (**Scheme 94**). In the presence of LiBr, however, bromide replaces the chloride in P(V)–Cl species to generate P(V)–Br species, which converts aliphatic alcohols to alkyl bromides.^[343]

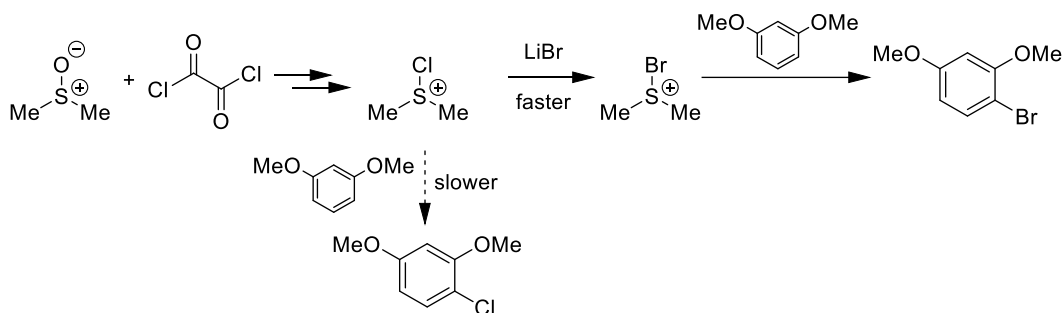


Scheme 94. Chlorination of alcohols by a phosphine oxide and oxalyl chloride. As highlighted, P–Cl species react with an external bromide to generate P–Br species for deoxybromination.^[343]

In the case of the S(IV) analogue, accordingly, the addition of inorganic halide may convert S(IV)–Cl species to other S(IV)–X species for oxidative halogenations of arenes. Thus, LiF, LiBr and LiI, respectively, was added to the oxalyl chloride/DMSO system for the oxidative halogenations of arene **51** (**Scheme 95**). With LiF, no fluorinated product was observed, and chlorinated product **59** was obtained. The addition of LiBr successfully brominated arene **51** and no chlorinated product was observed. The high selectivity for the bromination indicates that attack by bromide on the sulfonium cation intermediate is faster than the aromatic chlorination reaction (**Scheme 96**). At last, LiI produced chlorinated product **59** in 22% yield, while a dark solid precipitated immediately after the addition of the reagents. It is possible that iodide was oxidized to generate molecular iodine, which did not oxidize arene **51** under the given condition.



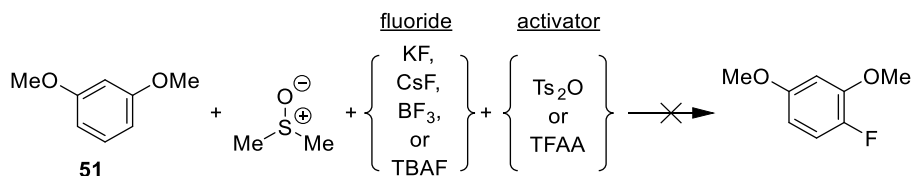
Scheme 95. Aromatic halogenations in the oxalyl chloride/DMSO system with external halides. Reaction conditions: **51** (1.0 mmol), DMSO (1.1 mmol), oxalyl chloride (2.2 mmol), LiX (3.0 mmol), DCM (3 mL), RT, 2 h. The yields were determined by GC-FID with decane as the internal standard.



Scheme 96. Assumed mechanism for aromatic bromination by the addition of LiBr to the oxalyl chloride/DMSO system.

5.2.2 Attempts towards oxidative fluorination

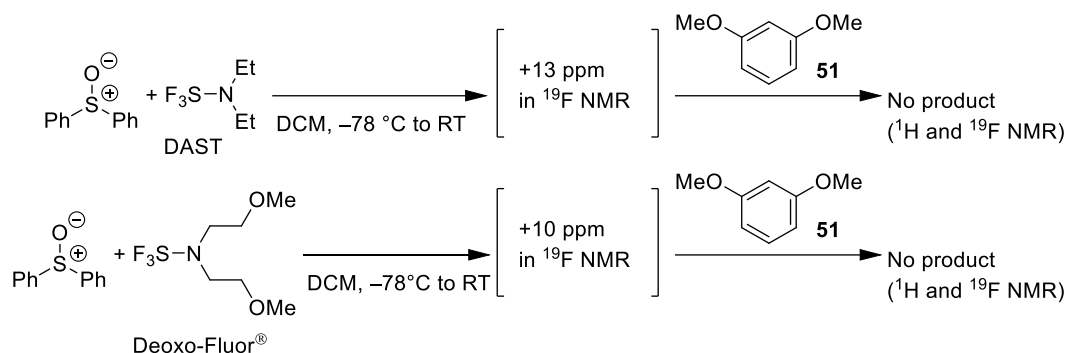
Although fluoride did not substitute chloride in S(IV)–Cl species (**Scheme 95**), fluorination of arenes by S(IV)–F species were further attempted. By the use of DMSO as an oxidant, several fluorides and activators were tested, but no oxidative fluorination was observed in any combination as illustrated in **Scheme 97**.



Scheme 97. Attempted oxidative fluorinations of arene **51** by using DMSO. Reaction conditions: **51** (1.0 mmol), DMSO (1.1 mmol), fluoride (3.0 mmol), activator (1.1 mmol), DCM (3 mL), RT, 2 h. The reaction mixtures were analyzed by ^1H and ^{19}F NMR.

In view of replacing O by F, the transformation of sulfoxides to S(IV)–F species is very similar to deoxyfluorination of alcohols (See Section 1.2.10). Therefore, DAST and Deoxo-Fluor[®] were employed to activate a sulfoxide for the attempt of fluorination of arene **51** (**Scheme 98**). A new

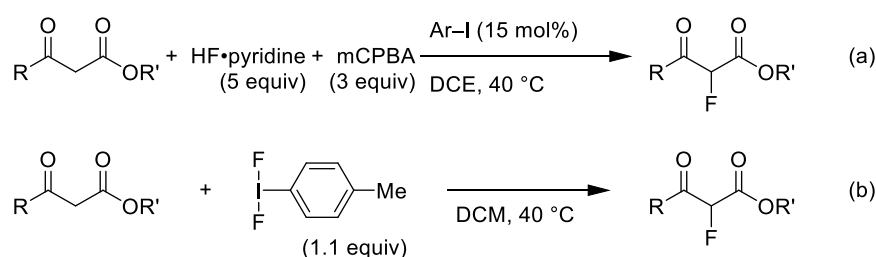
signal at 10–13 ppm in the ^{19}F NMR spectrum of the corresponding reaction mixtures was detected, although no fluorination of arene **51** could be detected.



Scheme 98. Activation of sulfoxides by deoxyfluorinating reagents for oxidative fluorination of arene **51**. Reaction conditions: diphenylsulfoxide (1.0 mmol), deoxyfluorinating reagent (1.0 mmol), DCM (3 mL), $-78\text{ }^{\circ}\text{C}$ to RT, 2 h; then **51** (1.0 mmol), RT, 2 h. The reaction mixtures were analyzed by ^1H and ^{19}F NMR.

5.3 Iodine-based oxidations

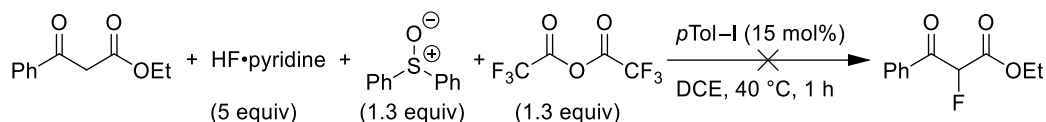
Apart from DMSO-based oxidations, an increasing number of oxidative fluorinations have been reported,^[41,345] including an interesting fluorination reaction reported by the group of Shibata (**Scheme 99a**).^[346] 1,3-Dicarbonyl compounds were fluorinated at the α -position by using HF and mCPBA, where aryl iodides were used as catalysts. This reaction is based on another report that I(III)–F reagents fluorinate the same class of compounds (**Scheme 99b**).^[347,348] Thus, it is believed that I(I) species, which are aryl iodides in this case, are converted to I(III)–F species by HF and mCPBA.



Scheme 99. (a) ArI-catalyzed α -fluorination of 1,3-dicarbonyl compounds.^[346] mCPBA=*m*-Chloroperoxybenzoic acid. (b) α -Fluorination of 1,3-dicarbonyl compounds using *p*-iodotoluene difluoride.^[348]

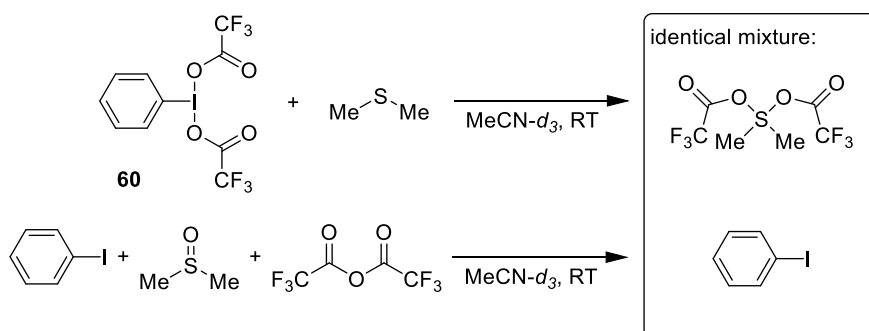
5.3.1 Redox reactions between organoiodine and organosulfur compounds

We attempted a similar oxidative fluorination by using the combination of a sulfoxide and TFAA as an oxidant instead of mCPBA (**Scheme 100**). However, no product was obtained regardless of the used catalysts and activators.



Scheme 100. Attempted ArI-catalyzed oxidative fluorination with a sulfoxide as an oxidant. Reaction conditions: ethyl benzoylacetate (0.5 mmol), hydrogen fluoride-pyridine (2.5 mmol), diphenylsulfonium hexafluoroantimonate (0.65 mmol), TFAA (0.65 mmol), 4-iodotoluene (0.075 mmol), DCE (10 mL), 40 °C, 1 h. The reaction mixture was analyzed by ^1H and ^{19}F NMR.

In order to examine the ability of a sulfoxide to oxidize an organoiodine catalyst, the experiments illustrated in **Scheme 101** were carried out. In one run, (bis(trifluoroacetoxy)iodo)benzene (**60**) and dimethyl sulfide were mixed in $\text{MeCN-}d_3$. In the other run, iodobenzene, DMSO and TFAA were mixed in $\text{MeCN-}d_3$. ^1H and ^{19}F NMR analyses of these mixtures showed identical spectra that correspond to a mixture of TFAA-activated DMSO and iodobenzene. The results indicate that the oxidizing power of activated sulfoxides is insufficient to oxidize I(I) species to I(III) species.

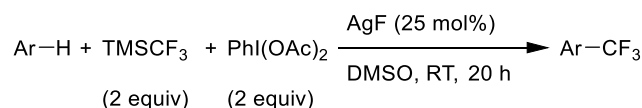


Scheme 101. Experiments to examine the ability of a sulfoxide to oxidize an iodine catalyst. Reaction conditions: **60** (0.2 mmol), dimethyl sulfide (0.2 mmol), $\text{MeCN-}d_3$ (2 mL), RT, 1 h; or, iodobenzene (0.2 mmol), DMSO (0.2 mmol), TFAA (0.2 mmol), $\text{MeCN-}d_3$ (2 mL), RT, 1 h. The reaction was analyzed by ^1H NMR.

5.3.2 Optimization towards facile oxidative trifluoromethylation

Since oxidation of organoiodine catalysts by DMSO seemed challenging, our interest was directed to the analogous trifluoromethylation. In a similar method to the oxidative fluorination by I(III)–F

reagents (**Scheme 99**), Ar-I mediated oxidative trifluoromethylation using TMSCF_3 and stoichiometric I(III) oxidants has been reported (**Scheme 102**).^[349] By combining the ideas corresponding to **Scheme 99** and **Scheme 102**, we focused on the ArI-catalyzed oxidative trifluoromethylation with external oxidants (**Scheme 103**).

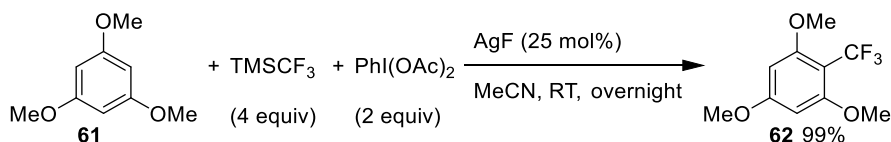


Scheme 102. Silver-catalyzed trifluoromethylation of arenes.^[349]

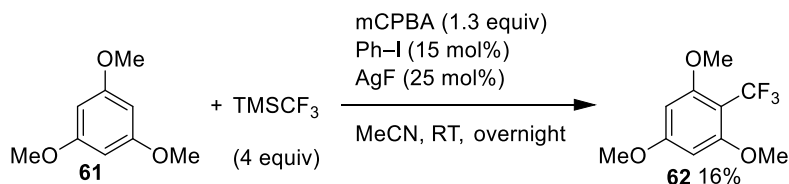


Scheme 103. The idea of ArI-catalyzed oxidative trifluoromethylation.

Because mCPBA and DMSO reacted highly exothermically, we first carried out the trifluoromethylation of arene **61** with TMSCF_3 and PhI(OAc)_2 in MeCN, yielding trifluoromethylated product **62** in 99% yield (**Scheme 104**). However, the replacement of the I(III) oxidant with mCPBA and catalytic PhI led to a low yield of the desired product (**Scheme 105**).

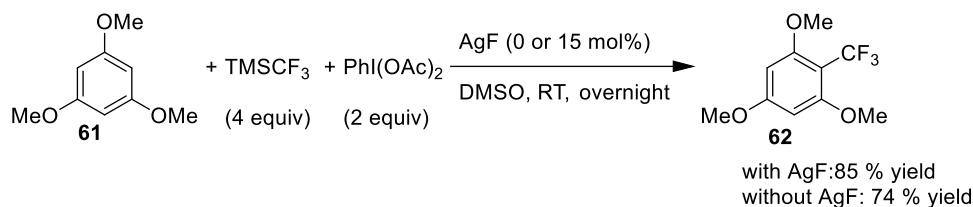


Scheme 104. Oxidative trifluoromethylation of arene **61** in MeCN. Reaction conditions: **61** (0.5 mmol), TMSCF_3 (2.0 mmol), PhI(OAc)_2 (1.0 mmol), AgF (0.125 mmol), MeCN (3 mL), RT, overnight. The yield was determined by ^{19}F NMR with PhCF_3 as the internal standard.



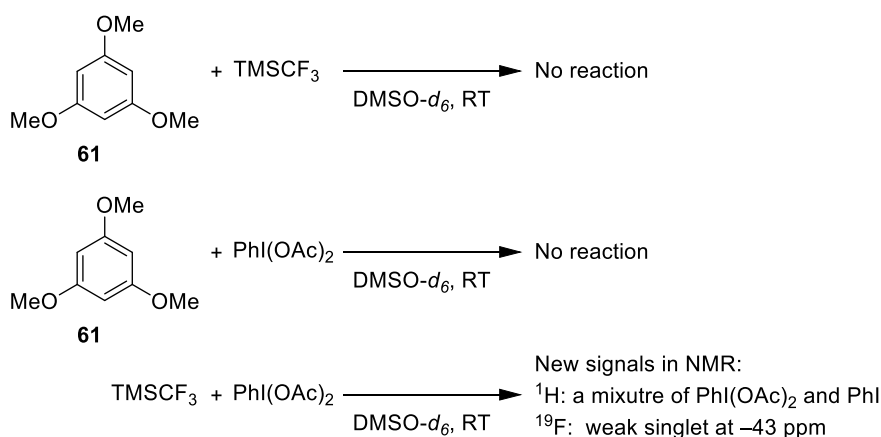
Scheme 105. Oxidative trifluoromethylation with TMSCF_3 and mCPBA in the presence of catalytic iodobenzene and AgF. Reaction conditions: **61** (0.5 mmol), TMSCF_3 (2.0 mmol), mCPBA (0.65 mmol), iodobenzene (0.075 mmol), AgF (0.125 mmol), MeCN (3 mL), RT, overnight. The yield was determined by ^{19}F NMR with PhCF_3 as the internal standard.

The trifluoromethylation reaction of arene **61** by TMSCF_3 and $\text{PhI}(\text{OAc})_2$ was carried out with or without AgF because the role of AgF was not clear in the corresponding report (**Scheme 106**).^[349] Unexpectedly, trifluoromethylated product **62** was produced in good yield in the absence of the catalyst.



Scheme 106. Trifluoromethylation of arene **61** by TMSCF_3 and $\text{PhI}(\text{OAc})_2$ with or without AgF. Reaction conditions: **61** (0.5 mmol), TMSCF_3 (2 mmol), $\text{PhI}(\text{OAc})_2$ (1 mmol), AgF (0 or 0.05 mmol), DMSO (3 mL), RT, overnight. The yields were determined by ^{19}F NMR with PhCF_3 as the internal standard.

To obtain deeper insight into the reaction, reactions of two of each reactant/reagent were carried out (**Scheme 107**). Arene **61** did not react with TMSCF_3 or $\text{PhI}(\text{OAc})_2$ alone. The mixture of TMSCF_3 and $\text{PhI}(\text{OAc})_2$ generated new signals in ^1H and ^{19}F NMR spectra, although the corresponding products could not be identified.⁵



Scheme 107. Reactions between two of the reactant/reagents. Reaction conditions: **61** (0 or 0.5 mmol), TMSCF_3 (0 or 2 mmol), $\text{PhI}(\text{OAc})_2$ (0 or 1 mmol), $\text{DMSO-}d_6$ (3 mL), RT, overnight. The reaction mixtures were analyzed by ^1H and ^{19}F NMR.

⁵ The reaction of TMSCF_3 and PhIX_2 have been studied. See; C. Xu, X. Song, J. Guo, S. Chen, J. Gao, J. Jiang, F. Gao, Y. Li, M. Wang, *Org. Lett.* **2018**, *20*, 3933. They reported that the reaction mixture must be cooled down in order to avoid quick degradation of $\text{ArI}(\text{CF}_3)\text{X}$ species.

5.4 Conclusion

DMSO-based oxidative functionalizations of arenes were investigated. Although TMSX reagents, except for TMSCl and TMSBr, did not activate DMSO, the combination of oxalyl chloride and DMSO chlorinated an arene efficiently. It was also found that the addition of an external bromide to the oxalyl chloride/DMSO system converts arenes to the corresponding aryl bromides. Apart from DMSO-based reactions, oxidative trifluoromethylation of an arene with TMSCF_3 and $\text{PhI}(\text{OAc})_2$ was studied. It was indicated that the reaction between TMSCF_3 and $\text{PhI}(\text{OAc})_2$ possibly generates a reactive intermediate, which could not be identified.

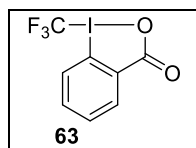
A variety of reactions of TMSCF_3 and I(III) oxidants have been reported.^[350] Acyclic I(III)- CF_3 compounds are usually considered to be less stable than cyclic I(III)- CF_3 compounds.^[204,351] Therefore, in order to further understand trifluoromethylations, the study of reactive intermediates occurring in such reactions by using cyclic I(III)- CF_3 compounds should be useful. The study of trifluoromethylation will be described in Chapter 6.

Chapter 6

Mechanistic Study of a Copper-catalyzed Trifluoromethylation Reaction of Arenes

6.1 Introduction

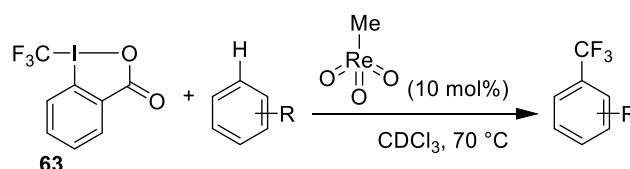
A trifluoromethylation reaction of an arene using our trifluoromethylating reagent **63** was investigated and is reported in this chapter. The goal of this study was to possibly identify reactive intermediates of the trifluoromethylation reaction that would contribute to the development of a DMSO-based oxidative trifluoromethylation reaction (Chapter 5).



6.1.1 Reported trifluoromethylation reactions by using our trifluoromethylating reagents

A general overview of trifluoromethylation reactions is described in Section 1.6. Among trifluoromethylation reactions by our reagents, Cu-catalyzed procedures constitute a significant proportion.^[205] The scope of reported nucleophiles includes silyl enol ethers,^[352] enamines,^[209] alkenes,^[353,354] alkynes,^[208] aryl boranes,^[355,356] alkynyl boranes,^[357] allyl silanes^[358] and aryl zincs.^[359] CuI is the most commonly used Cu(I) compound because of its availability and relative redox stability.^[360] Different kinds of copper species also showed catalytic activity in trifluoromethylation reactions; ionic species like $[\text{Cu}(\text{NCMe})_4]\text{PF}_6$ ^[209,353,354] have been used as stable Cu(I) sources as well as copper(I) thiophene-2-carboxylate (CuTC) and CuSCN.^[357,361] Not only Cu(I) species, but also Cu(II) species such as CuCl_2 and $\text{Cu}(\text{TFA})_2$ have been used with our trifluoromethylating reagents.^[356] In some cases, both Cu(I) and Cu(II) compounds catalyzed a trifluoromethylation reaction under the same reaction conditions.^[362]

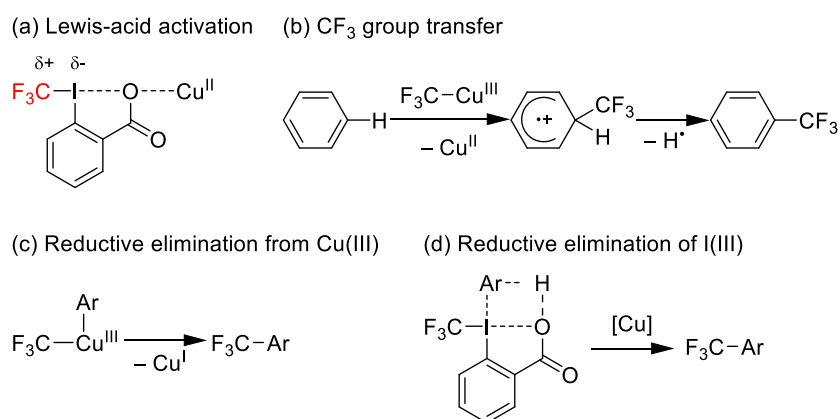
As for trifluoromethylation of arenes, our group reported a methyltrioxorhenium-catalyzed trifluoromethylation of a variety of arenes (**Scheme 108**).^[363] Other reports employed copper catalysts, although they focused on trifluoromethylation of specific substrates such as *N*-heteroarenes^[364,365] and arenes with directing groups.^[366,367]



Scheme 108. Rhenium-catalyzed trifluoromethylation of arenes.^[363]

6.1.2 Mechanistic insights

Many mechanistic studies on Cu-catalyzed trifluoromethylation reactions have been reported (**Scheme 109a, b** and **c**). They include the activation of the reagents by Cu(II) Lewis acids,^[213] the CF₃ group transfer by Cu(III)–CF₃ species^[215] and reductive eliminations of Ar–Cu(III)–CF₃ species,^[212,214,216] as illustrated more in depth in Section 1.6.2. In addition, other general possibilities must be considered. For example, an arene and the reagents may form an adduct or an intermediate in the presence of copper catalysts (**Scheme 109d**). This will lead to the formation of Ar–I(III)–CF₃ species, which may produce the corresponding trifluoromethylated arene by reductive elimination.^[368,369]

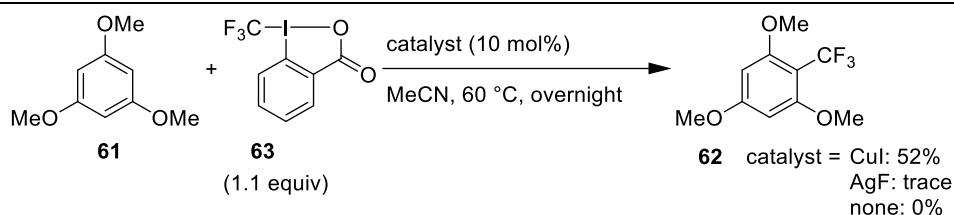


Scheme 109. Plausible mechanisms of Cu-catalyzed trifluoromethylation reactions. (a) Lewis-acid activation of trifluoromethylating reagents by Cu(II) species. (b) CF₃ group transfer to arenes *via* radical mechanisms. (c) Reductive elimination of Ar–Cu(III)–CF₃ species. (d) Reductive elimination of Ar–I(III)–CF₃ species.

6.2 Copper iodide-catalyzed reactions

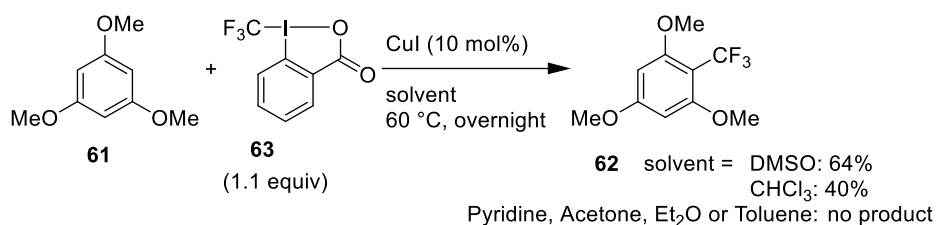
6.2.1 Model reaction

Referring to related examples,^[349,364–367] CuI and AgF were examined as catalysts for trifluoromethylation of arenes by using reagent **63** (**Scheme 110**). Symmetric and electron-rich arene **61** was trifluoromethylated successfully in the presence of CuI. Thus, the mechanistic study of this model reaction commenced.



Scheme 110. Trifluoromethylation of arene **61** by reagent **63**. Reaction conditions: **61** (0.5 mmol), **63** (0.55 mmol), catalyst (0.05 mmol), MeCN (5 mL), 60 °C, overnight. The yields in the crude mixtures were determined by ^1H NMR based on arene **61** with CH_2Br_2 as the internal standard.

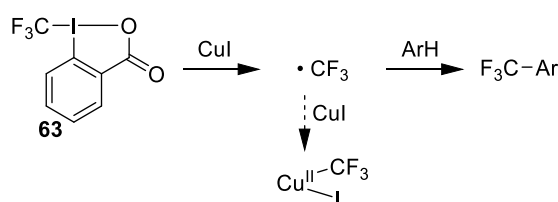
The CuI-catalyzed trifluoromethylation reaction was carried out in other solvents (**Scheme 111**). DMSO and CHCl_3 yielded the desired product, although only DMSO formed a homogeneous reaction mixture. Thus, DMSO was chosen as the solvent for further investigations. Pyridine, acetone, diethylether and toluene did not give trifluoromethylated product **62**.



Scheme 111. Solvent screening for CuI-catalyzed trifluoromethylation of arene **61** by reagent **63**. Reaction conditions: **61** (0.5 mmol), **63** (0.55 mmol), CuI (0.05 mmol), solvent (5 mL), 60 °C, overnight. The yields in the crude mixtures were determined by ^1H NMR based on arene **61** with CH_2Br_2 as the internal standard.

6.2.2 Reactions between CuI and our trifluoromethylating reagent 63

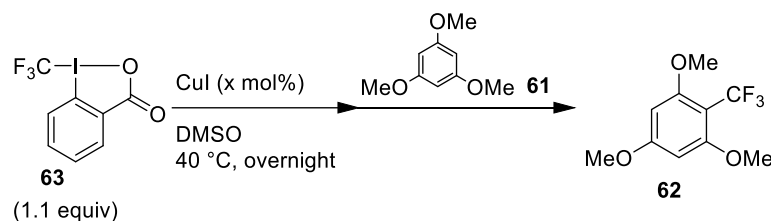
Many researchers describe the generation of the trifluoromethyl radical ($\cdot\text{CF}_3$) by activating reagent **63** towards trifluoromethylation reactions.^[205,370,371] To test this idea, various quantities of CuI were to be exposed to reagent **63**, because $\cdot\text{CF}_3$ should be consumed for the oxidation of excess Cu(I) species to Cu(II) or Cu(III) species (**Scheme 112**).



Scheme 112. Proposed generation of $\cdot\text{CF}_3$ and its trifluoromethylation reaction of arenes. However, $\cdot\text{CF}_3$ may also oxidize CuI to generate Cu(II) or Cu(III) species.

Trifluoromethylations of arene **61** by reagent **63** in the presence of 10–100 mol% of CuI were carried out (**Table 17**). These experiments show that the more CuI was used, the less product was obtained. Although the trend that high equivalents of CuI with respect to reagent **63** interferes with the reaction was as expected, the stoichiometric relation was different from that in **Scheme 112**. If CuI reacts with $\cdot\text{CF}_3$, 2 equivalents of CuI should consume 1 equivalent of reagent **63**. Interpolation of the data in **Table 17** shows that 0.6 equivalents of CuI and 1 equivalent of reagent **63** reacted. Therefore, the generation of $\cdot\text{CF}_3$ described in **Scheme 112** is not very likely in our reaction. It also should be noted that CF_3I was detected by ^{19}F NMR at -9.7 ppm in concentrations correlating to the amount of CuI used. Note that the quantification of CF_3I here is limited by volatility, because the boiling point of CF_3I is -22.5 °C, thus losses cannot be excluded.

Table 17. Trifluoromethylation of arene **61** by reagent **63** with various quantities of CuI.^[a]



entry	x (mol%)	Yield (%) ^[a]	
		62	CF_3I
1	10	59	9
2	40	30	36
3	70	0	60
4	100	0	60

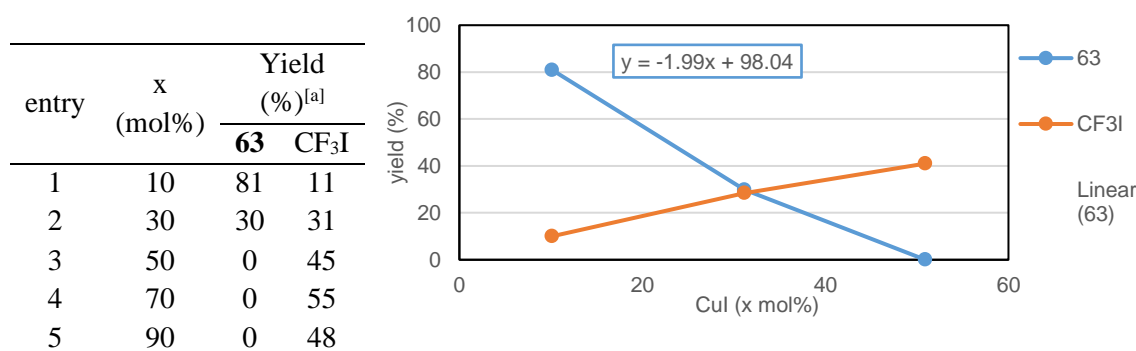
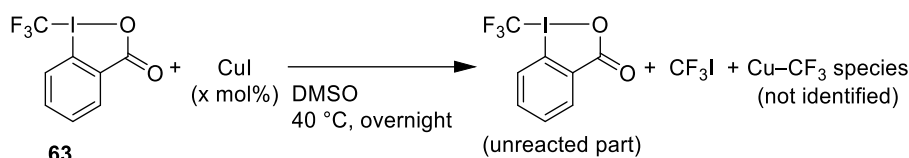
^[a] Reaction conditions: **63** (0.33 mmol), CuI (0.03–0.3 mmol), DMSO (3 mL), RT, 30 min; **61** (0.3 mmol), 40 °C, overnight.

^[b] Determined by ^{19}F NMR analysis of the reaction mixture based on arene **61** with PhCF_3 as the internal standard.

To get a better picture of the reaction between CuI and reagent **63**, simpler experiments without arene **61** were carried out (**Table 18**). Reagent **63** and 10–90 mol% of CuI with respect to reagent **63** were mixed in DMSO, and the consumption of reagent **63** was determined by ^{19}F NMR. The spectra were monitored until they became steady, which took overnight. The ^{19}F NMR signals for CF_3I and the unreacted part of reagent **63** were observed in the reaction mixtures. Additionally, weak signals were detected between -26 and -37 ppm in the ^{19}F NMR spectra, which reportedly correspond to $\text{CF}_3\text{-Cu}$ species.^[372] Yet, the total peak areas were smaller than the used amount of

reagent **63**. It is likely that Cu(II)–CF₃ species were generated in the reaction mixtures, which are known to be NMR inactive.^[212] Therefore, the missing parts of peak integrations should correspond to Cu(II)–CF₃ species. Based on the peak area for the unreacted reagent **63** and their slope in the chart, CuI seemed to consume 2 equivalents of reagent **63**.

Table 18. Reactions between reagent **63** and CuI.^[a] The chart describes the yield of unreacted parts of reagent **63** and CF₃I.



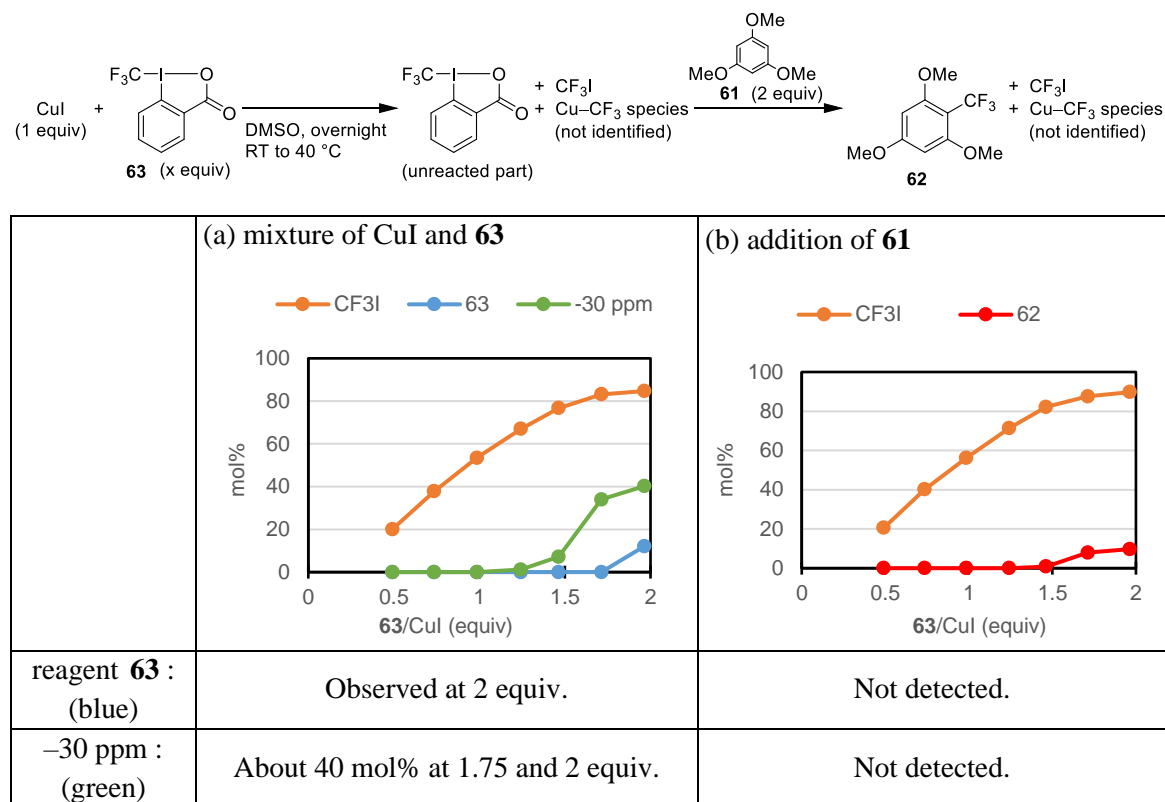
^[a] Reaction conditions: **63** (0.3 mmol), CuI (0.03–0.27 mmol), DMSO (3 mL), 40 °C, overnight.

^[b] Determined by ¹⁹F NMR analysis of the reaction mixture based on reagent **63** with PhCF₃ as the internal standard.

In order to obtain more information about the reaction between CuI and reagent **63**, between 0.5 and 2 equivalents of reagent **63** with respect to CuI were tested (**Table 19**). With 1.75 and 2 equivalents of reagent **63**, a new species characterized by a ¹⁹F NMR signal at –30 ppm appeared in the spectra. The signals for CF₃I and reagent **63** were also detected. Other weak signals for Cu–CF₃ species were observed with lower equivalents of reagent **63**. (They are not plotted in the chart.) The chart shown in **Table 19a** is the data from the experiments at room temperature, but no large difference was seen at 40 °C.

Table 19b shows a chart of the peak integrations of ¹⁹F NMR signals after arene **61** was added to the reaction mixtures. The signal at –30 ppm and the signal for reagent **63** disappeared, while the signal for trifluoromethylated product **62** in around 10% yield was observed. Although these experiments offer many data to interpret, it is important that CF₃I was generated almost proportionally to the used reagent **63** (orange points in the charts), and the signal at –30 ppm was observed before arene **61** was added (green points in the chart).

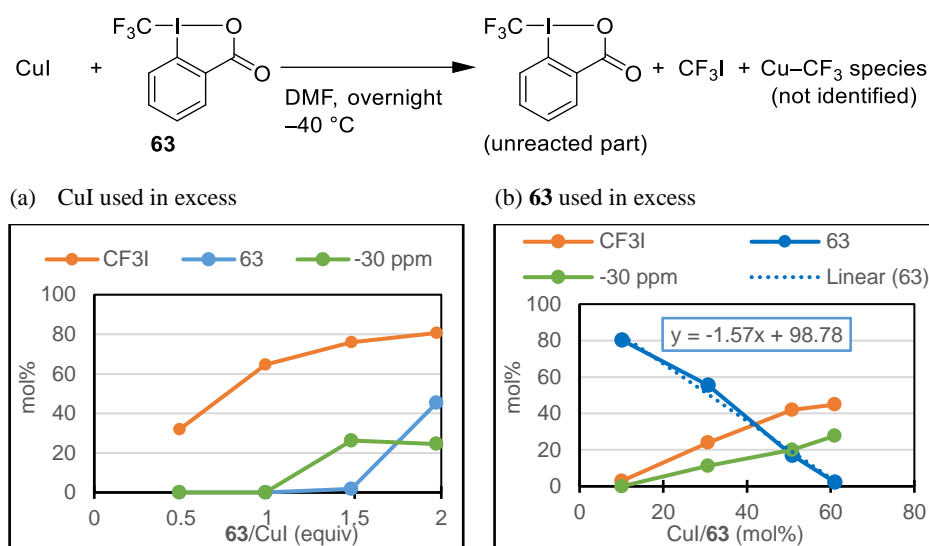
Table 19. Reactions between CuI and reagent **63**, followed by the addition of arene **61**.^[a] The charts describe the yield of observed components in ¹⁹F NMR spectra of the reaction mixtures.



^[a] Reaction conditions: **63** (0.075–0.3 mmol), CuI (0.15 mmol), DMSO (3 mL), RT, overnight; **61** (0.3 mmol), RT, overnight. ^[b] Determined by ¹⁹F NMR analysis of the reaction mixture based on CuI with PhCF₃ as the internal standard.

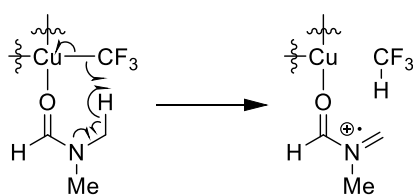
Minor components observed by ¹⁹F NMR might have been generated by the side reactions between CuI and reagent **63**. They are probably irrelevant to the formation of product **62**, because no changes in these signals were found by the addition of arene **61**. In order to prevent these side reactions, experiments were to be carried out at lower temperature in a different solvent, because the freezing point of DMSO is 19 °C. DMF is similarly polar to DMSO, and its melting point is –61 °C. Thus, reactions of CuI and reagent **63** were conducted in DMF at –40 °C where the mixture formed homogenous solutions like in DMSO (**Scheme 113**). As intended, minor signals were not detected in ¹⁹F NMR spectra, while they were detected when the reaction was carried out at 40 °C in DMF.

In order to determine the stoichiometric relation between CuI and reagent **63**, similar experiments with excess of reagent **63** were conducted (**Scheme 113b**, X-axis is CuI/**63** (mol%)). From the slope, it was found that CuI consumed 1.5 equivalents of reagent **63**. Also, an equimolar amount of CF₃I was detected with respect to CuI (**Scheme 113b**, orange). The peak area in ¹⁹F NMR spectrum at –30 ppm increased also proportionally to the used CuI (**Scheme 113b**, green).



Scheme 113. Cold reactions of CuI and reagent **63** in DMF. (a) CuI used in excess. (b) reagent **63** used in excess. Reaction conditions: **63** (0.075–0.3 mmol), CuI (0.015–0.09 mmol), DMF (3 mL), –40 °C, overnight. Yields were determined by ^{19}F NMR analysis of the reaction mixture with PhCF_3 as the internal standard, based on (a) CuI or (b) reagent **63**.

However, trifluoromethylation of arene **61** in DMF at 40 °C produced trifluoromethylated product **62** in low yield while CHF_3 was detected. CHF_3 was not detected when the reactions were carried out in DMSO or CHCl_3 (**Scheme 111**). This can be explained if CHF_3 is generated by abstraction of active hydrogen atoms from the solvent molecule associated with Cu-CF_3 species (**Scheme 114**). The hydrogen atoms on DMF and CHCl_3 are known to be easily abstracted compared to those on DMSO, and CHCl_3 does not coordinate to copper species.^[318] Therefore, the use of DMF as a solvent should be avoided for the production of product **62**. Yet, the data obtained from the experiments at low temperatures are useful, because CHF_3 is not formed at –40 °C.



Scheme 114. Hydrogen abstraction from Cu-coordinating DMF.

6.2.3 Dinuclear copper complex

A crystalline material was obtained from the reaction mixtures of trifluoromethylation reactions. X-ray analysis revealed its structure to be $[\text{Cu}_2(\text{OCOC}_6\text{H}_4)_4 \cdot 2\text{DMSO}]$ (**64**·2DMSO) (**Figure 20**). A similar dinuclear structure is known for $[\text{Cu}_2(\text{OAc})_4 \cdot 2\text{H}_2\text{O}]$ since 1953, where four acetate

ligands are bridging the two Cu(II) centers.^[238] An overview of dinuclear metal complexes is described in Section 1.6.3. The apical positions of the obtained structure are occupied by DMSO, and aromatic rings are tilted out of the carboxylate planes. One pair of aromatic rings is close to coplanar with the carboxylate group, as indicated by the torsion angle O9-C1-C11-C13 of 31.4°. The second pair, however, is almost perpendicular (the corresponding torsion angle is 73.5°). Similar complexes were reported by the group of Sodeoka.^[213]

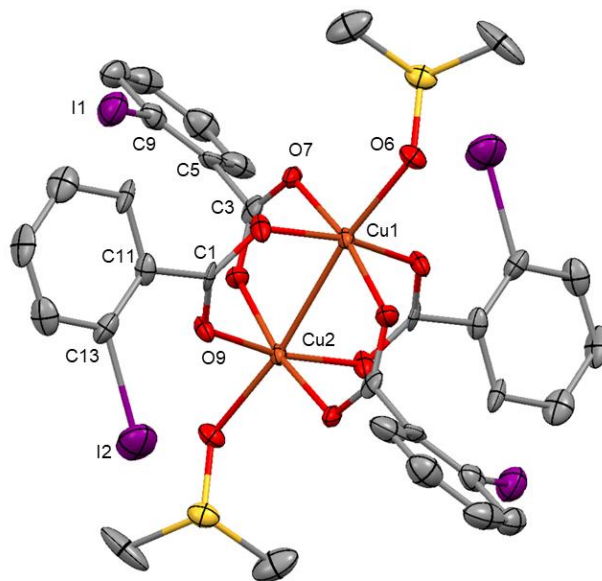
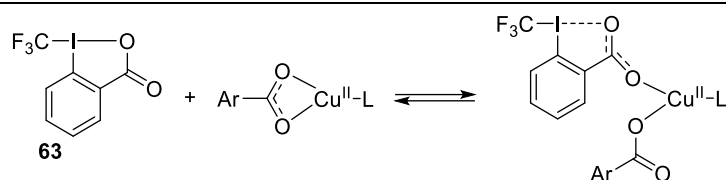


Figure 20. ORTEP representation of **64**·2DMSO obtained from our reaction mixture. H atoms are omitted for clarity. Thermal ellipsoids are set to 50% probability. Selected bond length (Å) and angles (°): Cu1-Cu2 2.620(2), Cu1-O6 2.093(7), Cu1-O7 1.973(8), Cu2-O9 1.960(8), O7-C3-C5-C9 -73.5(3), O9-C1-C11-C13 31.4(2).

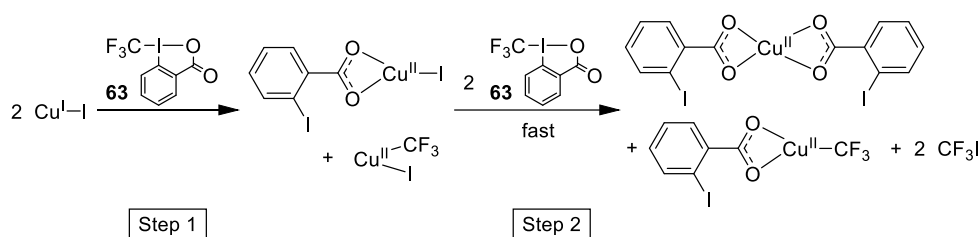
The group of Sodeoka observed a ¹⁹F NMR signal at -32 ppm in the mixture of CuI and reagent **63** in CD₂Cl₂.^[213] With other analyses such as ESI-MS of the mixtures of CuI and reagent **63**, they concluded that this signal at -32 ppm should correspond to an activated reagent by Cu(II) species (**Scheme 115**), shifted from the signal for pure reagent **63** at -35 ppm. This might be true also for our case, since the species corresponding to the -30 ppm signal seemed to react with arene **61** giving trifluoromethylated product **62** (**Table 19b**).



Scheme 115. Cu(II) activation of reagent **63** suggested by the group of Sodeoka.^[213]

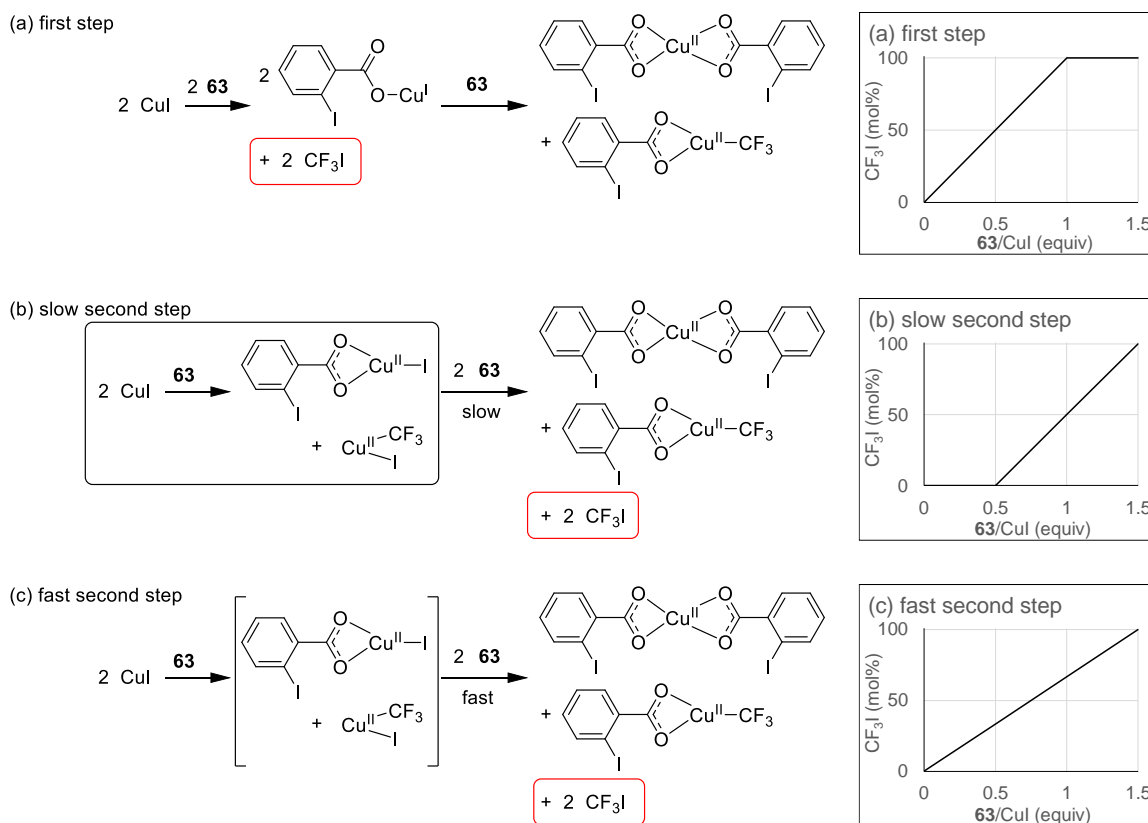
6.2.4 Tentative hypotheses

Drawing from the data so far, it is reasoned that 2 equivalents of CuI and 3 equivalents of reagent **63** react releasing 2 equivalents of CF₃I, where the resultant Cu(II) species bear CF₃ groups and/or carboxylates (**Scheme 116**). By this composition, the observations of the generation of CF₃I and the consumption of reagent **63** are reasonable. These Cu(II) species can possibly activate reagent **63** as Lewis acids or form Cu(III) species by further oxidations.



Scheme 116. Reaction of 2 equivalents of CuI and 3 equivalents of reagent **63** toward possible Cu(II) mixtures bearing CF₃ groups and/or carboxylates.

It is reasonable to assume that CF₃I is generated in a fast second step as shown in **Scheme 116** because **Scheme 113a** shows a gradual generation of CF₃I. First of all, the Cu–I bond is expected to break when the oxidation state of Cu is +II rather than +I, because Cu(II)–I bond is known to be weak compared to Cu(I)–I bond.^[373,374] Furthermore, if it occurs in the first step (**Scheme 117a**), all the iodide from CuI should be used for the generation of CF₃I by the addition of 1 equivalent of reagent **63**. Therefore, the generation of CF₃I in this case would be saturated with 1 equivalent of reagent **63** as drawn in the chart of **Scheme 117a**. Even though CF₃I is generated in the second step, this step must be faster than the first one. The slow generation of CF₃I in the second step (**Scheme 117b**) would lead to reaction with 0.5 equivalents of reagent **63** without the generation of CF₃I, followed by the addition of the other 1 equivalent of reagent **63** producing CF₃I. Therefore, CF₃I should be generated in the fast second step (**Scheme 117c**) to explain the observations in **Table 19** and **Scheme 113**.

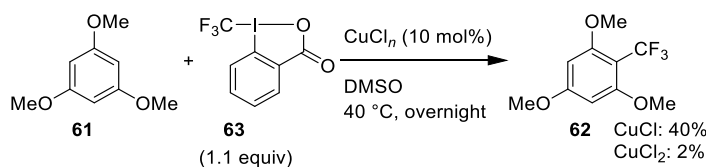


Scheme 117. Possible reaction patterns of CuI and reagent **63** and schematic representations of expected yield of CF₃I with respect to CuI depending on the stoichiometric ratio **63**/CuI. Three possibilities characterized by the reaction pattern and the relative rate of the two steps shown in **Scheme 116** are presented: (a) CF₃I generates in the first step. (b) CF₃I generates in the slow second step. (c) CF₃I generates in the fast second step.

6.3 Other copper catalysts

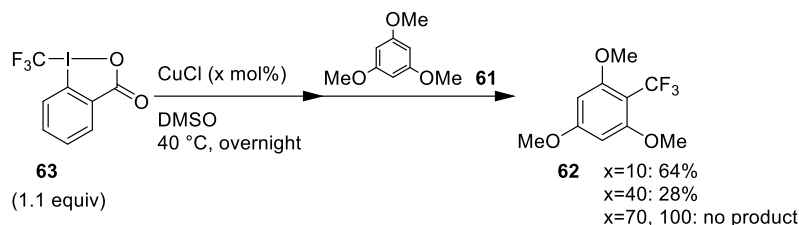
6.3.1 CuCl vs. CuCl₂

CuCl and CuCl₂ were tested for the model trifluoromethylation reaction (**Scheme 118**). CuCl₂ did not catalyze the reaction, but CuCl gave trifluoromethylated product **62** in 40% yield. This was surprising, as the literature showed that Cu(II) species also activate the trifluoromethylating reagents.^[362]



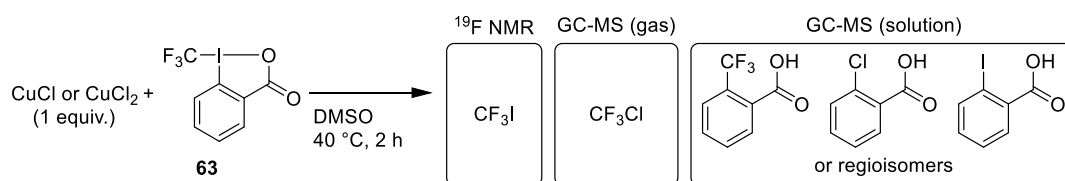
Scheme 118. CuCl_n-catalyzed trifluoromethylation of arene **61** by reagent **63**. Reaction conditions: **61** (0.5 mmol), **63** (0.55 mmol), CuCl_n (0.05 mmol), DMSO (10 mL), 40 °C, overnight. Yields were determined by ¹⁹F NMR analysis of the reaction mixture based on arene **61** with PhCF₃ as the internal standard.

Varying equivalents of CuCl were used to examine its effect on the reaction (**Scheme 119**). The yield decreased as more CuCl was used, and CF₃I was detected in trace amounts. It is likely that the possible formation of CF₃Cl could not be detected by ¹⁹F NMR because the boiling point of CF₃Cl is -81.5 °C.



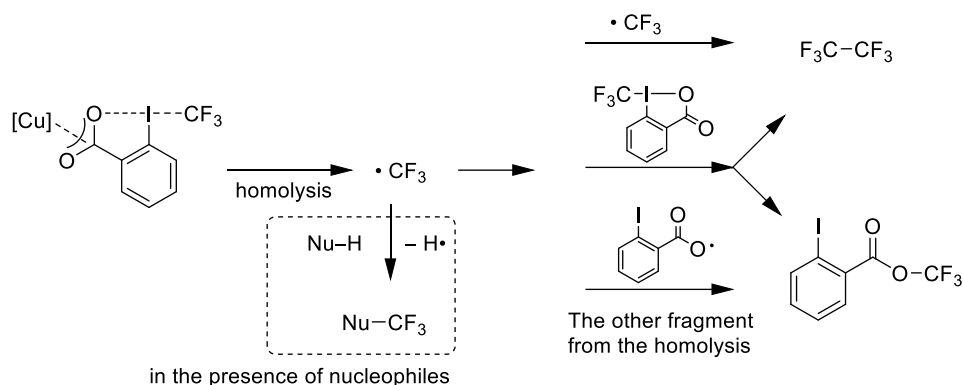
Scheme 119. Trifluoromethylation of arene **61** by reagent **63** in the presence of CuCl. Reaction conditions: **61** (0.3 mmol), **63** (0.33 mmol), CuCl (0.03–0.3 mmol), DMSO (3 mL), 40 °C, overnight. Yields were determined by ¹⁹F NMR analysis of the reaction mixture based on arene **61** with PhCF₃ as the internal standard.

Qualitative analyses of the reaction of CuCl_n and reagent **63**, without arene **61**, are summarized in **Scheme 120**. Similar products were detected with either of the CuCl_n precursors. It is important to note that C₂F₆ and trifluoromethyl iodobenzoate were not detected in the reaction mixtures, and their absence is a positive indication to exclude the involvement of ·CF₃ (**Scheme 121**). If the activation of reagent **63** leads to the generation of ·CF₃ without intended nucleophiles, which would be arene **61** in our case, the free radical should react with other components. C₂F₆ can be produced by recombination of ·CF₃ or reaction with another molecule of reagent **63**. The reaction of reagent **63** and ·CF₃ may produce trifluoromethyl 2-iodobenzoate,⁶ which also could be formed by radical recombination of ·CF₃ and the carboxyl radical generated from the homolysis. Copper precursors may react with ·CF₃, although this is unlikely as it has been already examined in Section 6.2.2.



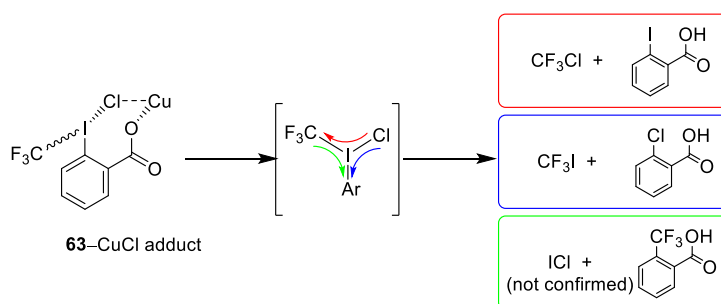
Scheme 120. Qualitative analyses of the reaction of CuCl_n and reagent **63**. Reaction conditions: **63** (0.5 mmol), CuCl_n (0.5 mmol), DMSO (3 mL), 40 °C, 2 h.

⁶ This compound is also the product of an isomerization of reagent **63** by reductive elimination, which has never been observed because of high activation barrier. See computational studies: T.-Y. Sun, X. Wang, H. Geng, Y. Xie, Y.-D. Wu, X. Zhang, H. F. Schaefer III, *Chem. Commun.* **2016**, 52, 5371; H. Jiang, T.-Y. Sun, Y. Chen, X. Zhang, Y.-D. Wu, Y. Xie, H. F. Schaefer, *Chem. Commun.* **2019**, 55, 5667.



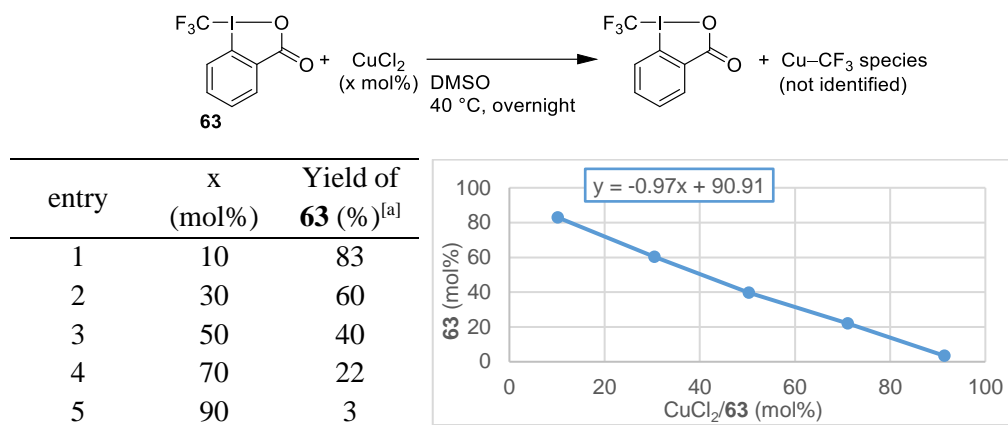
Scheme 121. Expected products that the reactions with $\cdot\text{CF}_3$ would produce in the absence of nucleophiles.

Liquid-phase GC-MS analyses of the reaction mixtures (**Scheme 120**) detected derivatives of iodobenzoic acid in which iodine was displaced by CF₃ or Cl. The formation of these products indicates that a **63**-CuCl adduct was generated, followed by different reductive eliminations to generate the observed products (**Scheme 122**). “CuCl” in **63**-CuCl species herein is not limited to Cu(I)Cl but it also can be Cu(II) species bearing chloride. Aromatic ring, CF₃ and Cl are coordinated to I(III) center, and three different patterns of reductive elimination of this adduct are possible. For example, if I-Cl and I-CF₃ bonds are broken, CF₃Cl and I-Ar species are produced as indicated in red in the scheme.

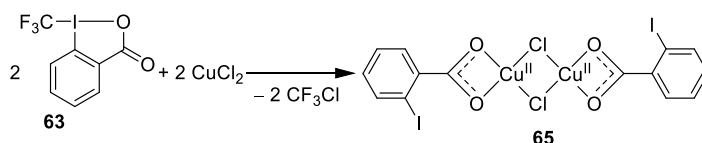


Scheme 122. Reductive eliminations of **63**-CuCl adduct.

Reactions of various equivalents of CuCl₂ and reagent **63** were carried out to find out the reason that CuCl₂ was catalytically inactive (**Table 20**). CuCl₂ consumed 1 equivalent of reagent **63**, and no ¹⁹F NMR signals in Cu-CF₃ region were found in these experiments. Considering that CF₃Cl was generated in the mixture of CuCl₂ and reagent **63**, the rest of the components may form complex such as [Cu(II)ClOCOA₂]₂ (**65**) (**Scheme 123**). This type of compound is known to form square planar dinuclear complexes.^[375]

Table 20. Reactions of CuCl₂ and reagent **63**.^[a] The chart describes the yield of unreacted parts of reagent **63**.


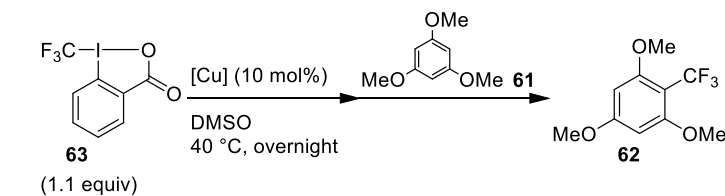
^[a] Reaction conditions: **63** (0.3 mmol), CuCl₂ (0.03–0.27 mmol), DMSO (3 mL), 40 °C, overnight. ^[b] Determined by ¹⁹F NMR analysis of the reaction mixture based on reagent **63** with PhCF₃ as the internal standard.


Scheme 123. Assumed generation of square planar dinuclear complex **65**.

6.3.2 Other copper precursors

CuCN, CuBr, CuBr₂ and CuF₂ were examined as precatalysts for the model trifluoromethylation reaction (**Table 21**). Cu(I) compounds (CuCN and CuBr) promoted the reaction (entries 1–2), although CuBr₂ and CuF₂·2H₂O showed poor activity (entries 3–4).

Table 21. Screening of copper precursors for trifluoromethylation of arene **61**.^[a]



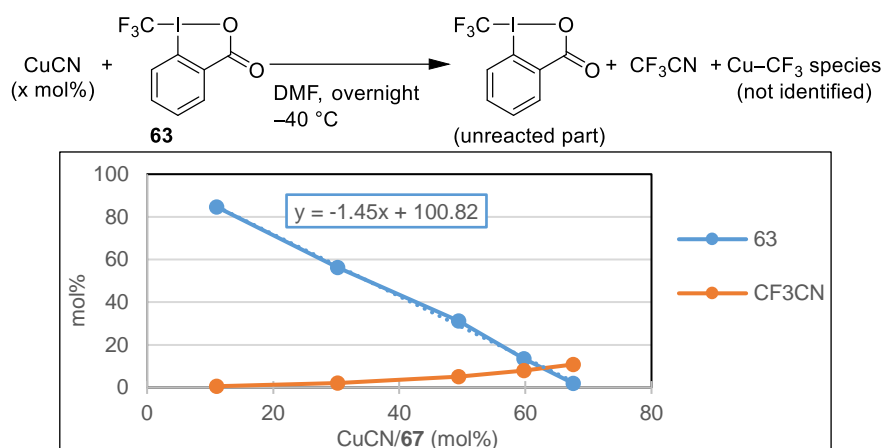
63 (1.1 equiv)

entry	[Cu]	Yield (%) ^[a]
1	CuCN	55
2	CuBr	79
3	CuBr ₂	4
4	CuF ₂ ·2H ₂ O	6

^[a] Reaction conditions: **63** (0.33 mmol), [Cu] (0.03 mmol), DMSO (3 mL), 40 °C, 4 h; **61** (0.3 mmol), 40 °C, overnight.

^[b] Determined by ¹⁹F NMR analysis of the reaction mixture based on arene **61** with PhCF₃ as the internal standard.

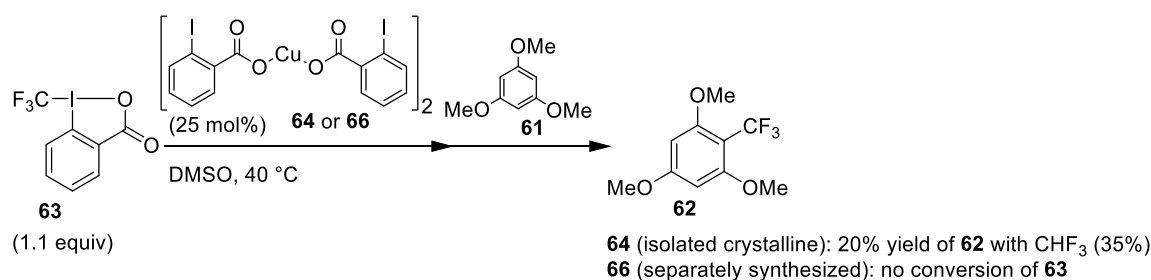
In order to determine the stoichiometry of the reaction of CuCN and reagent **63**, experiments with different ratios of CuCN and reagent **63** were carried out (**Scheme 124**). The observed slope in **Scheme 124** is 1.5, meaning that 2 equivalents of CuCN consumed 3 equivalents of **63**, similarly to CuI. CF₃CN was detected in smaller amounts than CF₃I from CuI, possibly because CF₃CN is volatile with a boiling point of -64 °C.



Scheme 124. Reactions between reagent **63** and CuCN. The chart describes the yield of unreacted parts of reagent **63**. Reaction conditions: **63** (0.15 mmol), CuCN (0.015–0.105 mmol), DMF (10 mL), -40 °C, overnight. Yields were determined by ¹⁹F NMR analysis of the reaction mixture based on reagent **63** with PhCF₃ as the internal standard.

6.3.3 Copper carboxylates

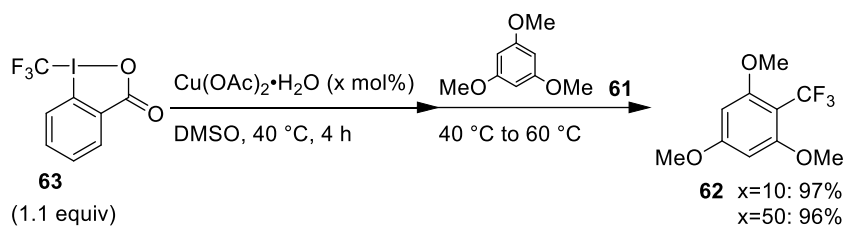
Crystallographically characterized dinuclear complex **64**·2DMSO (**Figure 20**) was used for the model trifluoromethylation (**Scheme 125**). However, the yield was lower than with CuI, and CHF₃ was detected in 35%. A solid material (**66**) obtained from the reaction of copper(II) hydroxide carbonate (Cu₂CO₃(OH)₂) and 2-iodobenzoic acid⁷ was also tested, but reagent **63** was fully recovered.



Scheme 125. Trifluoromethylation of arene **61** by reagent **63** with copper complex **64** or **66** as catalysts. Reaction conditions: **63** (0.33 mmol), **64** or **66** (0.075 mmol), DMSO (3 mL), 40 °C, 4 h; **61** (0.3 mmol), 40 °C, overnight. Determined by ¹⁹F NMR analysis of the reaction mixture based on arene **61** with PhCF₃ as the internal standard.

⁷ The chemical composition was confirmed to be the same as complex **64** by elemental analysis.

Similarly to copper carboxylate **66**, $\text{Cu}(\text{OAc})_2 \cdot \text{H}_2\text{O}$ did not catalyze the reaction at 40 °C (**Scheme 126**). However, it produced trifluoromethylated product **62** in high yield when the reaction mixtures were heated at 60 °C. Interestingly, when 50 mol% of $\text{Cu}(\text{OAc})_2 \cdot \text{H}_2\text{O}$ was used, the yield remained high. This is different from the behavior of CuI , meaning that $\text{Cu}(\text{OAc})_2 \cdot \text{H}_2\text{O}$ itself does not consume reagent **63**. These comparisons indicate that a part of reagent **63** was consumed to oxidize $\text{Cu}(\text{I})$ species, and thus, the possibility that $\text{Cu}(\text{I})$ is the active catalyst may be excluded.



Scheme 126. $\text{Cu}(\text{OAc})_2$ -catalyzed trifluoromethylation of arene **61** by reagent **63**. Reaction conditions: **63** (0.33 mmol), $\text{Cu}(\text{OAc})_2 \cdot \text{H}_2\text{O}$ (0.03 mmol), DMSO (3 mL), 40 °C, 4 h; **61** (0.3 mmol), 40 °C, overnight. Determined by ^{19}F NMR analysis of the reaction mixture based on arene **61** with PhCF_3 as the internal standard.

Having found that $\text{Cu}(\text{OAc})_2 \cdot \text{H}_2\text{O}$ required higher temperature for the trifluoromethylation, other $\text{Cu}(\text{II})$ compounds were tested at elevated temperatures (**Table 22**). Copper carboxylate **66** required 80 °C to promote the trifluoromethylation reaction (entry 2). This difference may be attributed to

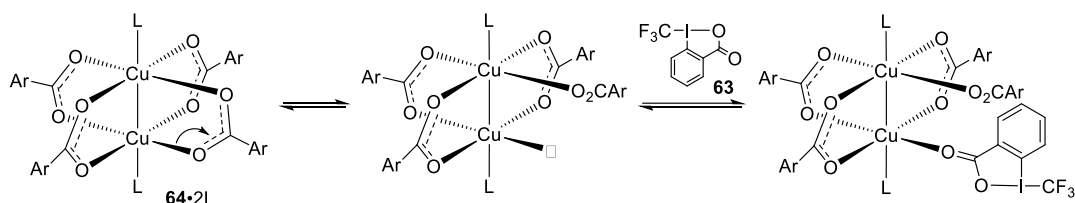
Table 22. Catalyst screening for trifluoromethylation of arene **61** at elevated temperature.^[a]

entry	catalyst	Yield (%) ^[b]		
		40 °C	60 °C	80 °C
1	$\text{Cu}(\text{OAc})_2 \cdot \text{H}_2\text{O}$	3	87	— ^[c]
2	66 (5 mol%)	1	10	84
3	$\text{CuF}_2 \cdot 2\text{H}_2\text{O}$	10	86	— ^[c]
4	CuCl_2	8	62	— ^[c]
5	CuBr_2	8	64	— ^[c]

^[a] Reaction conditions: **63** (0.3 mmol), catalyst (0.03 mmol), DMSO (3 mL), 40 °C, 4 h; **61** (0.6 mmol), 40 °C, overnight.

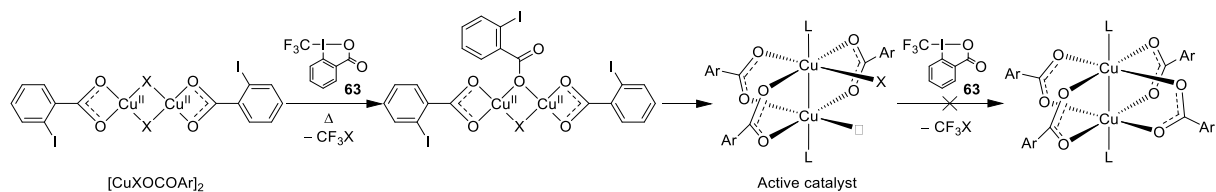
^[b] Determined by ^{19}F NMR analysis of the reaction mixture based on reagent **63** with PhCF_3 as the internal standard. ^[c] Reagent **63** was consumed at 60 °C.

the different acidity of the corresponding conjugated acids ($pK_a(\text{HOAc})=4.7$, $pK_a(\text{HOCOC}_6\text{H}_4\text{I})=2.8$, in H_2O),^[376] indicating that ligand dissociation may be involved in the reaction mechanism as illustrated in **Scheme 127**. One of the bidentate carboxylates dissociates to generate free coordination site, such that another molecule of reagent **63** may coordinate for activation towards trifluoromethylation. In addition to copper carboxylates, Cu(II) halides also catalyzed the reaction at 60 °C (entries 3–5).



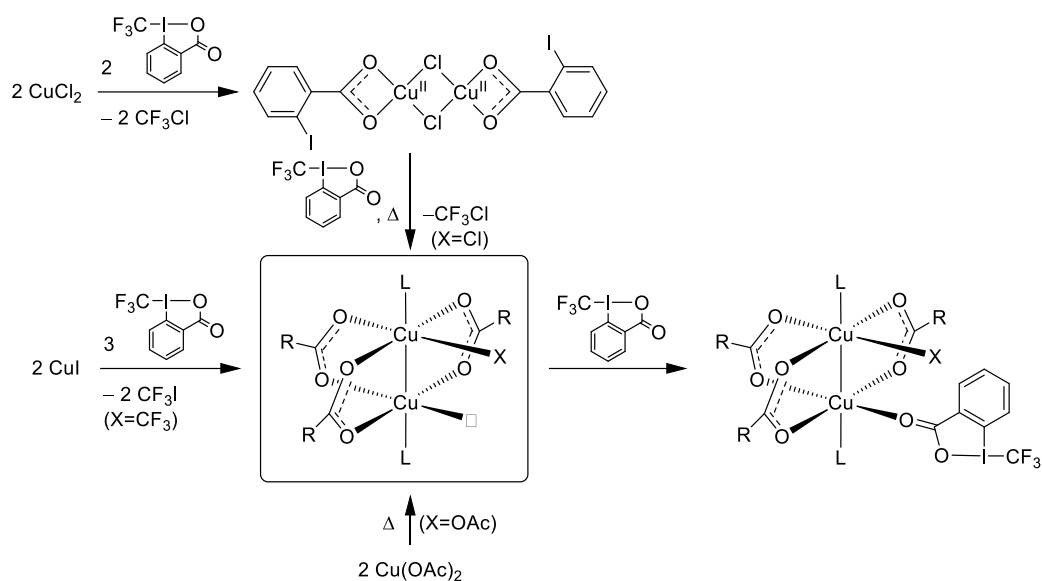
Scheme 127. Ligand dissociation of complex **64** and coordination of reagent **63**. (□ stands for an empty coordination site.)

Under these reaction conditions, reactions of copper(II) halides and reagent **63** may form complexes such as $[\text{CuXOCOAr}]_2$ as illustrated in **Scheme 123**. These species could react with another equivalent of reagent **63** at 60 °C giving a catalytically active species (**Scheme 128**), which is similar to the one described in **Scheme 127**. However, it should not form $[\text{Cu}_2(\text{OCOAr})_4]$ because the required temperatures were higher for complex **66** (**Table 22**, entry 2).



Scheme 128. Plausible reactions of $[\text{CuXOCOAr}]_2$ with reagent **63** to generate the active catalyst.

The most plausible hypothesis as to the catalytically active species is that this corresponds to complexes of the type $[\text{Cu}(\text{II})_2\text{X}(\text{OCOAr})_3]$ where X is CF_3 , halide or monodentate carboxylate (**Scheme 130**). The pathways from CuI, CuCl_2 and $\text{Cu}(\text{OAc})_2$ are described in discussions corresponding to **Scheme 116**, **Scheme 129** and **Scheme 127**, respectively. The different pathways of formation of these complexes, depending on the precursor, may explain the different required reaction temperature for trifluoromethylation of arene **61**. Another molecule of reagent **63** may coordinate to this intermediate for the activation towards trifluoromethylation reaction.



Scheme 130. Generations of the hypothesized active catalyst from CuI, CuCl₂ or Cu(OAc)₂. L is coordinating solvent molecule.

6.4 Supporting the hypothesis

6.4.1 Magnetic susceptibility measurement

According to the literature, dinuclear copper carboxylate complexes show lower magnetic susceptibility than mononuclear ones.^[377–379] Thus, the magnetic susceptibility of the reaction mixture was compared to that of isolated dinuclear complex **64**·2DMSO, [Cu(OAc)₂·H₂O]₂ as a reference for a dinuclear complex, and CuBr₂ as a reference for a mononuclear complex. The results are shown in **Table 23**. The magnetic susceptibility of the reaction mixture was close to that of the dinuclear complexes (entries 1–3), and much lower than that of CuBr₂ (entry 4). These data indicate that the majority of the copper species in trifluoromethylation reaction mixtures exist as dinuclear complexes.

Table 23. Magnetic susceptibility measurement.

entry	[Cu]	solvent	Magnetic susceptibility (B.M.)
1	Reaction mixture ^[a]	DMSO- <i>d</i> 6	1.74
2	64 ·2DMSO	DMSO- <i>d</i> 6	1.64
3	[Cu(OAc) ₂ ·H ₂ O] ₂	DMSO- <i>d</i> 6	1.50
4	CuBr ₂	DMSO- <i>d</i> 6	2.16

^[a] Reaction conditions: **63** (0.075 mmol), CuI (0.05 mmol), DMSO-*d*6 (2 mL), RT, overnight.

6.4.2 Other spectroscopic analyses

EPR measurements were carried out to characterize the active catalyst in a reaction mixture of CuI and reagent **63** by comparing it with copper carboxylate **66**. However, the signals were too weak to allow a reliable characterization (**Figure 21**). It has been reported that the signal intensities of antiferromagnetically-coupled copper(II) centers such as in [Cu(OAc)₂·H₂O]₂ are typically not observable due to a large axial zero-field splitting parameter.^[267,380] These data agree with the formation of dinuclear complexes.

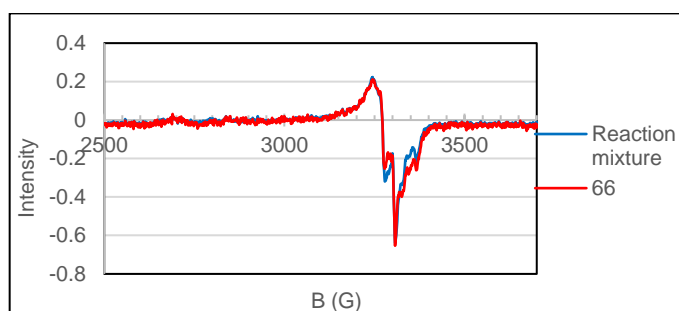


Figure 21. EPR spectra of the reaction mixture of CuI and reagent **63** (blue) and copper carboxylate **66** (red).

UV-VIS spectroscopy was used to compare the dimer/monomer ratio in a mixture of CuI and reagent **63** to copper carboxylate **66** (**Figure 22**). A peak at 370 nm reportedly should be characteristic for a dinuclear structure.^[381] Although the main peak was identical at 733 nm, unfortunately the absorption by aryl groups overlapped with peaks around 370 nm.

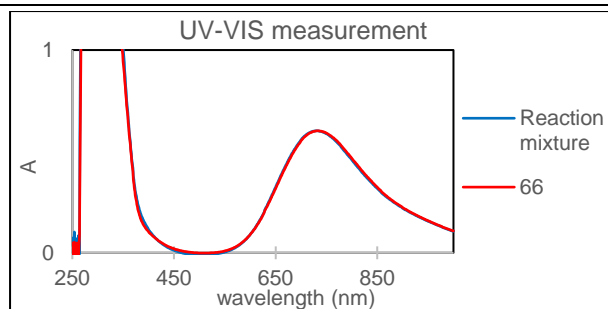
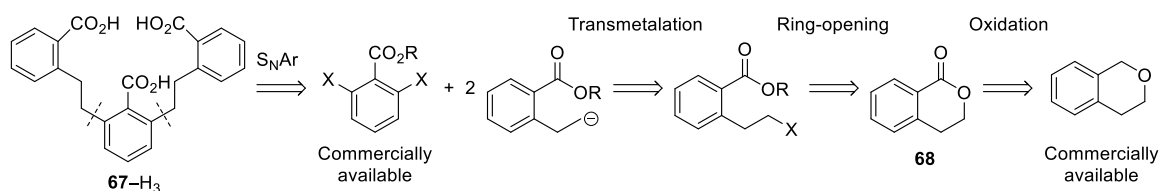


Figure 22. UV-VIS spectra of the reaction mixture of CuI and reagent **63** (blue) and copper carboxylate **66** (red).

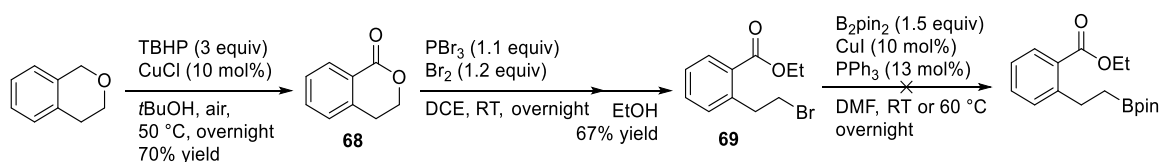
6.4.3 Tricarboxylato complexes

Tricarboxylato complexes were to be synthesized to support the idea that three carboxylate ligands are involved in the active catalyst. Thus, ligand **67**-H₃ was designed, and its retrosynthetic analysis is shown in **Scheme 131**.



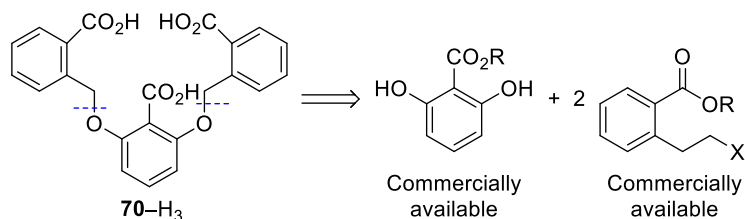
Scheme 131. Retrosynthesis of tricarboxylic acid **67**-H₃ by 4 steps from isochroman.

Procedures starting from isochroman gave the desired bromide (**69**) as shown in **Scheme 132**. However, the subsequently envisaged borylation of bromide **69** was not successful. The conversions were low at room temperature under several conditions, and high temperature promoted cyclization giving back compound **68**.



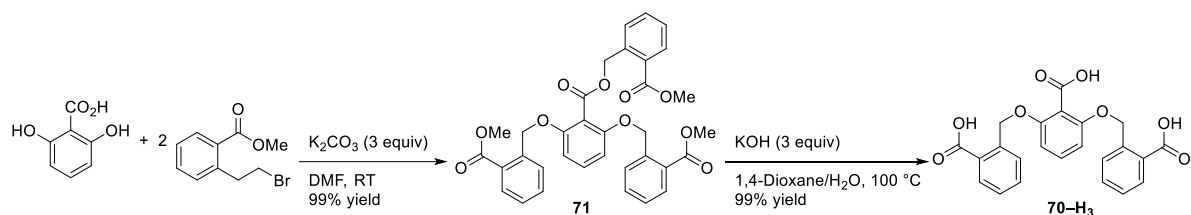
Scheme 132. Oxidation, bromination and borylation toward tricarboxylic acid **67**-H₃. Reaction conditions for oxidation: isochroman (20 mmol), *tert*-butyl hydroperoxide in decane (60mmol, 5.5 M), CuCl (1 mmol), *t*BuOH (200 mL), 50 °C, under air, overnight. Bromination: **68** (12 mmol), PBr₃ (13.2 mmol), Br₂ (14.4 mmol), 1,2-dichloroethane (DCE) (24 mL), RT, overnight; EtOH (12 mmol), RT, 1 h. Borylation: **69** (2 mmol), B₂pin₂ (3 mmol), CuI (0.2 mmol), PPh₃ (0.3 mmol), LiOMe (4 mmol), DMF (8 mL), RT, overnight.

Therefore, the target molecule was modified, such that the three benzoic acid moieties are linked through $-\text{OCH}_2-$ bridges (**Scheme 133**). This might affect the electron density on the central carboxylate, but it increases the flexibility of the chains.



Scheme 133. Retrosynthesis of tricarboxylic acid **70-H₃**.

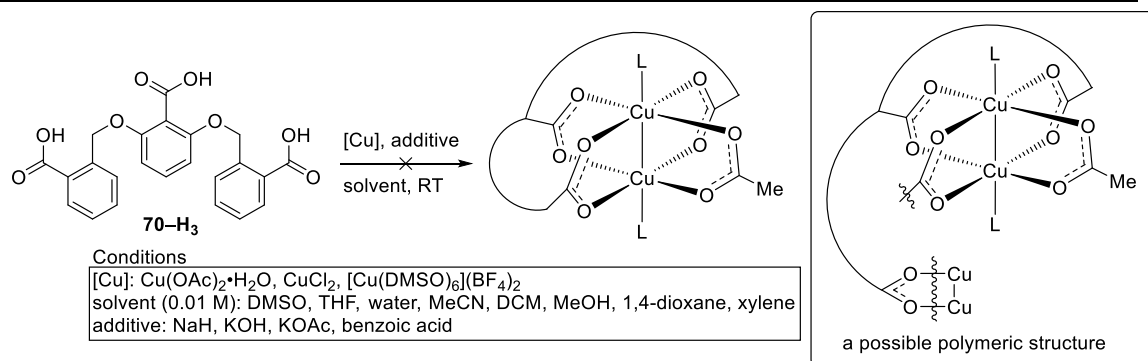
The etherification was carried out at room temperature and provided ester **71** in 99% yield (**Scheme 134**). Solvent choice for the saponification had an influence on the conversion, and the 1,4-dioxane/ H_2O mixed solvent led to a high yield of tricarboxylic acid **70-H₃**.



Scheme 134. Etherification and saponification for the synthesis of tricarboxylic acid **70-H₃**. Reaction conditions for etherification: 2,6-dihydroxybenzoic acid (6 mmol), methyl 2-bromomethylbenzoate (19.2 mmol), K_2CO_3 (28.8 mmol), RT, overnight. Saponification: **71** (3.5 mmol), KOH (30 mmol), 1,4-dioxane (8 mL), water (7 mL), 100 °C, overnight.

However, complexation experiments with ligand **70-H₃** were not successful. Various combinations of copper precursors, solvents and additives were tested, but only a poorly soluble green powdery material could be obtained (**Scheme 135**). We reasoned that the product might be a polymer. The results of corresponding elemental analyses are close to the value for the composition $\text{Cu}_2(\mathbf{70})(\text{OAc})$ (**Table 24**).⁸

⁸ The calculated values for the concerned compositions are listed in the experimental part (Section 8.6.10).



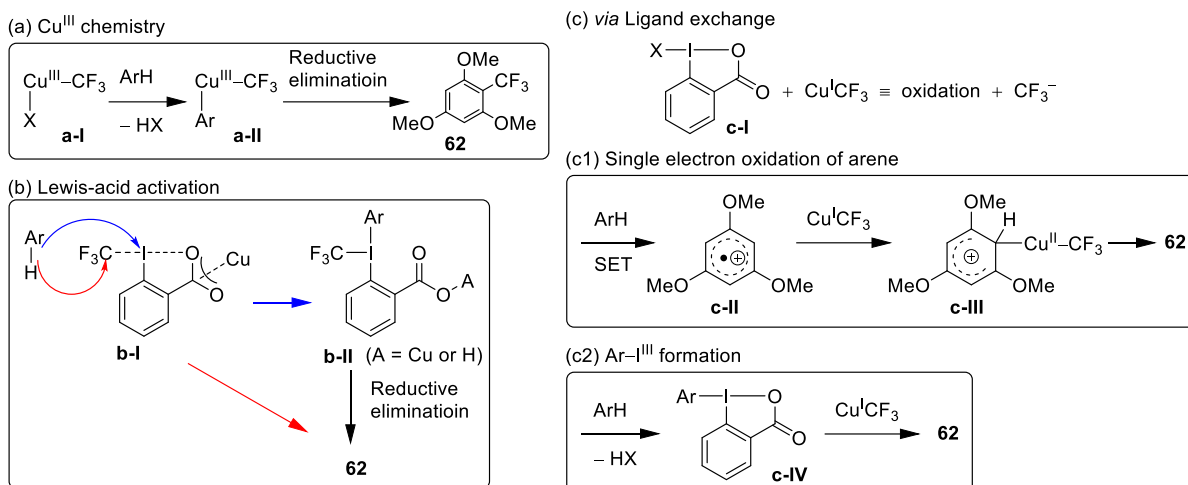
Scheme 135. Attempts of the complexation of Cu₂(**70**)(OAc).

Table 24. Results of elemental analyses and the calculated value for Cu₂(**70**)(OAc)(DMSO)_{0.23}.

Measured		Calculated for Cu ₂ (70)(OAc)(DMSO) _{0.23}	
Element	(wt%)	Element	(wt%)
Cu	21.80	Cu	20.39
C	49.69	C	49.04
H	3.66	H	3.11
O	23.57	O	26.28
S	1.28	S	1.18

6.5 Examination of reaction pathway

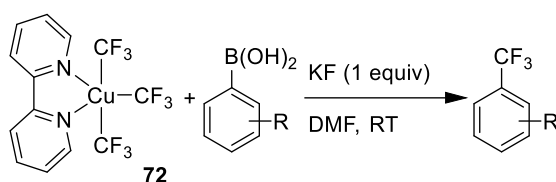
The experiments carried out so far indicate that CuI needs to react with reagent **63** first. Several reaction patterns of CuI and reagent **63** are possible as described in **Scheme 136**. One is the generation of Cu(III) species **a-I** (**Scheme 136a**), since electrophilic trifluoromethylations by Cu(III)–CF₃ species have been reported.^[382] This possibility will be discussed in the following Section 6.5.1. Another is Lewis-acid activation of reagent **63** (**Scheme 136b**), where the oxidation state of copper species may be +II or +III. The data shown thus far support this pathway. An activated reagent (**b-I**) may directly serve as an electrophilic trifluoromethylating species (red arrow). Alternatively, the nucleophilic arene replaces the carboxylate on the I(III) center to form intermediate **b-II** (blue arrow), followed by reductive elimination to yield product **62**. This possibility will be examined in Section 6.5.2. The other possibility is ligand exchange between Cu(I)–X and reagent **63** to give a mixture of **c-I** and Cu(I)CF₃ (**Scheme 136c**), which will be elaborated in Section 6.5.3. Single electron transfer (SET) between **c-I** and arene **61** may generate cation radical **c-II** (**Scheme 136c1**), which combines with Cu(I)CF₃ followed by hydrogen abstraction to give product **62**. Alternatively, arene **61** can substitute the halide of **c-I** to form **c-IV** (**Scheme 136c2**), which undergoes nucleophilic attack by Cu(I)CF₃ to give product **62**.



Scheme 136. Possible mechanisms following the reaction between CuI and reagent **63**.

6.5.1 Electrophilic trifluoromethylations by Cu(III)–CF₃ species

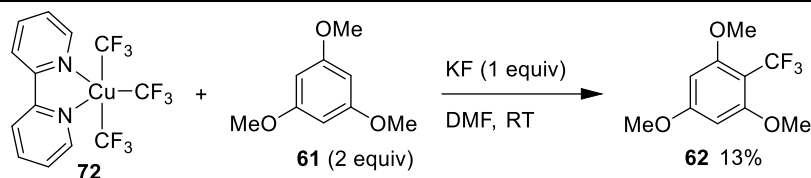
Trifluoromethylation of arene **61** by Cu(III)–CF₃ species is discussed herein. The possibility of the generation of Cu(III) species is low because the magnetic susceptibility measurement does not agree with their involvement (Section 6.4.1).⁹ Nevertheless, Cu(III)–CF₃ species **72** was prepared according to a report on a trifluoromethylation reaction of organoboranes (**Scheme 137**).^[383]



Scheme 137. Trifluoromethylation of organoboranes by Cu(III)–CF₃ species **72**.^[383]

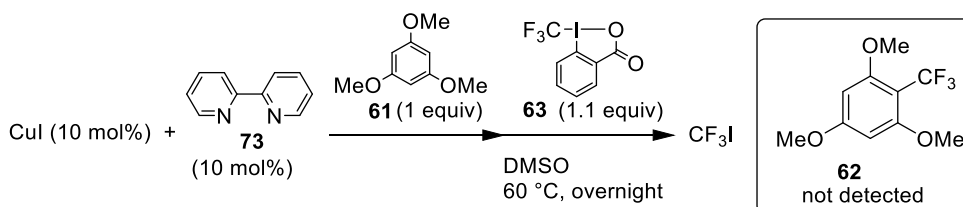
Reactions of reagent **72** with arene **61** were tested under similar conditions to the report (**Scheme 138**). However, conversions of arene **61** and reagent **72** were low. No improvement was observed with addition of bases (K₂CO₃ or NEt₃, 1.2 equivalents) and heating to 60 °C.

⁹ The magnetic susceptibility of Cu(III) species should be 0 (d⁸, low-spin) or about 2.8 B.M. (high-spin) depending on the geometry.

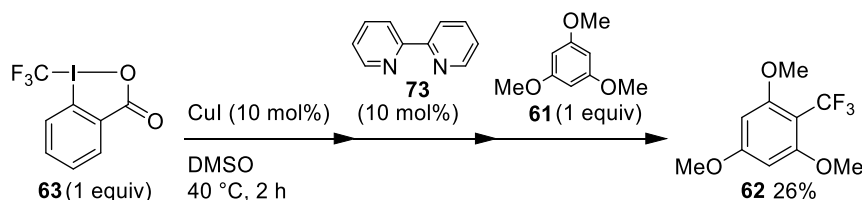


Scheme 138. Reaction of reagent **72** and arene **61**. Reaction conditions: **61** (0.6 mmol), **72** (0.3 mmol), KF (0.3 mmol), DMF (3 mL), RT, overnight. Yields were determined by ^{19}F NMR analysis of the reaction mixture based on reagent **72** with PhCF_3 as the internal standard.

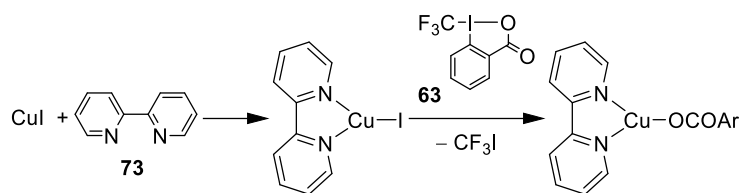
Bipyridine **73** is often used to stabilize copper complexes, and such complexes are also used for trifluoromethylation reactions.^[208,356] However, it also means that such a ligand lowers the reactivity of the corresponding copper species. In fact, when bipyridine **73** was added to the CuI-catalyzed trifluoromethylation reaction of arene **61**, the reaction was inhibited (**Scheme 139**). The role of ligand **73** was examined by changing the addition order (**Scheme 140**). In **Scheme 139**, CuI and ligand **73** were mixed first, followed by arene **61** and reagent **63**. On the other hand, when ligand **73** was added to the mixture of CuI and reagent **63** (**Scheme 140**), product **62** was obtained in 26% yield. This result indicates that the formation of CuI–**73** complexes inhibits the generation of the active catalyst. CF_3I was detected in equivalent amounts as the used CuI in both cases, meaning that the reaction of CuI–**73** and reagent **63** may generate CuOCOAr-73 and CF_3I (**Scheme 141**).



Scheme 139. Addition of bipyridine **73** to CuI-catalyzed trifluoromethylation of arene **61**. Reaction conditions: CuI (0.05 mmol), **73** (0.05 mmol), **61** (0.5 mmol), DMSO (10 mL), 60 °C, 2 h; **63** (0.55 mmol), 60 °C, overnight. The reaction mixture was analyzed by ^{19}F NMR.



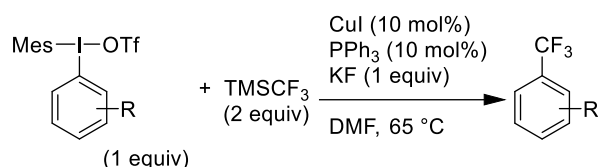
Scheme 140. Addition of bipyridine **73** in a different order. Reaction conditions: CuI (0.03 mmol), **63** (0.3 mmol), DMSO (3 mL), 40 °C, 2 h; **73** (0.03 mmol), 40 °C, 2 h; **61** (0.3 mmol), 40 °C, overnight. Yield was determined by ^{19}F NMR analysis of the reaction mixture based on arene **61** with PhCF_3 as the internal standard.



Scheme 141. The formation of non-productive CuI-**73** and CuOCOAr-**73**.

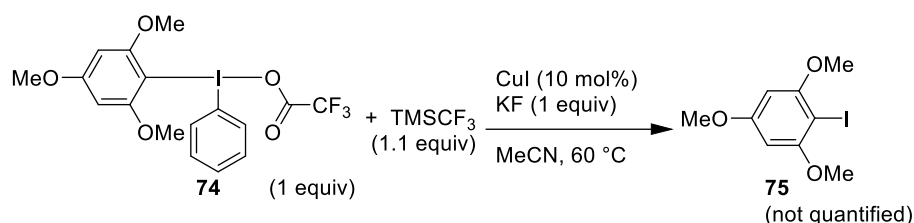
6.5.2 The formation of Diaryl- λ^3 -iodanes and their reactivity

It has been reported that Ar-I(III) species and nucleophilic CF₃ compounds react in the presence of copper catalysts to produce the corresponding Ar-CF₃ products (**Scheme 142**).^[384] Therefore, to examine the reactivity of possible I(III) intermediates (**b-II** and **c-IV** in **Scheme 136**), an Ar-I(III) compound was prepared and investigated.



Scheme 142. Cu-catalyzed synthesis of trifluoromethylated arenes from di(hetero)aryl- λ^3 -iodanes.^[384]

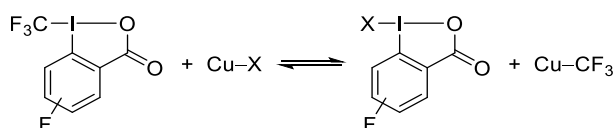
The known Ar-I(III) compound **74** was exposed to TMSCF₃ and catalytic CuI, but only undesired product **75** was obtained (**Scheme 143**). Although this data alone cannot exclude the possibility of the formation of Ar-I(III) intermediate in the CuI-catalyzed trifluoromethylation, the generation of Ar-I(I) product **75** seems to be favored in this pathway, which was not detected in the CuI-catalyzed trifluoromethylation.



Scheme 143. Reaction of Ar-I(III) compound **74** and TMSCF₃ in the presence of CuI. Reaction conditions: **74** (0.5 mmol), TMSCF₃ (0.55 mmol), CuI (0.05 mmol), MeCN (5 mL), 60 °C, overnight. The reaction mixture was analyzed by ¹H NMR.

6.5.3 Examination of ligand exchange by the use of fluorinated trifluoromethylating reagents

In order to test the possibility depicted in **Scheme 136c**, fluorinated $\text{CF}_3\text{-I(III)}$ reagents were synthesized. A possible ligand exchange between Cu-X and $\text{CF}_3\text{-I(III)}$ can be monitored by the ^{19}F NMR signal of the newly introduced fluorine atom into the trifluoromethylating reagent (**Scheme 144**). Although fluorinated reagent **76** could be prepared, it turned out to be unstable, and an unidentified impurity was detected in increasing amounts over time by ^1H NMR. The reaction mixture of reagent **76** and CuCl showed only a weak signal at -27 ppm in ^{19}F NMR spectrum (CF_3Cl), but the signals for Cu(I)-CF_3 and Ar-F compounds were not observed (**Scheme 145**).^[382] These data indicate that ligand exchange did not occur to any significant extent. Instead, missing ^{19}F NMR signals for CF_3 groups indicate redox reactions between reagent **76** and CuCl producing Cu(II) or high-spin Cu(III) species bearing the CF_3 groups. The missing ^{19}F NMR signals for Ar-F would imply coordination of 2-fluoro-6-iodobenzoic acid to paramagnetic copper(II) species.



Scheme 144. Possible ligand exchange between a fluorinated reagent and Cu-X .

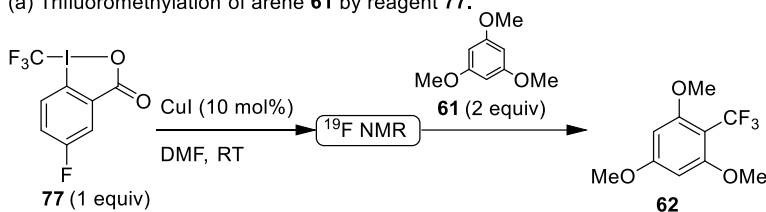


Scheme 145. Experiment for ligand exchange between reagent **76** and CuCl . Reaction conditions: **76** (0.3 mmol), CuI (0.3 mmol), DMSO (6 mL), RT, overnight. The reaction mixture was analyzed by ^{19}F NMR.

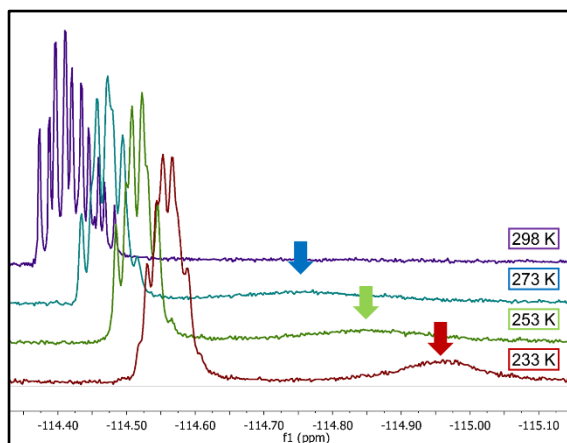
Another fluorinated isomeric reagent **77** was synthesized and found to be bench-stable. It was employed for the CuI -catalyzed trifluoromethylation reaction (**Scheme 146**). In the pretreatment with CuI , the signal for reagent **77** (Ar-F , -111.5 ppm) and another signal at -114.5 ppm were observed in the ^{19}F NMR spectrum. This -114.5 ppm signal was close to the Ar-F signal of the corresponding 5-fluoro-2-iodobenzoic acid that appears at -115.0 ppm. After the addition of arene **61**, only this -114.5 ppm signal was found in this region, but its integration corresponded to 60% of the amount of reagent **77** used. To examine the possibility of a fast ligand exchange of Cu-OCOAr that may cause reduced integrations, this reaction mixture was analyzed by ^{19}F NMR at lower temperature (**Scheme 146b**). In addition to a peak shift of these Ar-F signals, a broad peak

was separated from the main Ar–F peak, although the total peak area did not increase. Then, HCl was added to the reaction mixture to prompt the release of the carboxylic acid from paramagnetic Cu(II) species. The color change of the reaction mixture (green to yellow) and gas generation were observed. In the ^{19}F NMR spectrum, another Ar–F signal appeared at -113.8 ppm (**Scheme 146c**) and the total integration increased to 91% of reagent **77** used. The -113.8 ppm signal was likely generated by a different reductive elimination of I(III) species as illustrated in **Scheme 122** in Section 6.3.1 to generate I-displaced carboxylic acid. Cl or CF_3 could have displaced the iodine (**Scheme 146d**), although the corresponding Ar– CF_3 signal for 2-trifluoromethyl-5-fluorobenzoic acid was not found. Thus, the signal may indicate the generation of 2-chloro-5-fluorobenzoic acid.

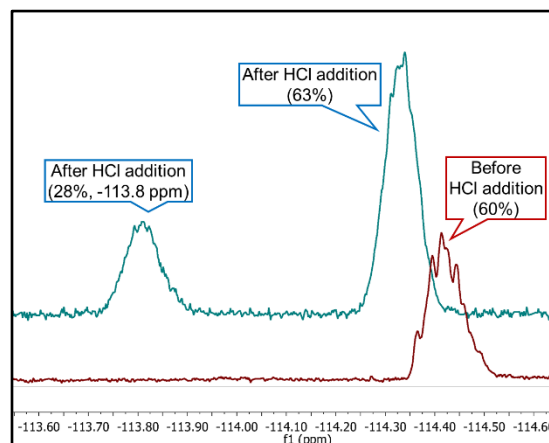
(a) Trifluoromethylation of arene **61** by reagent **77**.



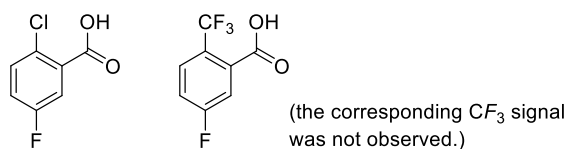
(b) ^{19}F NMR of the reaction mixture.



(c) Change in ^{19}F NMR by HCl addition.



(d) Possible species for the new -113.8 ppm peak in ^{19}F NMR spectrum.

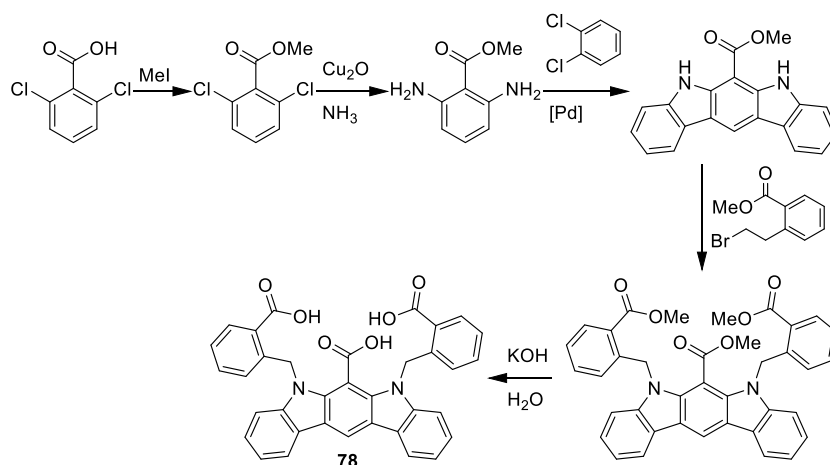


Scheme 146. (a) Trifluoromethylation of arene **61** by reagent **77**. (b) ^{19}F NMR spectra (500 MHz) of the reaction mixture at 233 K (red), 253 K (green), 273 K (blue) and 298 K (purple). Arrows indicate the separated broad peaks. (c) ^{19}F NMR spectra (300 MHz) before and after the addition of HCl. Numbers in parentheses are relative peak areas for Ar–F. (d) Possible species for the new -113.8 ppm signal in ^{19}F NMR spectrum.

6.6 Conclusion and outlook

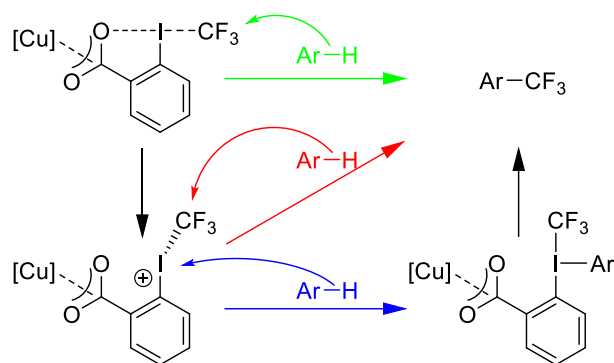
The reactive intermediate in the model Cu-catalyzed trifluoromethylation of 1,3,5-trimethoxybenzene (**61**) was studied. The available data indicate that the catalytically active species is $[\text{Cu}(\text{II})_2\text{X}(\text{OCOAr})_3]$, where X is CF_3 , halide or monodentate carboxylate. Magnetic susceptibility experiments agreed with the existence of dinuclear copper structures in the reaction mixture.

The synthesis of a tricarboxylato complex was not achieved because of the unexpected formation of insoluble polymeric complexes. To prevent this polymerization, conformationally more rigid ligand **78** was designed, where the relative positions of three carboxylic acids are fixed (**Scheme 147**). Starting from 2,6-dichlorobenzoic acid, methylation of the carboxylic acid, aminations of the aryl chloride,^[385] formation of heterocycles,^[386,387] coupling with side chains and saponification will produce ligand **78**.



Scheme 147. Synthetic route to position-fixed tricarboxylate ligand **78**.

The study herein only suggests the activation of reagent **63** by $[\text{Cu}(\text{II})_2\text{X}(\text{OCOAr})_3]$. The mechanism of the trifluoromethylation of arene **61** after the coordination of reagent **63** to the active catalyst is not yet clear. An activated reagent can be directly attacked by nucleophilic arenes (**Scheme 148** green). Possible I–O cleavage (**Scheme 136b** in Section 6.5) can lead to an iodonium cation. Arenes can react with this iodonium cation to yield the $\text{Ar}-\text{CF}_3$ product, or to form $\text{Ar}-\text{I}(\text{III})-\text{CF}_3$ species followed by reductive elimination towards $\text{Ar}-\text{CF}_3$ product.



Scheme 148. Possible formations of trifluoromethylated products from an activated reagent.

However, it is difficult to analyze these reactive intermediates, partly because of the involvement of Cu(II) species interfering with NMR analyses. One idea to differentiate these possibilities is a design of intramolecular reaction experiments (**Figure 23**). All three possible nucleophilic attacks should show different preferences of the chain length between the electrophilic part and the nucleophilic part.

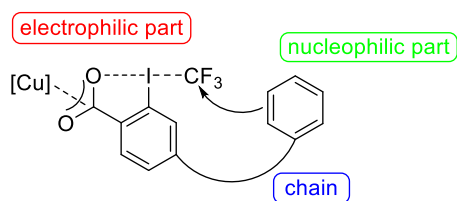


Figure 23. Motif of an intermolecular reaction experiment. The electrophilic part and the nucleophilic part are connected in a molecule.

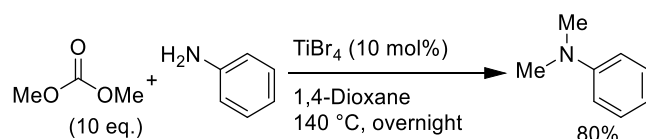
Chapter 7

General Conclusion and Outlook

7.1 Conclusion

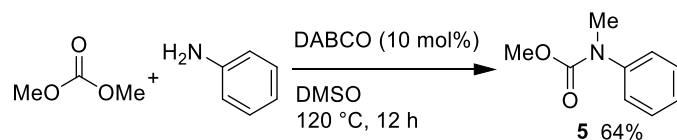
The original goal of this thesis was the development of a deoxyfluorination reaction of aliphatic alcohols, and the investigation started with the model reaction of amines and organic carbonates. Although fluorination was not achieved, activations of organic carbonates, DMSO-based oxidative functionalization reactions, and a trifluoromethylation reaction were studied.

Organic carbonates were activated by Lewis-acid catalysts towards methylation of amines. TiBr_4 was found to be an efficient catalyst for this transformation (**Scheme 149**). The bulkiness of the electrophilic alkyl group is significantly influential on reactivity. Also, phenyl carbonates suffered from the nucleophilic attack on the carbonyl group to produce carbamates and ureas. Various Lewis acids were tested as catalysts, but TiBr_4 showed a high catalytic activity. It is likely that TiBr_4 converts the alkyl group of an organic carbonate to a reactive electrophilic species, with which a nucleophile reacts to form an alkylated amine.



Scheme 149. The TiBr_4 -catalyzed methylation of aniline by DMC.

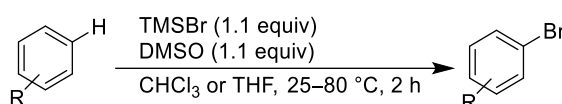
The base-catalyzed formation of carbamate **5** was unexpectedly found while investigating the methylation reaction of aniline by DMC, and was studied because the reaction was found interesting and attractive. DMSO is a good solvent and the transformation was achieved with a catalytic amount of base at 120°C (**Scheme 150**). The $\text{p}K_a$ value of amine substrates was influential on the reaction efficiency, and electron-deficient amines reacted with DMC smoothly. However, not only the deprotonation of amines but also the activation of DMC was apparently necessary and, therefore, non-amine bases such as *n*BuLi did not promote the reaction efficiently.



Scheme 150. The base-catalyzed transformation of DMC and aniline to *N,N*-disubstituted carbamate **5**.

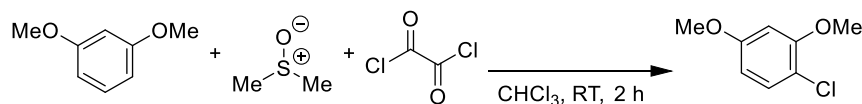
The DMSO-based oxidative bromination reaction of arenes with TMSBr as a bromide source was found to be a fast, mild and efficient reaction (**Scheme 151**). The substrate scope is limited to

electron-rich arenes, but acid-sensitive functional groups such as ester and acetal are tolerated. This protocol is suitable for large-scale syntheses, because all the by-products can be easily removed by evaporation. The advantages of this bromination protocol were emphasized by the three synthetic applications that directly transformed the produced aryl bromides to more complex molecules in short and efficient procedures.



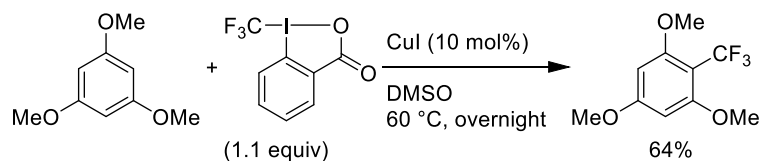
Scheme 151. The oxidative bromination of arenes in the TMSBr/DMSO system.

Other DMSO-based oxidative functionalizations were also investigated. An electron-rich arene is oxidatively chlorinated in the oxalyl chloride/DMSO system efficiently (**Scheme 152**). Interestingly, the addition of an external bromide achieved an oxidative bromination instead of chlorination. Unfortunately, the relatively low oxidizing power of sulfoxides was proven by redox exchange experiments, and thus, it was concluded that replacing I(III) oxidants by activated DMSO was difficult.

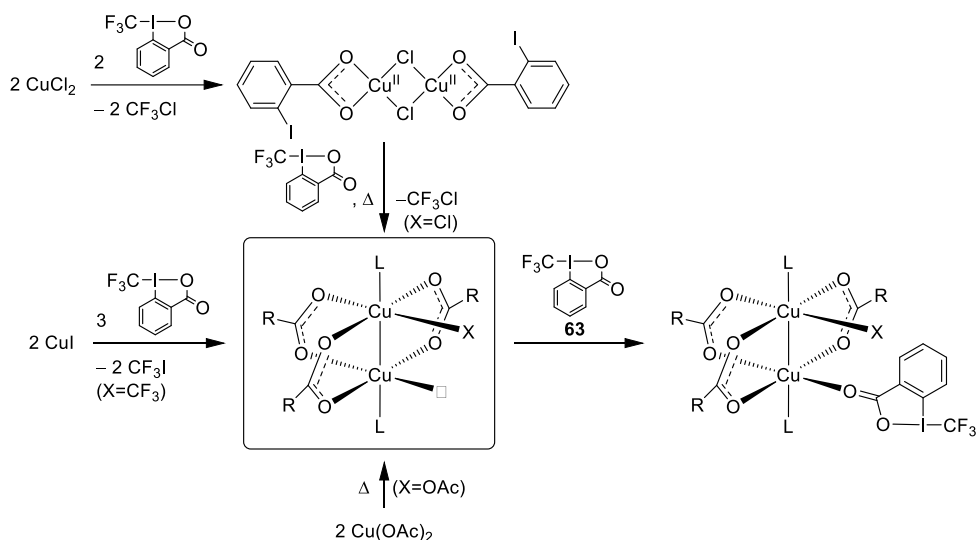


Scheme 152. Oxidative chlorination of an arene under Swern conditions.

Reactive intermediates of a copper-catalyzed trifluoromethylation reaction were studied (**Scheme 153**). The active catalyst is invoked to be $\text{Cu(II)}_2\text{X(OCOAr)}_3$, where X is CF_3 , halide or a monodentate carboxylate, and a trifluoromethylating reagent **63** may occupy an empty coordination site for activation (**Scheme 154**). Other possible reaction mechanisms were examined although they were found unlikely. Magnetic susceptibility experiments agreed with the existence of dinuclear copper structures in the reaction mixture.



Scheme 153. The CuI-catalyzed trifluoromethylation of an arene.



Scheme 154. Generations of the hypothesized active catalyst from CuI, CuCl₂ or Cu(OAc)₂.

7.2 Outlook

Selected suggestions based on the findings during the research of the reactions mentioned in this thesis are to be described.

7.2.1 Acid-activation of organic carbonates

As for the acid-catalyzed alkylation of amines by using organic carbonates, a ligand could be designed as described below. Acidic catalysts showed good selectivity towards methylation. Also, ligand exchange *in situ* between labile ligands and the alcohol that was produced as a by-product was observed and should be minimized. Considering these features, it is proposed that the type of complexes shown in **Figure 24** would be an ideal catalyst where acidic bidentate ligands control selectivity while being reluctant towards ligand exchange with a by-product alcohol.

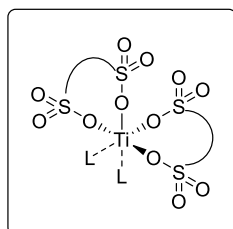


Figure 24. Suggested type of complex to improve the catalytic activity for methylation of amines with DMC.

7.2.2 DMSO-based oxidative bromination of arenes

The advantage of the oxidative bromination reaction of arenes in the TMSBr/DMSO system could be maximized by a flow chemistry application. A designed diagram of the flow reaction system is depicted in **Figure 25**. A flow of arenes and DMSO could be mixed with a TMSBr solution at low temperature before a heating column, followed by a continuous evaporation treatment to remove volatile compounds. As long as dry solvents are used, the system can be made of stainless steel, which is cheap, strong and easy to handle.

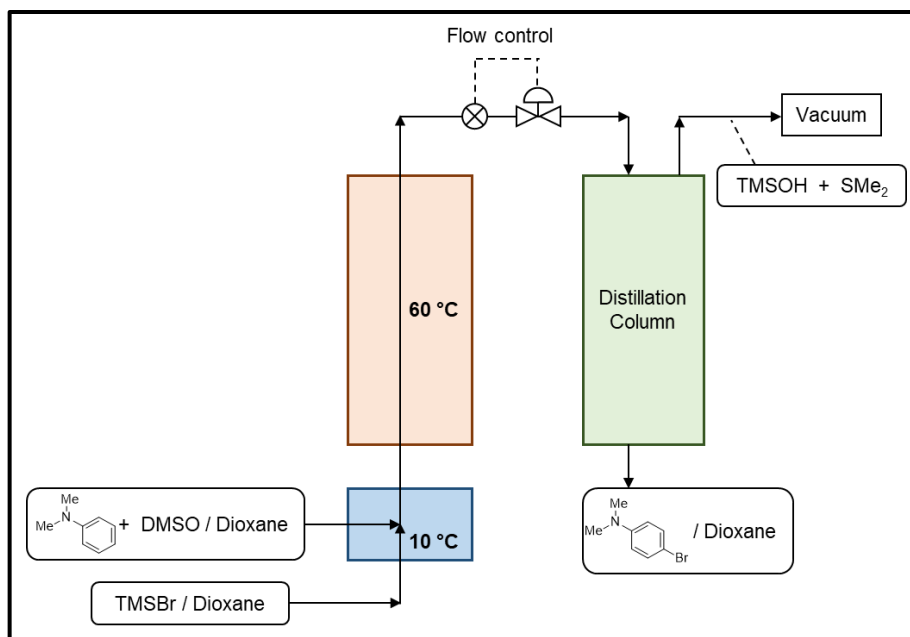
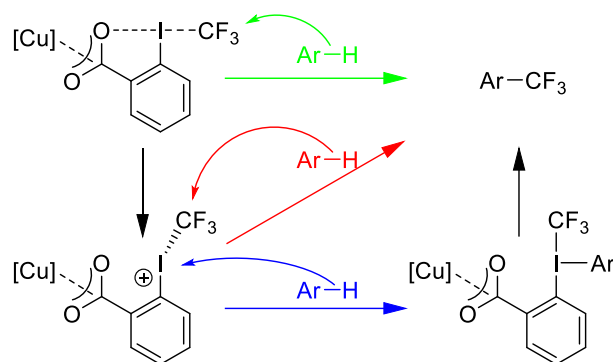


Figure 25. Diagram of a suggested flow system.

7.2.3 Copper-catalyzed trifluoromethylation of arenes

A plausible active catalyst of the trifluoromethylation reaction has been suggested, but this proposal needs more supportive evidence. The positions of three carboxylic acids of a tricarboxylate ligand should be fixed (ligand **78** shown in **Scheme 147**), so that it could form the corresponding copper complex without polymerization reactions. This ligand is assumed to form dinuclear complexes only. Experiments using such a complex as a catalyst will disclose the involvement of dinuclear copper structure with three carboxylate ligands unambiguously. Furthermore, isolation and use of $(\text{CuXOCOAr})_2$ such as **65** ($\text{X}=\text{Cl}$) for the reaction as catalysts should be effective in order to prove the pathway from CuCl to the active structure.

The present study only suggests the activation of reagent **63** by $[\text{Cu}(\text{II})_2\text{X}(\text{OCOAr})_3]$. The mechanism of the trifluoromethylation of arene **61** after the coordination of reagent **63** to the active catalyst is not yet clear. Some possibilities are depicted in **Scheme 155**; nucleophilic attack to an activated trifluoromethylating reagent, I–O cleavage of the reagent generating a reactive iodonium cation, or formation of $\text{Ar}-\text{I}(\text{III})-\text{CF}_3$ species followed by reductive elimination towards $\text{Ar}-\text{CF}_3$ product.



Scheme 155. Possible formations of trifluoromethylated products from an activated reagent.

In order to differentiate these possibilities, intramolecular reaction experiments could be designed (**Figure 26**). All three possible nucleophilic attacks above should show different preferences of the chain length between the electrophilic part and the nucleophilic part.

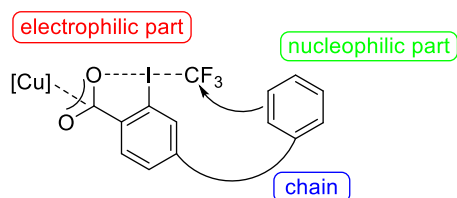


Figure 26. Motif of an intermolecular reaction experiment. The electrophilic part and the nucleophilic part are connected in a molecule.

Chapter 8

Experimental

8.1 General remarks

8.1.1 Techniques

Dry solvents.^[388] For oxygen and moisture sensitive reactions solvents were distilled under argon using an appropriate drying agent (toluene from Na, hexane from Na/benzophenone/tetraglyme, pentane from Na/benzophenone/diglyme, MeOH, DCM and MeCN from CaH₂, EtOH from Na/diethyl phthalate, Et₂O and THF from Na/benzophenone) or were purchased from Acros as bottled solvent over molecular sieves (3 Å for MeOH and MeCN, else 4 Å). CHCl₃ was washed with water to remove EtOH, passed through a column of silica gel and then dried over molecular sieves 4 Å, and stored in an amber glass bottle with pieces of copper wire and molecular sieves 4 Å.

Deuterated solvents. Deuterated solvents for NMR studies were purchased from Armar Chemicals (CDCl₃, CO(CD₃)₂) or Cambridge Isotope Laboratories (CD₂Cl₂, CD₃CN, C₆D₆). The solvents were used as received or transferred to a Young Schlenk over molecular sieves 4 Å under an argon atmosphere.

8.1.2 Chemicals

Chemicals were purchased from abcr, Acros, Apollo Scientific, Fluka, Fluorochem, Lancaster, Sigma-Aldrich, Strem, TCI and VWR and used without further purification unless otherwise noted.

8.1.3 Analytics

Flash column chromatography. Automated medium pressure liquid chromatography was carried out on a CombiFlash[®] Rf+ Lumen using RediSep prepacked columns (60 Å Pore Size, 230–400 Mesh). In some cases that the method above was not available, flash column chromatography was manually carried out on Fluka Silica gel 60 (230–400 mesh ASTM) with solvents reported as volume ratios under 0.1–0.3 bar overpressure.

Gas chromatography with Flame-Ionization Detector (GC-FID). Performed on a Thermo Finnigan series instrument equipped with a split-mode capillary injection system, Zebron Guardian ZB-5 column (30 m × 0.25 mm × 0.25 μm film) and FID detectors. Helium was used as carrier gas (1.4 ml/min), and the injector and detector were heated to 250 °C.

Calibrations were carried out for quantification by using GC-FID. Starting materials, products and decane (0.5 mmol, ranged 50–100 mg in this thesis) were dissolved in the solvent that was used in the reaction and EtOAc filling up to 10 mL. The mixture was analyzed by GC-FID. The procedures were repeated three times and averages were used for calculation unless they showed large errors. The factors were determined in the equation:

$$f_{i/0} = \frac{n_i A_0}{n_0 A_i}$$

, where 0 is the label for the internal standard, n_i is the used molar amount of the substance i , A_i is the peak area in FID for the substance i .

Gas chromatography-mass spectrometry (GC-MS). Performed on an Agilent GC 7890A with an HP-5MS column (30 m × 250 μm × 0.25 μm film), with a column flow of 1.7 mL/min using helium as carrier gas, and an Agilent mass spectrometer 5975C VL MSD operating in EI positive mode. Sample injection was done by an Agilent autosampler ALS 7693, 1 μL at <1 mg/mL in split mode (split ratio 100:1). The standard method consisted of the following temperature program: 2 min at 50 °C, ramp of 20 °C/min with 2 min hold time at 300 °C (16.5 min total time). For heavy or not so volatile compounds, a high mass method was used consisting of the following temperature program: 2 min at 50 °C, ramp of 20 °C/min with 8 min hold time at 300 °C (22.5 min total time).

For analysis of gas phase, the sample was taken from the headspace of the sample with a micro syringe, purged with the gas sample three times, and injected manually (5 μL). The temperature of the oven was constant at 40 °C, and the data are acquired for 5 min. After the acquisition, the oven was heat to 230 °C for 3 min.

High resolution mass spectrometry (HRMS). Performed by the Mass Spectrometry Service Lab in the Laboratory of Organic Chemistry at ETH Zurich. The signals are given as mass-to-charge ratio (m/z). Ions from EI sources were measured with a Waters Micromass AutoSpec Ultima EI-Sector-MS, from ESI sources with a Bruker maXis Qq-TOF-MS or a solariX FTICR-MS or from MALDI sources with a Bruker UltraFlex II MALDI-TOF-MS or a solariX FTICR-MS.

For structure elucidation by X-ray diffraction. intensity data for single crystals mounted on MiTeGen MicroLoops were collected. The crystals were cooled to 100 K for measurement and the diffraction pattern was collected by a Bruker SMART APEX, APEXII platform with CCD detector or Venture D8. Graphite monochromated Mo- K_{α} -radiation ($\lambda=0.71073 \text{ \AA}$) was applied. The

program SMART was used for data collection, integration was performed with SAINT.^[389] The structures were solved by direct or heavy atom (Patterson) method, respectively, or by charge flipping, using the program SHELXS-97.^[390] The refinement and all further calculations were carried out using SHELXL-97.^[391] All non-hydrogen atoms were refined anisotropically using weighted full-matrix leastsquares on F^2 . The hydrogen atoms were included in calculated positions and treated as riding atoms using the SHELXL default parameters. An absorption correction was applied (SADABS)^[392] and the weighting scheme was optimized in the final refinement cycles. The absolute configuration of chiral compounds was determined on the basis of the Flack parameter.^[393,394] The standard uncertainties are rounded according to *the Notes for Authors of Acta Crystallographica*.^[395] Detailed information about the crystal structures and their solutions is given in appendix B. All measurements and solutions were performed by Mona Wagner or Ewa Pietrasiak.

Nuclear magnetic resonance (NMR) spectra were recorded on a Bruker DPX-250, Avance Nanobay III-300, Avance III-400 and Avance III-500. All spectra were recorded in the given solvent at the given frequency in non-spinning mode, which were measured at room temperature unless otherwise noted. Chemical shifts (δ) are given in ppm relative to the residual solvent signal or the internal standard in ^1H , ^{13}C and ^{19}F spectra. Multiplicities are abbreviated as follows: s for singlet, d for doublet, t for triplet, q for quartet, quint for quintet, sext for sextet, sept for septet, and m for multiplet. The description br describes an obvious broadening of the signal. Coupling constants (J) are given in Hertz (Hz). Unresolved frequencies are cited as multiplets.

8.2 Acid-activation of organic carbonate (Chapter 2)

8.2.1 General procedure: Lewis acid-catalyzed reaction of aniline and an organic carbonate

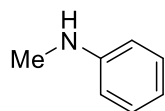
Lewis acid-catalyzed methylation reactions were carried out in a 20 mL Schlenk tube equipped with a small stirring bar. The tube was charged with catalysts before the tube was purged with argon by three vacuum/argon cycles, then aniline (95 mg, 1 mmol), organic carbonate (10 mmol) and decane (72 mg, 0.5 mmol, internal standard for GC-FID analysis) in 3 mL of solvent were quickly added to the tube with a slow counter flow of argon. In the case that DMC was used as a solvent, the added amount of DMC was 2.6 mL, 30 mmol. The tube was then closed with a PTFE stopcock. The tube was heated by a mean of oil bath at 140 °C overnight with vigorously stirred. After cooling it down to room temperature, 0.1 mL of the reaction mixture was filtered through a thin layer of silica gel, washed with EtOAc and submitted to GC-FID analysis. The rest of the reaction mixture was filtered through a thin layer of silica gel, washed with EtOAc, and solvents were removed under reduced pressure.

General analysis of catalysis samples

Quantitative analysis of reactions was fulfilled by GC-FID analysis. When necessary, a part of the crude mixture was taken for ^1H and ^{13}C NMR and GC-MS analyses. When separation was necessary, the crude mixture was separated using silica-gel flash chromatography (hexane with 1% triethylamine : EtOAc, gradient elution).

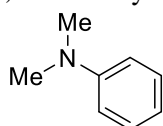
Compound data

N-Methylaniline (**1**), CAS No.: 100-61-8

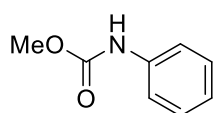


^1H NMR (300 MHz, Chloroform-*d*): δ = 7.20 (dt, J = 7.4, 2.2 Hz, 2H), 6.71 (tt, J = 7.2, 1.1 Hz, 1H), 6.62 (dd, J = 8.6, 1.0 Hz, 2H), 2.84 (s, 3H).

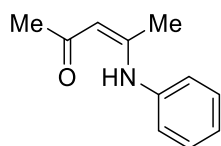
N,N-Dimethylaniline (**2**), CAS No.: 121-69-7



^1H NMR (300 MHz, Chloroform-*d*): δ = 7.26 (t, J = 7.8 Hz, 2H), 6.82 – 6.68 (m, 3H), 2.96 (s, 6H).

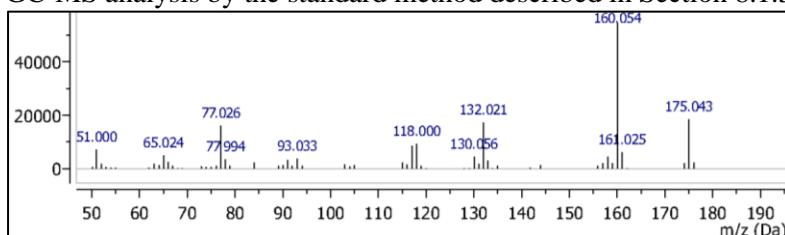
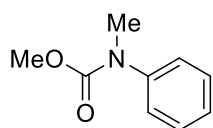
Methyl *N*-phenylcarbamate (**3**), CAS No.: 2603-10-3

$^1\text{H NMR}$ (300 MHz, Chloroform-*d*): $\delta = 7.38$ (d, $J = 8.0$ Hz, 2H), 7.31 (d, $J = 7.3$ Hz, 2H), 7.07 (tt, $J = 7.2, 1.4$ Hz, 1H), 6.57 (s, 1H), 3.78 (s, 3H).

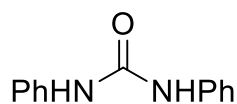
4-Anilinopent-3-en-2-one (**4**), CAS No.: 26567-78-2

$^1\text{H NMR}$ (300 MHz, Chloroform-*d*): $\delta = 12.47$ (s, 1H), 7.34 (t, $J = 7.7$ Hz, 2H), 7.18 (t, $J = 7.4$ Hz, 1H), 7.10 (d, $J = 7.6$ Hz, 2H), 5.18 (s, 1H), 2.10 (s, 3H), 1.99 (s, 3H).

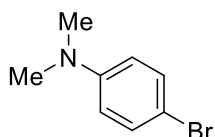
GC-MS analysis by the standard method described in Section 8.1.3.

Methyl *N*-methyl-*N*-phenylcarbamate (**5**), CAS No.: 28685-60-1

$^1\text{H NMR}$ (300 MHz, Chloroform-*d*): $\delta = 7.36$ (t, $J = 6.6$ Hz, 2H), 7.23 (d, $J = 7.5$ Hz, 3H), 3.71 (s, 3H), 3.30 (s, 3H).

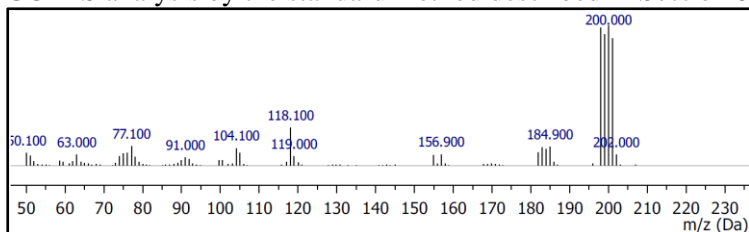
1,3-Diphenylurea (**10**), CAS No.: 102-07-8

$^1\text{H NMR}$ (300 MHz, Chloroform-*d*): $\delta = 7.45$ (s, 1H), 7.38 (d, $J = 7.7$ Hz, 2H), 7.29 (d, $J = 7.5$ Hz, 2H), 7.03 (t, $J = 7.3$ Hz, 1H).

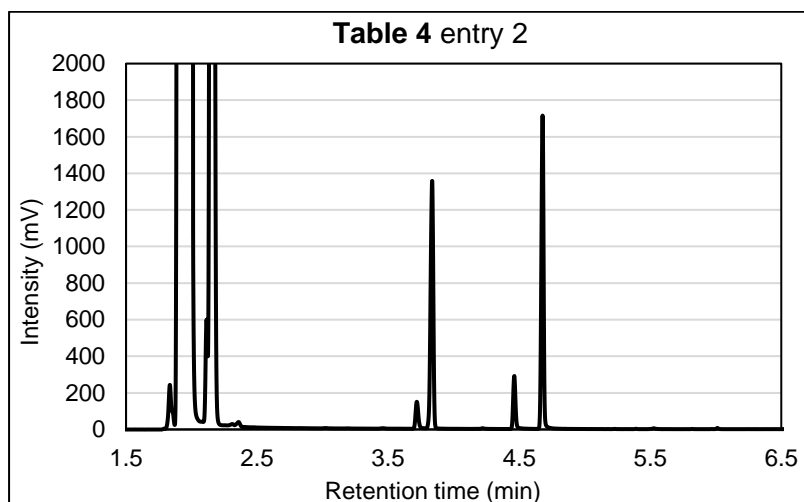
4-Bromo-*N,N*-dimethylaniline (**13**), CAS No.: 586-77-6

$^1\text{H NMR}$ (300 MHz, Chloroform-*d*): $\delta = 7.30$ (d, $J = 9.2$ Hz, 2H), 6.59 (d, $J = 9.1$ Hz, 2H), 2.92 (s, 6H).

GC-MS analysis by the standard method described in Section 8.1.3.



Selected GC chromatogram



Retention time (min)	Compound
1.5–2.5	solvents
3.72	Aniline
3.84	Decane
4.46	1
4.68	2
6.32	3

Method information:

Injection volume: 2 μ L. Carrier flow rate 1.4 mL/min.

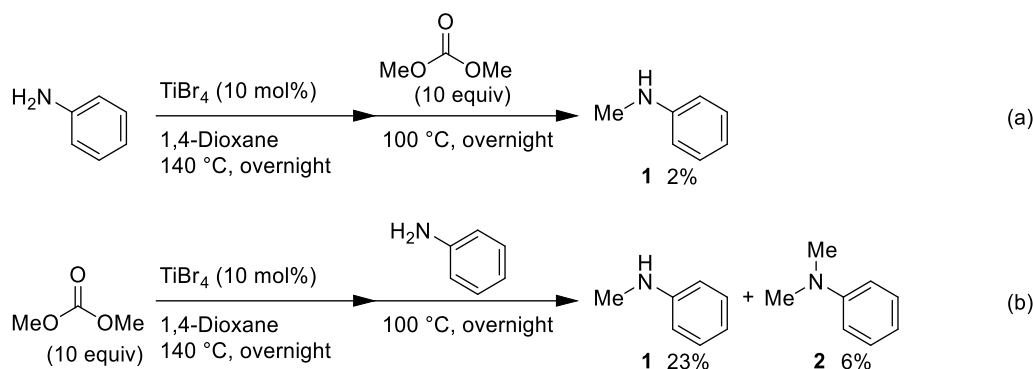
Retention time (min)	Rate ($^{\circ}$ C/min)	Target Value ($^{\circ}$ C)	Hold time (min)
0	Method start		
3	0	100	3
6.3	30	200	0
8.556	45	300	0
13	Method end		

More method/instrumental information is available in Section 8.1.3.

8.2.2 Reaction pathway experiments (Scheme 58)

In a 20 mL Schlenk tube equipped with a small stirring bar, TiBr_4 (38 mg, 0.1 mmol) was placed before the tube was purged with argon by three vacuum/argon cycles, then substrate **3** or **5** (1 mmol), DMC (910 mg, 10 mmol) and decane (72 mg, 0.5 mmol, GC-FID internal standard) in 3 mL of 1,4-dioxane were quickly added to the tube with a slow counter flow of argon. The tube was then closed with a PTFE stopcock. The tube was heated by a mean of oil bath at 140 $^{\circ}$ C overnight with vigorously stirred. After cooling it down to room temperature, 0.1 mL of the reaction mixture was filtered through a thin layer of silica gel, washed with EtOAc and submitted to GC-FID analysis.

8.2.3 Temperature separated experiment (Scheme 61)



Run (a):

TiBr₄ (37 mg, 0.1 mmol) was charged in a 20 mL Schlenk tube equipped with a small stirring bar, before the tube was purged with argon by three vacuum/argon cycles. Aniline (95 mg, 1 mmol) and decane (72 mg, 0.5 mmol, internal standard for GC-FID analysis) in 3 mL of 1,4-dioxane was quickly added to the tube with a slow counter flow of argon. The tube was then closed with a PTFE stopcock and was heated by a mean of oil bath at 140 °C overnight with vigorously stirred. After cooling it down to room temperature, DMC (910 mg, 10 mmol) was added to the tube. The tube was heated by a mean of oil bath at 100 °C overnight with vigorously stirred. After cooling it down to room temperature, 0.1 mL of the reaction mixture was filtered through a thin layer of silica gel, washed with EtOAc and submitted to GC-FID analysis.

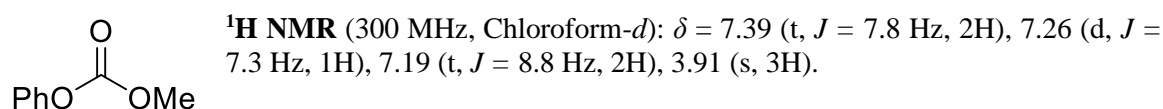
Run (b):

TiBr₄ (37 mg, 0.1 mmol) was charged in a 20 mL Schlenk tube equipped with a small stirring bar, before the tube was purged with argon by three vacuum/argon cycles. DMC (910 mg, 10 mmol) and decane (72 mg, 0.5 mmol, internal standard for GC-FID analysis) in 3 mL of 1,4-dioxane was quickly added to the tube with a slow counter flow of argon. The tube was then closed with a PTFE stopcock and was heated by a mean of oil bath at 140 °C overnight with vigorously stirred. After cooling it down to room temperature, aniline (95 mg, 1 mmol) was added to the tube. The tube was heated by a mean of oil bath at 100 °C overnight with vigorously stirred. After cooling it down to room temperature, 0.1 mL of the reaction mixture was filtered through a thin layer of silica gel, washed with EtOAc and submitted to GC-FID analysis.

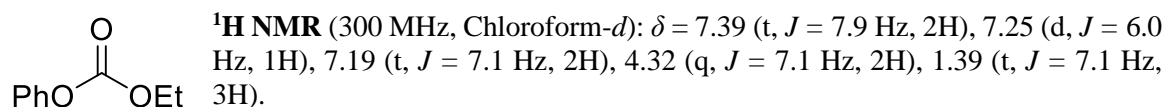
8.2.4 Synthesis of alkyl phenylcarbonates, used in Table 3

Following a modified procedure of Motoki et al.,^[396] phenol (950 mg, 10 mmol) was placed in a 100 mL flask equipped with a small stirring bar. The flask was purged with argon by three vacuum/argon cycles. Triethylamine (2.1 mL, 15 mmol) and 23 mL of dichloromethane was added to the flask and cooled down to 0 °C. Alkyl chloroformate (10 mmol) in 7 mL of dichloromethane was slowly added to the flask. The mixture was stirred at room temperature for 1 hour. It was poured into saturated NaHCO₃ solution, and extracted with dichloromethane, dried over MgSO₄, and solvents were removed under reduced pressure. The crude mixture was separated using silica-gel flash chromatography (hexane: EtOAc, gradient elution).

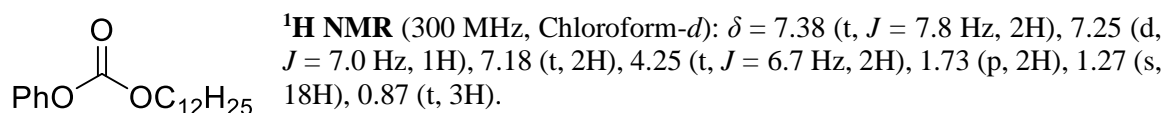
Methyl phenyl carbonate (**7**), colorless liquid (1.31 g, 86% yield), CAS No.: 13509-27-8



Ethyl phenyl carbonate (**8**), colorless liquid (0.84 g, 51% yield), CAS No.: 3878-46-4

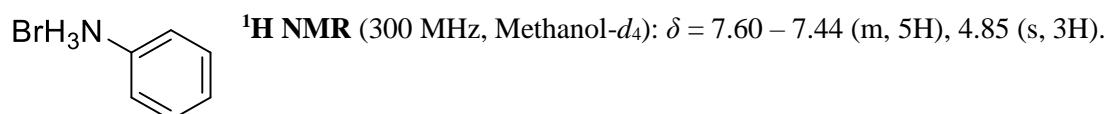


Dodecyl phenyl carbonate (**9**), colorless liquid (2.34 g, 76% yield), CAS No.: 127027-45-6

**8.2.5 Synthesis of aniline hydrobromide, used in Scheme 65**

Aniline (950 mg, 10 mmol) was placed in a 20 mL vial equipped with a small stirring bar. 5 mL of water and hydrobromic acid (8 mL, 48% in water, 50 mmol) was added to the vial sequentially. Immediate precipitation was observed. The vial was heated at 60 °C for 2 hours. After cooling down to room temperature, the mixture was filtered and the solid was washed with ether. The residual solvents were removed under reduced pressure. Colorless solid was obtained (1.09 g, 65% yield).

Aniline hydrobromide, colorless solid (1.09 g, 65% yield), CAS No.: 542-11-0



8.3 Base-activation of organic carbonates (Chapter 3)

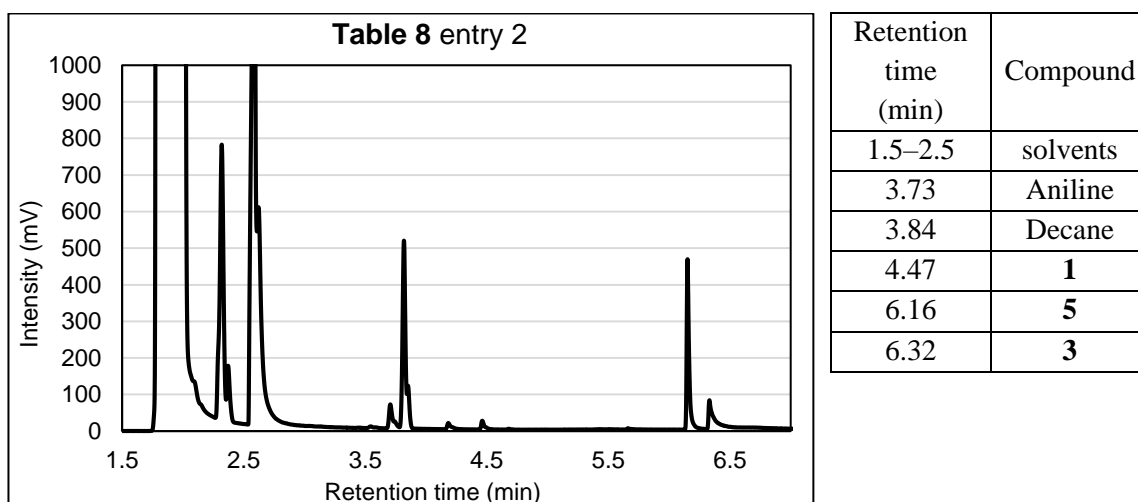
8.3.1 General procedure: Base-catalyzed reaction of amine and DMC

A 20 mL vial with a stirring bar was capped with a crimp seal, and purged with argon by three vacuum/argon cycles. A solution of amine substrate (1 mmol), catalyst (0.1 mmol, or the given equivalent) and decane (72 mg, 0.5 mmol, GC-FID internal standard) in 2 mL of solvent was added to the vial. DMC (910 mg, 10 mmol, or the given equivalent) in 1 mL of solvent was added to the vial. The solution was heated by a mean of aluminium heating block with vigorously stirred. After cooling it down to room temperature, 0.1 mL of the reaction mixture was filtered through a thin layer of silica gel, washed with EtOH and submitted to GC-FID analysis. The rest of the reaction mixture was filtered through a thin layer of silica gel, washed with EtOH, and solvents were removed under reduced pressure.

General analysis of catalysis sample

Quantitative analysis of reactions was fulfilled by GC-FID analysis. When necessary, a part of the crude mixture was taken for ^1H and ^{13}C NMR and GC-MS analyses. When separation was necessary, the crude mixture was separated using silica-gel flash chromatography (hexane with 1% triethylamine : EtOAc, gradient elution).

GC chromatogram example Table 8 entry 2



Method information:

Injection volume: 2 μ L. Carrier flow rate 1.4 mL/min.

Retention time (min)	Rate ($^{\circ}$ C/min)	Target Value ($^{\circ}$ C)	Hold time (min)
0	Method start		
3	0	100	3
6.3	30	200	0
8.556	45	300	0
13	Method end		

More method/instrumental information is available in Section 8.1.3.

8.3.2 Reaction of DMC and aniline with *n*BuLi (Table 9)

Aniline (95 mg, 1 mmol) was placed in a 20 mL vial with a stirring bar was capped with a crimp seal, and purged with argon by three vacuum/argon cycles. *n*BuLi solution (0.6 mL, 1.6 M in hexanes, 1 mmol) was added to the vial slowly at 0 $^{\circ}$ C. Decane (72 mg, 0.5 mmol, GC-FID internal standard) in 3 mL of DMC was added to the vial. The mixture was stirred at the given temperature overnight. After cooling it down to room temperature, 0.1 mL of the reaction mixture was filtered through a thin layer of silica gel, washed with EtOH and submitted to GC-FID analysis.

8.4 DMSO-based oxidative bromination of arenes (Chapter 4)

8.4.1 General procedure: Oxidative bromination of arenes in the TMSBr/DMSO system

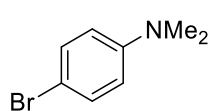
Arene (1 mmol) was placed in a 10 mL vial with a stirring bar, capped with a crimp seal, and purged with argon by three vacuum/argon cycles. DMSO (87 mg, 1.1 mmol) in 2 mL of solvent was added to the vial followed by the addition of TMSBr (174 mg, 1.1 mmol) in 1 mL of THF at 0 °C. The mixture was stirred at the given temperature for 2 hours. After cooling it down to room temperature, 5 mL of EtOAc, 0.1 mL of triethylamine and 1 mL of EtOH was added to the reaction mixture. After decane (72 mg, 0.5 mmol, GC-FID internal standard) in 2 mL of EtOAc, the quenched mixture was submitted to GC-FID analysis. The rest of the reaction mixture was filtered through a thin layer of silica gel, washed with EtOAc, and solvents were removed under reduced pressure.

General analysis of catalysis sample

Quantitative analysis of reactions was fulfilled by GC-FID analysis. When necessary, a part of the crude mixture was taken for ^1H and ^{13}C NMR and GC-MS analyses. When separation was necessary, the crude mixture was separated using silica-gel flash chromatography (hexane : EtOAc, gradient elution).

Compound data

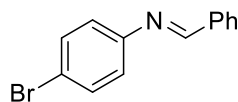
4-Bromo-*N,N*-dimethylaniline (**13**), colorless solid, CAS No.: 586-77-6



$^1\text{H NMR}$ (300 MHz, Chloroform-*d*): δ = 7.38 – 7.27 (m, 2H), 6.59 (d, J = 9.1 Hz, 2H), 2.92 (s, 6H).

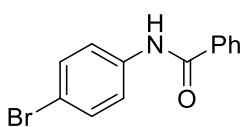
$^{13}\text{C NMR}$ (75 MHz, Chloroform-*d*): δ = 149.67, 131.82, 114.26, 108.67, 40.71.

4-Bromo-*N*-(phenylmethylene)benzenamine (**23**), orange solid, CAS No.: 780-20-1



$^1\text{H NMR}$ (300 MHz, Chloroform-*d*): δ = 8.47 (s, 1H), 7.91 (dd, J = 6.7, 2.9 Hz, 2H), 7.48 (dd, J = 5.0, 1.8 Hz, 3H), 7.46 – 7.34 (m, 2H), 7.27 – 7.17 (m, 2H).

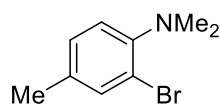
N-(4-Bromophenyl)benzamide (**24**), colorless solid, CAS No.: 7702-38-7



$^1\text{H NMR}$ (300 MHz, Chloroform-*d*): δ = 10.36 (s, 1H), 7.94 (dd, J = 6.7, 1.6 Hz, 2H), 7.77 (dd, J = 9.0, 2.0 Hz, 2H), 7.65 – 7.46 (m, 5H).

$^{13}\text{C NMR}$ (75 MHz, Chloroform-*d*): δ = 165.62, 138.54, 134.67, 131.68, 131.40, 128.39, 127.64, 122.18, 115.29.

N,N-Dimethyl-2-bromo-4-methylaniline (**22**), colorless liquid, CAS No.: 23667-06-3



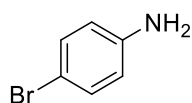
¹H NMR (300 MHz, Chloroform-*d*): δ = 7.39 (d, J = 1.0 Hz, 1H), 7.10 – 7.02 (m, 1H), 6.99 (d, J = 8.1 Hz, 1H), 2.77 (s, 6H), 2.27 (s, 3H).

¹³C NMR (75 MHz, Chloroform-*d*): δ = 149.53, 134.37, 134.06, 128.84, 120.39, 119.29, 44.60, 20.41.

IR (ATR, neat): 2922.66, 2861.32, 2828.48, 2777.12, 1726.47, 1493.77, 1452.82, 1316.12, 1272.51, 1212.27, 1188.50, 1162.61, 1137.60, 1050.09, 1038.62, 946.78, 851.91, 570.14, 814.18, 742.03, 692.43, 669.47 cm^{-1} .

HRMS (ESI⁺) calcd. (m/z) for C₉H₁₃BrN: [M+H⁺] 214.0226, found: 214.0227.

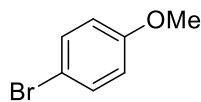
4-Bromoaniline (**25**), brown solid, CAS No.: 106-40-1



¹H NMR (300 MHz, Chloroform-*d*): δ = 7.23 (d, J = 8.7 Hz, 2H), 6.56 (d, J = 8.7 Hz, 2H), 3.67 (s, 2H).

¹³C NMR (75 MHz, Chloroform-*d*): δ = 145.45, 132.05, 116.75, 110.25.

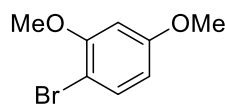
4-Bromoanisole (**26**), colorless liquid, CAS No.: 104-92-7



¹H NMR (300 MHz, Chloroform-*d*): δ = 7.38 (dd, J = 9.0, 2.3 Hz, 2H), 6.78 (dd, J = 9.0, 2.2 Hz, 2H), 3.78 (s, 3H).

¹³C NMR (75 MHz, Chloroform-*d*): δ = 158.85, 132.38, 115.88, 112.96, 55.58.

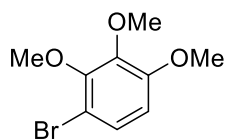
2,4-Dimethoxybromobenzene (**27**), colorless liquid, CAS No.: 17715-69-4



¹H NMR (300 MHz, Chloroform-*d*): δ = 7.39 (d, J = 8.7 Hz, 1H), 6.48 (d, J = 2.8 Hz, 1H), 6.39 (dd, J = 8.7, 2.8 Hz, 1H), 3.86 (s, 3H), 3.78 (s, 3H).

¹³C NMR (75 MHz, Chloroform-*d*): δ = 160.29, 156.59, 133.17, 105.97, 102.48, 100.03, 56.17, 55.60.

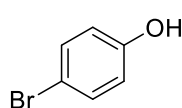
2,3,4-Trimethoxybromobenzene (**28**), slightly yellow liquid, CAS No.: 10385-36-1



¹H NMR (300 MHz, Chloroform-*d*): δ = 7.20 (d, J = 9.0 Hz, 1H), 6.58 (d, J = 9.0 Hz, 1H), 3.90 (s, 3H), 3.88 (s, 3H), 3.84 (s, 3H).

¹³C NMR (75 MHz, Chloroform-*d*): δ = 153.48, 151.15, 143.71, 126.89, 108.79, 108.54, 61.23, 61.15, 56.32.

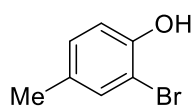
4-Bromophenol (**30**), green liquid, CAS No.: 106-41-2



¹H NMR (300 MHz, Chloroform-*d*): δ = 7.33 (d, J = 8.9 Hz, 2H), 6.73 (d, J = 8.8 Hz, 2H), 5.28 (s, 1H).

¹³C NMR (75 MHz, Chloroform-*d*): δ = 154.59, 132.55, 117.28, 112.99.

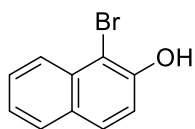
2-Bromo-4-cresol (**31**), Slightly yellow liquid, CAS No.: 6627-55-0



$^1\text{H NMR}$ (300 MHz, Chloroform-*d*): δ = 7.27 (d, J = 1.3 Hz, 1H), 7.01 (dd, J = 8.2, 2.0 Hz, 1H), 6.91 (d, J = 8.2 Hz, 1H), 5.32 (s, 1H), 2.27 (s, 3H).

$^{13}\text{C NMR}$ (75 MHz, Chloroform-*d*): δ = 150.13, 132.24, 131.54, 129.89, 115.87, 109.95, 20.32.

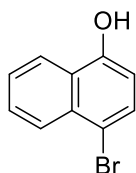
1-Bromo-2-naphthol (**32**), colorless solid, CAS No.: 573-97-7



$^1\text{H NMR}$ (300 MHz, Chloroform-*d*): δ = 8.10 – 7.99 (m, 1H), 7.84 – 7.71 (m, 2H), 7.57 (ddd, J = 8.4, 6.9, 1.3 Hz, 1H), 7.40 (ddd, J = 8.1, 6.9, 1.2 Hz, 1H), 7.27 (d, J = 8.8 Hz, 1H), 5.91 (s, 1H).

$^{13}\text{C NMR}$ (75 MHz, Chloroform-*d*): δ = 150.75, 132.46, 129.85, 129.49, 128.37, 127.99, 125.48, 124.30, 117.31, 106.29.

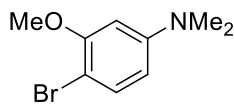
4-Bromo-1-naphthol (**33**), colorless crystal, CAS No.: 571-57-3



$^1\text{H NMR}$ (300 MHz, Chloroform-*d*): δ = 8.20 (t, J = 7.5 Hz, 2H), 7.70 – 7.48 (m, 3H), 6.71 (d, J = 8.0 Hz, 1H), 5.29 (s, 1H).

$^{13}\text{C NMR}$ (75 MHz, Chloroform-*d*): δ = 151.39, 132.88, 129.53, 128.02, 127.23, 126.18, 125.77, 122.30, 113.62, 109.32.

4-Bromo-3-methoxy-*N,N*-dimethyl-benzenamine (**34**), Green solid, CAS No.: 90642-46-9



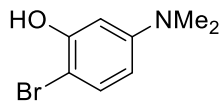
$^1\text{H NMR}$ (300 MHz, Chloroform-*d*): δ = 7.31 (d, J = 8.7 Hz, 1H), 6.37 – 6.13 (m, 2H), 3.88 (s, 3H), 2.95 (s, 6H).

$^{13}\text{C NMR}$ (75 MHz, Chloroform-*d*): δ = 156.45, 151.41, 133.14, 106.35, 98.17, 97.44, 56.17, 40.83.

IR (ATR, neat): 2833.88, 2803.03, 1591.00, 1561.15, 1497.92, 1463.55, 1432.83, 1407.33, 1359.47, 1246.56, 1162.56, 1048.69, 1011.40, 977.77, 931.79, 802.51, 789.14, 780.46, 706.44, 631.68, 609.81 cm^{-1} .

HRMS (EI⁺) calcd. (m/z) for $\text{C}_9\text{H}_{12}\text{BrNO}$: [M^+] 229.0102, found: 229.0097

2-Bromo-5-(dimethylamino)phenol (**35**), brown crystal, CAS No.: 90006-17-0



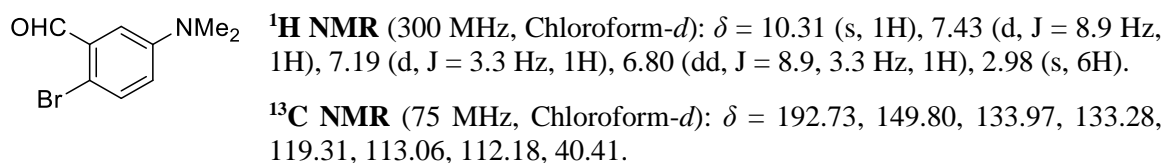
$^1\text{H NMR}$ (300 MHz, Chloroform-*d*): δ = 7.23 (d, J = 8.9 Hz, 1H), 6.39 (d, J = 2.9 Hz, 1H), 6.22 (dd, J = 8.9, 2.9 Hz, 1H), 5.37 (s, 1H), 2.92 (s, 6H).

$^{13}\text{C NMR}$ (75 MHz, Chloroform-*d*): δ = 152.79, 151.69, 131.82, 106.93, 100.02, 96.83, 40.69.

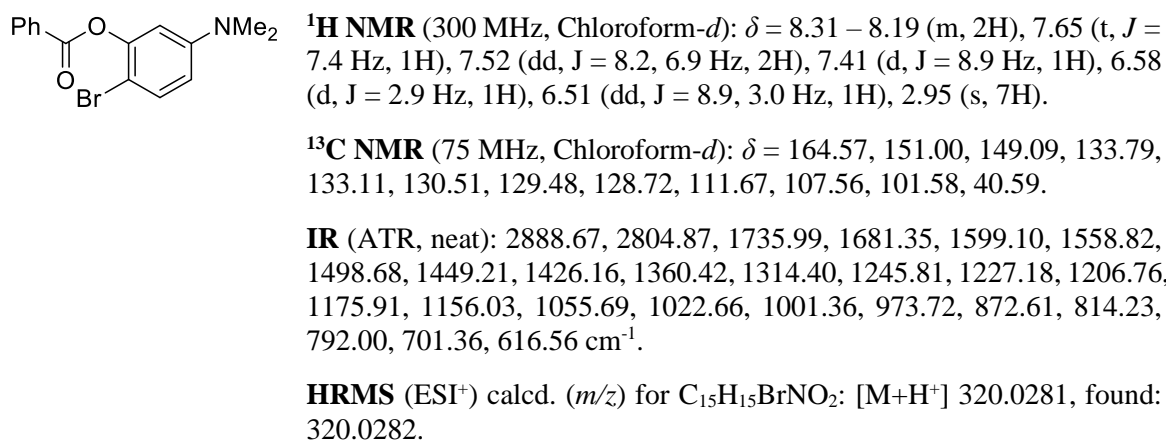
IR (ATR, neat): 2913.35, 2851.76, 1583.52, 1475.62, 1456.57, 1421.00, 1408.42, 1316.20, 1287.05, 1247.17, 1218.64, 1197.60, 1131.83, 1044.26, 1030.93, 977.96, 882.56, 798.65, 790.94, 711.37, 639.33 cm^{-1} .

HRMS (EI⁺) calcd. (m/z) for $\text{C}_8\text{H}_{10}\text{BrNO}$: [M^+] 214.9946, found: 214.9941

2-Bromo-5-(dimethylamino)-benzaldehyde (**37**), yellow solid, CAS No.: 828916-47-8

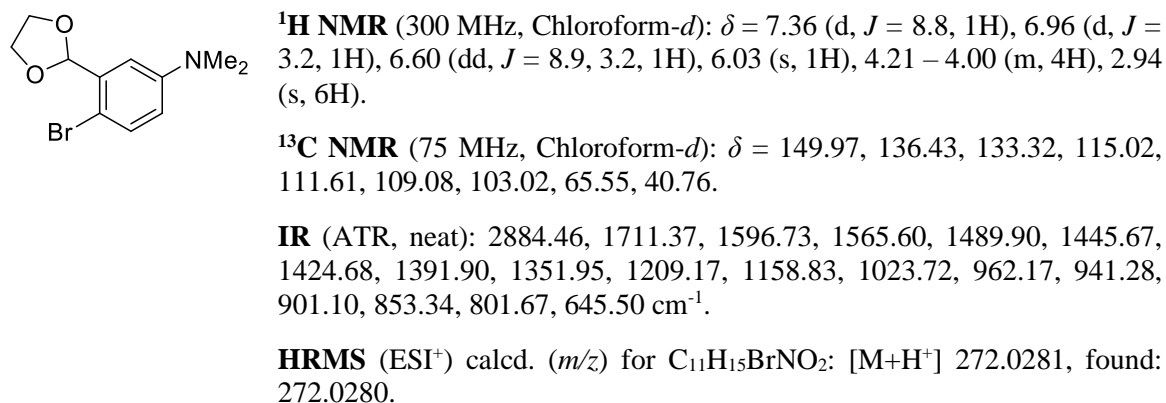


2-Bromo-5-(dimethylamino)phenyl benzoate (**36**), brown liquid, CAS No.: 2093970-40-0

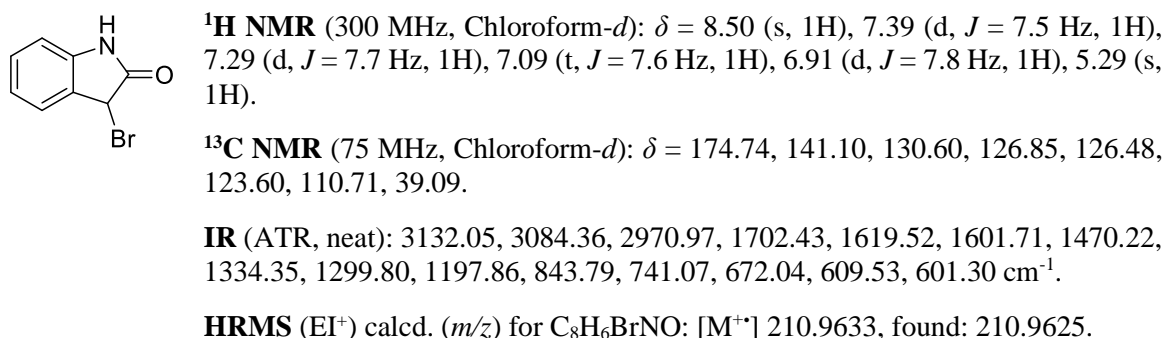


4-Bromo-3-(1,3-dioxolan-2-yl)-*N,N*-dimethyl-benzenamine (**38**),

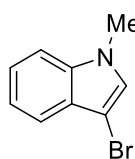
Orange liquid, CAS No.: 1257846-99-3



3-Bromo-2-indolinone (**39**), brown solid, CAS No.: 22942-87-6

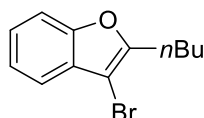


3-Bromo-1-methylindole (**40**), colorless liquid, CAS No.: 81471-20-7
(Unstable at room temperature to give dark solid over time.)



$^1\text{H NMR}$ (300 MHz, Chloroform-*d*): $\delta = 7.58$ (d, $J = 7.8$ Hz, 1H), 7.39 – 7.27 (m, 2H), 7.21 (ddd, $J = 8.0, 6.3, 1.9$ Hz, 1H), 7.08 (s, 1H), 3.78 (s, 3H).

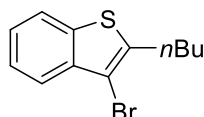
3-Bromo-2-butyl-1-benzofuran (**41**), slightly yellow liquid, CAS No.: 872400-06-1



$^1\text{H NMR}$ (300 MHz, Chloroform-*d*): $\delta = 7.59 - 7.36$ (m, 2H), 7.34 – 7.22 (m, 2H), 2.84 (t, $J = 7.5$ Hz, 2H), 1.84 – 1.66 (m, 2H), 1.51 – 1.33 (m, 2H), 0.97 (t, $J = 7.4$ Hz, 3H).

$^{13}\text{C NMR}$ (75 MHz, Chloroform-*d*): $\delta = 155.97, 153.61, 128.52, 124.47, 123.20, 119.22, 111.19, 94.34, 29.77, 26.48, 22.34, 13.90$.

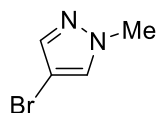
3-Bromo-2-butyl-1-benzothiophene (**42**), slightly yellow liquid, CAS No.: 872400-10-7



$^1\text{H NMR}$ (300 MHz, Chloroform-*d*): $\delta = 7.76$ (d, $J = 8.0$ Hz, 2H), 7.43 (ddd, $J = 8.0, 7.2, 1.2$ Hz, 1H), 7.39 – 7.30 (m, 1H), 2.98 (t, $J = 7.6$ Hz, 2H), 1.83 – 1.68 (m, 2H), 1.58 – 1.38 (m, 2H), 1.00 (t, $J = 7.3$ Hz, 3H).

$^{13}\text{C NMR}$ (75 MHz, Chloroform-*d*): $\delta = 141.06, 138.54, 137.25, 124.96, 124.80, 122.73, 122.37, 105.84, 32.59, 29.79, 22.38, 13.96$.

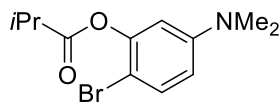
4-Bromo-1-methylpyrazole (**43**), colorless liquid, CAS No.: 15803-02-8



$^1\text{H NMR}$ (300 MHz, Chloroform-*d*): $\delta = 7.44$ (s, 1H), 7.38 (s, 1H), 3.90 (s, 3H).

$^{13}\text{C NMR}$ (75 MHz, Chloroform-*d*): $\delta = 139.81, 130.24, 93.14, 39.59$.

2-Bromo-5-(dimethylamino)phenyl isobutanoate (**48**), slightly yellow liquid, CAS No.: 2093970-42-2



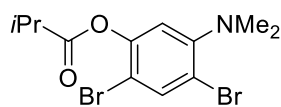
$^1\text{H NMR}$ (300 MHz, Chloroform-*d*): $\delta = 7.35$ (d, $J = 8.9$ Hz, 1H), 6.50 – 6.37 (m, 2H), 3.04 – 2.73 (m, 7H), 1.36 (d, $J = 7.0$ Hz, 6H).

$^{13}\text{C NMR}$ (75 MHz, Chloroform-*d*): $\delta = 174.69, 150.84, 148.80, 132.97, 111.43, 107.33, 101.50, 40.48, 34.29, 19.08$.

IR (ATR, neat): 2974.67, 2932.54, 2876.13, 1759.13, 1684.60, 1601.79, 1561.09, 1498.76, 1467.89, 1445.35, 1386.66, 1360.33, 1261.33, 1228.24, 1179.63, 1157.37, 1090.89, 1044.22, 1031.83, 977.26, 919.54, 880.18, 863.97, 814.62, 792.40 cm^{-1} .

HRMS (ESI⁺) calcd. (m/z) for $\text{C}_{12}\text{H}_{17}\text{BrNO}_2$: $[\text{M}+\text{H}^+]$ 286.0437, found: 286.0438.

2,4-Dibromo-5-(dimethylamino)phenyl isobutanoate (**50**), slightly yellow liquid, CAS No.: 2093970-43-3



¹H NMR (300 MHz, Chloroform-*d*): δ = 7.75 (s, 1H), 6.79 (s, 1H), 2.98 – 2.68 (m, 7H), 1.36 (d, J = 7.0 Hz, 6H).

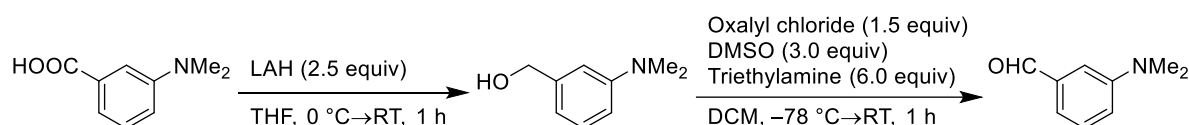
¹³C NMR (75 MHz, Chloroform-*d*): δ = 174.47, 152.41, 148.14, 137.03, 115.77, 115.64, 109.09, 44.05, 34.35, 19.10.

IR (ATR, neat): 2975.82, 2942.97, 2872.88, 2833.54, 2790.16, 1762.45, 1582.31, 1480.17, 1466.10, 1454.56, 1434.71, 1386.99, 1369.23, 1345.12, 1266.01, 1214.36, 1179.65, 1137.74, 1106.52, 1051.64, 996.20, 917.50, 889.48, 877.98, 736.31, 670.77, 648.49 cm^{-1} .

HRMS (ESI⁺) calcd. (m/z) for C₁₂H₁₆Br₂NO₂: [M+H⁺] 363.9542, found: 363.9543.

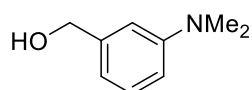
8.4.2 Preparation of substrates for the oxidative bromination

Synthesis of 3-(*N,N*-dimethylamino)benzaldehyde^[397]



Lithium aluminium hydride (LAH) (2.00 g, 50 mmol) was placed in a 250 mL flask equipped with a rubber septum and a magnetic stirring bar, and the atmosphere was replaced with argon. 100 mL of THF was added to the flask before the solution was cooled down to 0 °C. A solution of 3-(*N,N*-dimethylaminobenzoic acid (3.37 g, 20 mmol) in 20 mL of THF was added to the mixture slowly before it was allowed to warm up to room temperature. After 1 hour of stirring, the resultant reaction mixture was quenched with 10 mL of EtOH and 3.6 mL of water, and the solid was filtered off through a thin layer of MgSO₄ and silica gel. The filtrate was concentrated under reduced pressure. The residue was purified by using an automated preparative HPLC (10% EtOAc in hexane) to give 3-(*N,N*-dimethylamino)benzyl alcohol (1.29 g, 8.5 mmol, 43%).

3-(*N,N*-Dimethylamino)benzyl alcohol, slightly yellow liquid, CAS No.: 23501-93-1



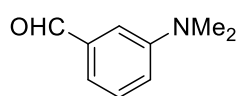
¹H NMR (300 MHz, Chloroform-*d*): δ = 7.22 (d, J = 7.9 Hz, 1H), 6.80 – 6.60 (m, 3H), 4.65 (s, 2H), 2.96 (s, 6H).

¹³C NMR (75 MHz, Chloroform-*d*): δ = 151.06, 142.00, 129.44, 115.33, 112.12, 111.23, 66.10, 40.77.

A flame-dried 100 mL flask equipped with a rubber septum and a magnetic stirring bar was charged under argon atmosphere subsequently with oxalyl chloride (1.30 g, 10 mmol) and 25 mL

of DCM. The solution was cooled down to $-78\text{ }^{\circ}\text{C}$ (acetone/dry ice bath) followed by a slow addition of DMSO (1.18 g, 15 mmol) in 5 mL of DCM. 3-(*N,N*-Dimethylamino)benzyl alcohol (756 mg, 5.0 mmol) in 5 mL of DCM was added to the mixture dropwise. 15 minutes later triethylamine (4.2 mL, 30 mmol) was added at once to the mixture before it was allowed to warm up to room temperature. The resultant reaction mixture was quenched with saturated NH_4Cl solution. The aqueous phase was extracted with DCM, washed with brine, dried over MgSO_4 , and was concentrated under reduced pressure. The residue was purified by using an automated preparative HPLC (5% EtOAc in hexane) to give 3-(*N,N*-dimethylamino)benzaldehyde (467 mg, 3.1 mmol, 62%).

3-(*N,N*-Dimethylamino)benzaldehyde, bright yellow liquid, CAS No.: 619-22-7



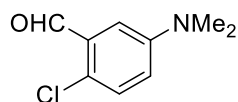
$^1\text{H NMR}$ (300 MHz, Chloroform-*d*): $\delta = 9.96$ (s, 1H), 7.39 (t, $J=8.1$, 1H), 7.23 – 7.15 (m, 2H), 7.02 – 6.93 (m, 1H), 3.02 (s, 6H).

$^{13}\text{C NMR}$ (75 MHz, Chloroform-*d*): $\delta = 193.34$, 150.95, 137.42, 129.74, 119.11, 118.46, 111.71, 40.57.

The original report employed MnO_2 for the oxidation in the second step. However, when we tried to reproduce it, a brown solid was found with a small quantity of the product. Demethylation of the dimethylamino group by using MnO_2 have been studied and reported.^[398,399] it is assumed that the demethylated amines were condensate with aldehyde to form an organic polymer. Therefore, the oxidation was replaced by the Swern oxidation.

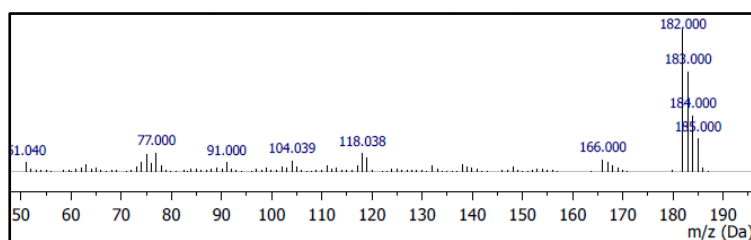
In the Swern oxidation, chlorinated products were found after separation. Refer to Section 5.2.1 for the theoretical background.

2-Chloro-5-(dimethylamino)benzaldehyde, CAS No.: 137548-17-5

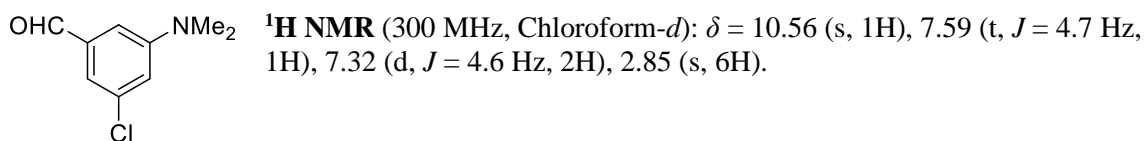


$^1\text{H NMR}$ (300 MHz, Chloroform-*d*): $\delta = 10.44$ (s, 1H), 7.27 (d, $J = 8.8$ Hz, 1H), 7.19 (d, $J = 3.3$ Hz, 1H), 6.87 (dd, $J = 8.9, 3.3$ Hz, 1H), 2.99 (s, 6H).

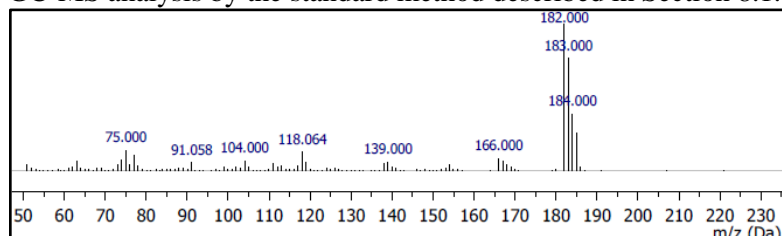
GC-MS analysis by the standard method described in Section 8.1.3.



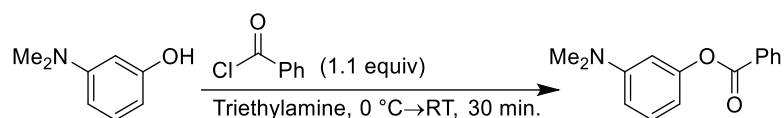
3-Chloro-5-(dimethylamino)benzaldehyde, CAS No.: 284047-90-1



GC-MS analysis by the standard method described in Section 8.1.3.

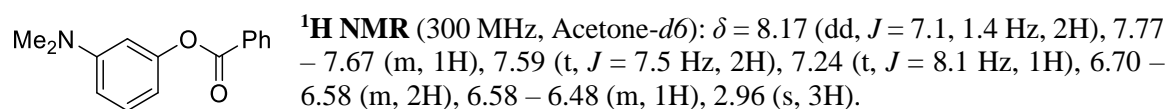


Synthesis of 3-(dimethylamino)phenyl benzoate



3-(Dimethylamino)phenol (707 mg, 5.0 mmol) was placed in a 10 mL vial with a magnetic stirring bar, and the atmosphere was replaced with argon. 5 mL of triethylamine was added to the vial through a septum before the solution was cooled down to 0 °C. Benzoyl chloride (814 mg, 5.5 mmol) was added to the mixture dropwise. After stirring for 30 minutes at room temperature, the resultant reaction mixture was directly loaded on an automated preparative HPLC for purification (5% EtOAc in hexane) to give 3-(dimethylamino)phenyl benzoate (1.01 g, 4.2 mmol, 84%).

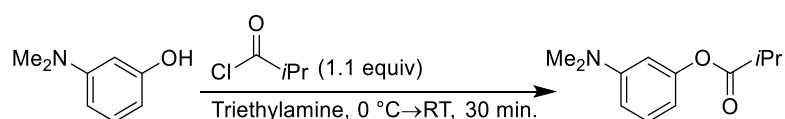
3-(Dimethylamino)phenyl benzoate, colorless crystal, CAS No.: 157279-47-5



¹³C NMR (75 MHz, Acetone-*d*₆): δ = 165.52, 153.25, 152.91, 134.39, 130.98, 130.68, 130.32, 129.61, 110.67, 110.18, 106.63, 40.54.

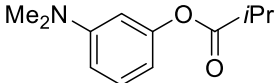
IR (ATR, neat): 2848.46, 1730.75, 1600.87, 1568.00, 1502.32, 1449.12, 1360.84, 1315.38, 1265.93, 1249.33, 1221.65, 1199.66, 1169.51, 1139.35, 1079.76, 1062.28, 1023.22, 997.16, 886.18, 842.74, 814.37, 800.90, 764.29, 725.08, 703.88, 688.19 cm⁻¹.

HRMS (ESI⁺) calcd. (m/z) for C₁₅H₁₆NO₂: [M+H⁺] 242.1176, found: 242.1174.

Synthesis of 3-(dimethylamino)phenyl isobutanoate

Similar procedure to the one for 3-(dimethylamino)phenyl benzoate, but isobutyryl chloride (598 mg, 5.5 mmol) was used as the reagent. (980 mg, 4.7 mmol, 94%).

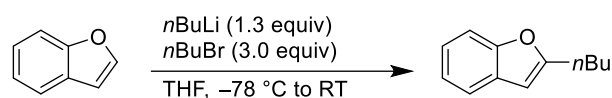
3-(Dimethylamino)phenyl isobutanoate, colorless liquid, CAS No.: 2093970-41-1

 **¹H NMR** (300 MHz, Acetone-*d*₆): δ = 7.17 (t, J = 8.2 Hz, 1H), 6.59 (dd, J = 8.4, 2.5 Hz, 1H), 6.43 (t, J = 2.3 Hz, 1H), 6.40 – 6.32 (m, 1H), 2.92 (s, 6H), 2.77 (p, J = 6.9 Hz, 1H), 1.26 (d, J = 7.0 Hz, 6H).

¹³C NMR (75 MHz, Acetone-*d*₆): δ = 206.05, 175.63, 153.19, 152.76, 130.14, 110.39, 110.09, 106.45, 40.49, 34.69, 30.59, 30.33, 30.07, 29.82, 29.56, 29.30, 29.05, 19.20.

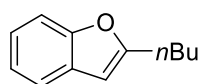
IR (ATR, neat): 2974.45, 2935.30, 2876.19, 2806.74, 1751.81, 1610.05, 1575.61, 1501.05, 1468.32, 1440.36, 1386.38, 1352.03, 1228.68, 1201.68, 1140.28, 1094.34, 1048.47, 998.92, 922.23, 879.73, 841.25, 759.73, 735.11, 701.91, 683.38 cm^{-1} .

HRMS (ESI⁺) calcd. (m/z) for C₁₂H₁₈NO₂: [M+H⁺] 208.1332, found: 208.1330.

Synthesis of 2-butyl-1-benzofuran

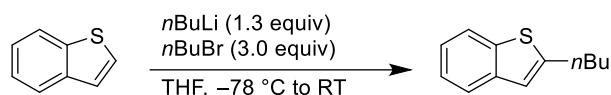
Following a modified procedure of Pfaltz et al.,^[400] benzofuran (1.19 g, 10 mmol) was placed in a 20 mL vial with a magnetic stirring bar, and the atmosphere was replaced with argon. 10 mL of THF was added to the vial through the septum before the solution was cooled down to -78 °C (acetone/dry ice bath). A solution of *n*BuLi (8.1 mL, 1.6 M in hexanes, 13 mmol) was added to the mixture dropwise. After stirring for 30 minutes, 1-bromobutane (3.3 mL, 30 mmol) was added to the mixture slowly before it was allowed to warm up to room temperature. The resultant reaction mixture was quenched with saturated NH₄Cl solution. The aqueous phase was extracted with EtOAc, washed with brine, dried over MgSO₄, and was concentrated under reduced pressure. The residue was purified by using an automated preparative HPLC (5% EtOAc in hexane) to give 2-butyl-1-benzofuran (1.78 g, 9.4 mmol, 94% yield).

2-Butyl-1-benzofuran, colorless liquid, CAS No.: 4265-27-4



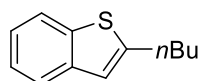
¹H NMR (300 MHz, Acetone-*d*₆): δ = 7.55 – 7.46 (m, 1H), 7.45 – 7.37 (m, 1H), 7.27 – 7.10 (m, 2H), 6.50 (d, *J* = 1.0 Hz, 1H), 2.79 (t, *J* = 7.5 Hz, 2H), 1.73 (p, *J* = 7.3 Hz, 2H), 1.43 (dt, *J* = 14.6, 7.3 Hz, 2H), 0.95 (t, *J* = 7.3 Hz, 3H).
¹³C NMR (75 MHz, Acetone-*d*₆): δ = 160.52, 155.56, 130.03, 123.98, 123.29, 121.12, 111.34, 102.71, 30.57, 28.57, 22.91, 14.04.

Synthesis of 2-butyl-1-benzothiophene



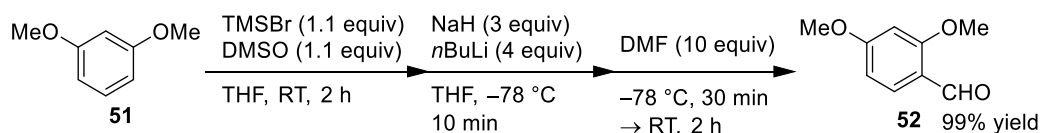
Similar procedure to the one for 2-butyl-1-benzofuran, but 1-benzothiophene (1.38 g, 10 mmol) was used as a substrate. (1.48 g, 8.5 mmol, 85% yield).

2-Butyl-1-benzothiophene, colorless liquid, CAS No.: 17890-53-8



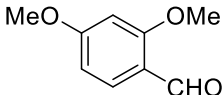
¹H NMR (300 MHz, Acetone-*d*₆): δ = 7.82 (d, *J* = 7.6 Hz, 1H), 7.70 (d, *J* = 7.4 Hz, 1H), 7.36 – 7.20 (m, 2H), 7.10 (s, 1H), 2.92 (t, *J* = 7.5 Hz, 2H), 1.73 (p, *J* = 7.4 Hz, 2H), 1.43 (h, *J* = 7.3 Hz, 2H), 0.95 (t, *J* = 7.3 Hz, 3H).
¹³C NMR (75 MHz, Acetone-*d*₆): δ = 147.40, 141.33, 140.14, 124.96, 124.33, 123.60, 122.87, 121.57, 34.06, 30.91, 22.82, 14.05.

8.4.3 Lithium–halogen exchange reaction and aldehyde formation^[320]



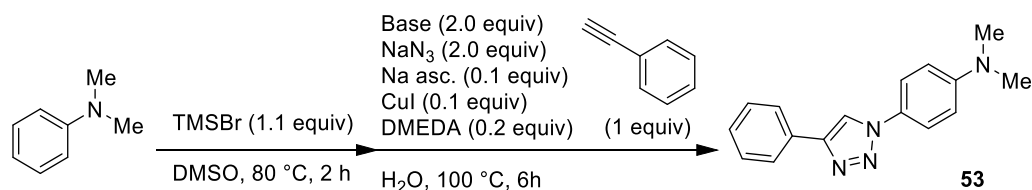
1,3-Dimethoxybenzene (**51**) (142 mg, 1.0 mmol) and DMSO (87 mg, 1.1 mmol) were placed in a 10 mL vial with a magnetic stirring bar, and the atmosphere was replaced with argon. After adding 2 mL of THF, a solution of trimethylsilyl bromide (174 mg, 1.1 mmol) in 1 mL of THF was added to the mixture at 0 °C. The mixture was stirred for 2 hours at room temperature. The mixture was transferred to a 10 mL Schlenk tube with sodium hydride (120 mg, 60% in oil, washed off with hexane, 3.0 mmol) and 2 mL of THF at 0 °C. This mixture was then added to another 20 mL Schlenk tube with *n*BuLi (2.5 mL, 1.6 M in hexane, 4 mmol) and 3 mL of THF at –78 °C slowly. After stirring for 5 minutes, DMF (7 mL, 10 mmol) was added to the tube slowly at –78 °C. The tube was allowed to warm up to room temperature and held for 2 hours. The resultant reaction mixture was quenched with saturated NH₄Cl solution. The aqueous phase was extracted with EtOAc, washed with brine, dried over MgSO₄, and was concentrated under reduced pressure. The residue was purified by using an automated preparative HPLC (5% EtOAc in hexane) to give 2,4-dimethoxybenzaldehyde (**52**) (164 mg, 0.99 mmol, 99% yield).

2,4-Dimethoxybenzaldehyde (**52**), colorless solid, CAS No.: 613-45-6

 **¹H NMR** (300 MHz, Chloroform-*d*): δ = 10.29 (s, 1H), 7.81 (d, J = 8.7 Hz, 1H), 6.55 (dd, J = 8.8, 2.0 Hz, 1H), 6.45 (d, J = 2.2 Hz, 1H), 3.90 (s, 3H), 3.88 (s, 3H).

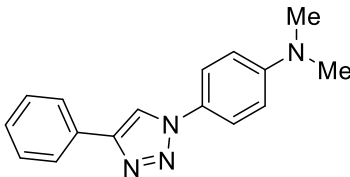
¹³C NMR (75 MHz, Chloroform-*d*): δ = 188.48, 166.33, 163.77, 130.93, 119.26, 105.89, 98.13, 55.77.

8.4.4 Azidation followed by cyclization with copper catalyst^[323]



Trimethylsilyl bromide (174 mg, 1.1 mmol) was placed in a 10 mL vial with a magnetic stirring bar, and the atmosphere was replaced with argon. *N,N*-Dimethylaniline (122 mg, 1.0 mmol) in 3 mL of DMSO was added to the vial through the septum at 0 °C. The mixture was stirred for 2 hours at 80 °C. A solution of NaHCO₃ (171 mg, 2.0 mmol) in 1 mL of water was added to the mixture. The resultant mixture was transferred to another vial with sodium azide (133 mg, 2.0 mmol), (+)-sodium L-ascorbate (Na asc.) (20 mg, 0.1 mmol), copper(I) iodide (19 mg, 0.1 mmol), *N,N'*-dimethylethylenediamine (DMEDA) (18 mg, 0.2 mmol) and phenylacetylene (104 mg, 1.0 mmol). The vial was then heated at 100 °C for 6 hours. The resultant reaction mixture was washed with brine, extracted with EtOAc, dried over MgSO₄, and was concentrated under reduced pressure. The residue was purified by using an automated preparative HPLC (5% EtOAc in hexane) to give *N,N*-dimethyl-4-(4-phenyl-1H-1,2,3-triazol-1-yl)-benzenamine (**53**) (167 mg, 0.63 mmol, 63% yield).

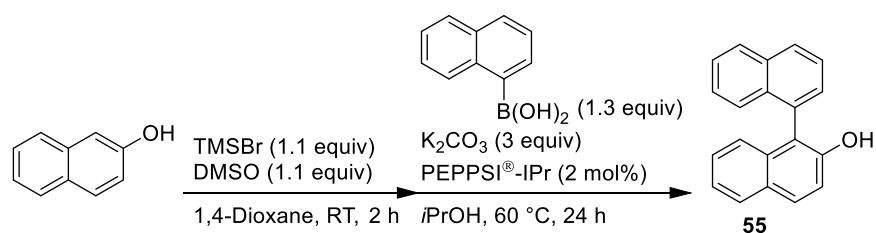
N,N-Dimethyl-4-(4-phenyl-1H-1,2,3-triazol-1-yl)-benzenamine (**53**), colorless crystal, CAS No.: 1603135-10-9

 **¹H NMR** (300 MHz, Chloroform-*d*): δ = 8.07 (s, 1H), 7.90 (d, J = 6.9 Hz, 2H), 7.60 (d, J = 9.1 Hz, 2H), 7.45 (t, J = 7.5 Hz, 2H), 7.35 (t, J = 7.4 Hz, 1H), 6.79 (d, J = 9.1 Hz, 2H), 3.03 (s, 6H).

¹³C NMR (75 MHz, Chloroform-*d*): δ = 150.78, 148.08, 130.83, 129.00, 128.29, 126.97, 125.95, 122.11, 117.88, 112.50, 40.63.

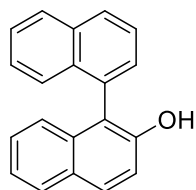
IR (ATR, neat): 2915.51, 1966.71, 1608.89, 1523.64, 1481.15, 1444.77, 1364.50, 1230.58, 1203.15, 1179.86, 1401.78, 1028.06, 1014.34, 950.70, 767.40, 705.55, 691.14 cm⁻¹.

HRMS (ESI⁺) calcd. (m/z) for C₁₆H₁₇N₄: [M+H⁺] 265.1448, found: 265.1450.

8.4.5 Suzuki–Miyaura cross coupling to form a binaphthyl backbone^[324]

2-Naphthol (146 mg, 1.0 mmol) and DMSO (87 mg, 1.1 mmol) were placed in a 10 mL vial with a magnetic stirring bar, and the atmosphere was replaced with argon. After 2 mL of 1,4-dioxane was added to the vial through the septum, a solution of trimethylsilyl bromide (174 mg, 1.1 mmol) in 1 mL of 1,4-dioxane was added to the mixture at 0 °C. The mixture was stirred for 2 hours at room temperature. The mixture was transferred to another vial with potassium carbonate (436 mg, 3.0 mmol). A solution of PEPPSI®-IPr (14 mg, 0.02 mmol) and 1-naphthaleneboronic acid (230 mg, 1.3 mmol) in 4 mL of *i*PrOH was added to the vial. After stirring the mixture at 60 °C for 24 hours, the resultant reaction mixture was quenched with saturated NH₄Cl solution. The aqueous phase was extracted with EtOAc, washed with brine, dried over MgSO₄, and was concentrated under reduced pressure. The residue was purified by using an automated preparative HPLC (5% EtOAc in hexane) to give 1,1'-binaphthyl-2'-ol (248 mg, 0.92 mmol, 92% yield).

1,1'-Binaphthyl-2'-ol (**55**), colorless crystal, CAS No.: 73572-12-0



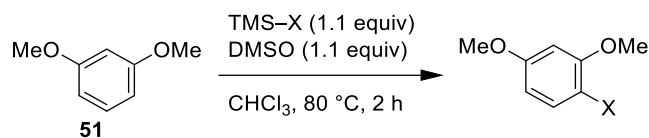
¹H NMR (300 MHz, Acetone-*d*₆): δ = 8.06 – 7.86 (m, 4H), 7.66 (dd, *J* = 8.2, 7.0 Hz, 1H), 7.55 – 7.43 (m, 2H), 7.41 – 7.16 (m, 5H), 7.01 (d, *J* = 8.8 Hz, 1H), 2.77 (t, *J* = 1.0 Hz, 1H).

¹³C NMR (75 MHz, Acetone-*d*₆): δ = 153.35, 135.50, 135.03, 134.87, 134.07, 130.27, 129.98, 129.97, 129.64, 129.17, 128.88, 128.84, 127.08, 126.83, 126.81, 126.71, 125.51, 123.69, 119.25, 119.14.

8.5 Exploring DMSO-based oxidative functionalizations

(Chapter 5)

8.5.1 Attempt of DMSO-base oxidative functionalization with TMSX (Table 16)

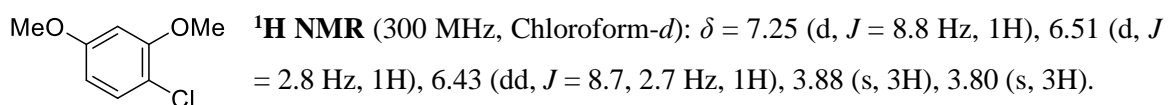


A 10 mL vial with **51** (142 mg, 1 mmol) and a stirring bar was capped with a crimp seal, and purged with argon by three vacuum/argon cycles. A solution of DMSO (87 mg, 1.1 mmol) and decane (72 mg, 0.5 mmol, GC-FID internal standard) in 2 mL of CHCl_3 was added to the vial. TMSX compound (1.1 mmol) in 1 mL of CHCl_3 was added to the vial at 0 °C. The solution was heated by a mean of aluminium heating block with vigorously stirred. After cooling it down to room temperature, 0.1 mL of the reaction mixture was quenched with 0.1 mL of triethylamine and 1 mL of EtOH, filtered through a thin layer of silica gel and submitted to GC-MS analysis. The rest of the reaction mixture was quenched with aqueous NaHCO_3 solution, extracted with EtOAc, dried over MgSO_4 and solvents were removed under reduced pressure.

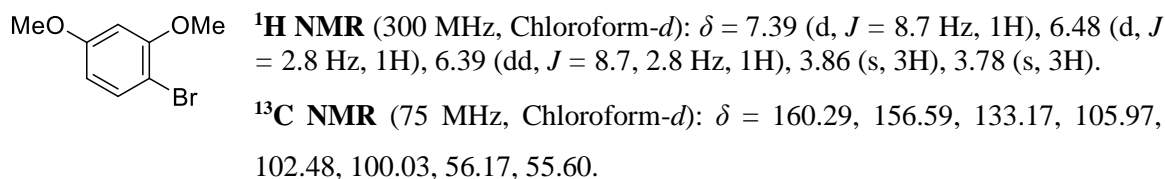
8.5.2 General procedure: Oxidative chlorination with oxalyl chloride

A 20 mL vial with **51** (142 mg, 1 mmol) and a stirring bar was capped with a crimp seal, and purged with argon by three vacuum/argon cycles. A solution of DMSO (174 mg, 2.2 mmol, or the given equivalent) and decane (72 mg, 0.5 mmol, GC-FID internal standard) in 2 mL of solvent was added to the vial. Oxalyl chloride (291 mg, 2.2 mmol, or the given equivalent) in 1 mL of solvent was added to the vial at 0 °C. The solution was stirred at room temperature for 2 hours. 0.1 mL of the reaction mixture was filtered through a thin layer of silica gel, washed with EtOH and submitted to GC-MS analysis. The rest of the reaction mixture was filtered through a thin layer of silica gel, washed with EtOH and solvents were removed under reduced pressure.

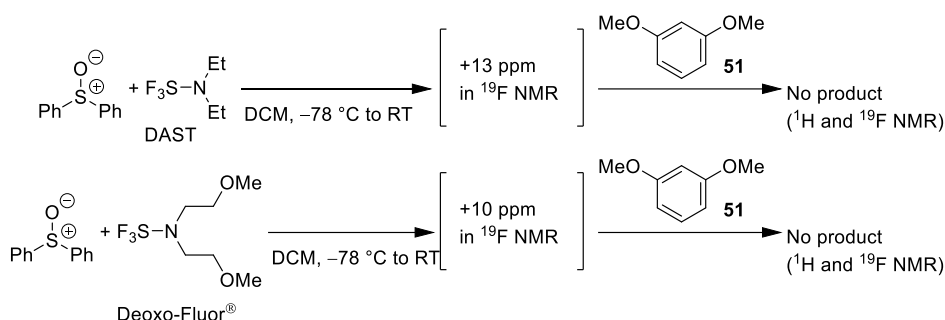
1-Chloro-2,4-dimethoxybenzene (**59**), CAS No.: 7051-13-0



2,4-Dimethoxybromobenzene (**27**), CAS No.: 17715-69-4

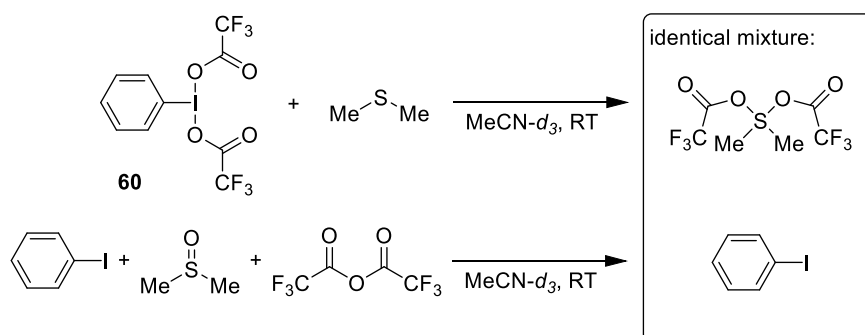


8.5.3 Activation of sulfoxides by deoxyfluorinating reagents (Scheme 98)



Diphenyl sulfoxide (206 mg, 1 mmol) was placed in a 20 mL Schlenk tube with a magnetic stirring bar, and the atmosphere was replaced with argon. After adding 3 mL of DCM, the tube was cooled down to -78 °C in MeOH/dry ice bath. DAST (332 mg, 2 mmol) in 1 mL of DCM was added to the mixture. The mixture was stirred overnight at room temperature. The cooling bath was allowed to warm up to room temperature without additional pieces of dry ice. Nitrogen gas was blown to the mixture to remove volatiles (HF and solvents) with aqueous NaOH solution trap behind. DCM was added to the residue, and white solid precipitated. This white solid was diluted in 2 mL of DCM and added to a 10 mL Schlenk tube with arene **51** (71 mg, 0.5 mmol), 3 mL of DCM and a stirring bar. The mixture was stirred at room temperature overnight. The reaction mixture was analyzed by GC-MS and ¹⁹F NMR.

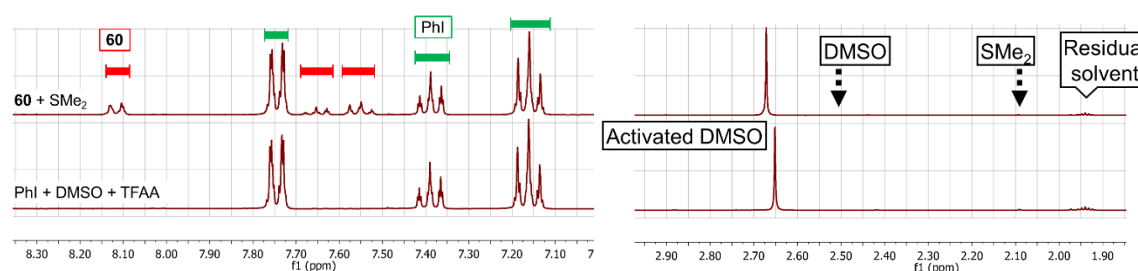
8.5.4 Redox experiments with a sulfoxide and an organoiodine (Scheme 101)



In one run, (bis(trifluoroacetoxy)iodo)benzene (**60**) (89 mg, 0.2 mmol) was placed in an NMR tube, and purged with argon by three vacuum/argon cycles. Dimethyl sulfide (13 mg, 0.2 mmol) in 2 mL of MeCN-*d*₃ was added to the tube with a slow counter flow of argon. After the tube was well shaken, the mixture was analyzed by ¹H and ¹⁹F NMR.

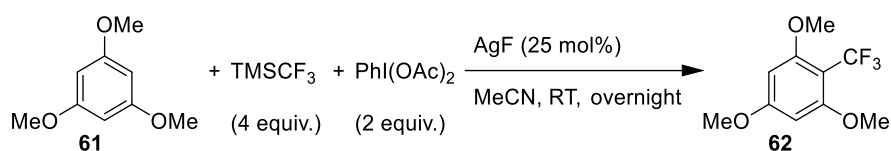
In the other run, iodobenzene (42 mg, 0.2 mmol) and DMSO (16 mg, 0.2 mmol) were placed in an NMR tube, and purged with argon by three vacuum/argon cycles. Trifluoroacetic anhydride (42 mg, 0.2 mmol) in 2 mL of MeCN-*d*₃ was added to the tube with a slow counter flow of argon. After the tube was well shaken, the mixture was analyzed by ¹H and ¹⁹F NMR.

¹H NMR spectra:



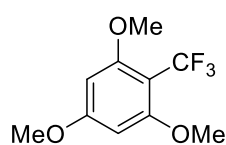
Signals for PhI (green) and trace amount of **60** (red) were detected in ¹H NMR spectra. Signals for both DMSO and SMe₂ were not detected but signals for activated DMSO were observed around 2 ppm frequency.

8.5.5 AgF-catalyzed trifluoromethylation of arene **61** (Scheme 104)



A 10 mL vial with AgF (16 mg, 0.125 mmol) and a stirring bar was capped with a crimp seal, and purged with argon by three vacuum/argon cycles. A solution of arene **61** (85 mg, 0.5 mmol) and TMSCF₃ (287 mg, 2 mmol) in 2 mL of MeCN was added to the vial. (Diacetoxyiodo)benzene (329 mg, 1 mmol) in 1 mL of MeCN was added to the vial at 0 °C. The solution was stirred at room temperature overnight. The mixture was filtered through a thin layer of silica gel, washed with DCM, and solvents were removed under reduced pressure. The crude mixture was analyzed by ¹H and ¹⁹F NMR with CH₂Br₂ as the internal standard.

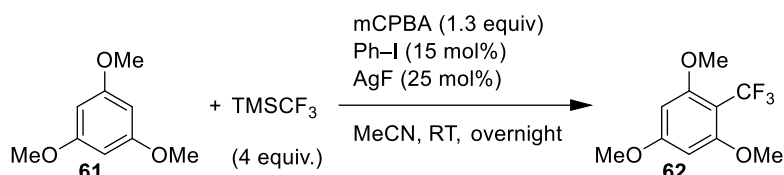
1,3,5-Trimethoxy-2-(trifluoromethyl)benzene (**62**), colorless solid, CAS No.: 1365122-33-3



$^1\text{H NMR}$ (300 MHz, Chloroform-*d*): δ = 6.12 (s, 2H), 3.83 (s, 9H).

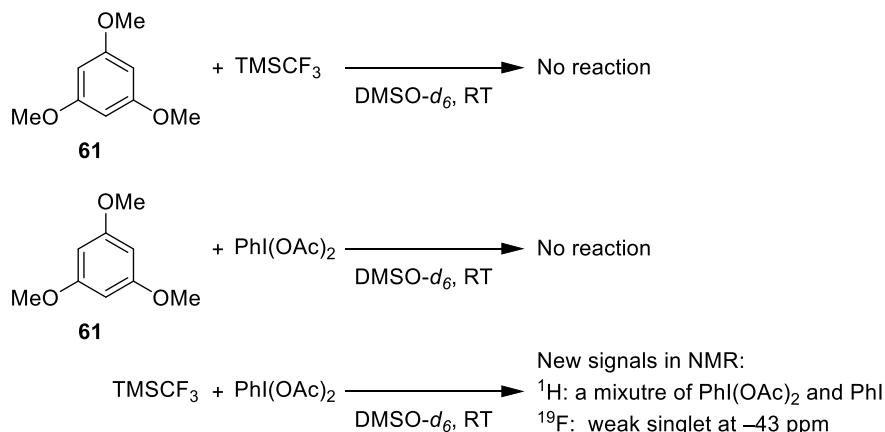
$^{19}\text{F NMR}$ (282 MHz, DMSO-*d*₆): δ = -52.00 (s).

8.5.6 Oxidative trifluoromethylation of arene **61** with catalytic amount of PhI (Scheme 105)



A 10 mL vial with AgF (16 mg, 0.125 mmol) and a stirring bar was capped with a crimp seal, and purged with argon by three vacuum/argon cycles. A solution of arene **61** (85 mg, 0.5 mmol), TMSCF₃ (287 mg, 2 mmol) and iodobenzene (16 mg, 0.075 mmol) in 2 mL of MeCN was added to the vial. mCPBA (160 mg, 70 wt%, 0.65 mmol) in 1 mL of MeCN was added to the vial at 0 °C. The solution was stirred at room temperature overnight. The mixture was filtered through a thin layer of silica gel, washed with DCM, and solvents were removed under reduced pressure. The crude mixture was analyzed by ^1H and ^{19}F NMR with CH₂Br₂ as the internal standard.

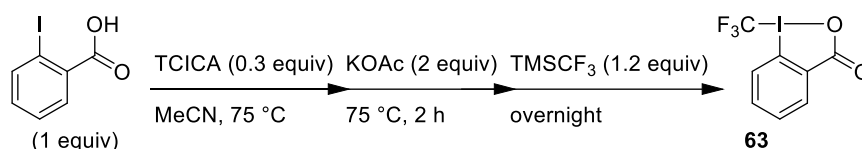
8.5.7 Examination of the reactivity of PhI(OAc)₂ with arene or TMSCF₃ (Scheme 107)



A 10 mL vial with (Diacetoxyiodo)benzene (33 mg, 0.1 mmol) and a stirring bar was capped with a crimp seal, and purged with argon by three vacuum/argon cycles. A solution of arene **61** (17 mg, 0.1 mmol) or TMSCF₃ (14 mg, 0.1 mmol) in DMSO-*d*₆ was added to the vial. The mixture was stirred until every ingredient was dissolved. 0.6 mL of the reaction mixture was transferred to an NMR tube with minimal contact to the air.

8.6 Mechanistic study of a copper-catalyzed trifluoromethylation Reaction of Arenes (Chapter 6)

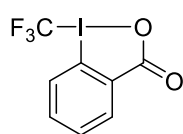
8.6.1 Synthesis of acid-type trifluoromethylating reagent **63**^[206]



A 250 mL flask equipped with a stirring bar, a condenser, a septum and a gas inlet was flame-dried and was filled with argon. 2-Iodobenzoic acid (5062 mg, 20 mmol) in 60 mL of MeCN was added to the flask, and heated up to 75 °C by a mean of oil bath. Trichloroisocyanuric acid (TCICA) (1878 mg, 8 mmol) in 10 mL of MeCN was added to the flask slowly over 5 minutes. Potassium acetate (3965 mg, 40 mmol, flame-dried) was quickly tossed into the flask with a slow counter flow of argon. The flask was vigorously stirred at 75 °C for 2 hours. After the flask was cooled down to room temperature, TMSCF_3 (3447 mg, 24 mmol) in 10 mL of MeCN was added to the flask, and the flask was stirred overnight at room temperature. Decant the liquid to a glass filter, the filtrate was cooled down in a freezer overnight. The solid was washed with MeCN and before it was filtered. The volume of this filtrate was reduced to half by evaporation and was cooled down in a freezer. Colorless crystal from both batches was collected and dried under reduced pressure. (3820 mg, 12 mmol, 60% yield)

Note that excess TMSCF_3 leads to low yields with generation of C_2F_6 (confirmed by GC-MS) and a brown reaction mixture.

1-Trifluoromethyl-1,2-benziodoxol-3-(1H)-one (**63**), colorless crystal, CAS No.: 887144-94-7



$^1\text{H NMR}$ (300 MHz, Chloroform-*d*): δ = 8.50 – 8.44 (m, 1H), 7.87 – 7.74 (m, 3H).

$^1\text{H NMR}$ (300 MHz, DMSO-*d*6): δ = 8.18 (dd, J = 7.7, 1.8 Hz, 1H), 7.93 (td, J = 8.5, 1.7 Hz, 1H), 7.86 – 7.77 (m, 2H).

$^{19}\text{F NMR}$ (282 MHz, Chloroform-*d*): δ = -33.87 (s).

$^{19}\text{F NMR}$ (282 MHz, DMSO-*d*6): δ = -33.61 (s).

8.6.2 Purification of Cu(I) compound^[388]

CuCl (3062 mg, 30 mmol) was placed on a glass filter and was washed with cold water. After removing down the water, change the reservoir to a flask with water. Saturated aqueous NH₄Cl solution was added to the filter and was stirred, before it was filtered. Precipitation was observed in the reservoir. This NH₄Cl/filtration cycle was repeated until the filtrate was Colorless although usually once was enough. The suspension was filtered and washed water, EtOH and distilled Et₂O (20 mL each). The collected solid was dried under reduced pressure.

CuBr and CuI were purified in a similar manner with NaBr and NaI instead of NH₄Cl, respectively.

8.6.3 General procedure for the trifluoromethylation reaction

Catalyst (0.015 mmol, or the given equivalent) was placed in a 10 mL vial with a stirring bar, capped with a crimp seal, and purged with argon by three vacuum/argon cycles. PhCF₃ (22 mg, 0.15 mmol, 1 equiv, ¹⁹F NMR internal standard), 1,3,5-trimethoxybenzene (**61**) (51 mg, 0.3 mmol, or the given equivalent) in 1 mL of solvent was added to the vial. Reagent **63** (48 mg, 0.15 mmol, or the given equivalent) in 2 mL of solvent was added to the vial dropwise at room temperature. The solution was stirred at room temperature before it was heated.

In the case with a pretreatment, catalyst, PhCF₃ and reagent **63** were added as above and the vial was stirred at room temperature. After ¹⁹F NMR analysis of this mixture, arene **61** in 1 mL of solvent was added and heated.

When the solvent was DMSO, 0.1 mL of the reaction mixture was diluted in DMSO-*d*₆ for ¹⁹F NMR analysis. Otherwise, 0.5 mL of the reaction mixture was submitted to the analysis, and the sample was injected back to the vial with a minimal contact to the air. In both cases, NMR tubes were charged with argon. In ¹⁹F NMR analysis, internal standard PhCF₃ was set at -60.94 ppm.

For isolation of product **62**, the reaction mixture was added to 0.1 M HCl solution, and extracted with EtOAc, washed with brine, dried over MgSO₄, and solvents were removed under reduced pressure. The crude mixture was separated using silica-gel flash chromatography (hexane: EtOAc, gradient elution).

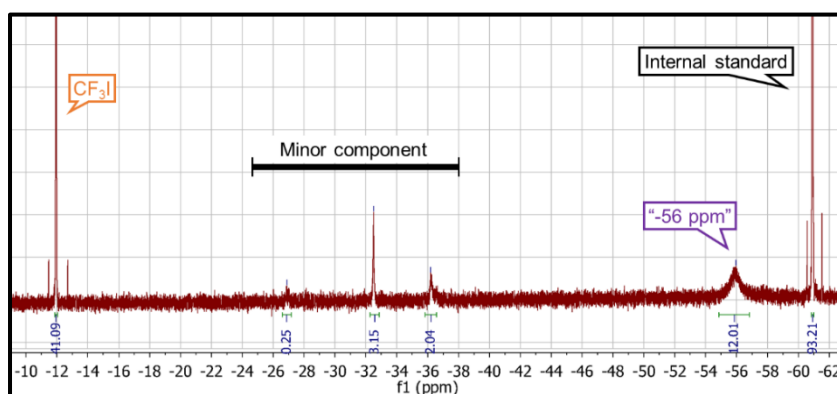
For the experiments in the dark, screw-capped amber glass vials were used.

8.6.4 General procedure for stoichiometry determination experiments

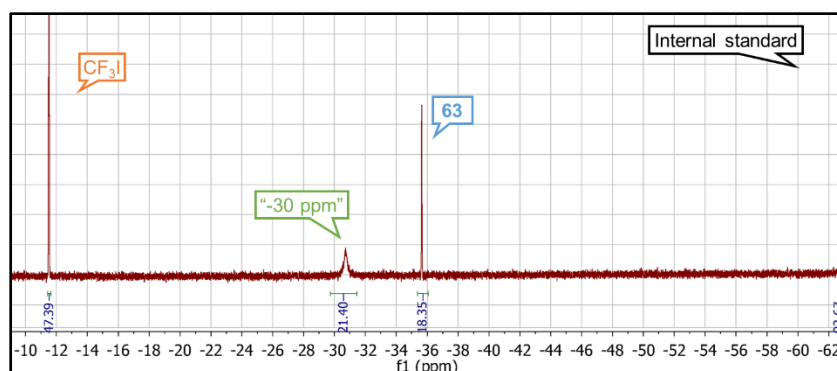
Catalyst was placed in a 20 mL vial with a stirring bar, capped with a crimp seal, and purged with argon by three vacuum/argon cycles. PhCF₃ (22 mg, 0.15 mmol, 1 equiv, ¹⁹F NMR internal standard) and 8 mL of solvent was added to the vial. Reagent **63** (48 mg, 0.15 mmol) in 2 mL of solvent was added to the vial dropwise. The solution was stirred overnight before ¹⁹F NMR analysis of the reaction mixture.

For **63**-excess conditions, CuI (29 mg, 0.15 mmol) and the given equivalent of reagent **63** were used. For cold experiments, the vial was cooled down to -40 °C in dry ice/MeCN bath before reagent **63** was added to the vial along the vial wall. The cooling bath was allowed to warm up to room temperature without additional pieces of dry ice. Arene **61** (51 mg, 0.3 mmol) was added to the vial with PhCF₃ when it was described in the scheme.

Selected ¹⁹F NMR spectra



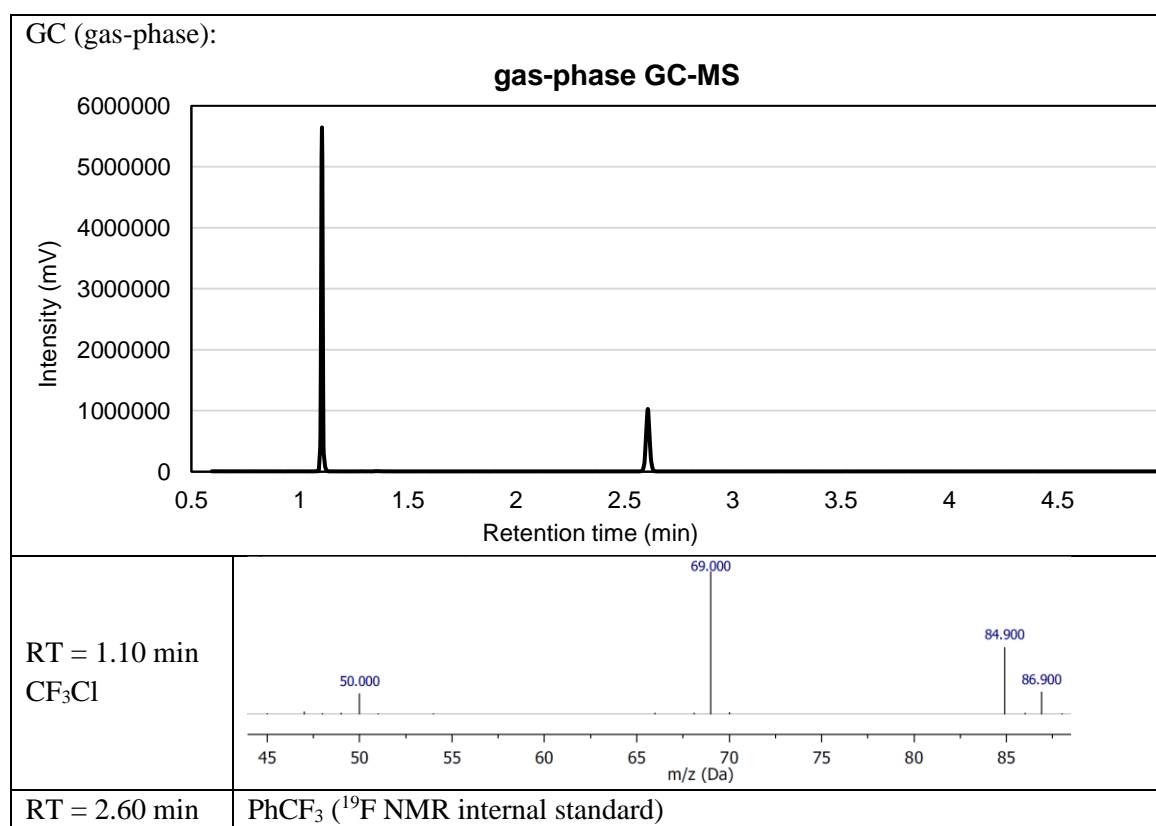
Reaction of CuI and reagent **63** in DMSO at RT (**Table 19**, **63**/CuI=0.75 (equiv)). Minor Cu–CF₃ components were observed.



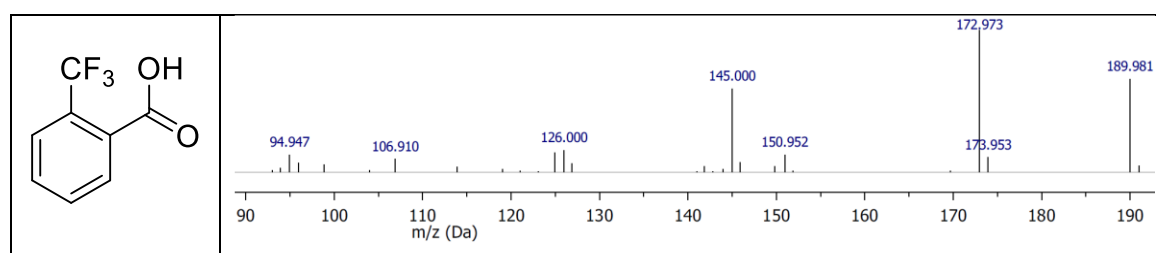
Cold reaction of CuI and reagent **63** in DMF (**Scheme 113b**, CuI/**63** (mol%)). No minor Cu–CF₃ components were observed.

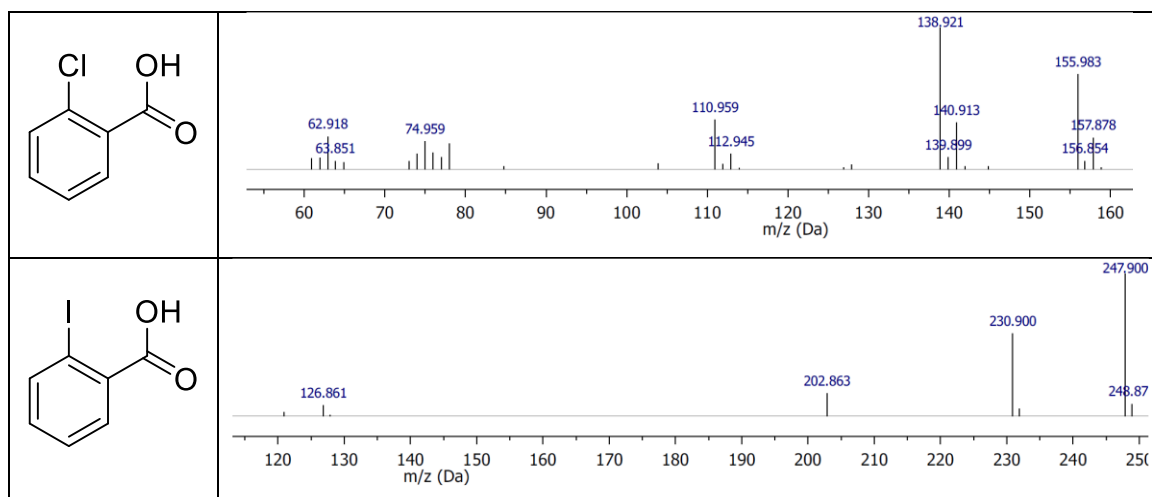
8.6.5 CuCl_n qualitative analyses (Scheme 120)

CuCl (51 mg, 0.5 mmol) or CuCl_2 (68 mg, 0.5 mmol) was placed in a 10 mL vial with a stirring bar, capped with a crimp seal, and purged with argon by three vacuum/argon cycles. PhCF_3 (74 mg, 0.5 mmol, ^{19}F NMR internal standard) and 1 mL of solvent was added to the vial. Reagent **63** (48 mg, 0.15 mmol) in 2 mL of solvent was added to the vial dropwise at room temperature. The solution was stirred at 40 °C for 2 hours. The gas sample from the vial was measured by GC-MS, and the solution was analyzed by ^{19}F NMR and GC-MS.

GC-MS analysis of the reaction of CuCl_n and reagent **63**

GC-MS (solution):



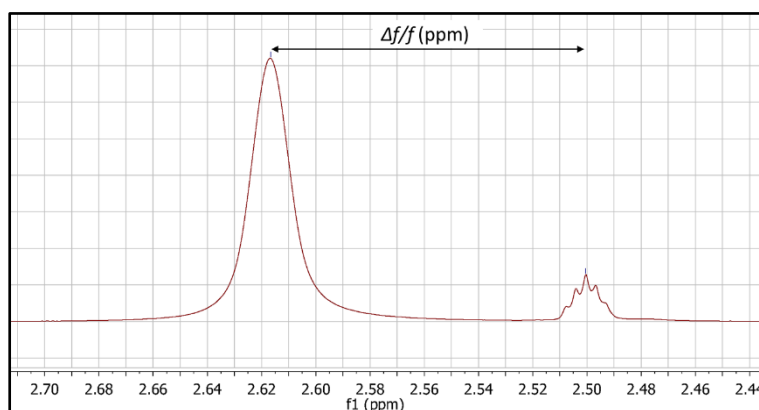


8.6.6 Magnetic susceptibility measurement (Table 23)

CuI (10 mg, 0.05 mmol) was placed in a 10 mL vial with a stirring bar, capped with a crimp seal, and purged with argon by three vacuum/argon cycles *via* a needle. The weight of this vial was recorded. Reagent **63** (24 mg, 0.075 mmol) in 2 mL of DMSO-*d*₆ was added dropwise to the vial, and the exact weight was recorded. The solution was stirred overnight. 1 mL of the mixture was transferred an NMR tube with a minimal contact to the air, and a capillary filled with DMSO-*d*₆ was added to the tube. The whole process was repeated for three samples.

Other samples were prepared as following and the exact values were recorded: **64**·2DMSO (8 mg, 0.0125 mmol) in 0.5 mL of DMSO-*d*₆ or CDCl₃, Cu(OAc)₂·H₂O (5 mg, 0.025 mmol) in 1 mL of DMSO-*d*₆, CuBr₂ (6 mg, 0.025 mmol) in 1 mL of DMSO-*d*₆. 1 mL of the mixture was transferred an NMR tube with a minimal contact to the air, and a capillary filled with DMSO-*d*₆ was added to the tube. The whole process was repeated for three samples.

Spectrum example: (Table 23, entry 1 (reaction mixture))



Calculations^[401]

The value of the effective magnetic moment (μ_{eff}) was determined from the magnetic susceptibility by paramagnetic contribution (χ_{para}) by the Curie Law equation:

$$\mu_{\text{eff}} = \sqrt{\frac{3kT\chi_{\text{para}}}{N\beta^2}}$$

, where k =Boltzmann constant ($1.3807 \times 10^{-16} \text{ cm}^2 \cdot \text{g} \cdot \text{s}^{-2} \cdot \text{K}^{-1}$), N =Avogadro's number ($6.0221409 \times 10^{23} \text{ mol}^{-1}$), β =Bohr magneton ($9.274009994 \times 10^7 \text{ erg} \cdot \text{G}^{-1}$) and T =the absolute temperature (K).

Here, we neglected the diamagnetic contribution because it is reportedly low ($\chi_{\text{para}} \approx \chi_{\text{M}}$). χ_{M} is the molar susceptibility of the sample in mL/mol, which can be determined by ¹H NMR.

$$\chi_{\text{M}} = \frac{3000 \Delta f}{4\pi c} \frac{1}{f} + \chi_{0, \text{M}}$$

, where c =concentration of the sample (M), $\Delta f/f$ = the difference in chemical shift (ppm). $\chi_{0, \text{M}}$ is the molar susceptibility of the solvent by the equation below, which was calculated to be -4.43×10^{-5} mL/mol.

$$\chi_{0, \text{V}} = \frac{\chi_{0, \text{V}} \text{Mw}}{d_0}$$

$\chi_{0, \text{V}}$ for DMSO-*d*6 = -6.09×10^{-7} mL/mL, d_0 is the density of DMSO-*d*6 (1.19 g/mL) and Mw is the molecular weight of DMSO-*d*6 (84.17 g/mol).

The volume of the solution was calculated from the weight of the solution and the density of DMSO-*d*6. The averages of three values are reported in **Table 23**.

The calculation data

Reaction mixture	_1	_2	_3
CuI (mg)	9.5	9.9	9.9
Volume of the solution (mL)	2.189	2.250	2.191
[Cu] (M)	0.0228	0.0231	0.0237
$\Delta f/f$ (ppm)	0.116	0.133	0.133
χ_M (mL/mol)	1.17×10^{-3}	1.33×10^{-3}	1.30×10^{-3}
μ_{eff} (B.M.)	1.67	1.78	1.76

^1H NMR was measured at 298 K with an external magnetic field of 500.26 MHz.

	64-2DMSO			Cu(OAc) ₂ ·H ₂ O			CuBr ₂		
[Cu] (mg)	7.9	7.8	7.8	5.0	5.0	4.7	6.2	5.7	5.8
Volume (mL)	0.569	0.536	0.543	1.022	1.018	1.032	1.043	1.113	1.031
[Cu] (M)	0.021	0.022	0.022	0.024	0.024	0.022	0.026	0.022	0.025
	9	9	6	5	6	8	6	9	2
$\Delta f/f$ (ppm)	0.108	0.110	0.111	0.098	0.102	0.094	0.221	0.192	0.208
χ_M (mL/mol)	1.14×10^{-3}	1.10×10^{-3}	1.13×10^{-3}	9.12×10^{-3}	9.46×10^{-3}	9.41×10^{-3}	1.94×10^{-3}	1.96×10^{-3}	1.93×10^{-3}
μ_{eff} (B.M.)	1.67	1.78	1.76	1.48	1.51	1.50	2.15	2.16	2.15

^1H NMR was measured at 299.4 K with an external magnetic field of 300.13 MHz.

64-2DMSO in CDCl ₃	_1	_2	_3
CuI (mg)	8.0	8.2	7.8
Volume of the solution (mL)	0.633	0.557	0.560
[Cu] (M)	0.0199	0.0232	0.0219
$\Delta f/f$ (ppm)	0.075	0.09	0.083
χ_M (mL/mol)	8.41×10^{-4}	8.68×10^{-4}	8.45×10^{-4}
μ_{eff} (B.M.)	1.42	1.44	1.42

^1H NMR was measured at 299.4 K with an external magnetic field of 300.13 MHz. $\chi_{0,V}$ for CDCl₃ = -7.40×10^{-7} mL/mL, $d_0 = 1.50$ g/mL, $M_w = 120.38$ g/mol, Therefore, $\chi_{0,M}$ for CDCl₃ = -5.94×10^{-5} mL/mol.

8.6.7 EPR and UV-VIS measurements

CuI (48 mg, 0.15 mmol) was placed in a 20 mL vial with a stirring bar, capped with a crimp seal, and purged with argon by three vacuum/argon cycles. PhCF₃ (22 mg, 0.15 mmol, ^{19}F NMR internal

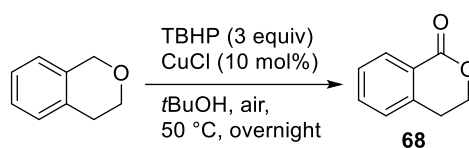
standard) and 8 mL of solvent was added to the vial. The vial was cooled down to $-40\text{ }^{\circ}\text{C}$ in dry ice/MeCN bath before reagent **63** (48 mg, 0.15 mmol) was added to the vial along the vial wall. The solution was stirred overnight with the cooling bath allowed to warm up to room temperature without additional pieces of dry ice.

For analysis by EPR spectroscopy 40 μL of a 2 mM solution of each sample in DMF were filled into 3 mm quartz capillaries, flash-frozen in liquid nitrogen and transferred frozen into the pre-cooled EPR spectrometer. Continuous wave (cw) EPR spectra were acquired at X-band (ca. 9.5 GHz) on an Elexsys E580 EPR spectrometer (Bruker Biospin, Rheinstetten, Germany) using a cylindrical resonator (Bruker SHQ) and an ESR900 helium flow cryostat (Oxford Instruments, Oxford, UK) to maintain a temperature of 20 K. Spectra were recorded under non-saturating conditions corresponding here to a microwave power of 13 μW , a B-field modulation amplitude of 0.2 mT and a conversion time of 81.92 ms for lock-in detection using 1024 points over a sweep width of 120 mT. EPR spectra were analyzed using the Matlab package EasySpin.^[402] The measurement and data analysis were carried out by Dr. Daniel Klose.

For analysis by UV-VIS spectroscopy, the reaction mixture was filled in 10 mm quartz cell. Spectra were acquired on Specord 250 spectrophotometer made by Analytik Jena (Jena, Germany). The measurement and data analysis were carried out by Dr. Reinhard Kissner.

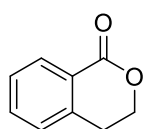
8.6.8 Attempt of the synthesis of tricarboxylic acid **67**-H₃ (Scheme 132)

Oxidation of isochroman^[403]



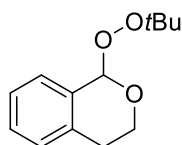
Isochroman (2711 mg, 20 mmol) and CuCl (99 mg, 1 mmol) was placed in a 500 mL flask equipped with a stirring bar, a condenser and a gas inlet. After 200 mL of *tert*-butyl alcohol was added to the flask, the mixture was stirred at 50 °C for 12 hours with a slow flow of air through the gas inlet to a gas trap. The mixture was cooled down to room temperature, poured into saturated Na₂S₂O₃ solution, extracted with EtOAc, dried over MgSO₄, and solvents were removed under reduced pressure. The crude mixture was separated using silica-gel flash chromatography (hexane: EtOAc, gradient elution). 3,4-Dihydroisocoumarin (**68**) was obtained (1.722 g, 11.63 mmol, 58% yield). The reported intermediate (**79**) was also obtained in 30% yield (1.350 g, 6.08 mmol).

3,4-Dihydroisocoumarin (**68**), CAS No.: 4702-34-5



$^1\text{H NMR}$ (300 MHz, Chloroform-*d*): δ = 8.10 (dd, J = 7.9, 1.1 Hz, 1H), 7.54 (td, J = 7.5, 1.4 Hz, 1H), 7.40 (t, J = 7.6 Hz, 1H), 7.26 (d, J = 7.5 Hz, 1H), 4.54 (d, J = 5.9 Hz, 2H), 3.06 (t, J = 6.0 Hz, 2H).

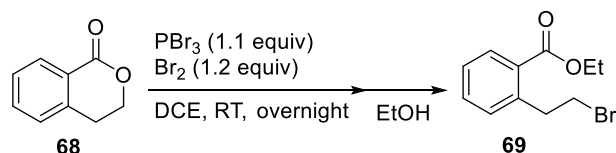
1-*tert*-butylperoxyisochroman (**79**), CAS No.: 131869-38-0



$^1\text{H NMR}$ (300 MHz, Chloroform-*d*): δ = 7.41 – 7.02 (m, 4H), 6.05 (s, 1H), 4.23 (td, J = 11.8, 3.3 Hz, 1H), 4.01 (ddd, J = 11.3, 6.1, 1.4 Hz, 1H), 3.04 (ddd, J = 17.8, 12.3, 6.1 Hz, 1H), 2.61 (dd, J = 16.6, 3.3 Hz, 1H), 1.36 (s, 9H).

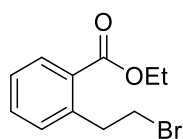
Intermediate **79** (1351 mg, 10 mmol) and CuCl (99 mg, 1 mmol) was placed in a 250 mL flask equipped with a stirring bar, a condenser and a gas inlet. After 100 mL of *tert*-butyl alcohol was added to the flask, the mixture was stirred at 50 °C for 12 hours with a slow flow of air through the gas inlet to a gas trap. The mixture was cooled down to room temperature, poured into saturated Na₂S₂O₃ solution, extracted with EtOAc, dried over MgSO₄, and solvents were removed under reduced pressure. The crude mixture was separated using silica-gel flash chromatography (hexane: EtOAc, gradient elution).

Bromination of dihydroisocoumarin^[404]



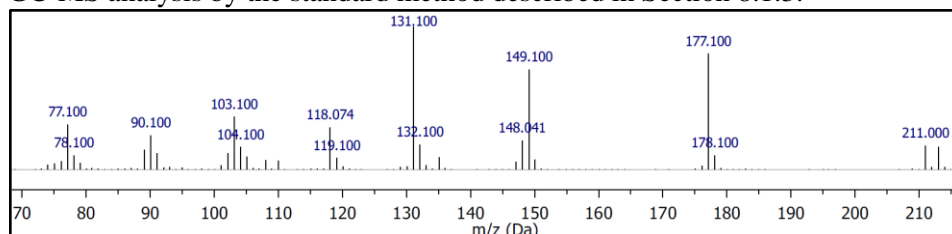
A 25 mL flask equipped with a stirring bar and a condenser was purged with argon by three vacuum/argon cycles. Bromine (775 mg, 4.8 mmol), 6 mL of 1,2-dichloroethane and a solution of phosphorus tribromide (1203 mg, 4.4 mmol) in 2 mL of 1,2-dichloroethane (DCE) was added to the flask with vigorously stirred. 3,4-dihydroisocoumarin (**68**) (599 mg, 4 mmol) in 2 mL of 1,2-dichloroethane was added to the flask slowly. The mixture was stirred at room temperature overnight, and then heated at 60 °C for 3 hours. The mixture was cooled down to 0 °C, and 4 mL of ethanol was added slowly. The mixture was stirred at room temperature for 1 hour, then was poured into water, extracted with DCM, washed with brine, dried over MgSO₄, and solvents were removed under reduced pressure. The crude mixture was separated using silica-gel flash chromatography (hexane: EtOAc, gradient elution). Ethyl 2-(2-bromoethyl)benzoate (**69**) was obtained (0.6958 g, 2.71 mmol, 67% yield).

Ethyl 2-(2-bromoethyl)benzoate (**69**), CAS No.: 179994-91-3

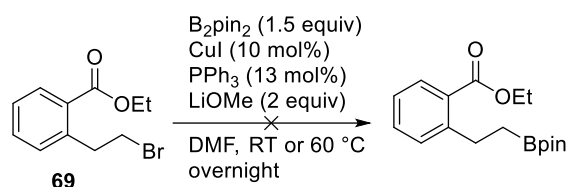


$^1\text{H NMR}$ (300 MHz, Chloroform-*d*): δ = 7.96 (dd, J = 7.8, 1.5 Hz, 1H), 7.47 (td, J = 7.5, 1.5 Hz, 1H), 7.38 – 7.27 (m, 2H), 4.37 (q, J = 7.1 Hz, 2H), 3.64 (t, J = 6.9 Hz, 2H), 3.49 (t, J = 6.6 Hz, 2H), 1.41 (t, J = 7.1 Hz, 3H).

GC-MS analysis by the standard method described in Section 8.1.3.

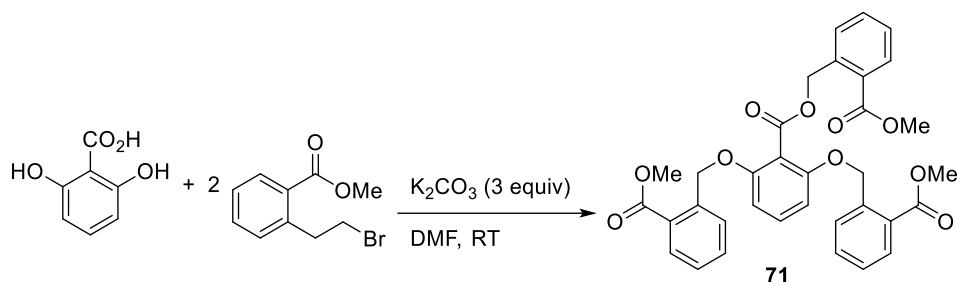


Attempted borylation of bromide **69**^[405]



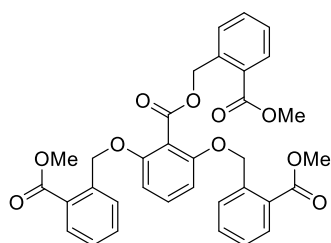
Bis(pinacolato)diboron (770 mg, 3 mmol), CuI (38 mg, 0.2 mmol), triphenylphosphine (80 mg, 0.3 mmol) and lithium methyllate (160 mg, 4 mmol) were placed in a 20 mL vial with a stirring bar. The vial was capped with a crimp seal, and purged with argon by three vacuum/argon cycles. 8 mL of DMF was added to the vial followed a slow addition of bromide **69** (520 mg, 2 mmol) in 2 mL of DMF. The mixture was stirred at room temperature overnight. The mixture was filtered through a thin layer of silica gel, then was poured into water, extracted with EtOAc, washed with brine, dried over MgSO_4 , and solvents were removed under reduced pressure. The crude mixture was analyzed by $^1\text{H NMR}$. However, $^1\text{H NMR}$ signals only for dihydroisocoumarin (**68**) and bromide **69** were detected.

In different runs, the vial was heated at 60 °C, and also PEPPSI®-IPr (7 mg, 0.01 mmol) and K_2CO_3 were used instead of CuI, triphenylphosphine and lithium methoxide, although only the $^1\text{H NMR}$ signals for dihydroisocoumarin (**68**) were detected in $^1\text{H NMR}$.

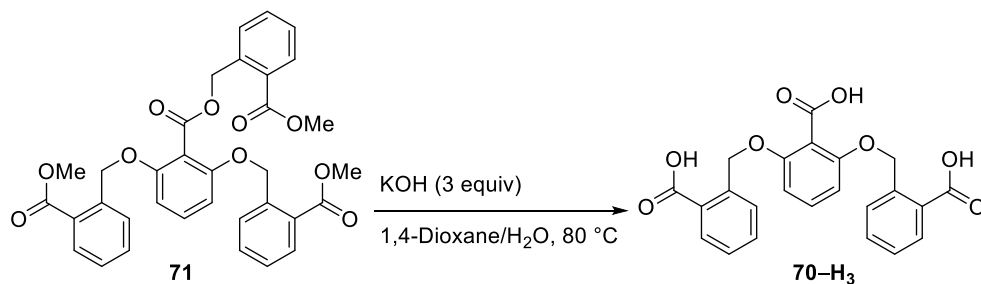
8.6.9 The synthesis of tricarboxylic acid **70-H₃** (Scheme 134)Synthesis of ester **71**

K_2CO_3 (4539 mg, 31.2 mmol) was placed in a 50 mL flask equipped with a stirring bar, and then was purged with argon by three vacuum/argon cycles. 12 mL of DMF, 2,6-dihydroxybenzoic acid (1022 mg, 6.5 mmol) in 8 mL of DMF, and methyl 2-bromomethylbenzoate (4862 mg, 20.8 mmol) in 4 mL of DMF were added to the flask sequentially. The mixture was stirred at room temperature overnight. The mixture was poured into water and toluene followed by filtration to collect the solid. The filtrate was acidified with 1 M HCl, extracted with DCM, dried over MgSO_4 , and solvents were removed under reduced pressure. Both the solid and residue were analyzed by ^1H NMR. The crude mixture was separated using silica-gel flash chromatography (hexane: EtOAc, gradient elution).

Ester **71**, white solid, (3.873 g, 6.47 mmol, 99% yield)



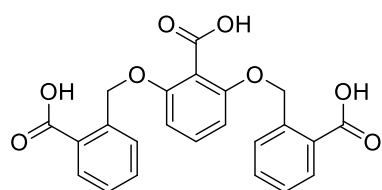
^1H NMR (300 MHz, Chloroform-*d*): δ = 8.02 (dd, J = 7.8, 1.4 Hz, 2H), 7.97 (dd, J = 7.4, 1.3 Hz, 2H), 7.72 (d, J = 7.9 Hz, 2H), 7.65 (d, J = 7.6 Hz, 1H), 7.47 (t, J = 7.7 Hz, 2H), 7.34 (t, J = 7.6 Hz, 2H), 7.22 (t, J = 8.1 Hz, 2H), 6.65 (d, J = 8.5 Hz, 2H), 5.88 (s, 2H), 5.58 (s, 4H), 3.91 (s, 6H), 3.88 (s, 3H).

Saponification of ester **71**

Ester **71** (120 mg, 0.2 mmol) was placed in a 10 mL vial with a stirring bar. The vial was capped with a crimp seal, and purged with argon by three vacuum/argon cycles. 5 mL of 1,4-dioxane was

added to the vial followed by KOH (528 mg, 85wt%, 8 mmol) in 7 mL water. The mixture was stirred at 80 °C overnight. The organic phase was isolated, and the solvent was removed in vacuum. The aqueous phase was washed with EtOAc, acidified with 1M HCl, extract with EtOAc, washed with 1M HCl again, and solvents were removed in reduced pressure. The residue was washed with CHCl₃, extract with MeOH, and solvents were removed under reduced pressure. Both fractions from the organic phase and aqueous phase were the desired product.

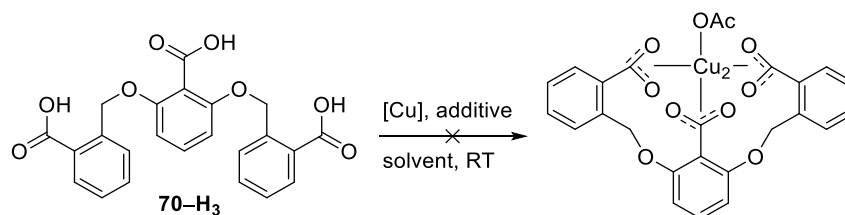
Tricarboxylic acid **70**-H₃, colorless solid (0.0840 g, 0.199 mmol, >99% yield)



¹H NMR (300 MHz, Methanol-*d*₄): δ = 8.06 (dd, *J* = 7.8, 1.4 Hz, 2H), 7.82 (d, *J* = 7.9 Hz, 2H), 7.58 (t, *J* = 7.5 Hz, 2H), 7.40 (t, *J* = 7.6 Hz, 2H), 7.29 (t, *J* = 8.4 Hz, 1H), 6.69 (d, *J* = 8.4 Hz, 2H), 5.57 (s, 4H).

HRMS (ESI⁺) calcd. (*m/z*) for C₂₃H₁₈O₈: [M+Na⁺] 445.0894, found: 445.0896.

Attempt to form Cu₂(**70**)OAc (Scheme 135)



Copper precursor was placed in a 20 mL vial with a stirring bar. The vial was capped with a crimp seal, and purged with argon by three vacuum/argon cycles. Solvent, carboxylic acid **70**-H₃ (43 mg, 0.1 mmol) and additive were added to the vial although the green powder appeared upon the addition of **70**-H₃. Poorly soluble green powdery material precipitated in the solution upon the mix of copper precursors and acid **70**-H₃. Having seen a gradual increase of the volume of green powdery material and its poor solubility, we reasoned that the powder might be a polymer.

Examined conditions:

Copper precursor: Cu(OAc)₂·H₂O, CuCl₂, [Cu(DMSO)₆](BF₄)₂

Solvent: DMSO, THF, water, MeCN, DCM, MeOH, 1,4-dioxane, xylene

Additive: none, NaH, KOH, KOAc, benzoic acid

Also, different concentrations, addition orders, reaction temperature and use of potassium salt **70**-K₃ were examined, but the green insoluble powder was always obtained.

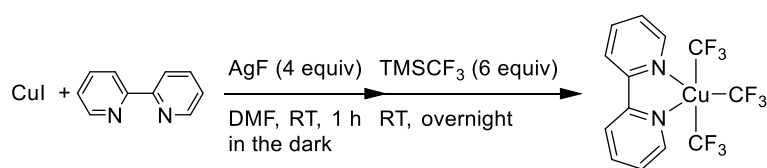
8.6.10 Elemental analysis of the green powder (Table 24)

All the complexation samples were combined and washed with DMSO at 60 °C. After DMSO was removed by filtration, the solid was washed with methanol. Then, methanol was removed by filtration and the solid was dried under reduced pressure. The elemental analyses of the resultant sample were carried out by the analysis service of the *Laboratorium für Organische Chemie der ETHZ (LOC)* for C, H and S, and copper content was determined by ICPMS technique. For ICPMS measurements, the samples were digested (1200 W, 220 °C, 40 bar) and further diluted by a factor of around 10^5 . The measurements were performed by atomic absorption spectroscopy (AAS, Perkin Elmer AAnalyst 200, Schwerzenbach, CH) using a standard addition approach to overcome possible matrix issues. The measurement and data analysis were carried out by Stephan Kradolfer from the group of Günther at ETH Zürich.

Calculated values of plausible compositions.

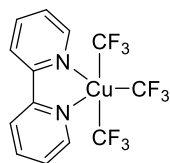
Composition	Cu	C	H	O	S	Comment
Experimental	21.8	49.69	3.66	23.565 ^[a]	1.285	
Cu ₂ (70)(OAc)(DMSO) _{0.23}	20.33	49.00	3.12	26.26	1.29	Suggested structure
Cu ₃ (70) ₃ (DMSO) _{0.43}	17.94	52.95	3.07	24.75	1.28	Cu too little
Cu ₂ (70)(OMe)(DMSO) _{0.24}	21.32	49.31	3.26	24.82	1.29	
Cu ₂ (70)(OH)(DMSO) _{0.23}	21.85	48.45	2.99	25.42	1.28	
Cu ₂ (70)(OCOPh)(DMSO) _{0.28}	18.44	53.25	3.15	23.88	1.28	Cu too little

^[a] Calculated to fill up the total to 100%.

8.6.11 Cu(III)–CF₃ (Scheme 138)**Synthesis of Cu(III)–CF₃ species **72**^[383]**

CuI (1924 mg, 10 mmol) and AgF (5126 mg, 40 mmol) and a stirring bar were placed in a 50 mL flask covered with an aluminium foil. The flask was purged with argon by three vacuum/argon cycles. 2,2'-Bipyridyl (1594 mg, 10 mmol) in 10 mL of DMF was added to the flask, and the mixture was stirred at room temperature for 1 hour. After 4 hours from the addition of TMSCF₃ (4309 mg, 30 mmol), another portion of TMSCF₃ (4309 mg, 30 mmol) was added to the flask, and was stirred overnight. The mixture was filtered, and the solid was washed with 20 mL of DCM. The filtrates were combined and washed with water. Silica gel was added to the organic phase, and then solvents were removed under reduced pressure. The obtained silica gel was loaded for Flash column chromatography.

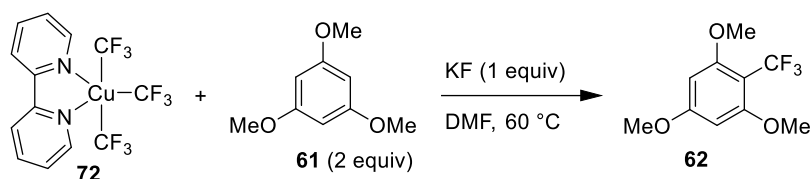
(2,2'-Bipyridyl- $\kappa N, \kappa N'$)tris(trifluoromethyl)copper(III) (**72**), yellow solid (1.314 g, 3.08 mmol, 31% yield), CAS No.: 1680206-12-5



$^1\text{H NMR}$ (300 MHz, $\text{DMSO-}d_6$): δ = 9.28 – 9.18 (m, 1H), 8.80 (d, J = 8.1 Hz, 1H), 8.38 (td, J = 7.9, 1.6 Hz, 1H), 7.91 (ddd, J = 7.6, 5.2, 1.2 Hz, 1H).

$^{19}\text{F NMR}$ (282 MHz, $\text{DMSO-}d_6$): δ = -23.70 (p, J = 9.1 Hz, 3F), -35.86 (q, J = 9.2 Hz, 6F).

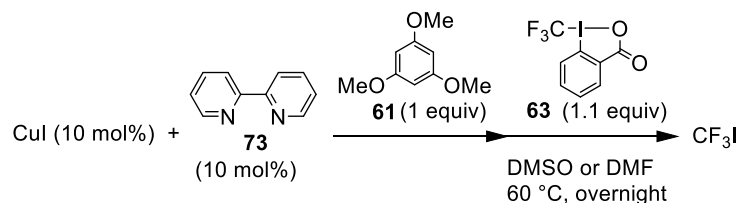
Trifluoromethylation of arene **61** by reagent **72**



KF (18 mg, 0.3 mmol) was placed in a 10 mL vial with a stirring bar, capped with a crimp seal, and purged with argon by three vacuum/argon cycles. PhCF_3 (44 mg, 0.3 mmol), 1,3,5-trimethoxybenzene (**61**) (51 mg, 0.3 mmol) in 1 mL of solvent was added to the vial. Reagent **72** (51 mg, 0.3 mmol) in 2 mL of solvent was added to the vial slowly at room temperature. The solution was stirred at room temperature overnight. After the mixture was cooled down to room temperature, 0.6 mL of the reaction mixture was taken to an NMR tube filled with argon for ^{19}F NMR analysis. Then, the mixture was heated at 60 °C and stirred overnight. Another 0.6 mL of the reaction mixture was taken to an NMR tube filled with argon for ^{19}F NMR analysis.

In the cases that additional bases were used, K_2CO_3 (50 mg, 0.36 mmol) was placed at the beginning, or triethylamine (37 mg, 0.36 mmol) was included in the solution of arene **61**.

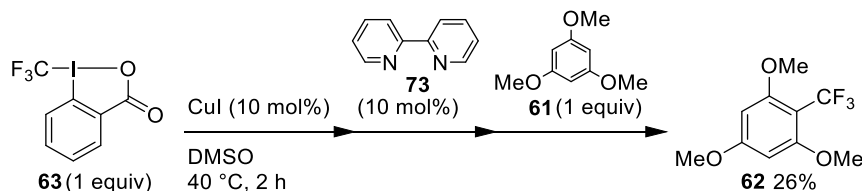
Reactions with 2,2'-bipyridyl (**73**) (CuI-73-61-63) (Scheme 139)



CuI (10 mg, 0.05 mmol) and ligand **73** (8 mg, 0.05 mmol) were placed in a 20 mL vial with a stirring bar, capped with a crimp seal, and purged with argon by three vacuum/argon cycles. 5 mL of DMSO or DMF was added to the vial, and the mixture was stirred at 60 °C for 4 hours. A solution of 1,3,5-trimethoxybenzene (**61**) (85 mg, 0.5 mmol) and PhCF_3 (74 mg, 0.5 mmol) in 3 mL of the solvent followed by reagent **63** (176 mg, 0.55 mmol) in 2 mL of the solvent was added to the vial

slowly at room temperature. The solution was stirred at 60 °C overnight. After the mixture was cooled down to room temperature, 0.6 mL of the reaction mixture was taken to an NMR tube filled with argon for ^{19}F NMR analysis, where only the signal for CF_3I was observed.

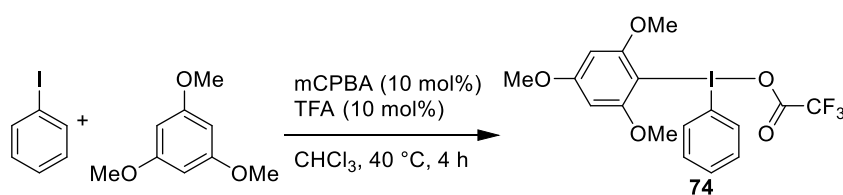
Reactions with 2,2'-bipyridyl (**73**) (CuI -**73**-**61**-**63**) (Scheme 140)



CuI (6 mg, 0.03 mmol) was placed in a 10 mL vial with a stirring bar, capped with a crimp seal, and purged with argon by three vacuum/argon cycles. A solution of reagent **63** (96 mg, 0.3 mmol) and PhCF_3 (44 mg, 0.3 mmol) in 2 mL of DMSO was added to the vial, and the mixture was stirred at 40 °C for 2 hours. Ligand **73** (8 mg, 0.05 mmol) in 1 mL of DMSO was added to the vial, and the mixture was stirred at 40 °C for 2 hours. 1,3,5-trimethoxybenzene (**61**) (51 mg, 0.3 mmol) in 1 mL of DMSO was added to the vial, and the mixture was stirred at 40 °C overnight. After the mixture was cooled down to room temperature, 0.6 mL of the reaction mixture was taken to an NMR tube filled with argon for ^{19}F NMR analysis.

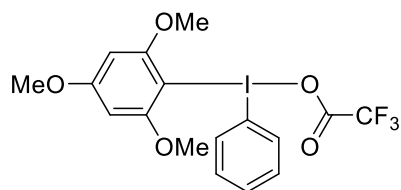
8.6.12 Diaryl- λ^3 -iodanes

The synthesis of Ar-I(III) compound **74**^[406]



3-Chloroperoxybenzoic acid (mCPBA) (814 mg, 70wt%, 3.3 mmol) and a stirring bar were placed in a 100 mL flask. The flask was purged with argon by three vacuum/argon cycles. 15 mL of CHCl_3 , iodobenzene (625 mg, 3 mmol) in 5 mL of CHCl_3 , trifluoroacetic acid (TFA) (380 mg, 3.3 mmol) in 5 mL of CHCl_3 and then 1,3,5-trimethoxybenzene (1529 mg, 9 mmol) in 5 mL of CHCl_3 were added to the flask, and the mixture was stirred at 40 °C for 4 hours. After solvents were removed in reduced pressure, Et_2O was added to the mixture and filtered to collect the solid. The product was recrystallized from $\text{DCM}/\text{Et}_2\text{O}$ at -20 °C (0.291 g, 0.60 mmol, 20% yield).

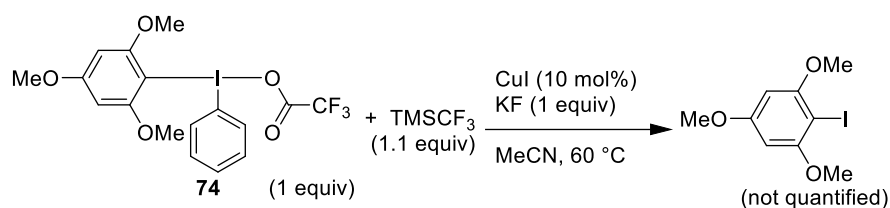
Phenyl(2,4,6-trimethoxyphenyl) iodonium trifluoroacetate (**74**), orange crystal, CAS No.: 2245026-78-0



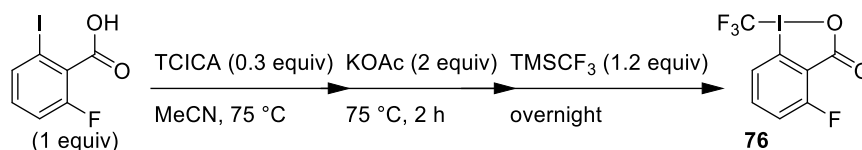
$^1\text{H NMR}$ (300 MHz, Chloroform-*d*): δ = 7.91 (dd, J = 8.6, 1.1 Hz, 2H), 7.51 – 7.43 (m, 1H), 7.33 (dd, J = 8.4, 7.1 Hz, 2H), 6.16 (s, 2H), 3.88 (s, 6H), 3.86 (s, 3H).

$^{19}\text{F NMR}$ (282 MHz, Chloroform-*d*): δ = -75.27 (s).

Reaction of **74** and TMSCF_3 in the presence of CuI (Scheme 143)

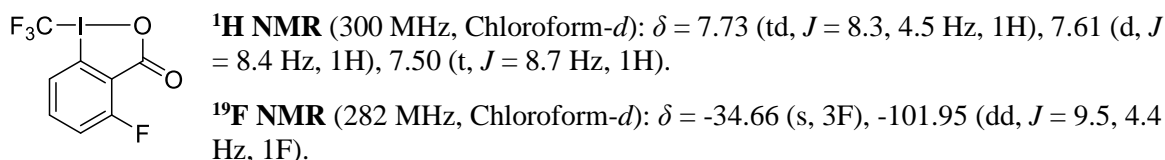


CuI (10mg, 0.05 mmol) was placed in a 10 mL vial with a stirring bar, capped with a crimp seal, and purged with argon by three vacuum/argon cycles. A solution of TMSCF_3 (79 mg, 0.55 mmol) and PhCF_3 (**74** mg, 0.5 mmol) in 3 mL of MeCN was added to the vial, followed by reagent **74** (245 mg, 0.5 mmol) in 2 mL of MeCN. The mixture was stirred at 60 °C for overnight. After the mixture was cooled down to room temperature, the mixture was filtered through a thin layer of silica gel, washed with DCM, and solvents were removed under reduced pressure. The crude mixture was analyzed by GC-MS and ^1H and ^{19}F NMR.

8.6.13 Trifluoromethylating reagents with ^{19}F NMR probeThe synthesis of 6-fluoro reagent **76**

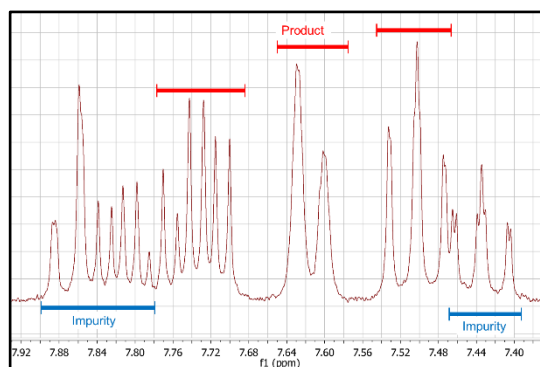
The synthetic procedure of reagent **76** was in the same manner as reagent **63** (Section 8.6.1), using 2-iodo-6-fluorobenzoic acid (1357 mg, 5 mmol). Recrystallization was repeated although the impurity was not removed and increased over time.

6-Fluoro-1-(trifluoromethyl)benzoic acid (**76**), colorless crystal (644 mg, 1.93 mmol, 39% yield)

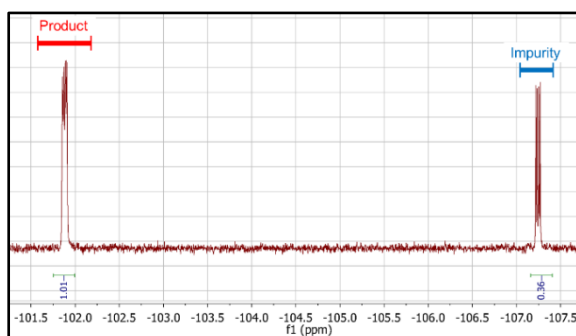


NMR spectra with impurities:

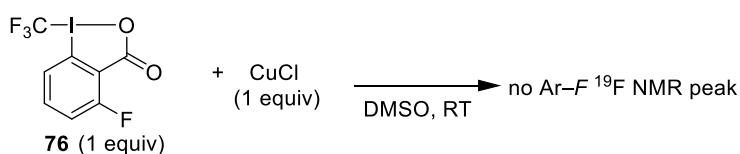
^1H NMR spectrum (7.4 – 8.0 ppm)



^{19}F NMR spectrum (-101 – -108 ppm)



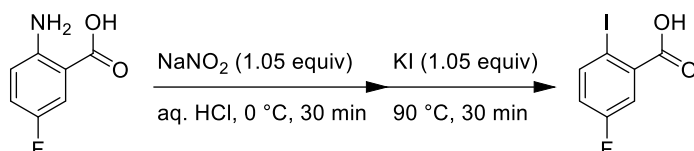
Red indicators: product. Blue indicators: impurities.

The reaction of reagent **76** and CuCl

CuCl (31 mg, 0.3 mmol) was placed in a 20 mL vial with a stirring bar, capped with a crimp seal, and purged with argon by three vacuum/argon cycles. PhCF₃ (44 mg, 0.3 mmol) and 4 mL of DMSO

were added to the vial, followed by a slow addition of reagent **76** (96 mg, 0.3 mmol) in 2 mL of DMSO. The mixture was stirred at room temperature overnight. After the mixture was cooled down to room temperature, 0.6 mL of the reaction mixture was taken to an NMR tube filled with argon for ^{19}F NMR analysis.

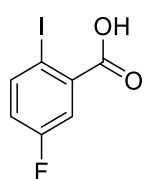
The synthesis of 5-fluoro reagent **77**



2-Amino-5-fluorobenzoic acid (7914 mg, 50 mmol) and a stirring bar were placed in a 250 mL flask. 65 mL of water and 35 mL of 35% aqueous HCl solution was added to the flask and the mixture was stirred until it became homogeneous. The flask was cooled down to 0 °C before a precooled solution of sodium nitrite (3659 mg, 52.5 mmol) in 10 mL of water was slowly added. After the mixture was stirred at 0 °C for 30 min, a precooled solution of potassium iodide (8803 mg, 52.5 mmol) in 10 mL of water was added to the flask slowly. After the mixture was stirred at 0 °C for 30 min, the flask was gradually heated up to 90 °C. After 30 min at 90 °C, the flask was cooled down to room temperature and was filtered and washed with water to collect the solid. The product was purified by recrystallization from EtOH/H₂O, and also, the crystal obtained upon concentration of the mother liquor was combined.

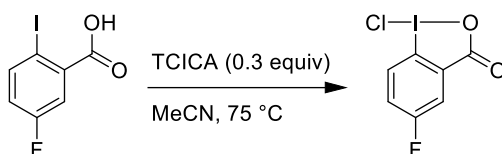
5-Fluoro-2-iodobenzoic acid, colorless crystal (8.832 g, 15.2 mmol, 30% yield),

CAS No.: 52548-63-7



^1H NMR (300 MHz, Chloroform-*d*): δ = 8.01 (dd, J = 8.7, 5.4 Hz, 1H), 7.73 (dd, J = 9.1, 3.0 Hz, 1H), 6.98 (ddd, J = 8.6, 7.6, 3.0 Hz, 1H).

^{19}F NMR (282 MHz, Chloroform-*d*): δ = -112.93 (ddd, J = 8.9, 7.7, 5.4 Hz).

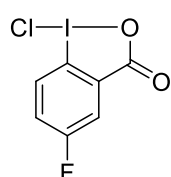


Since the purification of 5-fluoro-2-iodobenzoic acid was not successful, the chlorinated intermediated was isolated for purification. A 100 mL flask equipped with a stirring bar, a condenser, a septum and a gas inlet was flame-dried and was filled with argon. 5-fluoro-2-

iodobenzoic (2687 mg, 10 mmol) in 15 mL of MeCN was added to the flask, and heated up to 75 °C by a mean of oil bath. Trichloroisocyanuric acid (TCICA) (1878 mg, 8 mmol) in 5 mL of MeCN was added to the flask slowly over 5 minutes. The mixture was stirred at 75 °C for 5 min. After a hot filtration of the mixture, glassware and the solid was washed with warm CHCl₃ to combine with the first filtrate. The combined filtrate was cooled down to collect the crystal.

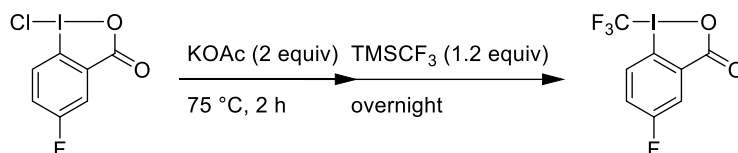
1-Chloro-5-fluoro-1,2-benziodoxol-3-(1H)-one, pale yellow crystal

(1.092 g, 3.6 mmol, 36% yield)



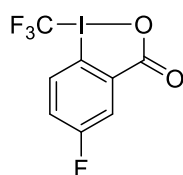
¹H NMR (300 MHz, Chloroform-*d*): δ = 8.16 (dd, J = 9.1, 4.1 Hz, 1H), 7.96 (dd, J = 7.5, 2.9 Hz, 1H), 7.70 (ddd, J = 9.1, 7.5, 2.9 Hz, 1H).

¹⁹F NMR (282 MHz, Chloroform-*d*): δ = -112.86 – -113.00 (m).



A 250 mL flask equipped with potassium acetate (6344 mg, 64 mmol), a stirring bar, a condenser, a septum and a gas inlet was flame-dried and was filled with argon. After 30 mL of MeCN was added to the flask, 1-chloro-5-fluoro-1,2-benziodoxol-3-(1H)-one (9712 mg, 32 mmol) in 20 mL of MeCN was added. The flask was stirred at 75 °C for 2 hours. After the flask was cooled down to room temperature, TMSCF₃ (5515 mg, 38.4 mmol) in 10 mL of MeCN was added to the flask, and the flask was stirred overnight at room temperature. Decant the liquid to a glass filter, the filtrate was cooled down in a freezer overnight. The solid was washed with CHCl₃ and before it was filtered. The volume of this filtrate was reduced to half by evaporation and was cooled down in a freezer. Colorless crystal from both batches was collected and dried under reduced pressure. (4.136 g, 12.4 mmol, 39% yield)

1-Trifluoromethyl-5-fluoro-1,2-benziodoxol-3-(1H)-one (**77**), colorless crystal

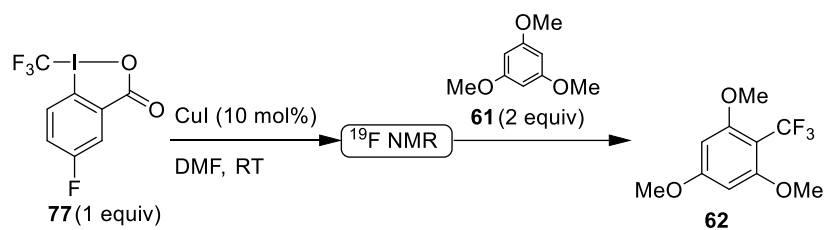


¹H NMR (300 MHz, Chloroform-*d*): δ = 8.17 (dd, J = 7.9, 3.0 Hz, 1H), 7.76 – 7.68 (m, 1H), 7.55 (ddd, J = 9.1, 7.2, 3.0 Hz, 1H).

¹⁹F NMR (282 MHz, Chloroform-*d*): δ = -33.69 (s, 3F), -107.51 (td, J = 7.5, 4.0 Hz, 1F).

Crystallographic data is available in APPENDIX B.

The trifluoromethylation of arene **61 by reagent **77****



CuI (3 mg, 0.015 mmol) was placed in a 10 mL vial with a stirring bar, capped with a crimp seal, and purged with argon by three vacuum/argon cycles. PhCF₃ (22 mg, 0.15 mmol) and reagent **77** (51 mg, 0.15 mmol) in 2 mL of DMF were added to the vial. The mixture was stirred at room temperature for overnight. 0.6 mL of the mixture was taken to an NMR tube with minimal contact to the air. After the ^{19}F NMR analysis, the sample was injected back to the vial, and 1,3,5-trimethoxybenzene (**61**) (51 mg, 0.3 mmol) in 1 mL of DMF was added to the vial. The mixture was stirred at 40 °C overnight. was added to the vial dropwise at room temperature. The mixture was analyzed by ^{19}F NMR.

Bibliography

- [1] T. Liang, T. Ritter, *Compr. Org. Synth. II* **2014**, 210.
- [2] L. Xing, D. C. Blakemore, A. Narayanan, R. Unwalla, F. Lovering, R. A. Denny, H. Zhou, M. E. Bunnage, *ChemMedChem* **2015**, *10*, 715.
- [3] E. P. Gillis, K. J. Eastman, M. D. Hill, D. J. Donnelly, N. A. Meanwell, *J. Med. Chem.* **2015**, *58*, 8315.
- [4] C. N. Neumann, T. Ritter, *Acc. Chem. Res.* **2017**, *50*, 2822.
- [5] A. Harsanyi, G. Sandford, *Green Chem.* **2015**, *17*, 2081.
- [6] W. R. Dolbier, *J. Fluor. Chem.* **2005**, *126*, 157.
- [7] S. Devotta, V. R. Pendyala, *Ind. Eng. Chem. Res.* **1992**, *31*, 2042.
- [8] C. J. Giunta, *Bull. Hist. Chem* **2006**, *31*, 66.
- [9] F. Swarts, *Bull. l'Académie R. des Sci. des lettres des B.-art. Belgique* **1892**, *24*, 309.
- [10] T. Midgley, A. L. Henne, *Ind. Eng. Chem.* **1930**, *22*, 542.
- [11] M. Rigby, R. G. Prinn, S. O'Doherty, S. A. Montzka, A. McCulloch, C. M. Harth, J. Mühle, P. K. Salameh, R. F. Weiss, D. Young, et al., *Atmos. Chem. Phys.* **2013**, *13*, 2691.
- [12] L. Vaitkus, V. Dagilis, *Int. J. Refrig.* **2017**, *76*, 160.
- [13] S. Devotta, *Indian Chem. Eng.* **2014**, *56*, 294.
- [14] D. H. Kim, H. W. Byun, S. H. Yoon, C. H. Song, K. H. Lee, O. J. Kim, *Int. J. Air-Conditioning Refrig.* **2016**, *24*, 1630009.
- [15] R. J. Plunkett, *TETRAFLUOROETHYLENE POLYMERS*, US 2230654, **1941**.
- [16] A. B. Garrett, *J. Chem. Educ.* **1962**, *39*, 288.
- [17] G. J. Puts, P. Crouse, B. M. Ameduri, *Chem. Rev.* **2019**, *119*, 1763.
- [18] H. Teng, *Appl. Sci.* **2012**, *2*, 496.
- [19] R. Dams, K. Hintzer, in *Fluorinated Polym. Vol. 2 Appl.*, The Royal Society Of Chemistry, **2017**, pp. 1–31.
- [20] *Global Fluoropolymer Market*, Acmite Market Intelligence, **2012**.
- [21] B. Ameduri, H. Sawada, *Fluorinated Polymers*, The Royal Society Of Chemistry, **2017**.
- [22] J. F. Gadberry, R. Otterson, R. M. Hill, G. Bognolo, R. R. Thomas, in *Chem. Technol. Surfactants*, Wiley-Blackwell, **2007**, pp. 153–235.
- [23] K. J. L. Paciorek, R. H. Kratzer, *J. Fluor. Chem.* **1994**, *67*, 169.
- [24] D. Shirakawa, K. Ohnishi, *IEEE Trans. Magn.* **2008**, *44*, 3710.
- [25] T. Okazoe, *Proc. Japan Acad. Ser. B* **2009**, *85*, 276.
- [26] T. Hoshino, Y. Morizawa, in *Fluorinated Polym. Vol. 2 Appl.*, The Royal Society Of

-
- Chemistry, **2017**, pp. 110–126.
- [27] J. Fried, E. F. Sabo, *J. Am. Chem. Soc.* **1954**, *76*, 1455.
- [28] M. C. Walker, M. C. Y. Chang, *Chem. Soc. Rev.* **2014**, *43*, 6527.
- [29] W. Sneader, in *Drug Discov. A Hist.*, Wiley-Blackwell, **2005**, pp. 248–268.
- [30] C. Heidelberger, N. K. Chaudhuri, P. Danneberg, D. Mooren, L. Griesbach, R. Duschinsky, R. J. Schnitzer, E. Plevin, J. Scheiner, *Nature* **1957**, *179*, 663.
- [31] V. P. Reddy, in *Organofluor. Compd. Biol. Med.* (Ed.: V.P. Reddy), Elsevier, Amsterdam, **2015**, pp. 29–57.
- [32] V. P. Reddy, in *Organofluor. Compd. Biol. Med.* (Ed.: V.P. Reddy), Elsevier, Amsterdam, **2015**, pp. 1–27.
- [33] Y. Zhou, J. Wang, Z. Gu, S. Wang, W. Zhu, J. L. Aceña, V. A. Soloshonok, K. Izawa, H. Liu, *Chem. Rev.* **2016**, *116*, 422.
- [34] J. Wang, M. Sánchez-Roselló, J. L. Aceña, C. del Pozo, A. E. Sorochinsky, S. Fustero, V. A. Soloshonok, H. Liu, *Chem. Rev.* **2014**, *114*, 2432.
- [35] T. Fujiwara, D. O'Hagan, *J. Fluor. Chem.* **2014**, *167*, 16.
- [36] R. J. Lagow, J. L. Margrave, in *Prog. Inorg. Chem.*, Wiley-Blackwell, **2007**, pp. 161–210.
- [37] L. A. Bigelow, J. H. Pearson, L. B. Cook, W. T. Miller, *J. Am. Chem. Soc.* **1933**, *55*, 4614.
- [38] T. Okazoe, *J. Fluor. Chem.* **2015**, *174*, 120.
- [39] C. B. McPake, G. Sandford, *Org. Process Res. Dev.* **2012**, *16*, 844.
- [40] A. C. Sather, S. L. Buchwald, *Acc. Chem. Res.* **2016**, *49*, 2146.
- [41] M. G. Campbell, T. Ritter, *Chem. Rev.* **2015**, *115*, 612.
- [42] P. A. Champagne, J. Desroches, J. D. Hamel, M. Vandamme, J. F. Paquin, *Chem. Rev.* **2015**, *115*, 9073.
- [43] G. Balz, G. Schiemann, *Ber. dtsh. Chem. Ges. A/B* **1927**, *60*, 1186.
- [44] D. J. Adams, J. H. Clark, *Chem. Soc. Rev.* **1999**, *28*, 225.
- [45] J. H. Simons, *J. Electrochem. Soc.* **1949**, *95*, 47.
- [46] I. N. Rozhkov, *Russ. Chem. Rev.* **1976**, *45*, 615.
- [47] I. L. Knunyants, I. N. Rozhkov, A. V Bukhtiarov, M. M. Gol'din, R. V Kudryavtsev, *Bull. Acad. Sci. USSR, Div. Chem. Sci.* **1970**, *19*, 1155.
- [48] K. Momota, M. Morita, Y. Matsuda, *Electrochim. Acta* **1993**, *38*, 619.
- [49] I. L. Knunyants, I. N. Rozhkov, A. V Bukhtiarov, M. M. Gol'din, R. V Kudryavtsev, *Bull. Acad. Sci. USSR, Div. Chem. Sci.* **1970**, *19*, 1155.
- [50] E. Differding, H. Ofner, *Synlett* **1991**, *3*, 187.
- [51] R. E. Banks, S. N. Mohialdin-Khaffaf, G. S. Lal, I. Sharif, R. G. Syvret, *J. Chem. Soc. Chem. Commun.* **1992**, *0*, 595.
- [52] K. L. Hull, W. Q. Anani, M. S. Sanford, *J. Am. Chem. Soc.* **2006**, *128*, 7134.
- [53] K. B. McMurtrey, J. M. Racowski, M. S. Sanford, *Org. Lett.* **2012**, *14*, 4094.
-

- [54] D. A. Watson, M. Su, G. Teverovskiy, Y. Zhang, J. García-Fortanet, T. Kinzel, S. L. Buchwald, *Science* **2009**, 325, 1661.
- [55] M. G. Campbell, A. J. Hoover, T. Ritter, in (Eds.: T. Braun, R.P. Hughes), Springer International Publishing, Cham, **2015**, pp. 1–53.
- [56] Z. Li, Z. Wang, L. Zhu, X. Tan, C. Li, *J. Am. Chem. Soc.* **2014**, 136, 16439.
- [57] B. Greedy, J.-M. Paris, T. Vidal, V. Gouverneur, *Angew. Chemie Int. Ed.* **2003**, 42, 3291.
- [58] E. Fuglseth, T. H. K. Thvedt, M. F. Møll, B. H. Hoff, *Tetrahedron* **2008**, 64, 7318.
- [59] E. P. A. Talbot, T. de A. Fernandes, J. M. McKenna, F. D. Toste, *J. Am. Chem. Soc.* **2014**, 136, 4101.
- [60] T. J. Barker, D. L. Boger, *J. Am. Chem. Soc.* **2012**, 134, 13588.
- [61] S. Qiu, T. Xu, J. Zhou, Y. Guo, G. Liu, *J. Am. Chem. Soc.* **2010**, 132, 2856.
- [62] R.-Y. Zhu, K. Tanaka, G.-C. Li, J. He, H.-Y. Fu, S.-H. Li, J.-Q. Yu, *J. Am. Chem. Soc.* **2015**, 137, 7067.
- [63] S. Bloom, C. R. Pitts, D. C. Miller, N. Haselton, M. G. Holl, E. Urheim, T. Lectka, *Angew. Chemie Int. Ed.* **2012**, 51, 10580.
- [64] T. Liang, C. N. Neumann, T. Ritter, *Angew. Chem., Int. Ed.* **2013**, 52, 8214.
- [65] M. R. C. Gerstenberger, A. Haas, *Angew. Chem., Int. Ed. Engl.* **1981**, 20, 647.
- [66] O. A. Mascaretti, *Aldrichimica Acta* **1993**, 26, 47.
- [67] H. Sun, S. G. DiMagno, *J. Am. Chem. Soc.* **2005**, 127, 2050.
- [68] V. H. Jadhav, H. J. Jeong, W. Choi, D. W. Kim, *Chem. Eng. J.* **2015**, 270, 36.
- [69] M. H. Katcher, A. G. Doyle, *J. Am. Chem. Soc.* **2010**, 132, 17402.
- [70] C. Hollingworth, A. Hazari, M. N. Hopkinson, M. Tredwell, E. Benedetto, M. Huiban, A. D. Gee, J. M. Brown, V. Gouverneur, *Angew. Chemie Int. Ed.* **2011**, 50, 2613.
- [71] E. Benedetto, M. Tredwell, C. Hollingworth, T. Khotavivattana, J. M. Brown, V. Gouverneur, *Chem. Sci.* **2013**, 4, 89.
- [72] W. L. Hu, X. G. Hu, L. Hunter, *Synthesis* **2017**, 49, 4917.
- [73] L. Kürti, B. Czako, *Strategic Applications of Named Reactions in Organic Synthesis*, Elsevier Academic Press, **2005**.
- [74] W. J. Middleton, *J. Org. Chem.* **1975**, 40, 574.
- [75] N. Al-Maharik, D. O'Hagan, *Aldrichimica Acta* **2011**, 44, 65.
- [76] S. Kobayashi, A. Yoneda, T. Fukuhara, S. Hara, *Tetrahedron* **2004**, 60, 6923.
- [77] G. Bellavance, P. Dubé, B. Nguyen, *Synlett* **2012**, 4, 569.
- [78] L. Li, C. Ni, F. Wang, J. Hu, *Nat. Commun.* **2016**, 7, 1.
- [79] S. Manna, J. R. Falck, C. Mioskowski, *Synth. Commun.* **1985**, 15, 663.
- [80] B. P. Bandgar, V. T. Kamble, A. V. Biradar, *Monatsh. Chem.* **2005**, 136, 1579.
- [81] J. Chen, J.-H. Lin, J.-C. Xiao, *Org. Lett.* **2018**, 20, 3061.
- [82] P. Tang, W. Wang, T. Ritter, *J. Am. Chem. Soc.* **2011**, 133, 11482.
-

-
- [83] F. Sladojevich, S. I. Arlow, P. Tang, T. Ritter, *J. Am. Chem. Soc.* **2013**, *135*, 2470.
- [84] C. N. Neumann, J. M. Hooker, T. Ritter, *Nature* **2016**, *534*, 369.
- [85] T. Fujimoto, T. Ritter, *Org. Lett.* **2015**, *17*, 544.
- [86] N. W. Goldberg, X. Shen, J. Li, T. Ritter, *Org. Lett.* **2016**, *18*, 6102.
- [87] M. K. Nielsen, C. R. Ugaz, W. Li, A. G. Doyle, *J. Am. Chem. Soc.* **2015**, *137*, 9571.
- [88] S. D. Schimmler, M. A. Cismesia, P. S. Hanley, R. D. J. Froese, M. J. Jansma, D. C. Bland, M. S. Sanford, *J. Am. Chem. Soc.* **2017**, *139*, 1452.
- [89] M. K. Nielsen, D. T. Ahneman, O. Riera, A. G. Doyle, *J. Am. Chem. Soc.* **2018**, *140*, 5004.
- [90] M. Schelhaas, H. Waldmann, *Angew. Chem., Int. Ed. Engl.* **1996**, *35*, 2056.
- [91] A. Isidro-Llobet, M. Álvarez, F. Albericio, *Chem. Rev.* **2009**, *109*, 2455.
- [92] P. G. M. Wuts, T. W. Greene, *Greene's Protective Groups in Organic Synthesis, Fourth Edition*, John Wiley & Sons, Inc., Hoboken, New Jersey, **2007**.
- [93] R. B. Bedford, R. L. Webster, C. J. Mitchell, *Org. Biomol. Chem.* **2009**, *7*, 4853.
- [94] V. Snieckus, *Chem. Rev.* **1990**, *90*, 879.
- [95] B. Xiao, Y. Fu, J. Xu, T.-J. Gong, J.-J. Dai, J. Yi, L. Liu, *J. Am. Chem. Soc.* **2010**, *132*, 468.
- [96] M. C. Whisler, S. MacNeil, V. Snieckus, P. Beak, *Angew. Chem., Int. Ed.* **2004**, *43*, 2206.
- [97] S. Florio, F. M. Perna, A. Salomone, P. Vitale, in *Compr. Org. Synth. Second Ed.*, **2014**, pp. 471–515.
- [98] L. N. Telegina, M. G. Ezernitskaya, I. A. Godovikov, K. K. Babievskii, B. V. Lokshin, T. V. Strelkova, Y. A. Borisov, N. M. Loim, *Eur. J. Inorg. Chem.* **2009**, 3636.
- [99] C. Neuhäuser, D. Domide, J. Mautz, E. Kaifer, H. J. Himmel, *Dalt. Trans.* **2008**, *4*, 1821.
- [100] C. S. McCowan, T. L. Groy, M. T. Caudle, *Inorg. Chem.* **2002**, *41*, 1120.
- [101] H. Zeng, Z. Qiu, A. Domínguez-Huerta, Z. Hearne, Z. Chen, C. J. Li, *ACS Catal.* **2017**, *7*, 510.
- [102] P. Tundo, M. Musolino, F. Aricò, *Green Chem.* **2018**, *20*, 28.
- [103] A. Ishizaki, Y. Hirose, *Agric. Biol. Chem.* **1973**, *37*, 1295.
- [104] P. S. Kalsi, *Organic Reactions and Their Mechanisms*, New Age Science, Tunbridge Wells, **2010**.
- [105] O. R. Suárez-Castillo, L. A. Montiel-Ortega, M. Meléndez-Rodríguez, M. Sánchez-Zavala, *Tetrahedron Lett.* **2007**, *48*, 17.
- [106] M. P. Shewalkar, R. R. Rao, V. Reddy, S. N. D. and D. B. Shinde, *Lett. Org. Chem.* **2013**, *10*, 60.
- [107] H. Yan, L. Zeng, Y. Xie, Y. Cui, L. Ye, S. Tu, *Res. Chem. Intermed.* **2016**, *42*, 5951.
- [108] R. N. Salvatore, H. Yoon, K. Woon, *Tetrahedron* **2001**, *57*, 7785.
- [109] A. Christine, in *Chem. Anal. Non-antimicrobial Vet. Drug Residues Food*, Wiley-Blackwell, **2016**, pp. 383–426.
- [110] S. M. David, D. B. Iliescu, I. Sandu, D. E. Paraschiv, C. Teodorescu, A. Knieling, in *Rev.*
-

- Chim. (Bucharest, Rom.)*, **2017**, pp. 1031–1034.
- [111] A. K. Ghosh, M. Brindisi, *J. Med. Chem.* **2015**, *58*, 2895.
- [112] H. W. Engels, H. G. Pirkl, R. Albers, R. W. Albach, J. Krause, A. Hoffmann, H. Casselmann, J. Dormish, *Angew. Chem., Int. Ed.* **2013**, *52*, 9422.
- [113] W. Yang, S. K. Both, G. J. V. M. Van Osch, Y. Wang, J. A. Jansen, F. Yang, *Eur. Cells Mater.* **2014**, *27*, 350.
- [114] X. Y. Zhang, G. H. Wang, D. Liu, Y. Wang, *Adv. Mater. Res.* **2013**, *608–609*, 1783.
- [115] J. S. Nowick, N. A. Powell, T. M. Nguyen, G. Noronha, *J. Org. Chem.* **1992**, *57*, 7364.
- [116] S. Ozaki, *Chem. Rev.* **1972**, *72*, 457.
- [117] R. Juárez, P. Concepción, A. Corma, V. Fornés, H. García, *Angew. Chem., Int. Ed.* **2010**, *49*, 1286.
- [118] P. Wang, S. Liu, Y. Deng, *Chinese J. Chem.* **2017**, *35*, 821.
- [119] S. Fukuoka, I. Fukawa, T. Adachi, H. Fujita, N. Sugiyama, T. Sawa, *Org. Process Res. Dev.* **2019**, *23*, 145.
- [120] D. F. VARMA, S. MULAY, *Toxicol. Organophosphate Carbamate Compd.* **2006**, 79.
- [121] J. Hu, A. Nand, P. Cantrell, *Ann. Work Expo. Heal.* **2017**, *61*, 1015.
- [122] S. Ghosh, N. Dey, *Paintindia* **2017**, *67*, 60.
- [123] A. PRONK, D. HEEDERIK, E. TIELEMANS, G. SKARPING, I. BOBELDIJK, J. VAN HEMMEN, L. PRELLER, *Ann. Occup. Hyg.* **2005**, *50*, 1.
- [124] K. Takeda, T. Kanoko, M. Hoshino, M. Kishino, H. Ogura, *Synthesis* **1987**, 557.
- [125] K. Sunggak, I. L. Jae, K. K. Young, *Tetrahedron Lett.* **1984**, *25*, 4943.
- [126] H. Ogura, T. Kobayashi, K. Shimizu, K. Kawabe, K. Takeda, *Tetrahedron Lett.* **1979**, *20*, 4745.
- [127] R. N. Salvatore, V. L. Flanders, D. Ha, K. W. Jung, *Org. Lett.* **2000**, *2*, 2797.
- [128] M. Abla, J.-C. Choi, T. Sakakura, *Chem. Commun.* **2001**, 2238.
- [129] S. L. Peterson, S. M. Stucka, C. J. Dinsmore, *Org. Lett.* **2010**, *12*, 1340.
- [130] F. Rivetti, U. Romano, D. Delledonne, in *Green Chem.* (Eds.: P.T. Anastas, T.C. Williamson), American Chemical Society, **1996**, pp. 70–80.
- [131] Y. Ono, *Appl. Catal., A* **1997**, *155*, 133.
- [132] M. Selva, A. Perosa, *Green Chem.* **2008**, *10*, 457.
- [133] A. H. Tamboli, A. A. Chaugule, H. Kim, *Chem. Eng. J.* **2017**, *323*, 530.
- [134] S. Huang, B. Yan, S. Wang, X. Ma, *Chem. Soc. Rev.* **2015**, *44*, 3079.
- [135] B. A. V. Santos, V. M. T. M. Silva, J. M. Loureiro, A. E. Rodrigues, *ChemBioEng Rev.* **2014**, *1*, 214.
- [136] H.-Z. Tan, Z.-Q. Wang, Z.-N. Xu, J. Sun, Y.-P. Xu, Q.-S. Chen, Y. Chen, G.-C. Guo, *Catal. Today* **2018**, *316*, 2.
- [137] F. Rivetti, *C. R. Acad. Sci., Ser. IIC: Chim.* **2000**, *3*, 497.

-
- [138] G. Fiorani, A. Perosa, M. Selva, *Green Chem.* **2018**, *20*, 288.
- [139] X. Zhao, L. Kang, N. Wang, H. An, F. Li, Y. Wang, *Ind. Eng. Chem. Res.* **2012**, *51*, 11335.
- [140] S. Grego, F. Aricò, P. Tundo, *Pure Appl. Chem.* **2011**, *84*, 695.
- [141] M. Distaso, E. Quaranta, *J. Catal.* **2008**, *253*, 278.
- [142] R. Tayebee, E. Rezaei Seresht, F. Jafari, S. Rabiei, *Ind. Eng. Chem. Res.* **2013**, *52*, 11001.
- [143] M. Selva, P. Tundo, *Synthesis of Mono-N-Substituted Functionalized Anilines*, EP1431274B1, **2007**.
- [144] R. Juarez, A. Padilla, A. Corma, H. Garcia, *Catal. Commun.* **2009**, *10*, 472.
- [145] P. N. Gooden, R. A. Bourne, A. J. Parrott, H. S. Bevinakatti, D. J. Irvine, M. Poliakoff, *Org. Process Res. Dev.* **2010**, *14*, 411.
- [146] A. Dhakshinamoorthy, M. Alvaro, H. Garcia, *Appl. Catal., A* **2010**, *378*, 19.
- [147] E. Jones-Mensah, M. Karki, J. Magolan, *Synthesis* **2016**, 1421.
- [148] N. Kornblum, J. W. Powers, G. J. Anderson, W. J. Jones, H. O. Larson, O. Levand, W. M. Weaver, *J. Am. Chem. Soc.* **1957**, *79*, 6562.
- [149] N. Kornblum, W. J. Jones, G. J. Anderson, *J. Am. Chem. Soc.* **1959**, *81*, 4113.
- [150] T. T. Tidwell, *Synthesis* **1990**, *10*, 857.
- [151] K. E. Pfitzner, J. G. Moffatt, *J. Am. Chem. Soc.* **1963**, *85*, 3027.
- [152] J. D. Albright, L. Goldman, *J. Am. Chem. Soc.* **1965**, *87*, 4214.
- [153] K. Onodera, S. Hirano, N. Kashimura, *J. Am. Chem. Soc.* **1965**, *87*, 4651.
- [154] J. R. Parikh, W. von E. Doering, *J. Am. Chem. Soc.* **1967**, *89*, 5505.
- [155] K. Omura, A. K. Sharma, D. Swern, *J. Org. Chem.* **1976**, *41*, 957.
- [156] K. Omura, D. Swern, *Tetrahedron* **1978**, *34*, 1651.
- [157] F. Saadati, K. Yousefi, *Synth. Commun.* **2014**, *44*, 2818.
- [158] L. De Luca, G. Giacomelli, A. Porcheddu, *J. Org. Chem.* **2001**, *66*, 7907.
- [159] T. Isobe, T. Ishikawa, *J. Org. Chem.* **1999**, *64*, 5832.
- [160] P. R. Sultane, C. W. Bielawski, *J. Org. Chem.* **2017**, *82*, 1046.
- [161] D. F. Taber, J. C. Amedio, K. Y. Jung, *J. Org. Chem.* **1987**, *52*, 5621.
- [162] H. J. Liu, J. M. Nyangulu, *Tetrahedron Lett.* **1988**, *29*, 3167.
- [163] S. K. Pandey, A. Bisai, V. K. Singh, *Synth. Commun.* **2007**, *37*, 4099.
- [164] A. Bisai, M. Chandrasekhar, V. K. Singh, *Tetrahedron Lett.* **2002**, *43*, 8355.
- [165] T. V. Nguyen, M. Hall, *Tetrahedron Lett.* **2014**, *55*, 6895.
- [166] H. Firouzabadi, H. Hassani, H. Hazarkhani, *Phosphorus, Sulfur Silicon Relat. Elem.* **2003**, *178*, 149.
- [167] Y. Wang, C. Wang, J. Sun, *Synth. Commun.* **2014**, *44*, 2961.
- [168] T. Lloyd Fletcher, H. L. Pan, *J. Am. Chem. Soc.* **1956**, *78*, 4812.
-

- [169] P. A. Zoretic, *J. Org. Chem.* **1975**, *40*, 1867.
- [170] E. Armani, A. Dossena, R. Marchelli, G. Casnati, *Tetrahedron* **1984**, *40*, 2035.
- [171] V. A. Alfonsov, O. V. Andreeva, G. A. Bakaleynik, D. V. Beskrovny, V. E. Kataev, G. I. Kovylyjaeva, I. A. Litvinov, O. I. Militsina, I. Y. Strobykina, *Mendeleev Commun.* **2003**, *13*, 234.
- [172] M. Guo, L. Varady, D. Fokas, C. Baldino, L. Yu, *Tetrahedron Lett.* **2006**, *47*, 3889.
- [173] K. Mal, A. Kaur, F. Haque, I. Das, *J. Org. Chem.* **2015**, *80*, 6400.
- [174] C. Song, P. Chen, Y. Tang, *RSC Adv.* **2017**, *7*, 11233.
- [175] R. Ding, J. Li, W. Jiao, M. Han, Y. Liu, H. Tian, B. Sun, *Synthesis* **2018**, *50*, 4325.
- [176] E. Sheikhi, M. Adib, R. Yazzaf, M. Jahani, M. Ghavidel, *Synlett* **2018**, *29*, 2046.
- [177] M. B. Floyd, M. T. Du, P. F. Fabio, L. A. Jacob, B. D. Johnson, *J. Org. Chem.* **1985**, *50*, 5022.
- [178] R. S. Phillips, S. Busby, L. Edenfield, K. Wickware, *Amino Acids* **2013**, *44*, 529.
- [179] C. Liu, R. Dai, G. Yao, Y. Deng, *J. Chem. Res.* **2014**, *38*, 593.
- [180] S. Song, X. Sun, X. Li, Y. Yuan, N. Jiao, *Org. Lett.* **2015**, *17*, 2886.
- [181] G. Majetich, R. Hicks, S. Reister, *J. Org. Chem.* **1997**, *62*, 4321.
- [182] K. Mislow, T. Simmons, J. T. Melillo, A. L. Ternay, *J. Am. Chem. Soc.* **1964**, *86*, 1452.
- [183] S. Antoniotti, E. Duñach, *J. Mol. Catal. A Chem.* **2004**, *208*, 135.
- [184] S. Klimczyk, X. Huang, C. Farès, N. Maulide, *Org. Biomol. Chem.* **2012**, *10*, 4327.
- [185] M. Tayu, K. Higuchi, M. Inaba, T. Kawasaki, *Org. Biomol. Chem.* **2013**, *11*, 496.
- [186] L. G. Voskressensky, N. E. Golantsov, A. M. Maharramov, *Synthesis* **2016**, *48*, 615.
- [187] A. M. Andrievsky, M. V Gorelik, *Russ. Chem. Rev.* **2011**, *80*, 421.
- [188] D. A. Klumpp, in *Arene Chemistry*, **2015**.
- [189] D. Kalyani, A. R. Dick, W. Q. Anani, M. S. Sanford, *Org. Lett.* **2006**, *8*, 2523.
- [190] A. Podgoršek, M. Zupan, J. Iskra, *Angew. Chem., Int. Ed.* **2009**, *48*, 8424.
- [191] I. P. Beletskaya, A. S. Sigeev, A. S. Peregudov, P. V. Petrovskii, *Synthesis* **2007**, *16*, 2534.
- [192] W. Kijrungaiboon, O. Chantarasriwong, W. Chavasiri, *Tetrahedron Lett.* **2012**, *53*, 674.
- [193] J. K. Kajorinne, J. C. M. Steers, M. E. Merchant, C. D. MacKinnon, *Can. J. Chem.* **2018**, *96*, 1087.
- [194] L. Qiao, X. Cao, K. Chai, J. Shen, J. Xu, P. Zhang, *Tetrahedron Lett.* **2018**, *59*, 2243.
- [195] Y. Satkar, V. Ramadoss, P. D. Nahide, E. García-Medina, K. A. Juárez-Ornelas, A. J. Alonso-Castro, R. Chávez-Rivera, J. O. C. Jiménez-Halla, C. R. Solorio-Alvarado, *RSC Adv.* **2018**, *8*, 17806.
- [196] C. Alonso, E. Martínez De Marigorta, G. Rubiales, F. Palacios, *Chem. Rev.* **2015**, *115*, 1847.
- [197] X. Yang, T. Wu, R. J. Phipps, F. D. Toste, *Chem. Rev.* **2015**, *115*, 826.
- [198] S. Purser, P. R. Moore, S. Swallow, V. Gouverneur, *Chem. Soc. Rev.* **2008**, *37*, 320.
-

-
- [199] K. Müller, C. Faeh, F. Diederich, *Science* **2007**, *317*, 1881.
- [200] I. Ruppert, K. Schlich, W. Volbach, *Tetrahedron Lett.* **1984**, *25*, 2195.
- [201] T. Umemoto, S. Ishihara, *Tetrahedron Lett.* **1990**, *31*, 3579.
- [202] T. Umemoto, S. Ishihara, *J. Am. Chem. Soc.* **1993**, *115*, 2156.
- [203] T. Umemoto, K. Adachi, *J. Org. Chem.* **1994**, *59*, 5692.
- [204] P. Eisenberger, S. Gischig, A. Togni, *Chem. Eur. J.* **2006**, *12*, 2579.
- [205] J. Charpentier, N. Früh, A. Togni, *Chem. Rev.* **2015**, *115*, 650.
- [206] V. Matoušek, E. Pietrasiak, R. Schwenk, A. Togni, *J. Org. Chem.* **2013**, *78*, 6763.
- [207] I. KIELTSCH, P. Eisenberger, A. Togni, *Angew. Chem., Int. Ed.* **2007**, *46*, 754.
- [208] Z. Weng, H. Li, W. He, L. F. Yao, J. Tan, J. Chen, Y. Yuan, K. W. Huang, *Tetrahedron* **2012**, *68*, 2527.
- [209] C. Feng, T. P. Loh, *Chem. Sci.* **2012**, *3*, 3458.
- [210] X. Liu, X. Wu, *Synlett* **2013**, *24*, 1882.
- [211] E. Pair, N. Monteiro, D. Bouyssi, O. Baudoin, *Angew. Chem., Int. Ed.* **2013**, *52*, 5346.
- [212] N. Nebra, V. V. Grushin, *J. Am. Chem. Soc.* **2014**, *136*, 16998.
- [213] S. Kawamura, H. Egami, M. Sodeoka, *J. Am. Chem. Soc.* **2015**, *137*, 4865.
- [214] A. I. Konovalov, A. Lishchynskyi, V. V. Grushin, *J. Am. Chem. Soc.* **2014**, *136*, 13410.
- [215] P. G. Janson, N. O. Ilchenko, A. Diez-Varga, K. J. Szabó, *Tetrahedron* **2015**, *71*, 922.
- [216] J. Jover, *ACS Catal.* **2014**, *4*, 4389.
- [217] F. A. Cotton, C. A. Murillo, R. A. Walton, in (Eds.: F.A. Cotton, C.A. Murillo, R.A. Walton), Springer US, Boston, MA, **2005**, pp. 1–21.
- [218] L. F. Dahl, E. Ishishi, R. E. Rundle, *J. Chem. Phys.* **1957**, *26*, 1750.
- [219] F. A. Cotton, N. F. Curtis, C. B. Harris, B. F. G. Johnson, S. J. Lippard, J. T. Mague, W. R. Robinson, J. S. Wood, *Science* **1964**, *145*, 1305 LP.
- [220] F. A. Cotton, *Inorg. Chem.* **1965**, *4*, 334.
- [221] J. A. Bertrand, F. A. Cotton, W. A. Dollase, *Inorg. Chem.* **1963**, *2*, 1166.
- [222] J. A. Bertrand, F. A. Cotton, W. A. Dollase, *J. Am. Chem. Soc.* **1963**, *85*, 1349.
- [223] W. T. Robinson, J. E. Fergusson, B. R. Penfold, *Proc. Chem. Soc.* **1963**, 116.
- [224] K. P. Kornecki, J. F. Berry, D. C. Powers, T. Ritter, *Prog. Inorg. Chem. Vol. 58* **2014**, 225.
- [225] R. H. Duncan Lyngdoh, H. F. Schaefer, R. B. King, *Chem. Rev.* **2018**, *118*, 11626.
- [226] A. Noor, G. Glatz, R. Müller, M. Kaupp, S. Demeshko, R. Kempe, *Zeitschrift für Anorg. und Allg. Chemie* **2009**, *635*, 1149.
- [227] A. Noor, R. Kempe, *Chem. Rec.* **2010**, *10*, 413.
- [228] F. A. Cotton, B. G. DeBoer, M. D. LaPrade, J. R. Pipal, D. A. Ucko, *Acta Crystallogr. Sect. B* **1971**, *27*, 1664.
-

- [229] F. A. Cotton, M. P. Diebold, M. Matusz, W. J. Roth, *Inorganica Chim. Acta* **1986**, *112*, 147.
- [230] I. G. Fomina, Z. V Dobrokhotova, M. A. Kiskin, G. G. Aleksandrov, O. Y. Proshenkina, A. L. Emelina, V. N. Ikorskii, V. M. Novotortsev, I. L. Eremenko, *Russ. Chem. Bull.* **2007**, *56*, 1712.
- [231] W. M. Kerlin, F. Poineau, K. R. Czerwinski, P. M. Forster, A. P. Sattelberger, *Polyhedron* **2013**, *58*, 115.
- [232] A. A. Sidorov, I. G. Fomina, G. G. Aleksandrov, Y. V Rakitin, V. M. Novotortsev, V. N. Ikorskii, M. A. Kiskin, I. L. Eremenko, *Russ. Chem. Bull.* **2004**, *53*, 483.
- [233] P. B. White, J. N. Jaworski, C. G. Fry, B. S. Dolinar, I. A. Guzei, S. S. Stahl, *J. Am. Chem. Soc.* **2016**, *138*, 4869.
- [234] J. Drew, M. B. Hursthouse, P. Thornton, A. J. Welch, *J. Chem. Soc. Chem. Commun.* **1973**, 52.
- [235] L. P. Olson, D. R. Whitcomb, M. Rajeswaran, T. N. Blanton, B. J. Stwertka, *Chem. Mater.* **2006**, *18*, 1667.
- [236] A. V Eremin, A. N. Belyaev, *Russ. J. Gen. Chem.* **2011**, *81*, 428.
- [237] M. H. Chisholm, J. A. Heppert, D. M. Hoffman, J. C. Huffman, *Inorg. Chem.* **1985**, *24*, 3214.
- [238] J. N. Van Niekerk, F. R. L. Schoening, *Acta Crystallogr.* **1953**, *6*, 227.
- [239] P. A. Koz'min, M. D. Surazhskaya, T. B. Larina, A. S. Kotel'nikova, T. V. Misailova, *Koord. Khimiya* **1980**, *6*, 1256.
- [240] F. A. Cotton, Z. C. Mester, T. R. Webb, *Acta Crystallogr. Sect. B* **1974**, *30*, 2768.
- [241] J. G. Bullitt, F. A. Cotton, *Inorganica Chim. Acta* **1971**, *5*, 406.
- [242] A. J. Lindsay, G. Wilkinson, M. Motevalli, M. B. Hursthouse, *J. Chem. Soc. Dalt. Trans.* **1985**, 2321.
- [243] N. Kanematsu, M. Ebihara, T. Kawamura, *J. Chem. Soc. Dalt. Trans.* **1999**, 4413.
- [244] T. Yamaguchi, Y. Sasaki, T. Ito, *J. Am. Chem. Soc.* **1990**, *112*, 4038.
- [245] D. J. Santure, J. C. Huffman, A. P. Sattelberger, *Inorg. Chem.* **1985**, *24*, 371.
- [246] R. Paulissen, H. Reimlinger, E. Hayez, A. J. Hubert, P. Teyssié, *Tetrahedron Lett.* **1973**, *14*, 2233.
- [247] A. J. HUBERT, A. F. NOELS, A. J. ANCIAUX, P. TEYSSIÉ, *Synthesis* **1976**, *1976*, 600.
- [248] E. Nakamura, N. Yoshikai, M. Yamanaka, *J. Am. Chem. Soc.* **2002**, *124*, 7181.
- [249] J. F. Berry, *Dalt. Trans.* **2012**, *41*, 700.
- [250] K. P. Kornecki, J. F. Briones, V. Boyarskikh, F. Fullilove, J. Autschbach, K. E. Schrote, K. M. Lancaster, H. M. L. Davies, J. F. Berry, *Science* **2013**, *342*, 351 LP.
- [251] A. F. Heyduk, D. G. Nocera, *Science* **2001**, *293*, 1639 LP.
- [252] K. R. Mann, N. S. Lewis, V. M. Miskowski, D. K. Erwin, G. S. Hammond, H. B. Gray, *J. Am. Chem. Soc.* **1977**, *99*, 5525.
- [253] A. J. Esswein, A. S. Veige, D. G. Nocera, *J. Am. Chem. Soc.* **2005**, *127*, 16641.

-
- [254] N. Elgrishi, T. S. Teets, M. B. Chambers, D. G. Nocera, *Chem. Commun.* **2012**, 48, 9474.
- [255] M. Kilner, A. Pietrzykowski, *Polyhedron* **1983**, 2, 1379.
- [256] J. Halfpenny, *Acta Crystallogr. Sect. C* **1995**, 51, 2542.
- [257] C. M. Harris, B. F. Hoskins, R. L. Martin, *J. Chem. Soc.* **1959**, 3728.
- [258] M. Corbett, B. F. Hoskins, N. J. McLeod, B. P. O'Day, *Aust. J. Chem.* **1975**, 28, 2377.
- [259] Y. Nishida, S. Kida, *Bull. Chem. Soc. Jpn.* **1985**, 58, 383.
- [260] M. Ueda, M. Itou, K. Okazawa, T. Mochida, H. Mori, *Polyhedron* **2005**, 24, 2189.
- [261] X. Li, G. Zhu, L. Dong, C. Ni, X. Yan, L. Yu, *Synth. React. Inorganic, Met. Nano-Metal Chem.* **2016**, 46, 659.
- [262] L. S. Forster, C. J. Ballhausen, *Acta Chem. Scand.* **1962**, 16, 1385.
- [263] B. N. Figgis, R. L. Martin, *J. Chem. Soc.* **1956**, 3837.
- [264] D. J. Royer, *Inorg. Chem.* **1965**, 4, 1830.
- [265] I. G. Ross, *Trans. Faraday Soc.* **1959**, 55, 1057.
- [266] R. Clérac, F. A. Cotton, L. M. Daniels, J. Gu, C. A. Murillo, H.-C. Zhou, *Inorg. Chem.* **2000**, 39, 4488.
- [267] B. Kozlevčar, *Croat. Chem. Acta* **2008**, 81, 369.
- [268] N. K. Shee, R. Verma, D. Kumar, D. Datta, *Comput. Theor. Chem.* **2015**, 1061, 1.
- [269] Bhaskaran, M. Trivedi, A. K. Yadav, G. Singh, A. Kumar, G. Kumar, A. Husain, N. P. Rath, *Dalt. Trans.* **2019**, DOI 10.1039/C9DT01457H.
- [270] J. Koshitani, M. Hiramatsu, Y. Ueno, T. Yoshida, *Bull. Chem. Soc. Jpn.* **1978**, 51, 3667.
- [271] J. Koshitani, T. Kado, Y. Ueno, T. Yoshida, *J. Org. Chem.* **1982**, 47, 2879.
- [272] P. Ratnasamy, D. Srinivas, *Catal. Today* **2009**, 141, 3.
- [273] I. Garcia-Bosch, R. E. Cowley, D. E. Díaz, R. L. Peterson, E. I. Solomon, K. D. Karlin, *J. Am. Chem. Soc.* **2017**, 139, 3186.
- [274] E. I. Solomon, D. E. Heppner, E. M. Johnston, J. W. Ginsbach, J. Cirera, M. Qayyum, M. T. Kieber-Emmons, C. H. Kjaergaard, R. G. Hadt, L. Tian, *Chem. Rev.* **2014**, 114, 3659.
- [275] Y. H. Kim, H. S. Park, *Synlett* **1998**, 3, 261.
- [276] C. Stock, R. Brückner, *Adv. Synth. Catal.* **2012**, 354, 2309.
- [277] C. Spino, M. A. Joly, C. Godbout, M. Arbour, *J. Org. Chem.* **2005**, 70, 6118.
- [278] F. Brotzel, C. C. Ying, H. Mayr, *J. Org. Chem.* **2007**, 72, 3679.
- [279] Z. L. Shen, X. Z. Jiang, *J. Mol. Catal. A Chem.* **2004**, 213, 193.
- [280] A. B. Shivarkar, S. P. Gupte, R. V. Chaudhari, *J. Mol. Catal. A Chem.* **2005**, 226, 49.
- [281] F. Aricò, P. Tundo, *Russ. Chem. Rev.* **2010**, 79, 479.
- [282] Z. Amara, E. S. Streng, R. A. Skilton, J. Jin, M. W. George, M. Poliakoff, *Eur. J. Org. Chem.* **2015**, 6141.
- [283] P. Tundo, *Pure Appl. Chem.* **2001**, 73, 1117.
-

- [284] N. Nagaraju, G. Kuriakose, *New J. Chem.* **2003**, 27, 765.
- [285] G. Towler, R. Sinnott, *Chemical Engineering Design: Principles, Practice and Economics of Plant and Process Design*, Elsevier Ltd., **2013**.
- [286] R. F. Rolsten, H. H. Sisler, *J. Am. Chem. Soc.* **1957**, 79, 1068.
- [287] R. F. Rolsten, H. H. Sisler, *J. Am. Chem. Soc.* **1957**, 79, 1819.
- [288] A. Linden, A. Petridis, B. D. James, *Helv. Chim. Acta* **2009**, 92, 29.
- [289] F. Trotta, P. Tundo, G. Moraglio, *J. Org. Chem.* **1987**, 52, 1300.
- [290] W. C. Shieh, S. Dell, A. Bach, O. Repič, T. J. Blacklock, *J. Org. Chem.* **2003**, 68, 1954.
- [291] T. N. Glasnov, J. D. Holbrey, C. O. Kappe, K. R. Seddon, T. Yan, *Green Chem.* **2012**, 14, 3071.
- [292] L. Zhang, Y. Yang, Y. Xue, X. Fu, Y. An, G. Gao, *Catal. Today* **2010**, 158, 279.
- [293] X. Jiang, C. Wang, Y. Wei, D. Xue, Z. Liu, J. Xiao, *Chem. – A Eur. J.* **2014**, 20, 58.
- [294] F. G. Bordwell, D. J. Algrim, *J. Am. Chem. Soc.* **1988**, 110, 2964.
- [295] F. G. Bordwell, H. E. Fried, *J. Org. Chem.* **1991**, 56, 4218.
- [296] Ö. REIS, H. KOYUNCU, I. ESIRINGU, Y. SAHIN, H. O. GULCAN, *A New Method for the Synthesis of Rasagiline*, EP2663545B1, **2011**.
- [297] W. N. Olmstead, Z. Margolin, F. G. Bordwell, *J. Org. Chem.* **1980**, 45, 3295.
- [298] C. C. C. Johansson Seechurn, M. O. Kitching, T. J. Colacot, V. Snieckus, *Angew. Chem., Int. Ed.* **2012**, 51, 5062.
- [299] C.-J. Li, L. Chen, *Chem. Soc. Rev.* **2006**, 35, 68.
- [300] U. M. Lindström, *Chem. Rev.* **2002**, 102, 2751.
- [301] C. J. Morten, J. A. Byers, A. R. Van Dyke, I. Vilotijevic, T. F. Jamison, *Chem. Soc. Rev.* **2009**, 38, 3175.
- [302] T. Kitanosono, K. Masuda, P. Xu, S. Kobayashi, *Chem. Rev.* **2018**, 118, 679.
- [303] R. N. Butler, A. G. Coyne, *Chem. Rev.* **2010**, 110, 6302.
- [304] M. B. Gawande, V. D. B. Bonifácio, R. Luque, P. S. Branco, R. S. Varma, *Chem. Soc. Rev.* **2013**, 42, 5522.
- [305] M.-O. Simon, C.-J. Li, *Chem. Soc. Rev.* **2012**, 41, 1415.
- [306] D. G. Blackmond, A. Armstrong, V. Coombe, A. Wells, *Angew. Chemie Int. Ed.* **2007**, 46, 3798.
- [307] A. P. Brogan, T. J. Dickerson, K. D. Janda, *Angew. Chemie Int. Ed.* **2006**, 45, 8100.
- [308] Y. Ni, D. Holtmann, F. Hollmann, *ChemCatChem* **2014**, 6, 930.
- [309] F. Tieves, F. Tonin, E. Fernández-Fueyo, J. M. Robbins, B. Bommarius, A. S. Bommarius, M. Alcalde, F. Hollmann, *Tetrahedron* **2019**, 75, 1311.
- [310] M. A. Oturan, J.-J. Aaron, *Crit. Rev. Environ. Sci. Technol.* **2014**, 44, 2577.
- [311] A. R. Rahmani, M. R. Samarghandi, D. Nematollahi, F. Zamani, *J. Environ. Chem. Eng.* **2019**, 7, 102785.

-
- [312] P. L. Fuchs, *Reagents for Silicon-Mediated Organic Synthesis*, Chichester : Wiley, **2011**.
- [313] G. Megyeri, T. Keve, *Synth. Commun.* **1989**, *19*, 3415.
- [314] C. Iwata, A. Tanaka, K. Miyashita, *Heterocycles* **1990**, *31*, 987.
- [315] K. Miyashita, A. Tanaka, H. Mizuno, M. Tanaka, C. Iwata, *J. Chem. Soc. Perkin Trans. 1* **1994**, 847.
- [316] F. M. Akwi, P. Watts, *Chem. Commun.* **2018**, *54*, 13894.
- [317] V. D. Parker, M. Tilset, *J. Am. Chem. Soc.* **1991**, *113*, 8778.
- [318] J. K. Kochi, R. V Subramanian, *J. Am. Chem. Soc.* **1965**, *87*, 4855.
- [319] S. Song, X. Li, X. Sun, Y. Yuan, N. Jiao, *Green Chem.* **2015**, *17*, 3285.
- [320] A. S. Kende, K. Koch, C. A. Smith, *J. Am. Chem. Soc.* **1988**, *110*, 2210.
- [321] N. S. Narasimhan, N. M. Sunder, R. Ammanamanchi, B. D. Bonde, *J. Am. Chem. Soc.* **1990**, *112*, 4431.
- [322] H. C. Kolb, K. B. Sharpless, *Drug Discov. Today* **2003**, *8*, 1128.
- [323] S. Potratz, A. Mishra, P. Bäuerle, *Beilstein J. Org. Chem.* **2012**, *8*, 683.
- [324] C. J. O'Brien, E. A. B. Kantchev, C. Valente, N. Hadei, G. A. Chass, A. Lough, A. C. Hopkinson, M. G. Organ, *Chem. Eur. J.* **2006**, *12*, 4743.
- [325] D. Masilamani, M. M. Rogic, *J. Org. Chem.* **1981**, *46*, 4486.
- [326] E. Roder, J. Lutz, *Arch. Pharm. (Weinheim)*. **1985**, *318*, 882.
- [327] R. Xu, J. Wan, H. Mao, Y. Pan, *Communications* **2010**, *132*, 15531.
- [328] S. K. R. Parumala, R. K. Peddinti, *Green Chem.* **2015**, *17*, 4068.
- [329] S. Saba, J. Rafique, A. L. Braga, *Adv. Synth. Catal.* **2015**, *357*, 1446.
- [330] L. Bettanin, S. Saba, F. Z. Galetto, G. A. Mike, J. Rafique, A. L. Braga, *Tetrahedron Lett.* **2017**, *58*, 4713.
- [331] M. S. Yusubov, E. A. Krasnokutskaya, V. P. Vasilyeva, V. D. Filimonov, K.-W. Chi, *Bull. Korean Chem. Soc.* **1995**, *16*, 86.
- [332] M. I. Javed, M. Brewer, *Org. Lett.* **2007**, *9*, 1789.
- [333] H. V. Le, B. Ganem, *Org. Lett.* **2011**, *13*, 2584.
- [334] R. Tomita, Y. Yasu, T. Koike, M. Akita, *Angew. Chem., Int. Ed.* **2014**, *53*, 7144.
- [335] H. Cui, X. Liu, W. Wei, D. Yang, C. He, T. Zhang, H. Wang, *J. Org. Chem.* **2016**, *81*, 2252.
- [336] D. Vaithialingam, D. Kumaraguru, S. Ayyanar, *New J. Chem.* **2016**, *40*, 7604.
- [337] J. Yin, C. E. Gallis, J. D. Chisholm, *J. Org. Chem.* **2007**, *72*, 7054.
- [338] B. Das, S. Vedachalam, D. Luo, T. Antonio, M. E. A. Reith, A. K. Dutta, *J. Med. Chem.* **2015**, *58*, 9179.
- [339] R. Pummerer, *Berichte der Dtsch. Chem. Gesellschaft* **1909**, *42*, 2282.
- [340] R. Pummerer, *Berichte der Dtsch. Chem. Gesellschaft* **1910**, *43*, 1401.
- [341] T. T. Tidwell, in *Organic Reactions*, John Wiley & Sons, Inc., Hoboken, New Jersey, **2004**,

- pp. 297–555.
- [342] M. Kennedy, M. Anthony Mckerverey, *Compr. Org. Synth.* **1991**, 193.
- [343] R. M. Denton, J. An, B. Adeniran, A. J. Blake, W. Lewis, A. M. Poulton, *J. Org. Chem.* **2011**, *76*, 6749.
- [344] J. An, R. M. Denton, T. H. Lambert, E. D. Nacsa, *Org. Biomol. Chem.* **2014**, *12*, 2993.
- [345] C. Ni, F. Jiang, Y. Zeng, J. Hu, *J. Fluor. Chem.* **2015**, *179*, 3.
- [346] S. Suzuki, T. Kamo, K. Fukushi, T. Hiramatsu, E. Tokunaga, T. Dohi, Y. Kita, N. Shibata, *Chem. Sci.* **2014**, *5*, 2754.
- [347] S. Hara, M. Sekiguchi, A. Ohmori, T. Fukuhara, N. Yoneda, *Chem. Commun.* **1996**, 1899.
- [348] M. Yoshida, K. Fujikawa, S. Sato, S. Hara, *ARKIVOC* **2003**, 36.
- [349] S. Seo, J. B. Taylor, M. F. Greaney, *Chem. Commun.* **2013**, *49*, 6385.
- [350] Z. Ji, T. C. Timothy, in *C-H Bond Act. Org. Synth.*, **2015**, pp. 251–266.
- [351] C. Xu, X. Song, J. Guo, S. Chen, J. Gao, J. Jiang, F. Gao, Y. Li, M. Wang, *Org. Lett.* **2018**, *20*, 3933.
- [352] L. Li, Q. Y. Chen, Y. Guo, *J. Org. Chem.* **2014**, *79*, 5145.
- [353] A. T. Parsons, S. L. Buchwald, *Angew. Chemie Int. Ed.* **2011**, *50*, 9120.
- [354] X. P. Wang, J. H. Lin, C. P. Zhang, J. C. Xiao, X. Zheng, *Beilstein J. Org. Chem.* **2013**, *9*, 2635.
- [355] T. Liu, Q. Shen, *Org. Lett.* **2011**, *13*, 2342.
- [356] Y. Huang, X. Fang, X. Lin, H. Li, W. He, K.-W. Huang, Y. Yuan, Z. Weng, *Tetrahedron* **2012**, *68*, 9949.
- [357] H. Zheng, Y. Huang, Z. Wang, H. Li, K.-W. Huang, Y. Yuan, Z. Weng, *Tetrahedron Lett.* **2012**, *53*, 6646.
- [358] S. Mizuta, O. Galicia-López, K. M. Engle, S. Verhoog, K. Wheelhouse, G. Rassias, V. Gouverneur, *Chem. Eur. J.* **2012**, *18*, 8583.
- [359] C.-S. Wang, H. Wang, C. Yao, *RSC Adv.* **2015**, *5*, 24783.
- [360] S. H. Bertz, E. H. Fairchild, G. Guillaumet, F. Suzenet, *Encycl. Reagents Org. Synth.* **2005**, DOI doi:10.1002/047084289X.rc229.pub2.
- [361] T. Liu, X. Shao, Y. Wu, Q. Shen, *Angew. Chemie Int. Ed.* **2012**, *51*, 540.
- [362] Z. He, P. Tan, J. Hu, *Org. Lett.* **2016**, *18*, 72.
- [363] E. Mejía, A. Togni, *ACS Catal.* **2012**, *2*, 521.
- [364] R. Shimizu, H. Egami, T. Nagi, J. Chae, Y. Hamashima, M. Sodeoka, *Tetrahedron Lett.* **2010**, *51*, 5947.
- [365] Y. Kuninobu, M. Nishi, M. Kanai, *Org. Biomol. Chem.* **2016**, *14*, 8092.
- [366] S. Cai, C. Chen, Z. Sun, C. Xi, *Chem. Commun.* **2013**, *49*, 4552.
- [367] L. Hu, X. Chen, Q. Gui, Z. Tan, G. Zhu, *Chem. Commun.* **2016**, *52*, 6845.
- [368] O. Sala, H. P. Lüthi, A. Togni, M. Iannuzzi, J. Hutter, *J. Comput. Chem.* **2015**, *36*, 785.

-
- [369] O. Sala, H. P. Lüthi, A. Togni, *J. Comput. Chem.* **2014**, *35*, 2122.
- [370] S.-M. Wang, J.-B. Han, C.-P. Zhang, H.-L. Qin, J.-C. Xiao, *Tetrahedron* **2015**, *71*, 7949.
- [371] F. Wang, P. Chen, G. Liu, *Acc. Chem. Res.* **2018**, *51*, 2036.
- [372] Y. Nakamura, M. Fujiu, T. Murase, Y. Itoh, H. Serizawa, K. Aikawa, K. Mikami, *Beilstein J. Org. Chem.* **2013**, *9*, 2404.
- [373] F. Akhtar, D. M. L. Goodgame, M. Goodgame, G. W. Rayner-Canham, A. C. Skapski, *Chem. Commun.* **1968**, 1389.
- [374] G. A. Bowmaker, C. Di Nicola, C. Pettinari, B. W. Skelton, N. Somers, A. H. White, *Dalt. Trans.* **2011**, *40*, 5102.
- [375] J. Zhao, H.-Y. Lin, G.-C. Liu, X. Wang, X.-L. Wang, *Inorganica Chim. Acta* **2017**, *464*, 114.
- [376] H. Yu, R. Kühne, R.-U. Ebert, G. Schüürmann, *J. Chem. Inf. Model.* **2011**, *51*, 2336.
- [377] M. Kato, H. B. Jonassen, J. C. Fanning, *Chem. Rev.* **1964**, *64*, 99.
- [378] M. Inoue, M. Kishita, M. Kubo, *Acta Crystallogr.* **1963**, *16*, 699.
- [379] J. Lewis, Y. C. Lin, L. K. Royston, R. C. Thompson, *J. Chem. Soc.* **1965**, 6464.
- [380] T. D. Smith, J. R. Pilbrow, *Coord. Chem. Rev.* **1974**, *13*, 173.
- [381] Y. Kikuchi, T. Suzuki, K. Sawada, *Bull. Chem. Soc. Jpn.* **1990**, *63*, 1819.
- [382] A. Zanardi, M. A. Novikov, E. Martin, J. Benet-Buchholz, V. V Grushin, *J. Am. Chem. Soc.* **2011**, *133*, 20901.
- [383] S.-L. Zhang, W.-F. Bie, *RSC Adv.* **2016**, *6*, 70902.
- [384] V. K. Pandey, P. Anbarasan, *RSC Adv.* **2016**, *6*, 18525.
- [385] H. Xu, C. Wolf, *Chem. Commun.* **2009**, 3035.
- [386] L. Ackermann, A. Althammer, *Angew. Chemie Int. Ed.* **2007**, *46*, 1627.
- [387] L. Ackermann, A. Althammer, P. Mayer, *Synthesis* **2009**, *2009*, 3493.
- [388] W. L. F. Armarego, C. Chai, *Purification of Laboratory Chemicals*, **2009**.
- [389] *SAINT+*; *Software for CCD Diffractometers*, v. 6.01 and *SAINT*, v. 6.02; *Bruker AXS, Inc., Madison, WI*, **2001**.
- [390] G. M. Sheldrick, *Acta Crystallogr. Sect. A* **1990**, *46*, 467.
- [391] G. M. Sheldrick, *Acta Crystallogr. Sect. C* **2015**, *71*, 3.
- [392] R. H. Blessing, *Acta Crystallogr. Sect. A* **1995**, *51*, 33.
- [393] H. D. Flack, *Acta Crystallogr. Sect. A* **1983**, *39*, 876.
- [394] G. Bernardinelli, H. D. Flack, *Acta Crystallogr. Sect. A* **1985**, *41*, 500.
- [395] *Acta Crystallogr. Sect. C* **2010**, *66*, e1.
- [396] T. Wakui, Y. Nakamura, S. Motoki, *Bull. Chem. Soc. Jpn.* **1978**, *51*, 3081.
- [397] J. Cody, C. J. Fahrni, *Tetrahedron* **2004**, *60*, 11099.
- [398] V. Weißkopf, H. Perst, *Justus Liebigs Ann. Chem.* **1978**, *1978*, 1634.
-

- [399] M. Skarpeli-Liati, S. G. Pati, J. Bolotin, S. N. Eustis, T. B. Hofstetter, *Environ. Sci. Technol.* **2012**, *46*, 7189.
- [400] L. Pauli, R. Tannert, R. Scheil, A. Pfaltz, *Chem. – A Eur. J.* **2015**, *21*, 1482.
- [401] A. B. Kudryavtsev, W. Linert, in *Physico-Chemical Appl. NMR*, WORLD SCIENTIFIC, **1996**, pp. 179–213.
- [402] S. Stoll, A. Schweiger, *J. Magn. Reson.* **2006**, *178*, 42.
- [403] H. Tanaka, K. Oisaki, M. Kanai, *Synlett* **2017**, *28*, 1576.
- [404] M. T. Miller, C. Anderson, V. Arumugam, B. R. Bear, H. M. Binch, J. J. Clemens, T. Cleveland, E. Conroy, T. R. Coon, B. A. Frieman, et al., *Modulators of Cystic Fibrosis Transmembrane Conductance Regulator*, US20160095858, **2015**.
- [405] X. Shao, T. Liu, L. Lu, Q. Shen, *Org. Lett.* **2014**, *16*, 4738.
- [406] J.-H. Chun, S. Telu, S. Lu, V. W. Pike, *Org. Biomol. Chem.* **2013**, *11*, 5094.

X. APPENDIX

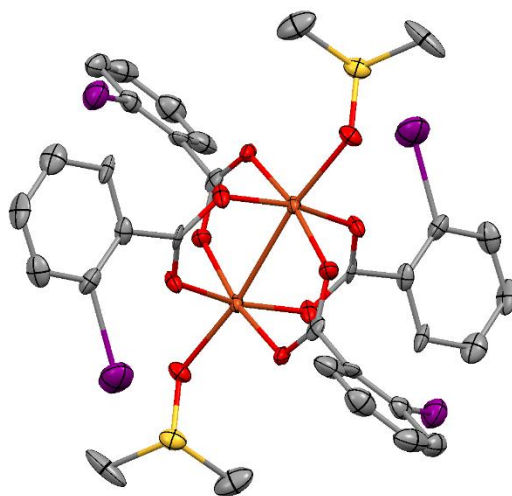
Appendix A: Abbreviations and Acronyms

acac	Acetylacetonato
aq.	Aqueous
Ar	Aryl
calcd.	calculated
DABCO	1,4-Diazabicyclo[2.2.2]octane
DAST	Diethylaminosulfur trifluoride
DCM	Dichloromethane
DMAP	4-Dimethylamino-pyridine
DMC	Dimethyl carbonate
DMF	<i>N,N</i> -Dimethylformamide
DMSO	Dimethyl sulfoxide
EI	Electron Ionization
ESI	Electrospray Ionization
FID	Flame-Ionization detector
GC	Gas Chromatography
HPLC	High Pressure Liquid Chromatography
HRMS	High-resolution mass spectrometry
IR spectroscopy	Infrared spectroscopy
<i>m/z</i>	Mass-to-charge ratio
mCPBA	<i>m</i> -Chloroperoxybenzoic acid
NBS	<i>N</i> -Bromosuccinimide
<i>n</i> Bu	<i>n</i> -Butyl
<i>n</i> BuLi	<i>n</i> -Butyllithium

NMP	<i>N</i> -Methyl-2-pyrrolidone
NMR	Nuclear Magnetic Resonance
PG	Protecting group
sat.	saturated
<i>s</i> BuLi	<i>sec</i> -Butyllithium
SET	Single-Electron Transfer
<i>t</i> BuCN	Pivalonitrile
Tf	Trifluoromethanesulfonyl
TFA	Trifluoroacetic acid
TFAA	Trifluoroacetic anhydride
THF	Tetrahydrofuran
TMS	Trimethylsilyl
Ts	Toluenesulfonyl

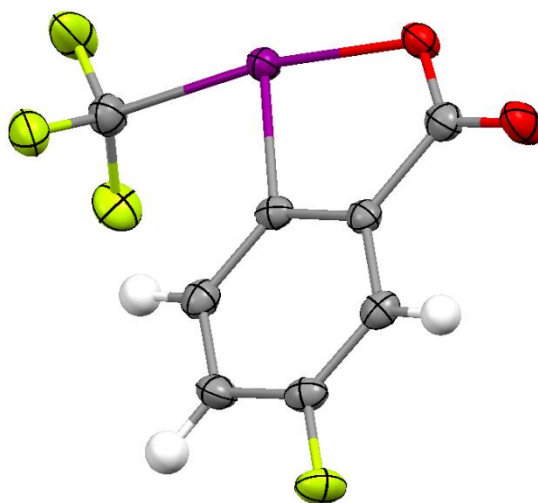
Appendix B: Crystallographic Data¹⁰

Dinuclear copper complex 64·2DMSO



Identification code	-	CCDC number	-
Empirical formula	C ₃₂ H ₂₈ Cu ₂ I ₄ O ₁₀ S ₂	Moiety formula	C ₃₂ H ₂₈ Cu ₂ I ₄ O ₁₀ S ₂
Formula weight	84.73	Crystallization method	Standing at RT
Temperature (K)	100.01	Crystal color, habit	green, block
Crystal system	monoclinic	Crystal size/mm ³	0.19 × 0.135 × 0.08
Space group	P21/c	Radiation	MoK α (λ = 0.71073)
a (Å)	19.8987(12)	2 θ range for data collection (°)	2.862 to 51.912
b (Å)	20.3908(12)	Index ranges	-24 ≤ h ≤ 24
c (Å)	9.7063(6)		-25 ≤ k ≤ 25
α (°)	90		-11 ≤ l ≤ 11
β (°)	93.3410(10)	Reflections collected	69302
γ (°)	90	Independent reflections	7674 [R _{int} = 0.0446, R _{sigma} = 0.0273]
Volume (Å ³)	3931.6(4)	Data/restraints/parameters	7674/0/456
Z	36	Goodness-of-fit on F ²	2.129
ρ_{calc} (g/cm ³)	1.288	Final R indexes [I ≥ 2 σ (I)]	R ₁ = 0.0817, wR ₂ = 0.2627
μ (mm ⁻¹)	0.409	Final R indexes [all data]	R ₁ = 0.1010, wR ₂ = 0.2756
F ₀₀₀	1618	Largest diff. peak/hole (e ⁻ ·Å ⁻³)	6.85/-4.20

¹⁰ The color coding of the atoms is as follows: grey = carbon, red = oxygen, blue = nitrogen, purple = iodine, orange = copper, green = fluorine, yellow = sulfur, pink = boron.

1-Trifluoromethyl-5-fluoro-1,2-benziodoxol-3-(1H)-one (77)

Identification code	KH527a_new_ortho	CCDC number	1896815
Empirical formula	C ₈ H ₃ F ₄ IO ₂	Moiety formula	C ₈ H ₃ F ₄ IO ₂
Formula weight	334.00	Crystallization method	MeCN
Temperature/K	100	Crystal color, habit	colorless, plate
Crystal system	orthorhombic	Crystal size/mm ³	0.045 × 0.022 × 0.013
Space group	Pbca	Radiation	MoKα (λ = 0.71073)
a (Å)	15.3616(18)	2θ range for data collection (°)	5.292 to 56.54
b (Å)	7.6441(9)	Index ranges	-20 ≤ h ≤ 20
c (Å)	15.3943(17)		-10 ≤ k ≤ 10
α (°)	90		-20 ≤ l ≤ 20
β (°)	90	Reflections collected	41213
γ (°)	90	Independent reflections	2238 [R _{int} = 0.0601, R _{sigma} = 0.0225]
Volume (Å ³)	1807.7(4)	Data/restraints/parameters	2238/0/136
Z	8	Goodness-of-fit on F ²	1.068
ρ _{calc} (g/cm ³)	2.455	Final R indexes [I ≥ 2σ (I)]	R ₁ = 0.0279, wR ₂ = 0.0595
μ (mm ⁻¹)	3.582	Final R indexes [all data]	R ₁ = 0.0410, wR ₂ = 0.0656
F ₀₀₀	1248.0	Largest diff. peak/hole (e ⁻ ·Å ⁻³)	1.34/-0.58

Appendix C: Curriculum Vitae

Name Harutake Kajita
Date of birth July 23, 1985
Nationality Japanese

Education

08.2014–04.2019 Dr. sc. ETH Zurich
Laboratory of Inorganic Chemistry, ETH Zurich
Supervisor: Prof. Antonio Togni
Co-examiner: Prof. Erick Carreira
04.2008–03.2010 Master of Engineering, Kyoto University
Supervisor: Prof. Seiji Matsubara
04.2004–03.2008 Bachelor of Engineering, Kyoto University

Work experience

04.2010–07.2014 Chemist/Chemical engineer, AGC Inc., Japan

Publications

1. "Magnesium-Catalyzed Electrophilic Trifluoromethylation: Facile Access to All-Carbon Quaternary Centers in Oxindoles" Dmitry Katayev, Harutake Kajita, Antonio Togni, *Chem. Eur. J.* **2017**, *23*, 8353–8357.
2. "A Oxidative Bromination of (Hetero)Arenes in the TMSBr/DMSO System: A Non-Aqueous Procedure Facilitates Synthetic Strategies" Harutake Kajita, Antonio Togni, *ChemistrySelect* **2017**, *2*, 1117–1121.